DIRECCION DE AGUAS

DFID
Department For
International Development

British Geological Survey

TECHNICAL REPORT WC/99/36
Overseas Geology Series

Arsenic and Other Quality Problems in Groundwater from Northern La Pampa Province, Argentina

Natural
Environment
Research
Council

British Geological Survey
Keyworth
Nottingham
United Kingdom NG12 5GG

DIRECCION DE AGUAS

DFID
Department For
International Development

British Geological Survey

TECHNICAL REPORT WC/99/36 PROJECT: R6491
Overseas Geology Series

Arsenic and Other Quality Problems in Groundwater from Northern La Pampa Province, Argentina

P L Smedley[1], D M J Macdonald[1], H B Nicolli[2], A J Barros[2], J O Tullio[3]
and J M Pearce[4]

[1]British Geological Survey (BGS), Wallingford, UK
[2]Instituto de Geoquímica (INGEOQUI), San Miguel, Provincia de Buenos Aires, Argentina
[3]Dirección de Aguas (DDA), Santa Rosa, Provincia de La Pampa, Argentina
[4]British Geological Survey (BGS), Keyworth, UK

This report is produced under a project funded by the UK Department for International Development (DFID) as part of the UK provision of technical assistance to developing countries. The views expressed are not necessarily those of the Department.

DFID classification:
Subsector: Geoscience
Theme: Identify and ameliorate minerals related and other geochemical toxic hazards
Project title: Environmental Arsenic Exposure: Health Risks and Geochemical Solutions
Project reference: R6491

Bibliographic reference:
P L Smedley, D M J Macdonald, H B Nicolli, A J Barros, J O Tullio and J M Pearce (2000).
Arsenic and Other Quality Problems in Groundwater from Northern La Pampa Province, Argentina
BGS Technical Report WC/99/36

Keywords: groundwater quality, arsenic, fluoride, loess, geochemistry, health

Front cover illustration: Typical Australian windmill discharging groundwater into a holding tank for agricultural use, La Pampa

Keyworth, Nottingham, British Geological Survey, 2000

BRITISH GEOLOGICAL SURVEY

The full range of Survey publications is available from the BGS Sales Desk at the Survey headquarters, Keyworth, Nottingham. The more popular maps and books may be purchased from BGS-approved stockists and agents and over the counter at the Bookshop, Gallery 37, Natural History Museum, Cromwell Road, (Earth Galleries), London. Sales Desks are also located at the BGS London Information Office, and at Murchison House, Edinburgh. The London Information Office maintains a reference collection of BGS publications including maps for consultation. Some BGS books and reports may also be obtained from HMSO Publications Centre or from HMSO bookshops and agents.

The Survey publishes an annual catalogue of maps, which lists published material and contains index maps for several of the BGS series.

The British Geological Survey carries out the geological survey of Great Britain and Northern Ireland (the latter as an agency service for the government of Northern Ireland), and of the surrounding continental shelf, as well as its basic research projects. It also undertakes programmes of British technical aid in geology in developing countries as arranged by the Department for International Development.

The British Geological Survey is a component body of the Natural Environment Research Council.

Keyworth, Nottingham NG12 5GG
☎ 0115-936 3100 Telex 378173 BGSKEY G
Fax 0115-936 3200

Murchison House, West Mains Road, Edinburgh, EH9 3LA
☎ 0131-667 1000 Telex 727343 SEISED G
Fax 0131-668 2683

London Information Office at the Natural History Museum, Earth Galleries, Exhibition Road, South Kensington, London SW7 2DE
☎ 0171-589 4090 Fax 0171-584 8270
☎ 0171-938 9056/57

St Just, 30 Pennsylvania Road, Exeter EX4 6BX
☎ 01392-78312 Fax 01392-437505

Geological Survey of Northern Ireland, 20 College Gardens, Belfast BT9 6BS
☎ 01232-666595 Fax 01232-662835

Maclean Building, Crowmarsh Gifford, Wallingford, Oxfordshire OX10 8BB
☎ 01491-838800 Fax 01491-692345

Parent Body
Natural Environment Research Council
Polaris House, North Star Avenue, Swindon, Wiltshire SN2 1EU
☎ 01793-411500 Telex 444293 ENVRE G
Fax 01793-411501

Contents

List of Figures

List of Tables

ACKNOWLEDGEMENTS

We are especially grateful to staff of Dirección de Aguas (DDA, formerly APA), Santa Rosa, La Pampa Province, for providing much assistance with groundwater sampling, transport and provision of hydrogeological and water-quality data. Staff of the public water-supply sites and numerous owners of private boreholes are also acknowledged for allowing sampling access.

Chemical analysis of water and sediment samples at BGS was carried out by K. Smith, S. Bourliakas, J. Thorns, J. Trafford, S. Burden, J. Robinson, L. Ault, B. Vickers and D. Gooddy. Stable-isotopic analysis was carried out by G. Darling and S. Bourliakas. Sulphur-isotopic analysis was carried out in part by B. Spiro of the NERC Isotope Geology Laboratory, BGS, Keyworth and part by Geochron Laboratories, Kreuger Enterprises, Cambridge, Massachusetts, USA. Radiocarbon and tritium analysis was carried out by Instituto de Geochronologia y geología Isotópica (INGEIS), Buenos Aires, Argentina.

Sediment samples from core material drilled at Eduardo Castex, Ingeniero Luiggi and La Maruja were provided by DDA. Drilling of cored boreholes at Tamagnoni and Talleres Norte was carried out by M. Blanco, Ingeniero Luiggi, La Pampa. Clay mineralogy was investigated by M. S. Alonso of INGEOQUI.

Cartographic work was carried out by G. Tyson.

We are also grateful to M. Blarasin of the University of Río Cuarto, Córdoba Province, Argentina and S. Foster of BGS for helpful hydrogeological discussions as well as to D. Kinniburgh (BGS) for hydrogeochemical discussions and review of this report.

Research was carried out with funding provided by UK-DFID under its Knowledge and Research (KAR) programme, project number R6491. INGEOQUI has participated with additional funding from PIP No. 4430, CONICET, Argentina.

EXECUTIVE SUMMARY

Groundwater is a vital resource in the semi-arid Chaco-Pampean Plain of central Argentina and is relied upon heavily for potable supply and agricultural production. However, the sustainability of the resource is under threat as a result of significant groundwater-quality problems from high salinity and high concentrations of potentially harmful elements such as arsenic (As), fluoride (F), nitrate (NO_3-N, boron (B), molybdenum (Mo) and uranium (U). Arsenic constitutes one of the most severe threats to health and the problems are recognised by water providers and health professionals. Symptoms typical of chronic arsenic poisoning, including skin lesions and some internal cancers, have been recorded in some of the areas where high groundwater concentrations exist. Problems resulting from chronic exposure to fluoride in the drinking water are also manifested by common occurrence of dental fluorosis. The extent of the groundwater-quality problems across the region is not well-defined, but is believed to cover an area of around 1 million square kilometres, extending from the Andes in the west to the Patagonian Plateau in the south and the Gran Chaco in the north. Up to 5 million people are thought to be exposed to As in drinking water in excess of the national standard for drinking water of 50 µg l^{-1}. Urgent mitigation of the water-quality problems in the region is needed in order to safeguard community health.

A hydrogeological and geochemical investigation has been carried out of part of the Chaco-Pampean Plain, the Eduardo Castex area of northern La Pampa Province, to assess the nature and causes of the As problems in the groundwaters, to characterise the scale of other water-quality problems and to make recommendations for groundwater mitigation.

The shallow aquifers of La Pampa are composed of Quaternary loess deposits formed by aeolian deposition and reworking. These deposits comprise mainly brown silts and fine sands and contain an important component of volcanic material (dacitic to rhyolitic ash, including volcanic glass and pumice) derived from Andean eruptions. The sediments have been diagenetically altered and have abundant calcrete in the form of nodules and cements, as well as occasional mottling resulting from manganese oxide nodules and cements. The diagenetic alterations are indicative of semi-arid climatic conditions over the Quaternary history of the aquifers.

Groundwater flow across the region is chiefly from west to east following the topographic gradient, but in the eastern area where a flatter plain exists with small depressions, localised shallow flow cells occur with internal drainage into the depressions. These act as discharge areas which fill with water during the wet season. During the dry season, water accumulated in the depressions evaporates and salt encrustations are deposited around the depression margins. Evaporation contributes significantly to the high salinity of many of the groundwaters.

Groundwaters from open wells and boreholes in the area have a large range of chemical compositions. Total dissolved solids in samples collected from this study vary between 700 mg l^{-1} and 11400 mg l^{-1} but concentrations are often at the high end of this range. The groundwaters also usually have high alkalinity (195 mg l^{-1} to 1440 mg l^{-1} as HCO_3) and a large range of concentrations of As (<4–5300 µg l^{-1}), F (0.03–29 mg l^{-1}), B (0.5–13.8 mg l^{-1}), V (0.02–5.4 mg l^{-1}), Mo (2.7–991 µg l^{-1}) and U (6.2–248 µg l^{-1}). Of groundwater samples investigated, 95% exceed the WHO guideline value for As in drinking water (10 µg l^{-1}) and 73 % exceed the Argentine national standard of 50 µg l^{-1}. In addition, 83 % exceed the WHO guideline value for F (1.5 mg l^{-1}), 99 % for B (0.3 mg l^{-1}), 39 % for Mo (70 µg l^{-1}) and 100 % for U (2 µg l^{-1}).

The groundwaters are universally oxidising with high dissolved-oxygen concentrations and generally high redox potentials. Groundwater pHs are neutral to alkaline (7.0–8.7). Under the ambient oxidising conditions, As is present in solution predominantly as the arsenate (As(V)) species.

Groundwater As correlates positively with pH, alkalinity (HCO_3) and with F and V. Weaker positive correlations are also observed between As and B, Mo and U as well as Be. The mobilisation of these elements which occur in solution as anion (fluoride) and oxyanion (arsenate, vanadate, borate and molybdate, uranyl) species is most likely to be promoted by desorption from iron, manganese and aluminium oxides in the sediments, particularly under the pertaining conditions of high pH and alkalinity. Competition between these anions and oxyanions for sorption sites on oxide minerals is also a factor likely to have enhanced mobilisation in solution.

Concentrations of As and other anions and oxyanions appear to be particularly high in groundwaters close to the low-lying depressions which act as localised groundwater-discharge zones. Concentrations up to 7490 $\mu g\ l^{-1}$ were found in porewaters extracted from a cored borehole adjacent to one such depression. Arsenic concentrations are also relatively high in some groundwaters close to the water table (ie. where the saturated depth of boreholes is small).

No monitoring of groundwater As has been carried out and variations in water quality with time are unknown. Since the As and other anion/oxyanion problems are naturally-derived, it is unlikely that significant changes with time will occur. However, seasonal or long-term variations in pumping regimes or recharge may effect some changes in water quality which are worthy of investigation.

Arsenic concentrations in the aquifer sediments are similar to average values for silty and sandy sediments. They contain no discernible discrete As minerals. Total As concentrations range between 3 mg kg^{-1} and 18 mg kg^{-1}, with finer-grained sediments being at the higher end of the range. Oxalate-extractable As concentrations (associated with mixed amorphous oxide minerals, especially iron oxides) vary between 0.5 mg kg^{-1} and 9.6 mg kg^{-1} (mean 2 mg kg^{-1}, roughly half the total As present in the solid phase) and hydroxylamine-extractable concentrations (associated with manganese oxide) vary between 0.02 mg kg^{-1} and 4.7 mg kg^{-1} (mean 1.0 mg kg^{-1}). This suggests that a significant amount of As present in the sediments is relatively labile and associated with poorly structured iron and manganese oxides. Release into solution can therefore be readily achieved given the appropriate pH and redox conditions. The data indicate that the As problem arises as a result of 'mobilisation' under favourable conditions, rather than the 'source' (high As in the aquifer) being the root of the problem.

The development of groundwaters with high pH and alkalinity results from pronounced silicate and carbonate reaction under closed conditions, facilitated by the arid climatic conditions. These factors, together with young age of the loess sediments and slow groundwater flow conditions (closed basins with low hydraulic heads and low recharge totals) has enabled the accumulation of high concentrations of As as well as F, B, P, Mo, and U in solution. Accumulation is particularly marked in the small depressions where potential groundwater flow away from the depression is limited. Dissolved salts accumulate at the near surface due to evaporation and lead to increased salinity, whilst at deeper levels, concentrations of anions and oxyanions including As accumulate without being flushed away.

Mitigation of As problems is difficult because groundwater constitutes the main source of drinking water and because it is only one of a number of elements of health concern present in the groundwater. However, quality problems can be minimised by future drilling being directed away from low-lying depressions and by completing boreholes in deeper parts of the aquifer so that high-As waters close to the water table are avoided. Measurement of pH and alkalinity could be useful as proxy indicators of high concentrations of As and other anions/oxyanions.

Given the fact that the majority of groundwaters in the Pampean aquifer are of unacceptable quality for potable use, only limited benefit is likely to be gained from optimal borehole-siting strategies in future drilling programmes. Despite the problems with groundwater treatment in terms of cost, maintenance and disposal of waste treatment materials, this remains one of the most appropriate mitigation steps. Wider application of groundwater treatment, particularly small-scale systems for rural areas is needed to protect public health. Rainwater harvesting may also have potential as a suitable mitigation measure. In terms of the Chaco-Pampean Plain as a whole, randomised surveying and mapping of groundwater quality are needed in order to delineate the scale of the problems nationally.

1. INTRODUCTION

Arsenic in groundwater and its associated health problems have received much scientific and media attention over the last few years. The concerns arise from a combination of the fact that As is highly toxic in solution so that recommended limits for drinking-water quality are low (the WHO guideline value being 10 $\mu g\ l^{-1}$) and the fact that As is potentially mobile over the typical range of pH and Eh conditions in groundwaters. Hence, although As is only problematic in aquifers in some areas, among the toxic trace elements, it ranks as one of the most significant.

Arsenic has traditionally not been an element routinely measured in analytical laboratories, particularly in developing countries, and hence newly emerging As problems in aquifers have often proved an unwelcome surprise. More problem areas are being identified as increasing volumes of As data become available.

Large aquifers have been identified with significant natural groundwater-As problems in various parts of the world, most notably Bangladesh, West Bengal (India), parts of northern China, Taiwan, Mexico, Hungary and south-west USA, as well as a large area of central Argentina and northern Chile. Arsenic problems related to sulphide mining and geothermal activity also occur in many other areas on a more localised scale.

In the developed world, As concentrations in groundwaters are typically much lower than those in the problem aquifers outlined above, but nonetheless are becoming of increasing concern because of moves to reduce the recommended limits for As in drinking water from 50 $\mu g\ l^{-1}$, the value currently adopted by most countries, to a value closer to that proposed by WHO (1993).

In light of the current concerns over As in groundwater, DFID commissioned BGS to carry out an investigation of the hydrogeological and geochemical aspects of the As problems in selected aquifers and to make recommendations for appropriate mitigation measures. The countries or regions chosen for study were Argentina, Bangladesh and Inner Mongolia. Investigations in Argentina and Inner Mongolia have been carried out under the DFID KAR programme, project R6491. Investigations in Bangladesh also began under this project but were expanded into a larger Technical Cooperation project between BGS and the Government of Bangladesh, which began in 1998.

This report describes the work carried out in northern La Pampa Province of Argentina as a collaboration between BGS Wallingford, Instituto de Geoquímica (INGEOQUI), Buenos Aires and Dirección de Aguas (DDA), Santa Rosa, Argentina.

2. ARSENIC PROBLEMS IN GROUNDWATER

2.1 Health effects

Arsenic has long been recognised as a toxin and carcinogen. Chronic ingestion has been noted to give rise to a number of health problems, particularly skin disorders, of which the most common are hypopigmentation, hyperpigmentation and keratosis. Additional reported symptoms include other more serious dermatological problems (e.g. skin cancer and Bowen's disease), cardiovascular (blackfoot disease, Raynaud's syndrome, hypertension), neurological, respiratory and hepatic diseases as well as diabetes mellitus (e.g. Gorby, 1994). A number of internal cancers have also been linked with As in drinking water, particularly lung, bladder, liver, prostate and kidney cancer (e.g. Smith et al., 1992; 1998). Clinical symptoms of As poisoning and their relative prevalence seem to vary between affected regions and there is no clear agreement on the definition of As poisoning.

Some studies have shown a clear dose-response relationship for As in drinking water (e.g. Tseng et al. 1968; Wu et al., 1989; Chiou et al., 1995; Hopenhayn-Rich et al., 1996). However, the relationship may be complicated by other factors such as nutritional and general health status (hepatitis B may exacerbate the problems) and water chemistry (e.g. As speciation, dissolved Fe concentration). Debate also remains over whether a threshold As concentration exists below which the element is effectively safe (e.g. Chappell et al., 1997; Clewell et al., 1999).

Latency periods of several years for the development of As-related health problems have been noted in several epidemiological investigations, a factor which in part explains why many of the problems in developing countries have only recently emerged despite several years of groundwater use. Albores et al. (1979) and Cebrián et al. (1983) studied the health effects of As exposure on rural populations in Lagunera Region of Mexico drinking water with As concentrations of 410 $\mu g\ l^{-1}$. They found an 8-year latency period for development of hypopigmentation, 12 years for hyperpigmentation and palmoplantar keratosis, 25 years for papular keratosis and 38 years for ulcerative lesions (Cebrián et al., 1994).

Many of the advanced and most serious clinical symptoms are incurable. Others can be treated and mild symptoms can go into remission provided a supply of low-As drinking water can be provided at a relatively early stage. Provision of As-free alternative drinking-water sources is therefore an important priority for exposed populations.

2.2 Regulation

Following the accumulation of evidence of the chronic toxicological effects of As in drinking water, recommended and regulatory limits of many authorities are being reduced. The WHO guideline value for As in drinking water was provisionally reduced in 1993 from 50 $\mu g\ l^{-1}$ to 10 $\mu g\ l^{-1}$. The new recommended value is based largely on analytical capability. Lifetime exposure to arsenic in drinking water at a concentration of just 1 $\mu g\ l^{-1}$ gives an estimated cancer risk of 1 in 1 million. Hence, a recommendation based on health alone would be still lower than 10 $\mu g\ l^{-1}$. The Japanese limit for drinking water is also 10 $\mu g\ l^{-1}$ and the Canadian limit has been set at 5 $\mu g\ l^{-1}$ but with an interim limit of 20 $\mu g\ l^{-1}$.

Whilst many regulatory authorities are seeking to reduce their limits in line with the WHO guideline value, many countries including Argentina, and indeed all affected developing countries, still operate to the 50 $\mu g\ l^{-1}$ standard, in part because of lack of adequate testing facilities for compliance monitoring at lower concentrations.

Both the current US-EPA limit and EC maximum admissible concentration (MAC) for As in drinking water are 50 $\mu g\ l^{-1}$ although both are planned to be reduced in line with the health evidence. For a number of years, the US-EPA has been debating the appropriate revised value to adopt. Although a decision has yet to be made, values in the range 2 $\mu g\, l^{-1}$ to 20 $\mu g\, l^{-1}$ are under consideration.

A new EC Directive has been agreed (98/83/EC) which incorporates a revised MAC for As in drinking water of 10 $\mu g\, l^{-1}$. The Directive is due to become EC regulation by the end of 2000 with the new standards being enforceable by the end of 2003.

2.3 World distribution of arsenic problems

A number of large aquifers worldwide have been identified with problems from As occurring at concentrations above 50 $\mu g\, l^{-1}$, often significantly so. The most noteworthy occurrences are in parts of West Bengal and Bangladesh, Taiwan, northern China, Hungary, Mexico, parts of south-west USA and Chile, as well as Argentina (Figure 2.1). Many of the occurrences affect aquifers over large areas and can therefore have a potentially severe impact on human health. It is unfortunate that many of the occurrences are in parts of the developing world where infrastructure and economy is least well able to mitigate the problems and hence raw groundwater is commonly used for drinking without treatment.

Most of the occurrences are due to natural contamination. However, in some areas As problems can be exacerbated by mining activity where As is released from sulphide minerals as they are oxidised during the mining operations. Arsenic problems can also be prevalent in geothermal waters. Arsenic contamination of water sources due to mining or geothermal inputs can often be severe, with concentrations in affected waters often being in the milligram-per-litre range. However, unlike As occurrences in major aquifers, the problems in these areas are typically localised rather than of widespread occurrence. Some of the best-documented As problems related to mining and geothermal activity are shown in Figure 2.1.

2.3.1 Natural occurrences in aquifers

Bangladesh and West Bengal

In terms of the population exposed, As problems in groundwater from the alluvial and deltaic aquifers of Bangladesh and West Bengal represent the most serious occurrences identified globally. Concentrations in groundwaters from the affected areas have a very large range from <0.5 $\mu g\, l^{-1}$ to ca. 3200 $\mu g\, l^{-1}$ (e.g. BGS/MML, 1999; CGWB, 1999). Resultant health problems were first identified in West Bengal in the late 1980s but the first diagnosis in Bangladesh was not until 1993. Around 30 million people in Bangladesh are thought be exposed to As in drinking water at concentrations above 50 $\mu g\, l^{-1}$ and around 6 million in West Bengal (Table 2.1). Skin disorders including hyper/hypopigmentation changes and keratosis are the most common manifestations, although skin cancer has also been identified. Around 5000 patients have been identified with As-related health problems in West Bengal (including skin pigmentation changes).

The two countries rely heavily on groundwater for public drinking-water supply, a policy which has been encouraged over the last few decades by government and other agencies as a means of reducing the incidence of bacterial and other water-borne diseases which arise from use of polluted surface water. In this, the increase in use of groundwater has been very successful. However, the identification of chronic health problems related to As was unforeseen and has taken several years to become manifest.

The affected aquifers are generally shallow (less than 100–150 m deep), of Holocene age and comprise a mixed sequence of micaceous sands, silts and clays deposited by the Ganges, Hugli, Brahmaputra and Meghna river systems and their precursors. The sediments are derived from the upland Himalayan catchments and from basement complexes of the northern and western parts of West Bengal. In most affected areas, the sediment sequence is capped by a layer of clay or silt (of variable thickness) which effectively restricts entry of air to the aquifers. This, together with recent

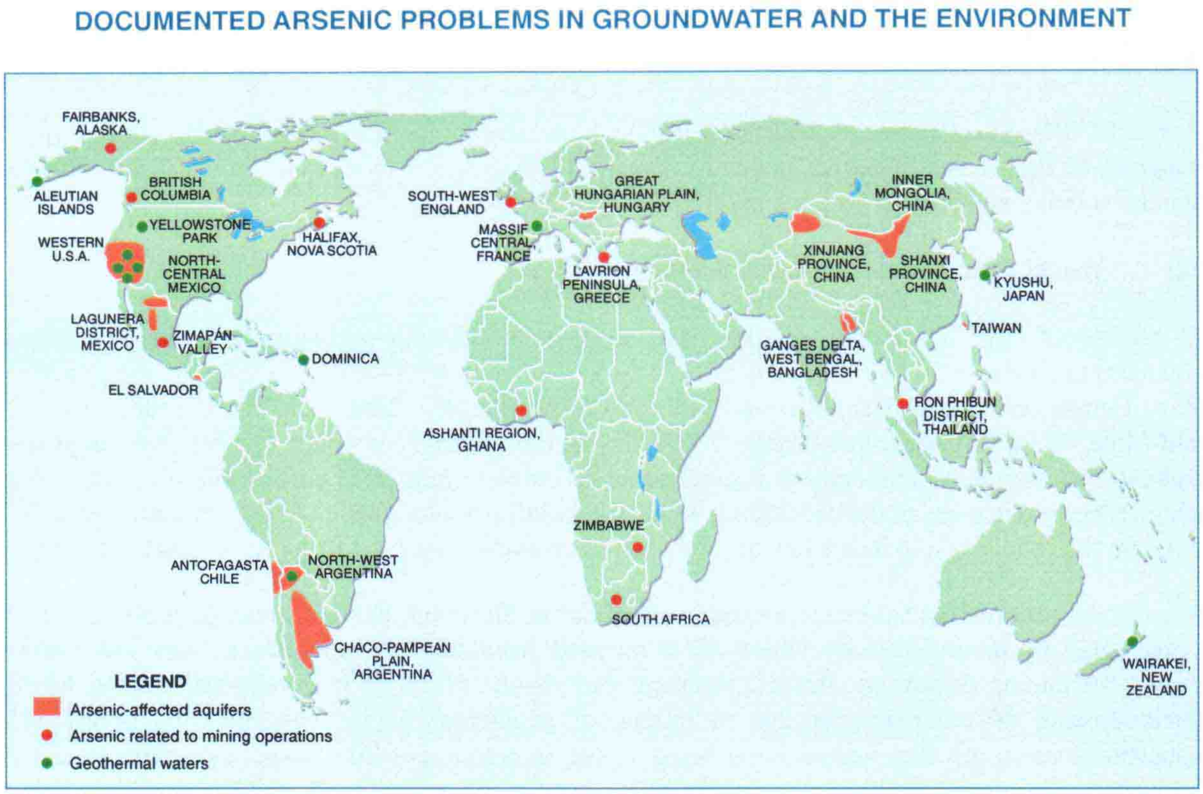
DOCUMENTED ARSENIC PROBLEMS IN GROUNDWATER AND THE ENVIRONMENT

Figure 2.1 **Distribution of documented world problems with As in groundwater in major aquifers as well as mining-related problems and geothermal sources**

solid organic matter deposited with the sediments, has resulted in development of highly reducing aquifer conditions which favour the mobilisation of As (largely as As(III), Section 2.4) by desorption of As species from iron-oxide surfaces and dissolution of iron oxides (BGS/MML, 1999). Deeper groundwaters from the sediment sequence (>100–150 m depth, probably of Pleistocene age) have generally low As concentrations ($<10\ \mu g\ l^{-1}$).

The characteristic chemical features of the high-arsenic groundwaters are high iron (> 0.2 mg l^{-1}), manganese (> 0.5 mg l^{-1}), bicarbonate (> 500 mg l^{-1}) and often phosphorus (> 0.5 mg l^{-1}) concentrations, and low chloride (< 60 mg l^{-1}), sulphate (< 1 mg l^{-1}), nitrate and fluoride (< 1 mg l^{-1}) concentrations, with pH values close to or greater than 7 (AIP Steering Committee, 1991; CGWB, 1999; BGS/MML, 1999).

Salinity increases further south in the near-coastal parts of the aquifers as a result of saline intrusion (Adyalkar et al., 1981; BGS/MML, 1999) and possibly also lack of flushing. In Bangladesh, the worst-affected areas are to the south and east of the capital, Dhaka, where in some villages, more than 90% of the wells have arsenic concentrations above $50\ \mu g\ l^{-1}$.

The groundwaters are predominantly reducing, as evidenced by the major-element chemistry. Some workers have found a positive correlation between arsenic and iron in localised studies (e.g. Nag et al., 1996), but this is not true of the Bengal Basin as a whole.

Arsenic speciation studies have revealed a large range in the relative proportions of dissolved arsenate and arsenite (e.g. Das et al., 1995; Acharyya, 1997; BGS/MML, 1999). The modal proportion of arsenite in Bangladesh groundwaters varies between <10–>90 %, but appears to be largely between 50–60% of the total (BGS/MML, 1999).

The regional distribution of the high-arsenic waters in West Bengal and Bangladesh is known to be extremely patchy (AIP Steering Committee, 1991; CSME, 1997; BGS/MML, 1999), presumably in part because of great variation in sedimentary characteristics and variations in abstraction depth. Estimates of the proportions of tubewells affected in West Bengal are not well-documented and difficult to assess. However, indications are that the degree of contamination is not as severe in West Bengal as in the worst-affected districts of Bangladesh (e.g. Dhar et al. 1997), where in some instances more than 90% of tubewells investigated exceed the Bangladesh and Indian drinking-water standard for arsenic (50 $\mu g\ l^{-1}$; BGS/MML, 1999). Certainly, the overall areal extent of contamination in West Bengal is less than in Bangladesh.

The arsenic-affected groundwaters in the Bengal Basin are associated with sediments having total arsenic concentrations in the range 2–20 mg kg^{-1}, ie. not exceptional by world averages. This is not surprising given the scale of the problem. These sediments are also derived from the drainage systems of three major rivers (Ganges, Brahmaputra and Meghna) which are themselves sourced from a wide area of the Himalaya. Therefore, while it could be argued that the source of much of the arsenic in the Bengal Basin sediments is derived from specific mineralised areas in the source region, these are likely to be so widespread as to be academic and of little practical relevance.

The distinction between As concentration ranges in the shallow and deep aquifers of the Bengal Basin is thought to be related to the history of aquifer flushing. Older, deeper sediments have had longer periods of groundwater movement, aided by greater hydraulic heads during the Pleistocene period when glacial sea levels were up to 120 m lower than today (e.g. Umitsu, 1993). Aquifer flushing is therefore likely to have been much more extensive than in the Holocene sediments deposited during the last 5,000–10,000 years.

Taiwan

The south-west coastal zone of Taiwan was perhaps the first area to be identified as a problem area for health effects arising from chronic arsenic exposure. Awareness of the problem began during the 1960s and health problems have been well-documented (e.g. Tseng et al., 1968; Chen et al., 1985). The region has been the focus of much epidemiological work over the last 30 years. Taiwan is the classic area for the identification of blackfoot disease but other peripheral vascular disorders as well as cardiovascular disease, neurological problems, diabetes and internal cancers have also been identified. A clear dose-response relationship has been found for many of the disorders, including blackfoot disease and bladder cancer (e.g. Chen et al., 1985).

Kuo (1968) observed As concentrations in groundwater samples from south-west Taiwan ranging between 10 $\mu g\ l^{-1}$ and 1800 $\mu g\ l^{-1}$ (mean 500 $\mu g\ l^{-1}$, n=126) and found that half the samples analysed had concentrations between 400 $\mu g\ l^{-1}$ and 700 $\mu g\ l^{-1}$. A large study carried out by the Taiwan Provincial Institute of Environmental Sanitation established that 119 townships in the affected area had As concentrations in groundwater of >50 $\mu g\ l^{-1}$ and 58 townships had >350 $\mu g\ l^{-1}$ (Lo et al., 1977). Chen et al. (1995) found As concentrations in the Pu-Tai endemic area in the range 437–897 $\mu g\ l^{-1}$ (mean 671 $\mu g\ l^{-1}$).

The high As concentrations are found in deep (100–280 m) artesian well waters abstracted from sediments which include deposits of black shale (Tseng et al., 1968). The groundwaters are therefore likely to be strongly reducing and hence analagous to groundwaters in the affected areas of Bangladesh and West Bengal. This is supported by the observation that the As is present largely as As(III) and the groundwaters commonly have high Fe and Mn concentrations and low Se concentrations (Chen et al., 1994; 1995). Some of the groundwaters appear to contain methane (Tseng et al., 1968) as well as humic substances. Groundwater from shallow wells in the area have low arsenic concentrations (Guo et al., 1994).

Table 2.1 Summary of documented cases of naturally-occurring As problems in world groundwaters (includes some mining cases)

Country/ Region	Area (km^2)	Population exposed*	Concentration ranges ($\mu g\ l^{-1}$)	Aquifer type	Groundwater conditions	Reference
Bangladesh	150,000	ca. $3x10^7$	<0.5 to 2500	Holocene alluvial/ deltaic sediments. Abundance of solid organic matter	Strongly reducing, neutral pH, high alkalinity, slow groundwater flow rates	BGS/MML (1999)
West Bengal	23,000	$6x10^6$	<10 to 3200	As Bangladesh	As Bangladesh	CGWB (1999); POA (1999)
China:						
Taiwan	4000	$?10^5$ (formerly)	10 to 1820	Sediments, including black shale	Strongly reducing, artesian conditions, some groundwaters contain humic acid	Kuo (1968), Tseng et al. (1968)
Inner Mongolia (Huhhot Basin (HB), Bayingao, Hexi, Ba Meng, Tumet Plain)	4300 (HB) ?30,000 total	? ca. 10^5 in HB	<1 to 2400	Holocene alluvial and lacustrine sediments	Strongly reducing conditions, neutral pH, high alkalinity. Deep groundwaters often artesian, some have high concentrations of humic acid	Luo et al. (1997), Ma et al. (1999), Zhai et al. (1998), Sun et al. (1999), Smedley et al. (2000)
Xinjiang (Tianshan Plain)	38,000	? (500 diagnosed)	40 to 750	Holocene alluvial plain	Reducing, deep wells (up to 660 m) are artesian	Wang and Huang (1994)
Shanxi				Alluvial plain	?Reducing	Sun et al. (1999)
Hungary (Danube Basin)	110,000	29,000	<2 to 150	Quaternary alluvial plain	Reducing groundwater, some high in humic acid	Varsányi et al. (1991)
Argentina (Chaco-Pampean Plain	10^6	$?5x10^6$	<1 to 11500 (up to 7800 in porewaters)	Holocene and earlier loess with rhyolitic volcanic ash	Oxidising, neutral to high pH, high alkalinity. Groundwaters often saline. As(V), accompanied by high B, V, Mo, U. Also high As concentrations in some river waters	Nicolli et al., 1989; Nicolli and Merino (1997), this study
Northern Chile (Antofagasta)	125,000		100 to 1000	?Quaternary volcanogenic sediment	Generally oxidising. Arid conditions, high salinity, high B. Also high-As river waters	Cáceres et al. (1992), Karcher et al. (1999)
South-west USA:		$3x10^5$ (tot)				
Basin & Range,	200,000		up to 1300	Alluvial basins, some	Oxidising, high pH. As (mainly As(V))	Robertson (1989)

Country/ Region	Area (km^2)	Population exposed*	Concentration ranges (µg l^{-1})	Aquifer type	Groundwater conditions	Reference
Arizona				evaporites	correlates positively with Mo, Se, V, F	
Tulare Basin, San Joaquin Valley, California	5000		<1 to 2600	Holocene and older basin-fill sediments	Internally-drained basin. Mixed redox conditions. Proportion of As(III) increases with well depth. High salinity in some shallow groundwaters. High Se, U, B, Mo	Fujii and Swain (1995)
Southern Carson Desert, Nevada	1300		up to 2600	Holocene mixed aeolian, alluvial, lacustrine sediments, some thin volcanic ash bands	Largely reducing, some high pH. Some with high salinity due to evaporation. Associated high U, P, Mn, DOC (Fe to a lesser extent)	Welch and Lico (1998)
Salton Sea Basin					Some saline groundwaters, with high U	Welch and Lico (1998)
Mexico (Lagunera)	32,000	4x10^5	8 to 620	Volcanic sediments	Oxidising, neutral to high pH, As mainly as As(V)	Del Razo et al. (1990)
Some problem areas related to mining activity and mineralised areas						
Thailand (Ron Phibun)	100	?15,000	1 to 5000	Dredged Quaternary alluvium (some problems in limestone), tailings	Oxidation of disseminated arsenopyrite due to former tin mining, subsequent groundwater rebound	Williams et al. (1996), Williams (1997)
Greece (Lavrion)				Mine tailings	Mining	
Fairbanks, Alaska, USA			up to 10,000	Schist, alluvium, mine tailings	Gold mining, arsenopyite, possibly scorodite	Wilson and Hawkins (1978); Welch et al. (1988)
Moira Lake, Ontario, Canada	100		50–3000	Mine tailings	Ore mining (gold, haematite, magnetite, lead, cobalt)	Azcue and Nriagu (1995)
Coeur d'Alene, Idaho, USA			up to 1400	Valley-fill deposits	River water and groundwater affected by lead-zinc-silver mining	Welch et al. (1988), Mok and Wai (1990)
Lake Oahe, South Dakota, USA			up to 2000	Lake sediments	As in sediment porewaters from gold mining in the Black Hills	Ficklin and Callender (1989)
Bowen Island, British Columbia	50		0.5–580	Sulphide mineral veins in volcanic country rocks	neutral to high-pH groundwaters (up to 8.9), As correlated with B, F	Boyle et al. (1998)

*Exposed refers to population drinking water with As >50 µg l^{-1} (drinking-water standard of most countries)

Northern China

Arsenic occurrence has been found at high concentrations (in excess of the Chinese national standard of 50 μg l^{-1}) in groundwaters from Inner Mongolia as well as Xinjiang and Shanxi Provinces (Figure 2.1; Wang, 1984; Wang and Huang, 1994; Niu et al., 1997). The first cases of As poisoning were recognised in Xinjiang Province in the early 1980s. Wang (1984) found As concentrations in groundwaters from the province at up to 1200 μg l^{-1}. Wang and Huang (1994) reported As concentrations of between 40 μg l^{-1} and 750 μg l^{-1} in deep artesian groundwater from the Dzungaria Basin on the north side of the Tianshan Mountains (from Aibi Lake in the west to Mamas River in the east, a stretch of ca. 250 km). Arsenic concentrations in artesian groundwater from deep boreholes (up to 660 m) were found to increase with depth. Shallow (non-artesian) groundwaters had observed As concentrations between <10 μg l^{-1} and 68 μg l^{-1}. The concentration of As in the saline Aibi Lake was reported as 175 μg l^{-1}, while local rivers had concentrations between 10 μg l^{-1} and 30 μg l^{-1}. Artesian groundwater has been used for drinking in the region since the 1960s and chronic health problems have been identified as a result (Wang and Huang, 1994).

In Inner Mongolia, concentrations of As in excess of the Chinese national standard have been identified in groundwaters from aquifers in the Huhhot Basin, Ba Meng Region, and Tumet Plain (e.g. Luo et al., 1997; Ma et al., 1999). These areas include the cities of Boutou and Togto. In the Huhhot Basin, the problem is found in groundwaters from Holocene alluvial and lacustrine aquifers under highly reducing conditions and is worst in the lowest-lying parts of the basin (Smedley et al., 2000). Concentrations up to 1500 μg l^{-1} have been found in the groundwaters, with a significant proportion of the As being present as As(III). Shallow groundwaters in the region are commonly saline as a result of evaporative concentration and many have high fluoride concentrations, although these do not generally correlate with high As concentrations. In the affected region, As-related disease has been identified by Luo et al. (1997). Recognised health effects include lung, skin and bladder cancer as well as prevalent keratosis and skin-pigmentation problems.

Hungary

Concentrations of As above 50 μg l^{-1} have been identified in groundwaters from alluvial sediments associated with the River Danube in the southern part of the Great Hungarian Plain (Figure 2.1). Concentrations of up to 150 μg l^{-1} (average 32 μg l^{-1}, 85 samples) have been found by Varsányi et al. (1991). The plain, some 110,000 km^2 in area, consists of a thick sequence of subsiding Quaternary sediments. Groundwaters vary from Ca-Mg-HCO_3-type in the recharge areas of the basin margins to Na-HCO_3-type in the low-lying discharge regions. Groundwaters in deep parts of the basin (80–560 m depth) with high As concentrations are reducing with elevated concentrations of Fe and NH_4 and many have reported high concentrations of humic acid (up to 20 mg l^{-1}; Varsányi et al., 1991). The groundwaters have highest As concentrations in the lowest parts of the basin, where the sediment is fine-grained.

Mexico

Parts of northern Mexico have significant problems with arsenic in groundwater. The best-documented is the Lagunera Region of north central Mexico where significant chronic health problems have been reported. The region is arid and groundwater is an important resource for potable supply. Groundwaters from the region are predominantly oxidising with neutral to high pH. Del Razo et al. (1990) quoted pH values for groundwaters in the range 6.3 to 8.9. They found As concentrations in the range 8 μg l^{-1} to 624 μg l^{-1} (average 100 μg l^{-1}, n=128), with half the samples having concentrations greater than 50 μg l^{-1}. They also noted that most (>90%) of the groundwater samples investigated had As present predominantly as As(V). Del Razo et al. (1994) determined the average concentration of As in drinking water from Santa Ana town in the region as 404 μg l^{-1}. The estimated population exposed to As in drinking water with >50 μg l^{-1} is around 400,000 in Lagunera Region (Del Razo et al., 1990).

Groundwaters from the region also have high concentrations of fluoride (up to 3.7 mg l^{-1}; Cebrián et al., 1994).

High As concentrations have also been identified in groundwaters from the state of Sonora in north-west Mexico. Wyatt et al. (1998) found concentrations in the range 2–305 µg l^{-1} (76 samples) with highest concentrations in groundwaters from the towns of Hermosillo, Etchojoa, Magdalena and Caborca. The As concentrations were also positively correlated with fluoride. Highest observed F concentration in the area was 7.4 mg l^{-1}.

South-western USA

Much research has been carried out on As in groundwater in the USA, particularly in view of the planned reduction in the US-EPA drinking-water limit and public concerns over the possible long-term health effects. Occurrences in groundwater are therefore noted to be widespread, although exceedances are often reported relative to lower guideline values than reported in other affected countries. Welch et al. (1999) noted elevated concentrations in groundwaters from parts of Maine, Michigan, Minnesota, South Dakota, Oklahoma and Wisconsin. Of 17,000 water analyses, they found that around 40% exceeded 1 µg l^{-1} (percentage above 50 µg l^{-1} unknown). The As is thought to derive from various sources, including natural dissolution/desorption reactions, geothermal water and mining activity. To date, no studies in the USA have found a clear relationship between As in drinking water and development of specific health effects.

The main areas where naturally-high concentrations of As occur in groundwater in the USA are in the south-western states (e.g. Nevada, California, Arizona, Utah). These areas include some localised mining- and geothermal-related As occurrences, but many of the affected groundwaters are from alluvial basins which occur under a range of redox conditions.

In Nevada, at least 1000 private wells are thought to contain As concentrations in excess of 50 µg l^{-1} (Fontaine, 1994). Many of the high concentrations are found in groundwaters from the Carson Desert. The city of Fallon (population 6000) is served by a groundwater supply with an As concentration of 100 µg l^{-1} which for many years has been supplied without treatment. Welch and Lico (1998) reported high As concentrations (often exceeding 100 µg l^{-1}, but with extremes up 2600 µg l^{-1}) in shallow groundwaters from the southern Carson Desert. These are apparently largely present under reducing conditions, having low dissolved-oxygen concentrations and high concentrations of dissolved organic C, Mn and Fe. The groundwaters also have associated high pH (>8) and high concentrations of P (locally >4 mg l^{-1}) and U (>100 µg l^{-1}; Welch and Lico, 1998). The high As and U concentrations were thought to be due to evaporative concentration of groundwater, together with the influence of redox and desorption processes involving metal oxides.

In groundwaters from the Tulare Basin of the San Joaquin Valley, California, a large range of As concentrations from <1 µg l^{-1} to 2600 µg l^{-1} have been found (Fujii and Swain, 1995). Redox conditions in the aquifers appear to be highly variable and elevated As concentrations are found in both reducing and oxidising conditions. The proportion of As present as As(III) apparently increases in different wells with increasing depth. The groundwaters from the Basin are often strongly affected by evaporative concentration with resulting high TDS values. Many also have high concentrations of Se (up to 1000 µg l^{-1}), U (up to 5400 µg l^{-1}), B (up to 73,000 µg l^{-1}) and Mo (up to 15,000 µg l^{-1}; Fujii and Swain, 1995).

Robertson (1989) also noted the occurrence of high As concentrations in groundwaters under oxidising conditions in alluvial aquifers in the Basin & Range Province in Arizona. Arsenic in the groundwater is present predominantly as As(V) and was observed to correlate well with Mo, Se, V, F and pH. Of the 467 samples analysed, 7% had As concentrations greater than 50 µg l^{-1}. Arsenic concentrations in the sediments were reported as 2–88 mg kg^{-1}. Oxidising conditions were found to persist in the aquifers down to significant depths (600 m) despite significant groundwater age (up to 10,000 years old). The elevated As (and other oxyanion) concentrations are a feature of the closed basins of the province.

Argentina

Large parts of the Chaco-Pampean Plain of central Argentina are known to have groundwaters with high concentrations of As. Nicolli et al. (1989) found that 84% of samples investigated in Córdoba Province north of La Pampa had concentrations greater than 50 $\mu g\ l^{-1}$. Nicolli and Merino (2000) found that 89% of groundwater samples investigated from the Carcarañá River Basin (Córdoba and Santa Fe Provinces) exceeded 50 $\mu g\ l^{-1}$ (most concentrations falling in the range 50–250 $\mu g\ l^{-1}$). In these areas, the aquifer conditions are similar to those of La Pampa. The sediments comprise Quaternary loess deposits with sporadic occurrences of acidic volcanic ash. Groundwaters are neutral to slightly alkaline (pH up to 8.3) and many are saline with high alkalinity and associated high concentrations of F, V, U, Mo and Se (Nicolli et al., 1989; Nicolli and Merino, 2000). River waters in the region have also been found to have high As and V concentrations (Lerda and Prosperi, 1996). Arsenic concentrations in loess sediments investigated from Córdoba Province range between 5.5–17 mg kg^{-1} (Nicolli et al., 1989).

High concentrations of As have also been identified in groundwaters from north-west Argentina. The area around the Andean village of San Antonio de los Cobres (altitude 3800 m) in Salta Province has groundwaters used for potable supply with As concentrations in the range 200–500 $\mu g\ l^{-1}$. The cause is uncertain but sulphide minerals are known to be present in the volcanic bedrocks and thermal springs have been found in the area with reported As concentrations up to 10 mg l^{-1} (Vahter et al., 1995). Thermal springs discharge to surface waters and hence As concentrations in these are also high in the area: the concentration in river water from San Antonio de los Cobres has been measured at 800 $\mu g\ l^{-1}$ (Vahter et al., 1995).

Chile

Health problems related to As in drinking water were first recognised in northern Chile in 1962. Typical symptoms included skin-pigmentation changes, keratosis, squamous-cell carcinoma (skin cancer), cardiovascular problems and respiratory disease (Zaldivar, 1974). More recently, As ingestion has been linked to lung and bladder cancer. Smith et al. (1998) estimated that around 7% of all deaths occurring in Antofagasta between 1989 and 1993 were due to past exposure to As in drinking water. Since exposure was chiefly in the period 1955–1970, this pointed to a long latency period of cancer mortality (Smith et al., 1998). Other reported symptoms include impaired resistance to viral infection and lip herpes (Karcher et al., 1999).

High As concentrations have been recorded in surface waters and groundwaters from Administrative Region II (incorporating the cities of Antofagasta, Calama and Tocopilla) of northern Chile (Cáceres et al., 1992). The region is arid (Atacama Desert) and water resources are limited. High As concentrations are accompanied by high salinity (due to evaporation) and high B concentrations. Arsenic values below 100 $\mu g\ l^{-1}$ in surface waters and groundwaters are apparently quite rare, and concentrations up to 21,000 $\mu g\ l^{-1}$ have been found. Karcher et al. (1999) quoted ranges of 100 $\mu g\ l^{-1}$ to 1000 $\mu g\ l^{-1}$ in raw waters (average 440 $\mu g\ l^{-1}$). The As is present in waters mostly as arsenate (Thornton and Farago, 1997 and references cited therein). The aquifers are composed of volcanogenic sediments. In Antofagasta, concentrations of As in the sediments are ca. 3.2 mg kg^{-1} (Cáceres et al., 1992). Additional As exposure from smelting of copper ore has also been noted in northern Chile (Cáceres et al., 1992).

Arsenic treatment plants were installed in the towns of Antofagasta and Calama in 1969 to mitigate the problems. Today, the urban populations of the major towns are supplied with treated water from the Rivers Toconce and Loa (Karcher et al., 1999) which is transported from the foot of the Andes mountains to the treatment works. However, rural communities still largely rely on untreated water supplies which contain As.

2.3.2 *Geothermal sources*

Arsenic associated with geothermal waters has been reported in several areas, including hot springs from parts of the USA, Japan, New Zealand, France and Dominica (e.g. Welch et al., 1988; Criaud and Fouillac, 1989). As noted above, parts of Salta Province of north-west Argentina also have thermal springs with high As concentrations.

In the USA, occurrences of As linked to geothermal sources have been summarised by Welch et al. (1988). Reported occurrences include Honey Lake Basin, California (As up to 2600 µg l^{-1}), Coso Hot Springs, California (up to 7500 µg l^{-1}), Imperial Valley, California (up to 15000 µg l^{-1}), Long Valley, California (up to 2500 µg l^{-1}) and Steamboat Springs, Nevada (up to 2700 µg l^{-1}). Geothermal waters in Yellowstone National Park also contain As and have given rise to elevated concentrations (up to 370 µg l^{-1}) in waters of the Madison and Missouri Rivers (Nimick et al., 1998). Geothermal inputs from Long Valley, California are believed to be responsible for elevated concentrations (20 µg l^{-1}) of As in the Los Angeles Aqueduct which provides the water supply for the city of Los Angeles (Wilkie and Hering, 1998).

Welch et al. (1988) noted a general relationship between As and salinity in geothermal waters from the USA. Despite a lack of good positive correlation between As and Cl, geothermal waters with As greater than ca. 1000 µg l^{-1} generally had Cl concentrations of 800 mg l^{-1} or more. Wilkie and Hering (1998) noted the high alkalinity and pH values (average pH 8.3) as well as high Cl and B concentrations of geothermal waters in Long Valley.

Geothermal waters from Kyushu, Japan have been found with As concentrations in the range 500–4600 µg l^{-1}. The waters are typically of Na-Cl type and the As is present almost entirely as As(III) (Yokoyama et al., 1993).

Elevated As concentrations have been documented in waters from the geothermal areas of New Zealand. Robinson et al. (1995) found As in groundwater from the Wairakei geothermal field at a concentration of 3800 µg l^{-1} and found river and lake waters receiving inputs of geothermal water from the Wairakei, Broadlands, Orakei Korako and Atiamuri geothermal fields to have concentrations up to 121 µg l^{-1}, although concentrations diminished significantly downstream away from the geothermal input areas.

2.3.3 *Arsenic problems in mining and mineralised areas*

Thailand

In terms of documented health problems, probably the worst case of As poisoning related to mining activity is that of Ron Phibun District in Nakhon Si Thammarat Province of southern Thailand. Health problems were first recognised in the area in 1987. Around 1000 people have been diagnosed with As-related skin disorders, particularly in and close to Ron Phibun town (Williams, 1997). The affected area lies within the South-East Asian Tin Belt. Arsenic concentrations have been found at up to 5000 µg l^{-1} in shallow groundwaters from Quaternary alluvial sediment that has been extensively dredged during ore extraction. Deeper groundwaters from older limestone aquifers have been found to be less contaminated (Williams et al., 1996) although a few high As concentrations occur, presumably also as a result of contamination from the mine workings. The mobilisation of As is taken to be caused by oxidation of arsenopyrite, exacerbated by the former tin-mining activities and subsequent mobilisation in groundwater during post-mining groundwater rebound (Williams, 1997).

Ghana

Several workers have reported the effects of mining activity on the environment in Ghana. Ghana is an important gold-mining country and mining has taken place since the late 19th century. Today, Ghana produces about one third of the world's gold. The most important mining area is the Ashanti Region of central Ghana. The gold is associated with sulphide mineralisation, particularly arsenopyrite. Arsenic mobilises in the local environment as a result of arsenopyrite oxidation, induced (or exacerbated) by the mining activity. Around the town of Obuasi, high As concentrations have been noted in soils close to the mines and treatment works (Amasa, 1975; Bowell, 1992; 1993). Some high concentrations have also been reported in river waters close to the mining activity (Smedley et al., 1996a).

Despite the presence of high As concentrations in the contaminated soils and in bedrocks close to the mines, Smedley et al. (1996a) found that many of the groundwaters of the Obuasi area had low As concentrations, with a median concentration in tubewell waters of just 2 $\mu g\ l^{-1}$. Some elevated concentrations were observed (up to 64 $\mu g\ l^{-1}$) but these were not generally in the vicinity of the mines or related directly to mining activity. Rather, the higher concentrations were found to be present in relatively reducing groundwaters (Eh of 220–250 mV). Oxidising groundwaters, especially from shallow hand-dug wells, had low As concentrations. This was taken to be due to retardation of As by sorption onto ferric hydroxides under the ambient low pH condition of the groundwaters (median pH 5.4 in dug wells; 5.8 in tubewells; Smedley et al., 1996a; b).

United States

Arsenic contamination from mining activities has been identified in numerous areas of the USA, many of which have been summarised by Welch et al. (1988). Groundwater from some areas has been reported to have very high As concentrations locally (up to 48000 $\mu g\ l^{-1}$). Well-documented cases of As contamination include the Fairbanks gold-mining district of Alaska (Wilson and Hawkins, 1978; Welch et al., 1988), the Coeur d'Alene lead-zinc-silver mining area of Idaho, (Mok and Wai, 1990), Leviathan Mine, California (Welch et al., 1988), Kelly Creek Valley, Nevada (Grimes et al., 1995) and Lake Oahe in South Dakota (Ficklin and Callender, 1989).

Other areas

Many other areas have been reported with elevated concentrations of As in soils, sediments and waters as a result of mining activity. Documented cases include the Lavrion region of Greece, associated with lead- and silver-mining activity (Komnitsas et al., 1995), the Zimapán Valley of Mexico, parts of south-west England (Thornton and Farago, 1997), South Africa and Zimbabwe. Although severe contamination of the environment has often been documented in these areas, the impact on groundwaters used for potable supply is usually minor.

Arsenic problems have also been recognised in mineralised areas where sulphide minerals undergo natural oxidation. Boyle et al. (1998) found As concentrations of 0.5–580 $\mu g\ l^{-1}$ in groundwaters close to sulphide mineral veins in volcanic rocks from Bowen Island, British Columbia.

2.4 Arsenic associations in minerals

Arsenic occurs as a major constituent in more than 200 minerals, including elemental arsenic, arsenides, sulphides, oxides, arsenates and arsenites. Most are ore minerals and their alteration products. The greatest concentrations of these minerals therefore occur in mineralised areas associated with basement rocks and active volcanic areas. In these, As is commonly found in close association with the transition metals as well as Cd, Pb, Ag, Au, Sb, P, W and Mo. The most abundant and widespread As ore mineral is arsenopyrite, FeAsS. Arsenopyrite, together with the other dominant As-sulphide minerals realgar and orpiment, are only formed under high-temperature conditions in the earth's crust.

Table 2.2 **Arsenic concentrations in the major rock-forming minerals**

Mineral	As concentration range (mg kg^{-1})	References
Sulphide minerals:		
Pyrite	100–10000	Baur and Onishi (1969);
Pyrite (gold ores)	300–54000	Arehart et al. (1993)
Pyrrhotite	5–100	Boyle and Jonasson (1973);
Marcasite	20–600	Dudas (1984)
Galena	5–10000	
Sphalerite	5–17000	
Chalcopyrite	10–5000	
Oxide minerals:		
Haematite	up to 160	
Fe oxide (undifferentiated)	up to 2000	
Fe(III) oxyhydroxide	up to 76000	Pichler et al. (1999)
Magnetite	2.7–41	
Ilmenite	<1	
Silicate minerals:		
Quartz	0.4–1.3	
Feldspar	<0.1–2.1	
Biotite	1.4	
Amphibole	1.1–2.3	
Olivine	0.08–0.17	
Pyroxene	0.05–0.8	
Carbonates minerals:		
Calcite	1–8	
Dolomite	<3	
Siderite	<3	
Sulphate minerals:		
Gypsum/anhydrite	<1–6	
Barite	<1–12	
Jarosite	34–1000	
Other minerals:		
Apatite	<1–1000	
Halite	<3	
Fluorite	<2	

Arsenic is also often present in varying concentrations in other common rock-forming minerals. As the chemistry of arsenic follows closely that of sulphur, the greatest concentrations of the element tend to occur in sulphide minerals, of which pyrite is the most abundant. Concentrations in pyrite, chalcopyrite and galena can be very variable, even within a given grain, but in some cases reach up to several weight percent (Table 2.2). Arsenic is present in the crystal structure of many sulphide minerals as a substitute for sulphur.

Besides being an important component of ore bodies, pyrite is also formed in low-temperature sedimentary environments under reducing conditions (authigenic pyrite). Authigenic pyrite plays a very important role in present-day geochemical cycles. It is present in the sediments of many rivers, lakes and the oceans as well as of many aquifers.

High As concentrations are also found in many oxide minerals and hydrous metal oxides, either as part of the mineral structure or as adsorbed species. Concentrations in Fe oxides can also reach weight percent values (Table 2.2), particularly where they form as the oxidation products of primary iron sulphide minerals which have an abundant supply of As. Sorption of arsenate to hydrous iron oxides is particularly strong, even at very low As concentrations (Goldberg, 1986; Manning and Goldberg, 1996). Sorption to hydrous Al and Mn oxides may also be important if these oxides are present in quantity (e.g. Peterson and Carpenter, 1986; Manning and Goldberg, 1996). Arsenic may also be sorbed to the edges of clays and on the surface of calcite. These sorption reactions are responsible for the relatively low (and non-toxic) concentrations of As found in most natural waters.

Arsenic concentrations in phosphate minerals are variable but can also reach high values, for example up to 1000 mg kg^{-1} in apatite. However, phosphate minerals are much less abundant than oxide minerals and so make a correspondingly small contribution to the arsenic load of most sediments.

Arsenic can also substitute for Si^{4+}, Al^{3+}, Fe^{3+} and Ti^{4+} in many mineral structures and is therefore present in many other rock-forming minerals, albeit at much lower concentrations. Most common silicate minerals contain around 1 mg kg^{-1} or less. Carbonate minerals usually contain less than 10 mg kg^{-1} (Table 2.2).

2.5 Hydrogeochemistry of arsenic

Arsenic is perhaps unique among the heavy metalloids in its capacity to mobilise at the pHs of natural groundwaters and over a wide range of redox conditions. Arsenic can occur in the environment in several oxidation states (-3 to +5) but in natural waters is mostly found as an oxyanion, in trivalent (arsenite) or pentavalent (arsenate) form. Most other toxic trace metals occur in solution as cations (e.g. Pb^{2+}, Cu^{2+}, Ni^{2+}, Cd^{2+}, Co^{2+}, Zn^{2+}) and hence solubilise preferentially at low pH. Selenium is mobile as an oxyanion under oxidised conditions, but may be reduced to the metal under reducing conditions. Chromium can also be mobilised as a stable oxyanion under oxidising conditions, but forms a cation species (Cr^{3+}) in reducing environments and hence behaves like other trace cations (ie. is relatively immobile at the neutral to high pHs of natural groundwaters). These factors, together with the high toxicity of As, render the element one of the most serious problems for potable groundwater quality.

Equilibrium speciation of As has been described in detail by Brookins (1988) and Cullen and Reimer (1989). In oxidising environments, arsenate is the dominant form. Under acidic conditions (pH less than about 6.9), $H_2AsO_4^-$ is preferentially stabilised, whilst at higher pH, $HAsO_4^{2-}$ will be more stable (H_3AsO_4 and AsO_4^{3-} may be present in extremely acidic and alkaline conditions respectively). Under reducing conditions at pH less than about 9.2, the arsenite species $H_3AsO_3^0$ should predominate (Brookins, 1988). However, under reducing conditions in the presence of sulphur, As concentrations may be limited by the low solubility of As sulphide minerals, such as realgar and orpiment.

The rate of oxidation of As(III) is known to be relatively slow. The rate may be enhanced significantly in the presence of manganese oxide (Mn(IV)O_2). Driehaus et al. (1995) noted from experiments that oxidation of As(III) to As(V) in the presence of manganese oxide was highly effective and followed a second-order rate law, possibly catalysed by bacteria. Wilkie and Hering (1998) also noted rapid oxidation of As(III) in streamwaters with inputs of As from geothermal sources in the USA and concluded that the rapid oxidation was bacterially mediated.

Most of the As in natural waters is present in inorganic form (e.g. Cebrián et al., 1994). Organic arsenicals are known to be stabilised by methylation reactions involving bacteria and algae (Mok and Wai, 1994): monomethylarsonic acid (MMAA) and dimethylarsinic acid (DMAA) have for example been observed, albeit in small quantities, in some river waters and porewaters by biotransformation of inorganic As compounds (e.g. Faust et al., 1987). Demethylation reactions are also known to occur in water. However, it is generally accepted that the dominant forms, particularly in groundwater, are the inorganic species.

As noted above, mobility of As in water is limited principally by adsorption onto iron oxides and hydroxides, as well as oxides of aluminium and manganese (e.g. Bowell, 1994; Mok and Wai, 1994; Driehaus et al., 1995). Iron oxides in particular have long been recognised as effective adsorption minerals and indeed, precipitation of these (for example, by coagulation of ferric chloride) is used as an effective water-treatment technology for removal of As from water (e.g. Wilkie and Hering, 1996).

As the pH_{PZC} of hydrous ferric oxides (Hfo) is generally high (pH 8.0 for ferrihydrite, Kinniburgh et al., 1976), its surfaces have a net positive surface charge in the pH range of most natural waters. Hence anions and oxyanions including As species have a strong surface attraction and are potentially readily adsorbed. Arsenic is also bound significantly to Hfo by specific adsorption. Dzombak and Morel (1990) summarised the limited amount of available experimental data for sorption of As (and other oxyanions) onto Hfo. For As, they demonstrated the importance of both speciation and pH on sorption capacity. They showed that arsenate has a greater tendency to sorb onto Hfo than arsenite, although arsenate sorption capacity diminishes at high pH (ie. alkaline). Arsenite sorption appears to be most effective at near-neutral pH (Dzombak and Morel, 1990). pH-dependent anion trends similar to those for arsenate are observed for vanadate (VO_4) molybdate (MoO_4), selenate (SeO_4), sulphate (SO_4), chromate (CrO_4) and to a lesser extent, borate (H_3BO_3) (Dzombak and Morel, 1990; Manning and Goldberg, 1996).

The sorption capacity is greater for the poorly ordered amorphous iron oxides than for more structured forms (goethite, haematite) due to their larger surface area and hence increased availability of binding sites (Dzombak and Morel, 1990).

Presence of dissolved phosphate has been shown to compete with As, particularly arsenate, for binding sites on Hfo and other Fe oxides. Hence As sorption is likely to be reduced in the presence of high concentrations of dissolved phosphate (e.g. Livesey and Huang, 1981; Manning and Goldberg, 1996).

Arsenic sorption onto Mn oxides might be expected to be less pronounced than onto iron oxides because the pH_{pzc} for Mn oxide is generally more acidic, although variable at around 2–7 (Kinniburgh and Jackson, 1981; Stumm and Morgan, 1981). With a lower pH_{pzc}, the surface charge of the Mn oxide will be negative and oxyanions such as arsenite and arsenate should not have such a strong electrostatic attraction. However, it has been suggested that specific adsorption of cations (e.g. Ca, Mg, Mn, Sr, Ba, Ni) on Mn oxide surfaces can increase the pH_{pzc} and hence enhance the capacity for sorption of anionic species including As (e.g. Stumm and Morgan, 1981). Takamatsu et al. (1985) explained the effect as exchange of divalent cations for H^+ ions on Mn-oxide surfaces, leading to generation of positive surface charge and attraction of the As oxyanion species. Peterson and Carpenter (1986) found a strong association between As and Mn (as well as Fe) concentrations in surficial marine sediments and suggested that As mobilisation was controlled principally by sorption reactions on Mn- and Fe-oxide phases. Azcue and Nriagu (1995) also found strong associations between As, Fe and Mn in mining-contaminated lake porewaters and suggested that the As was derived from both Fe and Mn oxide sorption sites.

Given the available information for controls on As speciation and mobility, it is apparent that As can be mobilised in solution over a range of groundwater redox conditions in either the oxidised (arsenate) or reduced (arsenite) form. Reducing conditions favour stabilisation of most of the As present as arsenite which binds less effectively to Fe, Al and Mn oxides. Under such conditions, Fe and Mn oxides may also themselves be dissolved, leading to additional As release into solution (Peterson and Carpenter, 1986). Presence of high concentrations (1 mg l^{-1} or more) of dissolved phosphorus may further enhance As release from iron oxides due to competition between phosphate and arsenate ions. Under oxidising conditions, As is potentially mobile in groundwaters as arsenate under conditions of high pH.

3. LA PAMPA - REGIONAL SETTING

3.1 Background

The Province of La Pampa is situated in central Argentina, in the 'Pampa Hundida' (Lowland Pampas). The capital, Santa Rosa, is situated in the north-eastern part of the Province and has a population of around 80,000 people. The region forms part of the vast Chaco-Pampean Plain extending throughout a large part of Argentina from the Paraguay border in the north to the Patagonian Mountains in the south to the east of the Andean Cordillera. The study area lies in northern La Pampa, incorporating the Departments of Rancul, Réalico, Trenel, Conhelo and Maraco, an area of around 110 km x 70 km, in which the largest town is Eduardo Castex, some 80 km north of Santa Rosa (Figure 3.1).

The region is predominantly rural with a low population density. The density is lowest in the west: Rancul Department has a population of around 0–2 per km^2, whilst the other Departments have population densities of 2.1–7 per km^2. The population substantially consists of immigrants from Italy and other parts of Europe and their descendants. In 1980, almost 50% of inhabitants aged 65 or more were foreign-born.

La Pampa experiences a semi-arid temperate climate. Annual rainfall is around 650 mm in Eduardo Castex but increases towards the north and north-east (range 500–700 mm; Michelena and Irurtia, 1995). There is a distinct dry season in the winter (May–September). Average temperatures range between 10ºC in winter (July) and 24ºC in summer (January). Average annual temperature for Santa Rosa is 15.5ºC.

Elevation of the study area ranges between 300 m in the west to around 150 m in the east, although numerous small-scale topographic variations exist. Terrain is typically undulating (Plate 3.2) with some sand dunes in the west but comprises a largely flat plain further east. There is little permanent surface drainage but localised small-scale depressions in the eastern plain fill with water during the wet season (October–April) and evaporate during the dry season (May–September), forming encrustations of salts, including calcium carbonate.

The economy of La Pampa is dominated by agriculture which consists mainly of cattle ranching and grain cultivation. The plains are highly fertile although the arid climate restricts arable cropping. Crop production is most common in the east and cattle rearing in the west. The main crops produced are wheat, sorghum, corn, rye, millet and alfalfa (Michelena and Irurtia, 1995). Natural vegetation consists

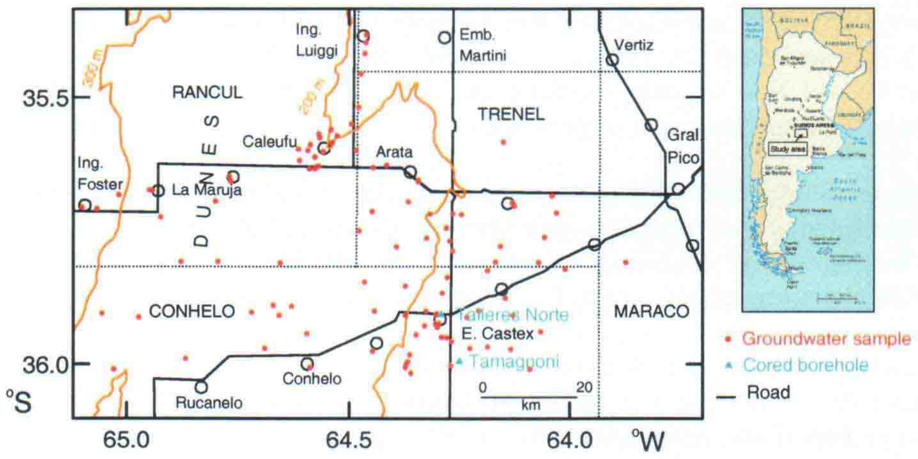

Figure 3.1 Sketch map of the study area of northern La Pampa

of Pampean steppe in the eastern area and caldén forest in the western upland area.

Soils in the region have largely evolved from aeolian sediments and have good permeability, low porosity and deep profiles. They are generally organic-poor. Soil degradation from wind erosion has been significant, particularly in cultivated areas (Michelena and Irurtia, 1995).

3.2 Water-related Argentine health problems

Various studies of the Chaco-Pampean Plain have reported health problems that are considered to be related to high As concentrations in drinking water. The problems are worst in the Provinces of Córdoba, Santiago del Estero, Chaco, La Pampa, Santa Fe and Buenos Aires. As early as 1917, reports were made of skin disorders in populations from Córdoba. The health problems were labelled as 'Bell Ville' disease after the town where the prevalence was particularly high (Circulo Médico del Rosario, 1917). Keratosis, skin-pigmentation disorders and skin cancer were reported from Córdoba Province by Argüello et al. (1938). Biagini et al. (1978) also noted the occurrence of these disorders as well as lung cancer, mainly from cases in Córdoba and Santiago del Estero Provinces. Of 276 patients examined, 15 presented with lung cancer (Biagini et al., 1978). The health problems are regionally known as 'HACRE' (Hidro Arsenicismo Crónico Regional Endémico).

Besuschio et al. (1980) described the increased incidence of several types of neoplasms, particularly of the skin, bladder and digestive tract from medical records of hospital patients in central Argentina, including La Pampa. The As concentration of the drinking water was reported as within the range 100–1200 $\mu g\,l^{-1}$. Besuschio et al. (1980) found that the most common type of cancer recorded was skin cancer (16.4% for all primary skin carcinomas, excluding melanoma). The most common occurrence was of squamous-cell carcinoma and this was found to be slightly more prevalent in covered areas of the skin (6.3%) compared to exposed areas (5.1%). Such features have been recorded in As-endemic cases elsewhere (e.g. Taiwan).

Hopenhayn-Rich et al. (1996) reported an increased incidence of bladder cancer among populations in Córdoba Province drinking water with high As concentrations. They reported standardised mortality ratios for bladder cancer in the same range as values given by other workers for populations in Taiwan. Given the relatively high intake of meat protein (Argentina having one of the highest per capita rates of beef consumption in the world), they suggested that this discounted poor nutritional status as a critical factor in development of carcinogenic effects. They also discounted genetic factors given the widely differing ethnic backgrounds of populations in Argentina and Taiwan (Hopenhayn-Rich et al., 1996).

Vahter et al. (1995) investigated the health of Andean women (age 19–47) from villages around San Antonio de los Cobres drinking water with up to 200 $\mu g\,l^{-1}$ As. They found a significant correlation between As concentrations in the water supply and As concentrations in urine (ca. 2% as MMA, 60–75% as DMA and 25–40% as inorganic As). They estimated that average daily intake of As from water and food sources was ca. 270–370 μg per day. Clinical signs of As poisoning (keratosis, pigmentation changes, skin cancer) were sought but no evidence was found. However, Dulout et al. (1996) found evidence of chromosomal abnormalities in the As-exposed populations of the region.

Over large parts of the Chaco-Pampean Plain, high F concentrations in the drinking water have given rise to the development of prominent dental fluorosis. No data are available for the occurrence of skeletal fluorosis.

Plate 3.1 Wind-blown silts and fine sands in northern La Pampa

Plate 3.2 Typical scenery with grassland on undulating hills in the western part of the La Pampa study area

4. REGIONAL GEOLOGY AND HYDROGEOLOGY

4.1 Geological setting

The central plains of Argentina occupy a major geosyncline that flanks the western side of the Brazilian Shield and dates from the Mesozoic. Sediments of the geosyncline comprise marine and continental deposits accumulated from Mesozoic to Lower Tertiary times and include many intercalations of lava and ash resulting from periods of volcanic activity. Between the Upper Palaeozoic and Miocene periods, parts of this area emerged above sea level and as a result, internal basins were formed where a variety of continental sediments were deposited. During the Upper Miocene, central and western parts of Argentina became a single vast plain (United Nations, 1976).

Epeirogenic movements associated with the formation of the Andean Cordillera during the Miocene resulted in marine transgression in the eastern, central and southern regions of Argentina and accumulation of a thick sequence of Upper Tertiary and Quaternary deposits. In the western Andean edges and central areas, the movements generated important faults, mostly oriented north-south which created block structures (central areas, Sierras Pampeanas) and numerous fold and fault structures (United Nations, 1976).

4.2 Argentine (Pampean) loess

The Argentine Pampas consists of a vast flat plain resulting from the accumulation of a blanketing sequence of aeolian (loess) deposits which in places reach several hundred metres in thickness. The plains stretch from the Andes in the west to the coast and from the Patagonian Mountains in the south, to the Gran Chaco in the north, covering an area of approximately 1.2 x 10^6 km^2. The deposits are mainly of Quaternary age.

Loess is defined as a terrestrial clastic sediment, composed predominantly of silt-size particles and formed essentially by the accumulation of wind-blown dust. There are three fundamental requirements for its formation: (i) a sustained source of dust, (ii) adequate wind energy to transport the dust, and (iii) a suitable accumulation site (Pye, 1995). Formation of this type of aeolian deposit typically coincides with Quaternary glacial episodes. Under such conditions, strong winds blowing off ice-caps can remove much fine-grained material from the vegetation-free proglacial landscape and are capable of transporting it for long distances before deposition.

The Pampean loess deposits are considered to be principally of Pleistocene age, having accumulated during the Late Glacial Maximum of the Andes at around 30–14 ka BP. During this period, a mountain ice field covered a large area south of 28°S (Clapperton, 1983), with winds blowing from the south-south-west. North of 28°S, the Argentine Cordillera was a cold, arid environment which allowed efficient production of fine silt by periglacial processes.

During Quaternary interglacial periods (e.g. the significant ice retreat around 14 ka BP; Clapperton, 1990) the silt was transported south by the Bermejo–Desaguardo–Salado fluvial system, fed by glacial meltwater in the Andes. This fluvial system formed a 25–35 km wide floodplain during the Upper Pleistocene. The sediments deposited by this fluvial system display a grain size zonation along the river system, with coarse gravels in the upper Andean basin and silty sands and sandy silts in the lower basins. These then became source materials for subsequent transportation northwards by the south-south-west winds from the Patagonian ice field, to form the Pampean sand desert and loess deposits.

The loess deposits have been substantially reworked by aeolian and fluvial processes since initial deposition. Well-developed dunes are present in some areas. Variations in loess thickness reflect local topography and degree of reworking.

Volcanic activity has had an important impact on the composition of the Pampean loess. Ash falls were frequent throughout the Tertiary and Quaternary and continue to the present. The last major ashfall in the region (1932) was from Quiza Pu volcano on the Argentine-Chilean border (Zárate and Fasano, 1989). The presence of volcanic material is an indication that deposition was contemporaneous with explosive volcanism but in some cases may result from reworking of Patagonian pyroclastic rocks and transportation by ice action (Sayago, 1995).

The Pampean loess is typically brown or light yellow in colour, sometimes with a reddish or grey tinge (Teruggi, 1957). The deposits are relatively homogeneous and on a local scale are well-sorted. Relative to loess deposits in other parts of the world, the Pampean loess has a coarse grain size with the modal range being coarse silt to very fine sand. The sand fraction typically comprises 20% of the sediment (Zárate and Blasi, 1993). Direct volcanic ashfall provided a small but frequent input in the form of pumice fragments and euhedral crystals (Zárate and Blasi, 1993). As a result of the small amounts of clay and calcium carbonate cement that are almost always present, the loess is slightly to moderately cohesive.

The loess deposits typically have an abundance of volcanic glass and plagioclase with quartz as a minor mineral and with occasional lithic fragments. Iron and manganese oxides are also usually present. Illite is the dominant clay mineral in most Pleistocene-Holocene loess sequences (Nicolli et al., 1989). Smectite and kaolinite are also typically present but are minor components except in reworked material ascribed to the Pliocene and Early Pleistocene (Sayago, 1995).

4.3 Secondary processes: calcrete and palaeosol formation

The deposits display abundant evidence of post-depositional alteration including carbonate cementation and soil-forming processes. Secondary carbonate occurs in the form of calcrete layers (locally known as 'tosca') as well as concretions, veins, scattered cementing dust or as extensive sheets or duricrusts with thicknesses of 1–3 m throughout the loess sequence (Rabassa and de Francesco, 1986). The calcretes may have formed over periods of several thousand years and are an indicator of semi-arid conditions. Zárate and Fasano (1989) suggested that the Pampean calcretes formed by a combination of pedogenic processes and by non-pedogenic processes involving biological activity, fluctuating shallow water tables and evaporation from surface waters.

Clayey palaeosols are also apparent in the loess deposits. These indicate periods of non-deposition and are considered to have formed during warmer climatic episodes (Zárate and Fasano, 1989). Mottling as a result of development of secondary manganese oxides is also evident in some horizons. In places, nodules of manganese oxide are also present.

Sedimentary sequences throughout La Pampa reveal much evidence for variable climatic conditions throughout the Quaternary, with generally cold, arid glacial intervals and warmer, wetter interglacial episodes (Kröhling, 1999; Tonni et al., 1999). Climatic variability following the loess deposition is evidenced by the abundant occurrence of calcretes and palaeosols throughout the loess sequence. The sediments also record potentially long intervals of non-deposition during the Pleistocene and Holocene periods.

4.4 Pre-Pampean geology

The Pampean sediments are underlain by Mesozoic and Cenozoic formations of variable thickness, which in turn overlie a crystalline basement of granitic and metamorphic rocks. In parts of the Chaco-Pampean Plain at least, the loess sequence is underlain by a sequence of fluvial deposits known as the Puelche Formation (thought to be mainly of Pliocene, but possibly also Pleistocene age). The Puelche Formation has been best described in profiles from neighbouring Buenos Aires Province and is composed primarily of quartzose friable sand, reported to range from 10–50 m in thickness (Auge, 1986). Hernández and González (1999) described a clayey to silty clay layer at the base of the

Plate 4.1 Typical layer of rhyolitic ash (ca. 2cm thick) in road cutting from La Pampa

Plate 4.2 Calcrete layer (ca. 50 cm thick; locally known as 'tosca') at ground surface, exposed in a shallow hand-dug well from La Pampa

Pampean deposits that underlie Buenos Aires city which acts as a confining layer to the Puelche sands, the main source of water in the region.

LANDSAT images from the study area have established that the crystalline basement is highly fractured. Lineaments corresponding to a fault system with a north-north-west strike have influenced the surface topography, producing elongate flat depressions. Bannert (1974) reported these depressions having a width of 100 m to 200 m, spaced approximately 2 km apart. Subsurface structure has had an important influence on surface topography (Elorriaga and Tullio, 2000).

4.5 Geology of the Eduardo Castex area

Information concerning the geology of the study area was obtained from approximately 50 logs of water supply boreholes provided by the Dirección de Aquas (DDA) of La Pampa. Depths ranged from 220 m in the west to typically 60 m in the east. These provided a good coverage of the area. In addition, information on the depth to basement was obtained from deeper exploratory boreholes drilled by DDA and as part of oil-exploration exercises.

Loess deposits blanket the whole area. These are dominantly brown to red-brown silts and sands with abundant calcrete. Volcanic material is also common. The topmost part of the loess sequence is largely composed of coarser sandy material, typically 1–6 m thick. Such upward coarsening of the loess deposits has been noted elsewhere in the Chaco-Pampean Plain (Rabassa and de Francesco, 1986). In most cases, abstraction boreholes appear to lie totally within the Pampean loess sequence, although in some locations, fine sands are found at depth that may be part of the older Puelche Formation.

A layer of white rhyolitic volcanic ash 0.05 to 2 cm thick can be traced over much of the study area within the upper part of the loess profile, typically just a few centimetres below surface (Plate 4.1). In a few places, it has been reworked but usually is maintained as a distinct horizon. The ash is widely considered to be derived from the 1932 Quiza Pu eruption.

Calcium carbonate epigenetic material is much in evidence in the form of cement, discrete calcrete layers and irregular concretions throughout much of the loess sequence. A layer of calcrete (tosca) 0.4 to 2 m in thickness can be found across much of the area, particularly in the east where the terrain comprises a flat plain (Section 3.1), typically at a depth of 1 m below ground level (Plate 4.2). This gives rise in the eastern part of the area to a largely flat-lying plain.

In the west of the region where the topography is undulating, calcrete is seen at surface on the higher ground and appears to have had some control on the topography. In the western part of the study area around La Maruja and Pichi Huinca, approximately north-south-trending bands of sand dunes are also visible, typically a few metres in height (Figure 2.1).

Palaeosol layers are evident in several lithological logs from the study area and provide evidence of past periods of non-deposition and soil development. Palaeosol horizons are not readily correlated between logs.

The pre-Pampean geology underlying the study area is poorly characterised. It is thought that sediments of Mesozoic and Cenozoic age infill a south-south-west to north-north-east-trending fault-controlled valley in the basement. The presence or extent of sediments of the Puelche Formation is not known. Basement rocks have been proved in boreholes in the west and central-west parts of the region at a depth of < 80 m, in La Maruja at a much greater depth of 708 m, and beneath Eduardo Castex in the east at a depth of around 180 m (154 m at Trenel; 162 m at Conhelo).

Where recorded, sediments of Triassic age appear to be largely continental red-brown sandy and partly conglomeratic sequences with some intercalations of clay. Both depth to the top of the Triassic sequence, and thickness, vary considerably. In the west around Ingeniero Foster, lithological logs record the presence of an unconformity with deposits of Triassic age immediately underlying Pampean deposits. One log from the area (Rancul) records likely Triassic sediments at 120 m depth. Another from La Trinchera (65°05' W 35°33' S, north-western area) records Triassic red sands and conglomerates with some calcrete at depths between 41–220 m. At La Maruja, Triassic sediments occur between 276–708 m depth (DDA, unpublished records).

4.6 Hydrogeology

4.6.1 General hydrogeology of Pampean sediments

The aquifer of greatest interest to this study is the loess aquifer of Pampean (Pleistocene) age. The upper, coarser-grained, and therefore likely more permeable sections of the formation, form an unconfined aquifer in the study area. Sediments underlying the Pampean loess may be fluvial sands of the Puelche Formation which is typically a highly productive aquifer. The presence and extent of Puelche sands is not known in detail and, if present, the degree of hydraulic continuity with the overlying Pampean aquifer is also unknown. In the Ingeniero Foster area, abstraction is mainly from Triassic sediments below the Pampean strata and boreholes typically abstract from depths of 120–150 m (DDA unpublished data).

4.6.2 Aquifer parameters

Very few publications in English are available that describe the hydrogeology of Pampean aquifers or give values for aquifer parameters. Auge (1986), in a study of groundwater dynamics from Buenos Aires Province, estimates parameters for the Pampean loess aquifer as well as the underlying Puelche Formation. Hydraulic conductivities of 1 and 10–40 m day^{-1} respectively are given. The thicknesses of the two formations are 30–70 m and 10–50 m respectively. Hernández and González (1999) described the aquifer underlying Buenos Aires in a study of the impact of rising piezometric levels on urban structures in the city. The unconfined Pampean aquifer is approximately 15 m thick with a hydraulic conductivity of 10 m day^{-1} and storativity of 2×10^{-2}. It is separated from the underlying Puelche aquifer, the main groundwater supply for Buenos Aires city, by an aquitard of the Lower Pampean (possibly an indication of the downward-fining of the formation, see Section 4.5). The semi-confined Puelche aquifer is approximately 20 m thick with a hydraulic conductivity of 30–50 m day^{-1} and storativity of 5×10^{-3}–3×10^{-4}.

Loess deposits worldwide have a general tendency to be aquitards, which drape over more permeable sediments (Mathers and Zalasiewicz, 1994). In La Pampa, this is the case where the loess is clayey and has no secondary permeability. However, the hydraulic conductivities given for the Pampean aquifer are within the upper range (10^{-5} m s^{-1}, ca. 10 m day^{-1}) for loess deposits quoted by Freeze and Cherry (1979), corresponding to coarse clean loess with secondary permeability. These authors also quote porosity of such deposits in the range of 40–50%. The secondary permeability that exists in loess is caused by fractures, root channels and animal burrows. This often exceeds the primary permeability. At a larger scale, however, the overall permeability of loess is decreased by the common presence of widespread clayey palaeosol layers formed during warmer climatic cycles.

4.6.3 Groundwater flow systems

The Pampean Plains are extremely flat and as a result devoid of surface drainage over much of their area. The great thickness of sediments and their relative homogeneity, coupled with this lack of regional topography, means that regional groundwater flow in these sediments is often very slow. In such terrain, local small-scale variations in the topography can have a significant control on groundwater recharge (Logan and Rudolph, 1996). This results in shallow groundwater flow systems with flow directions sometimes in opposition to the regional flow.

The local variations in topography can be the result of faulting in the underlying basement rocks (Bannert, 1974) and/or aeolian (Pye, 1995) or fluvial erosion. In the study area, thick shallow layers of calcrete have an influence on erosion, being coincident with topographic highs in the western part. Two conceptual models are put forward here to describe the influence that these topographical variations may have. These have relevance to the discussion of the groundwater flow system in the Eduardo Castex area.

i) Where the water-table intersects or is close to the surface at a topographic depression, it is likely that a discharge zone will occur there for at least part of the year with evaporation from the soil or free-water surface and/or transpiration by vegetation. Where these depressions occur along with topographic highs, shallow flow cells can be set-up, where a significant proportion of the groundwater recharging on the high ground, particularly where this was formed from sand dunes, discharges in the depression. Palaeosols constrain vertical flow (O'Brien et al., 1996) and may play a role in establishing these flow cells, as may the higher permeability of the upper zones of the loess aquifer.

ii) Depressions may also be zones of recharge under certain water-table and rainfall conditions, ie. where the water table does not rise to the ground surface and where rainfall is sufficiently intense to cause runoff and ponding of water in the depressions. Localised zones of recharge underlying depressions have been characterised by relatively fresh groundwater of low salinity (Bannert, 1974).

Variations in rainfall as a result of climatic cycles that occur in the Pampean region (cyclicity of ca. 10 years) are accompanied by associated fluctuations in groundwater levels (M. Blarasin, pers comm., 1998). The appropriate model for a given area will depend on the position of the water table in relation to the ground surface. During drier periods of the cycle when groundwater levels are relatively low, depressions which previously may have been zones of discharge, may become zones of intermittent recharge.

4.6.4 Hydrogeology of the Eduardo Castex area

Climate

The Eduardo Castex area of La Pampa experiences a semi-arid climate. Climatic data for Santa Rosa, located 80 km south of Eduardo Castex, are available for a 20-year period up to 1988. These data

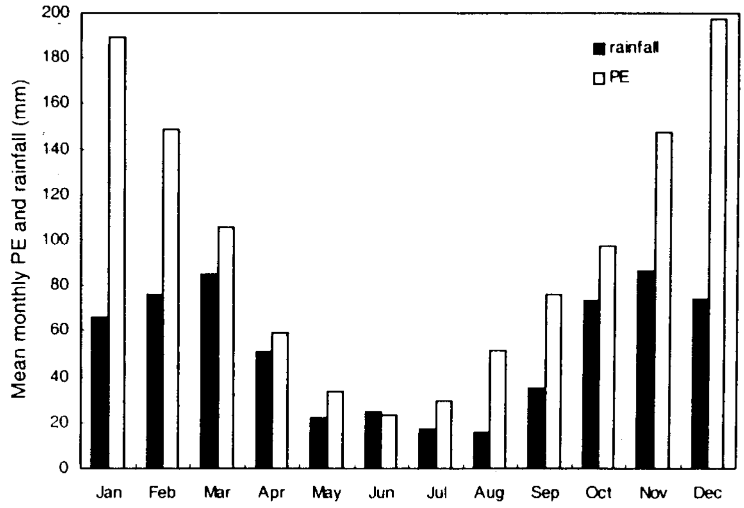

Figure 4.1 **Histograms of average monthly potential evapotranspiration (PE) and rainfall for Santa Rosa meteorological station**

indicate a mean monthly temperature maximum of 31.6 °C in January and a minimum of 1.7 °C in July. The mean annual rainfall for Santa Rosa is 626 mm.

The data also enable calculation of the potential evapotranspiration. The calculation is based on the revised FAO radiation method (Verhoef and Fettes, 1991) and assumes a short-grassland cover. This method gives a mean annual potential evapotranspiration of 1157 mm. The mean monthly rainfall and potential evapotranspiration are plotted in Figure 4.1. Although it must be emphasised that the evapotranspiration quoted here is potential, still it is significant when comparing the monthly mean of potential evapotranspiration and rainfall, that the former is greater for 11 months of the year. This is likely to result in a relatively lower groundwater recharge compared to other regions with similar annual totals where the rainfall is greatest during periods of the year when potential evapotranspiration is at its minimum (see below).

Information on the spatial variability of rainfall and the longer-term rainfall trend dating from the 1920s is available from records for 9 stations across the study area. Data were only available until the end of 1996. Rainfall increases from west to east. Ingeniero Foster in the west has a long-term average annual rainfall of 582 mm, while Monte Nievas in the south-east has an annual average of 691 mm.

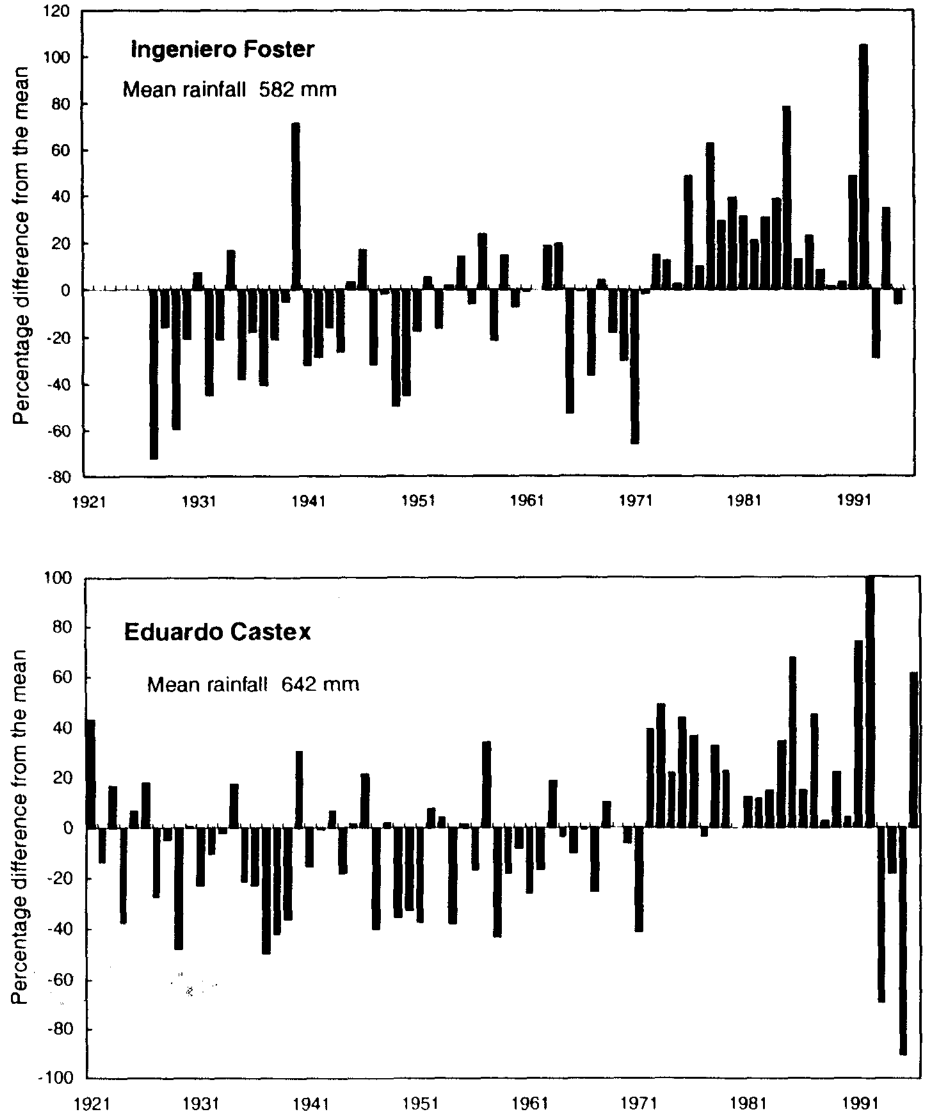

Figure 4.2 **Rainfall records for the period 1920–1996 for stations at Ingeniero Foster and Eduardo Castex**

That at Eduardo Castex is 642 mm.

Station records show a consistent rainfall trend over the period. Rainfall prior to the 1970s was generally below the long-term average. Since that time, annual rainfall has been significantly greater than the average. The data for Eduardo Castex and Ingeniero Foster rainfall stations are shown in Figure 4.2. The mean rainfall at Eduardo Castex for the period up to and including 1971 is 576 mm and for the period since is 778 mm. Corresponding rainfall totals for Ingeniero Foster over these periods were 499 mm and 730 mm respectively. The lower-than-average totals in the 1990s at Eduardo Castex station appear to be atypical of the study area and are not in evidence from the Ingeniero Foster rainfall record (Figure 4.2).

Topography

The ground surface decreases in height from around 300 m above OD in the west to 150 m above OD in the east. The overall topographical gradient is ca. 0.0015. There is also a change in landform from west to east. The terrain is more undulating in the west and central regions. The hills are roughly 30 m in height and 1–5 km apart. It appears that calcrete has some control on the topography in this area, being noticeable at outcrop on the tops of hills. A series of north-south trending sand dunes are also present, again occurring mainly in the west of the study area. The terrain in the east is generally very flat.

Groundwater use

The lack of perennial surface water sources in northern La Pampa makes groundwater a critical source for public water supply, domestic and agricultural use. In rural areas, most dwellings have at least one well. Domestic wells and boreholes are usually equipped with small motorised pumps with low pumping capacity. Some groundwater supplies are also abstracted by wind energy. In the rural areas, groundwater is typically used for potable supply without prior treatment. Boreholes and wells installed with Australian-style wind-driven pumps (cover illustration) are abundant in fields throughout the region and provide water for cattle and other farm animals.

Some dwellings in the urban and suburban areas also have private boreholes for water supply, although the majority of water is obtained from public groundwater sources where water is treated by reverse osmosis to reduce concentrations of inorganic constituents. Public-supply boreholes in the towns have large pumps with higher discharge rates. Towns in the area typically have 2 or 3 public-supply boreholes. Eduardo Castex has 5 public-supply boreholes and a reverse-osmosis treatment plant, principally designed for removal of F (capacity 1.2 m^3 hr^{-1}). Almost all boreholes used for groundwater tap the shallow Pampean loess aquifer.

Groundwater levels

Piezometric contour maps produced by DDA indicate the large number of groundwater sources. The map for the region Norte Zone II (DDA, 1983), an area of ca. 6360 km^2 including Eduardo Castex, uses data from a total of 1,124 wells. These wells occur at a density of 0.10 per km^2 in the west of the zone to 0.26 per km^2 in the east. The increase coincides with an increase in population density but also a decrease in the depth to groundwater.

Figure 4.3 shows a representative cross-section of groundwater levels. The depth to groundwater is typically 120 m in the west and 3.5 m in the east, with an overall gradient of ca. 0.0005. However, great variations in groundwater levels occur, particularly in the central region, probably due to the occurrence of localised recharge zones. Analysis by DDA has shown that afforestation has reduced groundwater recharge and groundwater levels underlying forested areas are lower as a result.

No data are available for groundwater-level fluctuations. The scant anecdotal information indicates generally small seasonal fluctuations across the whole area, typically of around 0.5–1.0 m. In the west, the thick unsaturated zone will attenuate seasonal fluctuations. In the east, fluctuations are constrained by the shallow thickness of the unsaturated zone. There is also anecdotal evidence that groundwater levels have risen overall in the region since the early 1970s as a result of the increased rainfall. This has also been accompanied by the appearance of a large number of newly-formed small lakes and ponds.

Groundwater flow system

The annual groundwater recharge has been estimated as 30 mm in the Eduardo Castex area and as 60–100 mm beneath the sand dunes in the west of the study area (using the chloride balance method; DDA, pers. commun. 1998). These estimates are rather low, bearing in mind that there are no significant discharge zones within the area. It is likely that due to the similar patterns in rainfall and evapotranspiration described above, much of the rainfall is evaporated or transpired and does not infiltrate below the root zone.

Based on these recharge estimates, a simple water-balance calculation indicates that a significant proportion of the flow beneath it must occur within deeper, necessarily more permeable, aquifers below the loess aquifer. The relatively low hydraulic conductivity of the loess does not allow the estimated amounts of water being recharged over the study area to flow out of the eastern boundary.

Groundwater flow within the loess aquifer will be a combination of deeper regional and shallow localised flow. This will be controlled in part by the zonation of loess aquifers by palaeosols. Regional groundwater-flow velocities will be slow in the loess aquifer. As an indication, using the regional groundwater-level gradient (0.0005) with parameters for a loess aquifer defined by Hernández and González (1999) and Freeze and Cherry (1979), the travel time for groundwater to flow a distance of 100 km (ie. from the west to the east of the study area) is in the order of 10^4 years.

In the west, the depths to groundwater are such that there will be no groundwater discharge from the aquifer. As mentioned above, there are no rivers or lakes in the area and the topography is variable compared to that in the east. Groundwater recharge will be concentrated in topographical depressions and beneath sand dunes.

In the east, the water table is much closer to the ground surface. In recent years, standing water has been seen in this area, coincident with greater amounts of rainfall. The occurrence of standing water may be due to perched water tables caused by the presence of extensive, thick deposits of calcrete at shallow levels. It may also be an indication of the reduced infiltration capacity of the unsaturated zone. Where this is the case, discharge from the groundwater system will occur.

Based on the observations above, a conceptual model of the groundwater flow system is described in Figure 4.3. Regional groundwater flow paths are from the higher regions of the west towards the east. This regional flow occurs both within the loess and underlying aquifers. Superimposed on this system are shallow flow cells which occur in zones of higher recharge where pockets of younger groundwater will be found. To the east, the terrain levels out and groundwater recharge is more diffuse. Here, discharge zones driven by evaporative processes, may cause the recycling of recently recharged water but may also cause deeper, regionally-flowing groundwaters to be brought nearer to the surface.

This model applies under the present climatic conditions, under which increased rainfall has brought groundwater levels in the east near to the surface. The model may not have applied during periods of lower rainfall that occurred in the area prior to the 1970s. If groundwater levels were significantly lower, discharge from the system may not have occurred within the study area, but further downgradient.

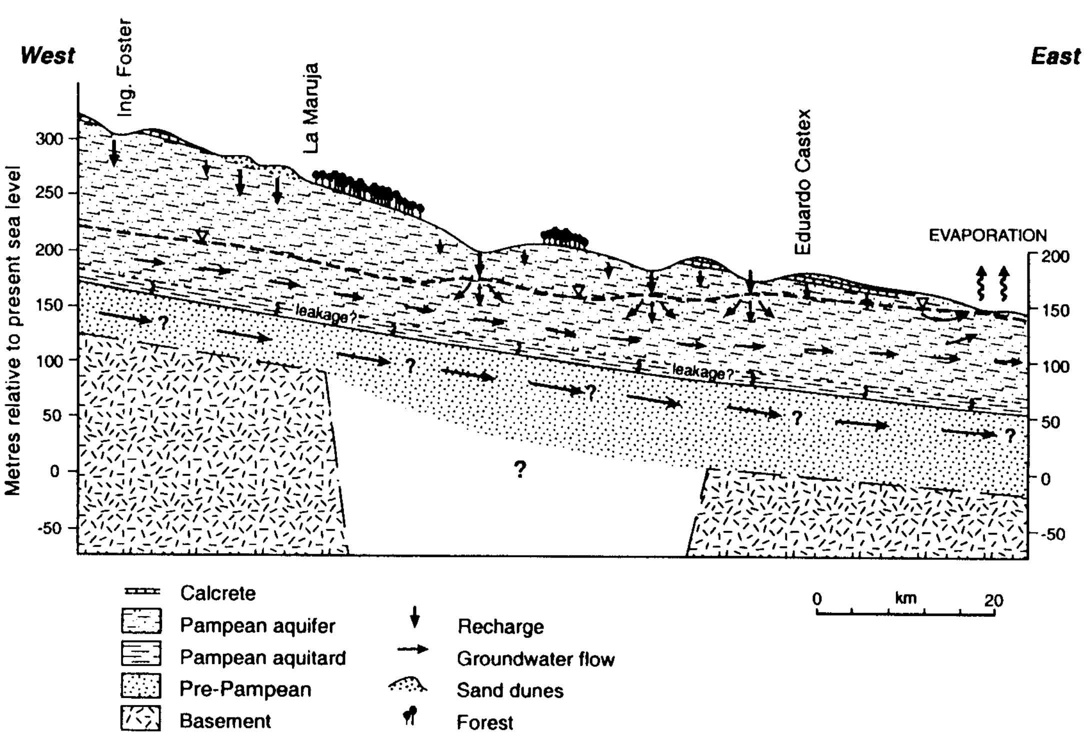

Figure 4.3 **Conceptual model of groundwater flow in the Pampean and deeper aquifers of the study area, showing regional flow gradient and localised zones of discharge in low-lying areas**

5. SAMPLING AND ANALYSIS

5.1 Water samples

5.1.1 Sampling

Groundwater samples were collected from boreholes in an area covering 110 km by 70 km. Sites included 17 public water-supply boreholes and 90 private boreholes or hand-dug wells. Private sources were selected largely at random within the constraints of accessibility, and all samples were collected without prior knowledge of groundwater quality. Sampling density was about 1 per 50 km^2. Surface-water samples were also collected by bailing from two sites (Santa Rita pond (sample 970685) and an unnamed lake next to Tamagnoni borehole (sample 970701)).

On-site analysis included water temperature, pH, Eh, dissolved oxygen, specific electrical conductance (SEC, 25°C) and alkalinity (H_2SO_4 titration). Alkalinity results are quoted as HCO_3. Wherever possible, pH, Eh and dissolved oxygen were measured in an anaerobic flow-through cell whilst the borehole was being pumped and values monitored until stable Eh readings were obtained (10–30 minutes). Where not possible, on-site measurements were made on freshly abstracted water samples in order to minimise changes in water condition before measurement.

At each site, water samples were also collected for subsequent laboratory analysis. Samples for major- and trace-element analysis were filtered (0.45 µm) on site into acid-washed polyethylene bottles. Those collected for analysis of cations and SO_4 were acidified to 1% v/v (Erbatron HNO_3, Carlo Erba). Samples for As analysis were acidified to pH 4 (HCl) ready for analysis of As(III) and subsequently to 2% v/v (Erbatron HCl) for analysis of total As (As_T). Samples for anion analysis were not acidified. Separate samples were collected for analysis of dissolved organic carbon (DOC). These were filtered using silver-impregnated 0.45 µm filters and glass syringes into acid-washed glass bottles. Several samples were collected in duplicate.

Unfiltered samples were also collected at some sites for isotopic analysis. Aliquots were collected in glass bottles for $\delta^{18}O$, δ^2H and $\delta^{13}C$, in acid-washed polyethylene bottles for $\delta^{34}S$, in 1-litre polythene bottles for tritium and in large polythene containers (ca. 20 litres, sufficient to collect 6 g of C) for ^{14}C analysis.

Where possible, sample bottles were refrigerated during storage before analysis and attempts were made to analyse samples as soon as possible after collection.

Aliquots for $\delta^{34}S$ analysis were prepared by adding a solution of 10% $BaCl_2$ and HCl (to pH 2) to the water samples and stirring until $BaSO_4$ precipitates formed. Excess $BaCl_2$ was added to ensure that all SO_4 was precipitated. The precipitates were then filtered off and dried ready for analysis. Aliquots for radiocarbon analysis were prepared by adding a solution of 10% $BaCl_2$, allowing precipitation and settling of $BaCO_3$ and decanting off the precipitate from a funnel at the base of the container.

Precipitates for ^{14}C analysis were prepared using an 80-litre steel separating funnel with 1-litre polyethylene bottle attached to the base. Water samples were poured into the funnel and sufficient $BaCl_2.2H_2O$ added to precipitate all carbonate. An additional 5 g $FeSO_4.7H_2O$ was added to aid flocculation. Solutions were adjusted to pH 11.0–11.3 using carbonate-free NaOH. Once formed, precipitates were decanted into the polyethylene bottles till brim full and sent for ^{14}C analysis.

5.1.2 Chemical analysis

Major cations, SO_4 and trace elements were analysed by ICP-AES (ARL3400 optical-emission spectrometer). Data were drift- and blank-corrected and with periodic checks of standard reference materials. During the course of analysis, NIST standard 1643d gave mean values (four analyses,

Table 5.1 Analytical results for reference standards TM23 and 1643d measured by ICP-MS at the time of sample analysis, compared with certified values

Determinand	Li μg l^{-1}	Be μg l^{-1}	Al μg l^{-1}	Cr μg l^{-1}	Mn μg l^{-1}	Co μg l^{-1}	Ni μg l^{-1}	Cu μg l^{-1}	Zn μg l^{-1}	Mo μg l^{-1}	Cd μg l^{-1}	Ba μg l^{-1}	Pb μg l^{-1}
TM23													
Certified	**3.3**	**0.6**	**37**	**8.3**	**8.5**	**8.0**	**8.6**	**9.2**	**5.6**	**5.8**	**2.6**	**13.4**	**3.4**
Certified 2σ	2.4	0.4	18	2.8	2.3	2.7	2.9	2.3	2.4	2.6	1.0	4.0	1.8
Measured	2.4	0.49	35	6.9	7.8	7.2	8.3	8.2	6.3	5.4	2.51	12.9	3.2
Measured 2σ	0.8	0.1	10	1.8	2	1.4	2.4	1.4	2.4	0.2	0.56	0.4	0.4
n	4	4	4	4	4	4	4	4	4	4	4	4	4
1643d													
Certified	**16.5**	**12.6**	**128**	**18.5**	**37.7**	**25.0**	**58.1**	**20.5**	**73**	**113**	**6.5**	**507**	**18.2**
Certified 2σ	0.6	0.3	4	0.2	0.8	0.6	2.7	3.8	1	2	0.4	9	0.6
Measured	16.1	10.7	130	17.8	38.5	25.2	59	20.0	64	118	5.9	548	19.8
Measured 2σ	1.8	1.0	0.006	1.4	1.2	1.2	4	2	2	4	0.5	36	4.6
n	2	2	2	2	2	2	2	2	2	2	2	2	2

certified values in parentheses) as Na: 22.07 mg l^{-1} (21.75 mg l^{-1}), K: 2.35 mg l^{-1} (2.28 mg l^{-1}), Ca: 31.04 mg l^{-1} (30.4 mg l^{-1}) Mg: 7.99 mg l^{-1} (8.06 mg l^{-1}), B: 145 μg l^{-1} (137 μg l^{-1}), Li: 16.5 μg l^{-1} (15.9 μg l^{-1}), Sr: 294 μg l^{-1} (285 μg l^{-1}), Mn: 38 μg l^{-1} (38 μg l^{-1}), Fe: 91 μg l^{-1} (90 μg l^{-1}) V: 35 μg l^{-1} (34 μg l^{-1}), Mo: 113 μg l^{-1} (109 μg l^{-1}), Al: 128 μg l^{-1} (121 μg l^{-1}).

Arsenic analysis was carried out by ICP-AES with hydride generation (using an ARL 341 hydride generator). Total As was analysed by pre-reduction of all As(V) to As(III) in samples 24 hours before analysis using 5% KI (2.5 ml 20% KI in 7.5 ml sample solution), followed by on-line hydride generation using 1% w/v $NaBH_4$ in 0.1% w/v NaOH (Trafford, 1986). Arsenic(III) was analysed using a modified version of the method given by Driehaus and Jekel (1992). Arsenic(III) was reduced to arsine by $NaBH_4$ at pH > 3.5 using 0.5 M acetic acid as buffer solution (to prevent As(V) also being reduced at lower pH; Driehaus and Jeckel, 1992). The acetic-acid method has the limitation that it fails to separate As(III) from DMAA (Anderson et al., 1984) and therefore analyses quoted for As(III) are strictly for the two species. However, since methylated As species usually have very low concentrations in natural waters (Section 2.4), the values listed are taken to be dominated by As(III). Interference problems from Fe, Ni and Cu are considered to be negligible. Organic arsenic compounds were not analysed for in this study.

During the course of As_T analysis, a Spex standard with nominal As concentration of 10 μg l^{-1} gave a value of 9.6 μg l^{-1} (n=2) and one analysis of TM23 (certified value 9.9 ± 3.6 μg l^{-1}) gave a value of 10.2 μg l^{-1}.

A large suite of trace elements was also analysed by ICP-MS (VG PQ1). Results were internal-standard (In, Pt) and blank-corrected and samples interspersed with standard reference materials. Average ICP-MS results for reference standards TM23 and 1643d measured during the course of sample analysis are given in Table 5.1.

Unacidified aliquots were analysed for NO_3-N, NO_2-N, NH_4-N, F, Br and I by automated colorimetry.

Saturated-zone porewaters were extracted from core sediments (Section 5.2) by high-speed centrifugation under partial vacuum, using sealed nylon centrifuge cups to minimise CO_2 degassing during centrifugation. Extracted porewaters were filtered (0.45 μm) and measurements made of pH, HCO_3 and SEC. The porewaters were then separated into two aliquots and one acidified to 1% HNO_3 (v/v) using Aristar acid. Analysis of major and trace elements was then carried out as for the groundwater samples described above, except anions (Br, I, F) were determined simultaneously by ion chromatography. Porewaters were also analysed for Se by atomic fluorescence spectrometry (AFS) with hydride generation.

Duplicate samples were also analysed by INGEOQUI for Na and K (flame spectroscopy), Ca + Mg and Ca only (by EDTA titration), SO_4 ($BaCl_2$ colorimetry) and Cl ($AgNO_3$ titration) and F by ion-selective electrode. Results for Na, K and K generally agreed well, mostly to better than 10%. Results for SO_4 and Cl were worse, but generally within about 20%.

Analytical charge imbalances for BGS analyses were less than 3% in all but one sample (4.8%) and the BGS results have therefore been used. Analytical charge imbalances for porewater analyses were usually less than 2% (the worst being 5%).

Stable-isotopic analysis was carried out by mass spectrometry. Analyses of $\delta^{18}O$, $\delta^{2}H$ and $\delta^{13}C$ were determined at BGS Wallingford and analyses of $\delta^{34}S$ were determined in part at the NERC Isotope Geology Laboratory, BGS Keyworth and in part by Geochron Laboratories, USA. Results for $\delta^{18}O$ and $\delta^{2}H$ are reported relative to SMOW, $\delta^{13}C$ relative to PDB and $\delta^{34}S$ relative to CDT.

Analysis of tritium and ^{14}C was carried out by liquid scintillation counting at the INGEIS laboratories in Buenos Aires. Results of ^{14}C analyses are corrected for isotopic fractionation using the BGS-measured $\delta^{13}C$ values. Precision of tritium analyses is better than 1 TU.

5.2 Sediment samples

Sediment samples were collated from various sources for chemical and mineralogical analysis. Archive samples of cored sediment were provided by DDA from Eduardo Castex from No 9 Cooperative [35°54.48'S 64°18.28'W] and No 2, Campo de Soria, 10 km south-west of Eduardo Castex, [64°22'S 36°01'S], Ingeniero Luiggi No 7 and La Maruja. Samples were also collected during the groundwater-sampling campaign from quarries and road cuttings at various locations across the province. Most were samples of brown silty loess but a few samples of rhyolitic ash from thin (a few

Table 5.2 Details of augering sites in the study area and samples collected

Site	Location relative to water well	Sample depth interval (m)		Material	Colour	Comment
Santa Rita	8 m west of well	0.0	0.8	silty clay	grey brown	hole abandoned due to slow progress
		0.8	1.4	sandy silt	medium brown	
Talleres Norte	200 m west of water borehole	0.0	0.25	silt	dark brown	hit calcrete
E. Castex No. 9 Cooperative	5 m from borehole	0.0	0.3	silt	dark brown	hit calcrete
La Invernada	20 m east of well	0.2	1.0	sandy silt	greyish brown	water strike ca. 0.8 m
		1.0	2.0	sandy	medium brown	abandoned hole due to low recovery in wet conditions
Piorno	10 m west of well	0.15	1.0	silt	medium brown	
		1.0	1.4	silt	medium brown	abandoned hole, very dry, difficult to dig
Nicola	15 m south of well	0.0	0.3	silt	dark brown	hit calcrete

cm) ash horizons were also collected.

A few sediment samples were collected by augering. Sites close to water wells sampled in the study were chosen for the auger sampling and the operation was carried out using a 2.5-inch hollow-stem auger. In the event, significant difficulties were experienced with the augering, principally because of the development of hard calcrete layers at shallow depths. Hence only a few shallow samples were successfully collected. Details of the augered sites and sediment samples collected are given in Table 5.2. Samples collected were sealed in polyethylene bottles and freighted to the UK for analysis.

5.2.1 Core drilling

Newly cored boreholes were drilled at Talleres Norte in Eduardo Castex [35°54.3S 64°18.07W] and Tamagnoni, 10 km south of Eduardo Castex [35°59.55S 64°15.57W]. Both sites are located in the east of the study area (Figure 3.1). Tamagnoni is sited close to a slight topographical depression which forms a small ephemeral lake (area around 5 km^2) during wet periods and is likely to be a zone of groundwater discharge resulting in upward groundwater flow. The Talleres Norte site lies within the Eduardo Castex urban area. Here, the topography is flat and there are no features likely to cause concentrated recharge or discharge.

The two boreholes were located next to existing private groundwater supply boreholes that had been previously sampled on the project (Table 5.3) and were selected because high groundwater-As concentrations had been measured (Appendix 1.2). A further criterion for choice of location was favourable drilling conditions ie. the thickness of near-surface calcrete was expected to be small. In addition, to ensure as much saturated material as possible could be retrieved (acknowledging the depth limitations that can be achieved from the core-drilling method), sites were identified where the depth to water table was small (less than 5 m). For logistical reasons, the distance of the sites from accommodation and laboratory facilities in Eduardo Castex was also taken into account.

The cored boreholes were drilled to depths of 26.5 m at Talleres Norte and 30.5 m at Tamagnoni. The core-drilling method involved hammering a hollow core barrel lined with a plastic sleeve into the ground and recovering undisturbed sediment and porewater. The drilling was undertaken by local contractors, supervised by a BGS hydrogeologist and assisted by personnel from DDA and INGEOQUI. The drilling programme was undertaken in December 1997.

Some experimentation was required on-site before the drilling method and equipment used was finalised. The larger diameter 'clear-out tool' was used to drill the hole in the unsaturated zone to speed-up drilling. Here it was not necessary to obtain undisturbed samples. The clear-out tool was used in the saturated zone to ream out the hole once a sample had been collected using the smaller diameter lined core barrel. A siphon tool was used to remove any loose material that could not be collected by the clear-out tool.

During drilling at Talleres Norte, a thick layer of calcrete was encountered at 1.45–4.2 m depth which led to considerable drilling difficulties and slow progress with use of the clear-out tool. A 'chisel' tool was used to penetrate this layer which required use of drilling fluid to produce a slurry for removal of chippings. The siphon tool was then used to remove the slurry. In this procedure, distilled water (50 l) was used as drilling fluid to minimise effects of contamination.

The 'valvator' system used, ensures that the core is held securely within the clear-out tool and the lined core barrel and does not fall back into the hole as the drill string is returned to the surface. The valvators are rubber discs which are located between the cutting shoe and the core barrel. The centres of the disks are split so that the material is forced through the rubber disk as it enters the core barrel. The ribbed arms of the split disk then hold the core in place. Two discs are included in-line.

Table 5.3 **Details of the water boreholes adjacent to cored boreholes at Talleres Norte and Tamagnoni. Water levels were measured at the time of core drilling**

Boreholes	Latitude		Longitude		Depth	Water level
	°S	'	°W	'	(m)	(mbgl)
Talleres Norte	35	54.3	64	18.07	42	4.65
Talleres Norte	35	54.3	64	18.07	18	4.65
Tamagnoni	36	0.083	64	16.20	14	4.8

A sliding hammer allows the hammering motion imparted by the drilling rig to be conveyed to the core barrel without the core barrel having to be raised and lowered with each blow. A heavy weight (ca. 300 kg) in the form of an iron bar is included in the drill string to increase the force of the hammer blow. The drill string is raised and lowered by a metal cable attached to the pulleys of the drill rig which is powered by a tractor engine (Plates 5.1–5.2).

The penetration of the core barrel is measured by marks on the drill cable. A typical length of core cut per run was 0.5 m. The number of blows required per run provided a means of estimating the degree of consolidation of the rock material. Once a full run was completed and the drill string had been returned to the surface the core barrel was emptied. The lined core barrel was then broken, allowing the liner with sample to be removed. The plastic liner and core was then split in two to allow sediment logging and sub-sampling. The percentage of the core from the run that had been retrieved was used to identify the depth interval of the core. Considerable efforts were made to minimise cross-contamination of the porewaters in the core by water from the borehole annulus above, but possible breaches were noted.

Sediments were logged and a representative sub-sample was taken. Where a significant change in lithology occurred within a run, two sub-samples were taken. The samples were bulked over the intervals selected (typically 0.5 m) and divided into aliquots, one sent to INGEOQUI for XRD analysis and a second placed into tightly-sealed plastic 500 ml containers and freighted to UK for porewater extraction, mineralogical and chemical analysis. All samples freighted to the UK were transported within 3 weeks of the end of the drilling programme.

5.2.2 *Sediment sample preparation*

Polished thin sections were prepared from 12 of the Talleres Norte and Tamagnoni core samples and investigated using a Leo 435VP scanning electron microscope (SEM) fitted with a solid-state four-element backscattered electron detector. Imaging in backscattered mode (BSEM) allows differentiation of phases of differing average atomic mass, by their ranges of grey levels correlating positively with atomic number and density. Mineral identification was aided using qualitative chemical information determined by energy-dispersive X-ray microanalysis (EDXA). EDXA spectra were acquired using a Link ISIS 300 system fitted to the SEM.

Table 5.4 **Details of drilling of the Talleres Norte and Tamagnoni cored boreholes**

	Talleres Norte	Tamagnoni
Depth of borehole (m)	26.5	30.5
Days to complete borehole	4	5
No. of samples collected	47	61
No. of samples collected in saturated zone	43	55
Approximate depth to saturated zone (m)	4.4	3.5
Overall percentage of core recovered	78	87

Selected samples from the cored boreholes were also investigated by XRD in the INGEOQUI laboratory. Each sample was first washed with distilled water to solubilise salts present. Clay minerals were then gravity-separated in Atterberg tubes until particles less than 2 μm in size were obtained. Separate aliquots were then prepared: one being air-dried, a second by exposing to a glycol atmosphere for 24 hours and a third being calcined at 550°C for 2 hours before being analysed by XRD.

Selected sediment samples from the two cored boreholes and samples collected from road cuttings and quarries were prepared for chemical analysis by first air drying and disaggregating with a pestle and mortar.

5.2.3 Sediment chemical analysis

Archive sediment samples from DDA cored boreholes at Eduardo Castex, Ingeniero Luiggi and La Maruja, together with quarry and road-cutting samples and selected samples from the Talleres Norte and Tamagnoni boreholes (a total of 50 samples) were analysed by XRF (Philips PW2400 spectrometer, BGS Keyworth) for major oxides and trace elements. Samples were pre-dried at 105°C. Major elements were determined on fused glass beads and trace elements on pressed-powder pellets. Loss on ignition was also calculated for the samples by ignition for 1 hour at 1050°C.

Solid organic carbon was determined using a Carlo Erba CNS analyser after initial dissolution of sediment aliquots in 10% HCl to remove inorganic carbon. Aliquots were then combusted at 1070°C. Interfering gases (halogens and sulphur compounds) were retained using chromium-oxide and cobaltous-oxide catalysts. The carbon present (as CO_2) was then re-reduced (using Cu), separated on a chromatographic column and detected by a thermal-conductivity detector. Calibration was performed using standard organic materials.

Acid-ammonium-oxalate extracts were prepared (following the method of McKeague and Day, 1966) from selected sediments from the Talleres Norte and Tamagnoni boreholes (about half the samples) and from quarry and road-cutting samples. Acid oxalate is commonly used to selectively dissolve amorphous Fe, Al and Mn oxides and associated trace elements. Samples were weighed (1.25 g) into acid-washed Oak Ridge centrifuge tubes and 25 ml of 0.2 M acid oxalate solution (700 ml ammonium oxalate plus 535 ml 0.2 M oxalic acid, adjusted to pH 3; ie. Tamm's Reagent) added. Solutions were then shaken in the dark (to prevent photochemical reactions) for 4 hours, centrifuged and supernatants decanted ready for chemical analysis.

Analysis of oxalate solutions for major and trace elements was carried out by ICP-AES using matrix-matched standards, and As and Se were measured by AFS with hydride generation. Three procedural blanks were measured with the sample batches. These gave a maximum As concentration of 0.06 μg. Samples were not blank-corrected.

The oxalate solutions were also measured for F by ion-selective electrode using TISAB IV (ionic-strength buffer solution). During the analysis, the WRc Aquacheck standard gave an average recovery for F of 97.99% (RSD 4.32% on 7 replicate analyses).

Sediment extracts from the Talleres Norte and Tamagnoni boreholes were also prepared using hydroxylamine hydrochloride reagent, following the method of Chou (1972). Hydroxylamine hydrochloride is used as a selective extractant for Mn oxide. Samples were prepared by adding 25 ml of 0.1 M $NH_2OH.HCl$ (pH 2) to sediment aliquots (0.5 g) and following the procedure as for acid-oxalate extraction, but shaking for only 30 minutes in order to restrict additional dissolution of iron oxide during the process. Approximately 10% of samples were extracted in duplicate and six procedural blanks were interspersed with the samples. Chemical analysis was carried out as for the oxalate solutions. Arsenic concentrations in the procedural blanks were in all cases <13 ng. No blank corrections have been applied to the data.

Plate 5.1 Talleres Norte drilling site, Eduardo Castex

Plate 5.2 Tamagnoni drilling site, 10 km south of Eduardo Castex

6. GROUNDWATER CHEMISTRY

6.1 Regional variations in well depth

Results of the chemical analysis of groundwater samples from La Pampa are presented in Appendices 1.1 to 1.6. As described in Section 3, samples were collected over an area of 7700 km^2 and with a regional west to east slope of around 150 m in 100 km, considerable variations in depth to water table and hence total well depth are observed. Well depths in the west of the study area are typically of the order of 140 m whilst in the east they are of the order of 20 m or less. In the west around Ingeniero Foster, it is possible that one or two groundwater samples collected from depths >100 m are from older, Triassic red-bed sediments rather than the Pampean aquifer. However, most (including deeper samples from the Conhelo area in the south-west), are considered to be from the Pampean loess.

As a result of the regional variation in well depth, large variations in groundwater temperature are observed in response to the geothermal gradient (Figure 6.1). As noted in Section 4, depth of the unsaturated zone is also greater in the western part than in the lower-lying eastern area. Around Ingeniero Foster, water levels are typically 120 m below ground surface, whereas water levels around Eduardo Castex are commonly within 5 m of the ground surface. The regional distribution of well depths is shown in Figure 6.2.

6.2 Major-element variation

Numerous water-quality investigations have been carried out in northern La Pampa by DDA, including a major survey of Pampean groundwaters from the region between 1978–1987. Contoured maps of the distribution of total dissolved solids, hardness, Cl, SO_4, As and F as well as piezometric level have been produced for the region. These maps show a considerable degree of spatial variation in water quality, often over short distances. The variations have little obvious relationship with topography, terrain or local geology and are difficult to interpret in detail.

Results of chemical analysis from the present study confirm the large variations in chemical composition. They also highlight the high salinity of many of the groundwaters, with TDS values of 734–11,460 mg l^{-1} and SEC values in the range 773–17520 μS cm^{-1}. Most are of Na-HCO_3 or Na-mixed-anion type, (HCO_3-SO_4-Cl) although the most saline groundwaters are of Na-Cl type (maximum Cl concentration 4580 mg l^{-1}; Table 6.1). Sulphate concentrations reach up to 3170 mg l^{-1} and groundwaters with the highest concentrations approach (though do not reach) saturation with respect to gypsum. The distribution of salinity does not show any clear regional trend but shows much spatial variability over scales of a few kilometres. Regional distributions of Cl are given in Figure 6.2.

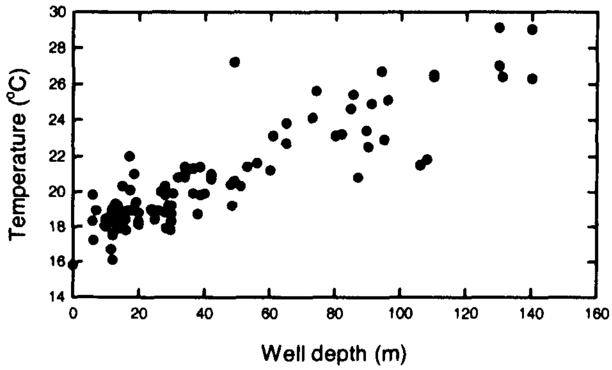

Figure 6.1 Variation between well depth and groundwater temperature in La Pampa. The deepest groundwaters are from the western part of the study area

Table 6.1 Statistical summary of field-collected data and major chemical constituents of the Pampean groundwaters

Determinand	Units	Min	Max	Median	Mean	10th centile	90th centile	n
Well depth	m	6.0	140	29.1	42	12	95	103
Water level	m	2.1	129	14.1	28	4.0	74	93
Temperature	°C	16.1	29.1	19.8	20.6	18.1	25.2	108
pH		6.99	8.66	7.85	7.82	7.39	8.25	108
Eh	mV	131	492	325	327	242	425	102
Dissolved oxygen	mg l^{-1}	0.8	9.9	6.1	5.9	3.9	8.0	106
SEC	µS cm^{-1}	773	17520	2610	3341	1307	6168	108
Ca	mg l^{-1}	1.55	599	20.9	45.1	4.468	100	108
Mg	mg l^{-1}	2.01	521	21.5	45.3	5.97	118	108
Na	mg l^{-1}	120	3100	543	667	290	1208	108
K	mg l^{-1}	3.3	70.6	11.8	14.8	5.78	26	108
Cl	mg l^{-1}	8.5	4580	192	458	20	1260	108
SO_4	mg l^{-1}	6.80	3170	285	432	72.1	916	108
HCO_3	mg l^{-1}	195	1440	653	716	400	1243	108
NO_3-N	mg l^{-1}	<0.2	144	9.06	19.35	1.56	49.74	108
NO_2-N	mg l^{-1}	<0.003	0.169	0.003	0.011	<0.005	0.020	108
NH_4-N	mg l^{-1}	<0.01	0.14	<0.02	0.01	<0.02	<0.02	108
Si	mg l^{-1}	21.1	39.2	29.2	29.6	26.0	34.0	108

Carbonate minerals are important components of the mineralogy of the Pampean aquifer and groundwater chemistry is strongly controlled by carbonate reaction. Most of the groundwaters are saturated with respect to calcite and dolomite and a few are supersaturated with respect to dolomite. Alkalinities are very variable but often high, with a range of 195–1440 mg l^{-1}. Groundwater pHs are neutral to alkaline (7.0–8.7), the highest values corresponding to low pCO_2 values, which have minima of around $10^{-3.0}$ atm (Appendix 1.2). Calcium varies between 1.6–599 mg l^{-1} but is mostly low at less than 100 mg l^{-1}. Carbonate reaction of the form:

$$CaCO_3(s) + CO_2 + H_2O \rightarrow Ca^{2+} + 2HCO_3^-$$

is likely to have been an important process in the groundwaters, with generation of high pHs due to consumption of CO_2 in a closed system and resultant development of low pCO_2 values.

Like Ca, concentrations of Mg are also generally low (range 2–521 mg l^{-1}; median 45 mg l^{-1}; Table 6.1). Molar Mg/Ca ratios are very variable, ranging between <1 and 4, but average around 1.8.

The groundwaters are universally oxidising with dissolved-oxygen concentrations between 0.8 mg l^{-1} and 9.9 mg l^{-1} (Table 6.1) and redox potentials (Ehs) up to 492 mV. As a result, observed concentrations of NO_3-N are often high, while concentrations of NO_2-N and NH_4-N are low (Table 6.1). Concentrations of NO_3-N reach up to 144 mg l^{-1}. Of the groundwaters investigated, 47% exceed the WHO guideline value for NO_3-N in drinking water of 11.3 mg l^{-1}. While it is likely that much of the NO_3-N in the groundwaters derives from pollution (fertilisers especially), it is thought that a significant contribution is made by evaporation. Highest concentrations are typically observed at shallow depths where the thickness of unsaturated zone is small (Figure 6.3). Accumulation of highest concentrations in this zone would be expected from both pollution and evaporative concentration.

Concentrations of K are often high (range 3.3–70.6 mg l^{-1}; Table 6.1). Some of this may be derived from pollution, although evaporation is likely to be responsible for many of the higher concentrations and reaction of K-bearing minerals and ion-exchange reactions may also be involved.

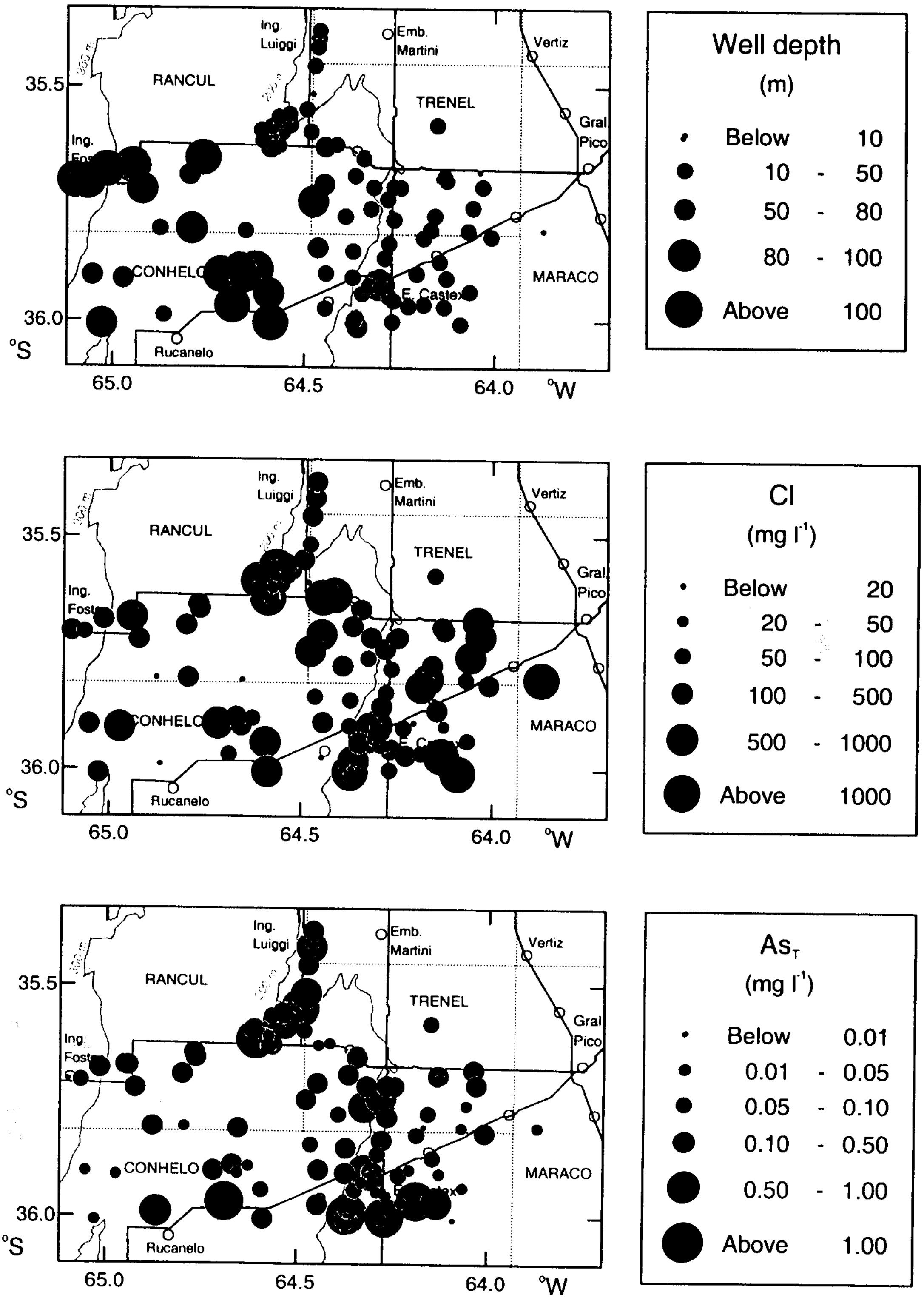

Figure 6.2 Variation in well depth, Cl and As_T concentration in groundwaters from La Pampa

Table 6.2 **Statistical summary of trace-element and stable-isotopic data for the Pampean groundwaters**

	Units	Min	Max	Median	Mean	10th centile	90th centile	n
As(III)	μg l^{-1}	<3	105	4.2	10.7	<4	28.3	108
As$_T$	μg l^{-1}	<4	5280	149	414	20	726	108
Fe$_T$	μg l^{-1}	<6	1160	55.0	125	10.0	337	108
Mn	μg l^{-1}	<1	79	2.0	5.17	<1	11.0	108
Ba	μg l^{-1}	5.0	259	36	45	19	81.2	108
Sr	mg l^{-1}	0.066	13.3	0.595	1.27	0.197	2.99	108
V	mg l^{-1}	0.019	5.43	0.558	0.837	0.160	1.65	108
B	mg l^{-1}	0.46	13.8	2.97	3.47	1.52	6.40	108
P$_T$	mg l^{-1}	<0.2	0.70	<0.2	0.191	<0.2	0.40	108
F	mg l^{-1}	0.034	29.2	3.84	5.24	1.30	9.94	108
Br	mg l^{-1}	0.055	11.6	0.67	1.18	0.148	2.50	108
I	μg l^{-1}	17.4	730	121	159	40.0	292	108
Li	μg l^{-1}	5.7	147.4	26.1	32.1	11.7	57.3	107
Be	μg l^{-1}	<0.01	0.40	0.01	0.05	<0.09	0.11	107
Al	μg l^{-1}	2.88	991	16.1	55.1	6.9	111	107
Cr	μg l^{-1}	0.40	20.4	2.30	2.98	1.02	5.59	107
Co	μg l^{-1}	<0.03	1.28	0.13	0.21	0.02	0.45	107
Ni	μg l^{-1}	<0.15	18.7	0.88	1.96	<0.30	4.39	107
Cu	μg l^{-1}	0.41	88.6	7.10	11.96	1.29	27.6	107
Zn	μg l^{-1}	2.51	1438	58.3	112	18.8	260	107
Ga	μg l^{-1}	<0.01	0.18	<2.2	0.09	<0.41	0.011	107
Ge	μg l^{-1}	<0.02	0.45	<2.4	0.14	<0.46	0.17	107
Rb	μg l^{-1}	1.45	31.6	5.0	6.38	2.62	12.0	107
Y	μg l^{-1}	<0.002	0.510	0.033	0.284	<0.18	0.115	107
Mo	μg l^{-1}	2.72	991	61.5	107	9.18	180	107
Cd	μg l^{-1}	<0.02	2.70	0.11	0.28	<0.11	0.46	107
Sb	μg l^{-1}	<0.05	0.92					107
Cs	μg l^{-1}	<0.01	0.22	0.02	0.10	<0.44	0.062	107
Tl	μg l^{-1}	<0.01	0.14			<0.45	0.04	107
Pb	μg l^{-1}	<0.45	13.8	0.39	0.82	<1.34	1.23	107
Bi	μg l^{-1}	<0.02	<1.9					106
Ag	μg l^{-1}	<0.04	0.04					106
La	μg l^{-1}	<0.013	6.43	<0.81	0.158	<0.27	0.13	107
Ce	μg l^{-1}	<0.008	1.65	<1.7	0.148	<0.52	0.117	107
Pr	μg l^{-1}	<0.004	0.163					107
Nd	μg l^{-1}	<0.009	0.49					107
Sm	μg l^{-1}	<0.01	0.11					107
Eu	μg l^{-1}	<0.004	0.030					107
Gd	μg l^{-1}	<0.01	0.14					107
Tb	μg l^{-1}	<0.003	0.015					107
Dy	μg l^{-1}	<0.007	0.098					107
Ho	μg l^{-1}	<0.002	0.011					107
Er	μg l^{-1}	<0.007	0.051					107
Tm	μg l^{-1}	<0.002	0.008					107
Yb	μg l^{-1}	<0.006	0.039					107
Lu	μg l^{-1}	<0.002	0.004					107
Th	μg l^{-1}	<0.004	0.45	0.005	0.085	<0.32	0.087	107
U	μg l^{-1}	6.16	248	30.6	42.1	16.7	81.5	107
δ^{18}O	‰	-6.4	-3.8	-4.8	-4.8	-5.3	-4.4	60
δ^{2}H	‰	-36	-23	-27	-27	-32	-24	60
δ^{13}C	‰	-12.8	-4.0	-8.5	-8.1	-11.6	-5.0	34
δ^{34}S	‰	6.3	8.7	7.9	7.9	7.1	8.6	20

Mean values were calculated by substituting a value of half the detection limit where values were found to be below detection limit. Median and mean values have not been quoted where a significant number of samples were below detection limit

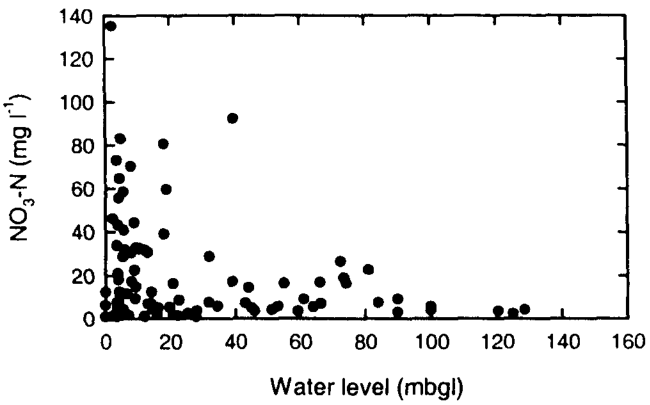

Figure 6.3 **Variation of NO_3-N with water level in groundwaters from La Pampa**

Concentrations of Si are also variable but generally high (21–39 mg l^{-1}; Table 6.1). The range reflects both high groundwater temperatures and pronounced reaction of silicate minerals in the aquifer. Many of the silicate minerals in the aquifer are fine-grained (e.g. clays) and easily dissolved (e.g. feldspar, volcanic glass). The groundwaters are saturated with respect to quartz, chalcedony and cristobalite. Reaction of silicate minerals is also a key process responsible for the generation of high-pH groundwaters. Reaction of sodic feldspar for example, consumes protons and hence causes a pH rise. Reaction of albite ($NaAlSi_3O_8$) to form kaolinite ($Al_2Si_2O_5(OH)_4$) can be described as:

$$2NaAlSi_3O_8 + 2H^+ + 9H_2O \rightarrow Al_2Si_2O_5(OH)_4 + 2Na^+ + 4H_4SiO_4.$$

The reaction also accounts for the origin of high Na concentrations in the groundwaters. A similar reaction may also produce gibbsite ($Al(OH)_3$) which is found to be saturated in most of the groundwaters.

By contrast, the two surface-water samples from Santa Rita pond and the small 'lake' next to Tamagnoni borehole (see Appendix 1.1 for locations) collected in April 1997, have low concentrations of dissolved solutes (TDS 145 mg l^{-1} and 192 mg l^{-1} respectively). They are oxidising and dominated by Ca and HCO_3 ions. No pH determination was made on Santa Rita pond but that of the Tamagnoni sample was 8.1 (Appendix 1.1). The low salinity of the samples, which were taken during the wet season, indicates that the surface-water bodies contain a large component of direct recharge, much of which may have been runoff collected in the depressions.

6.3 Iron, manganese and aluminium

As the groundwaters are usually oxidising, solubility of Fe and Mn minerals is low and concentrations of dissolved Fe and Mn are therefore mostly low. Many samples have concentrations below detection limits and most have <300 µg l^{-1} Fe and <15 µg l^{-1} Mn. However, Fe in a few samples reaches up to 1160 µg l^{-1} and Mn up to 79 µg l^{-1} (Table 6.2). At the pH of the groundwaters, the few high concentrations are most likely to be due to presence of colloidal particles which passed through the 0.45 µm filter. Neither Fe nor Mn correlates with pH. None of the samples exceeds the WHO guideline value for Mn in drinking water (500 µg l^{-1}) and few exceed the recommended upper limit for Fe on aesthetic grounds (Table 6.3).

Most samples also have less than around 200 µg l^{-1} Al, although a few have high concentrations (up to 991 µg l^{-1}; Table 6.2). In these, Al correlates with Fe. The sample of surface water collected from Santa Rita pond, which was visibly cloudy, has the highest concentrations of Fe, Mn and Al and reflects the dispersion of clays and colloids at low salinity. Although a few samples appear to have a colloidal component which can have a major effect on concentrations of trace elements due to adsorption reactions, most are clear groundwaters with negligible amounts of colloids. Colloidal transport is therefore not thought to have a major impact on the regional groundwater chemistry.

6.4 Arsenic

Arsenic concentrations in the groundwaters vary over four orders of magnitude (<4–5280 µg l^{-1}, median 149 µg l^{-1}). Of the 108 groundwaters collected, 95 % exceed the WHO guideline value of 10 µg l^{-1} and 73 % exceed the Argentine national standard of 50 µg l^{-1}. Concentrations show little distinct regional trend (Figure 6.2) but as with many other determinands, display a large spatial variability over short distances, typically of a few kilometres.

Of the 6 samples taken from the western area around Ingeniero Foster and possibly deriving from an older Triassic aquifer rather than the Pampean, only one contains As at a concentration less than the WHO guideline value (sample 962090; 8 µg l^{-1}). This sample has a relatively low HCO_3 concentration (258 mg l^{-1}) but has otherwise similar characteristics to groundwaters from the Pampean aquifer (Na-HCO_3 dominant, high Cl, SO_4; Appendix 1.1). It is likely, though not certain, that groundwater from this location is hydraulically connected to that from the overlying Pampean aquifer.

Arsenic shows no correlation with Fe, Mn or Al, although the few samples with high concentrations of these elements (taken to be colloidal) have relatively low As concentrations. This involves only around five groundwater samples and the surface-water sample from Santa Rita pond. In the remainder of samples, colloidal influence is thought to be negligible.

As a result of the oxidising condition of the groundwaters, As(V) (arsenate) is the dominant species present. Arsenic(III)/As_T ratios are typically low at around 0.017 (Figure 6.4) and the maximum observed As(III) concentration is 105 µg l^{-1} (with an As_T concentration of 4.93 mg l^{-1}).

Arsenic in the groundwaters shows a positive correlation with pH (r^2 0.46) and alkalinity (HCO_3; r^2 0.64; Figure 6.5). The high pHs generated by high degrees of silicate and carbonate reaction are thought to be the dominant control on arsenic mobilisation. At high pH, arsenate sorption onto Fe oxides in particular (but also Mn and Al oxides) is most restricted (Section 2.5). Correlations are also notable between As and other anions and oxanions, especially F (r^2 0.70), V (r^2 0.85), B, Mo, U and to a lesser extent Be (Figure 6.5). In solution, these are likely to occur dominantly as fluoride, vanadate, borate, molybdate and uranyl-carbonate species which are preferentially mobilised at high pH for the same reason as As. Mutual competition between these species as well as HCO_3 for available adsorption sites is a potential additional factor which contributes to high dissolved concentrations in the groundwaters with the highest pH values.

Although the distribution of As in the groundwaters is highly variable, there is a tendency for some of the high concentrations to occur in low-lying areas (localised depressions). Examples include groundwaters from the low terrain around Tamagnoni (adjacent to the lake which seasonally occupies the depression), and De Soria and Santa Rita in the south. The associations between terrain and groundwater chemistry are not entirely clear, but are considered to be related to the local patterns of groundwater circulation. Flow models suggest (Section 4) that the depressions are the centres of convergent localised flow which act as discharge zones during periods of high groundwater level. Although potentially diluted by surface recharge during wet periods, the depressions are likely to be zones of limited groundwater movement and lack of exit of groundwater. In this case, the degree of aquifer flushing and associated removal of desorbed ions will be restricted. Generation of high pHs in these zones can also be generated by dissolution of calcite in the aquifer under closed-system conditions with resultant reduction in pCO_2 values. As described above, high pH is considered a key process in the mobilisation of As in the Pampean groundwaters.

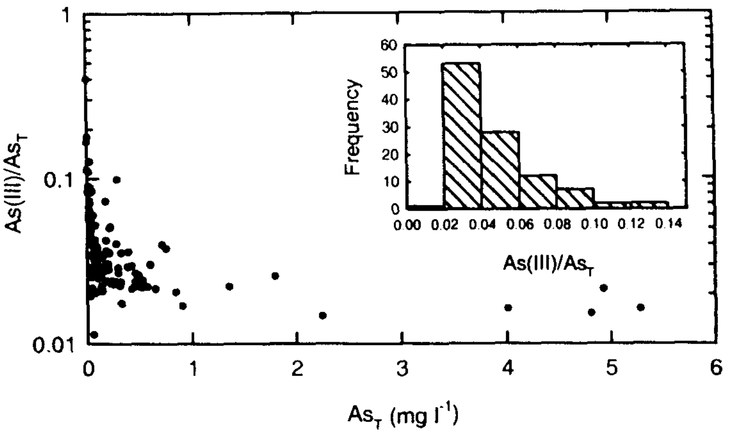

Figure 6.4 Variation of As(III)/As$_T$ ratio with As$_T$ concentration in the Pampean groundwaters

Highest concentrations of arsenic also tend to be found in wells where the saturated thickness is small, ie. those wells which penetrate only a few metres below the water table (Figure 6.6). It appears that more chemical reaction is occurring in the zone of water-table fluctuation than at greater depths.

Speciation modelling (PHREEQC using the WATEQ4F database) suggests that the groundwaters are undersaturated with respect to arsenic minerals, with the exception of barium arsenate ($Ba_3(AsO_4)_2$) which is supersaturated in many. However, this mineral has not been identified in the loess deposits and hence it is likely that the mineral saturation reflects inadequately known thermodynamic data for the mineral (Cullen and Reimer, 1989) rather than true oversaturation.

6.5 Other anions and oxyanions

As noted above, elements which form anions and oxyanions in solution generally have good positive correlations with As as a result of the high pH and alkalinity of the groundwaters and a common geochemical process, desorption, accounts for their accumulation. Of these elements, highest concentrations are observed for F which occurs in solution mainly as the fluoride ion (F^-). Concentrations range between 0.03–29.2 mg l^{-1} and 83% of groundwaters investigated exceed the WHO guideline value of 1.5 mg l^{-1} for F in drinking water (Table 6.3). Many of the high-F groundwaters are saturated with respect to fluorite. Most are significantly higher than the guideline value and the high risk of development of fluorosis problems from chronic exposure to such drinking water is clear. Fluoride correlates well with As (Figure 6.5).

Concentrations of B range between 0.46–13.8 mg l^{-1}. As with the other oxyanions, there is little distinct regional trend in concentrations (Figure 6.7). The WHO revised (1998) guideline value for B in drinking water is 0.5 mg l^{-1}. Of the samples investigated, all but one exceed this value (99% exceedance; Table 6.3) and many are significantly in excess. Boron in drinking water has been linked with gastrointestinal irritation and mutagenic effects in mice, though the health risks to humans are not well understood.

Vanadium varies between 0.02–5.4 mg l^{-1} (Table 6.2). Such concentrations are very high by world groundwater standards. No WHO guideline value exists for V and the health consequences of ingestion of the element are poorly understood. Vanadium is likely to be dominated in solution by vanadate (HVO_4^{2-}, $H_2VO_4^-$) ions. Vanadium shows a strong positive correlation with As (Figure 6.5; 6.7) and is likely to derive from similar mineral sources as well as being preferentially mobilised in the same way by high pH and alkalinity.

Table 6.3 **Exceedances of various chemical constituents above WHO guideline values (health-based) and aesthetic recommendations**

Determinand	WHO guideline value (GV)	Units	Number of samples	Number exceeding GV or recommendation	% exceedance
*Na	200	mg l^{-1}	108	105	97
*Cl	250	mg l^{-1}	108	47	44
*SO_4	250	mg l^{-1}	108	61	56
NO_3-N	11.3	mg l^{-1}	108	51	47
NO_2-N	0.91	mg l^{-1}	108	0	0
*NH_4-N	1.24	mg l^{-1}	83	0	0
As_T	10 (P)	μg l^{-1}	108	103	95
*Al	200	μg l^{-1}	108	6	5.6
*Fe_T	0.3	mg l^{-1}	108	12	11
Mn	500	μg l^{-1}	108	0	0
Ba	700	μg l^{-1}	108	0	0
**B	500 (P)	μg l^{-1}	108	107	99
F	1.5	mg l^{-1}	108	90	83
Cr	50 (P)	μg l^{-1}	107	0	0
Ni	20	μg l^{-1}	107	0	0
Cu	2000 (P)	μg l^{-1}	107	0	0
*Zn	3000	μg l^{-1}	107	0	0
Mo	70	μg l^{-1}	107	42	39
Cd	4	μg l^{-1}	107	0	0
Sb	5 (P)	μg l^{-1}	107	0	0
Ba	700	μg l^{-1}	107	0	0
Pb	10	μg l^{-1}	107	1	1
**U	2 (P)	μg l^{-1}	107	107	100

*WHO recommendation on aesthetic grounds
**1998 addendum to 1993 Volume
P: provisional value

Molybdenum varies in concentration between 2.7–991 μg l^{-1} (Table 6.2). Of the sources investigated, 39% exceed the WHO guideline value of 70 μg l^{-1}. Molybdenum is weakly correlated with As (Figure 6.5).

Uranium concentrations range from 6–248 μg l^{-1} (all samples exceed the revised WHO (1998) guideline value for drinking water of 2 μg l^{-1}; Table 6.3). At the pHs of the groundwaters, the dominant dissolved species are likely to be uranyl carbonate complexes ($UO_2(CO_3)_2^{2-}$, $UO_2(CO_3)_3^{4-}$). A good positive correlation is observed between U and HCO_3 in the groundwaters (as for the other oxyanions).

Concentrations of P are high in some samples, the range varying between <0.2–0.7 mg l^{-1}. Beryllium concentrations vary between <0.01–0.4 μg l^{-1}. The absolute concentrations are low but are relatively high compared to average groundwater compositions. Beryllium shows a weak positive correlation with As (Figure 6.5).

The mineral sources of all these anions and oxyanions are not clearly identified. Important sources could be the primary volcanic minerals in the loess and ash deposits. For example, F is likely to be present in detrital minerals such as biotite and apatite. However, adsorption on surfaces of Fe, Mn and Al oxide minerals also seems likely and desorption from these surfaces under the ambient high-pH and high-alkalinity conditions is believed to be a potentially important controlling process.

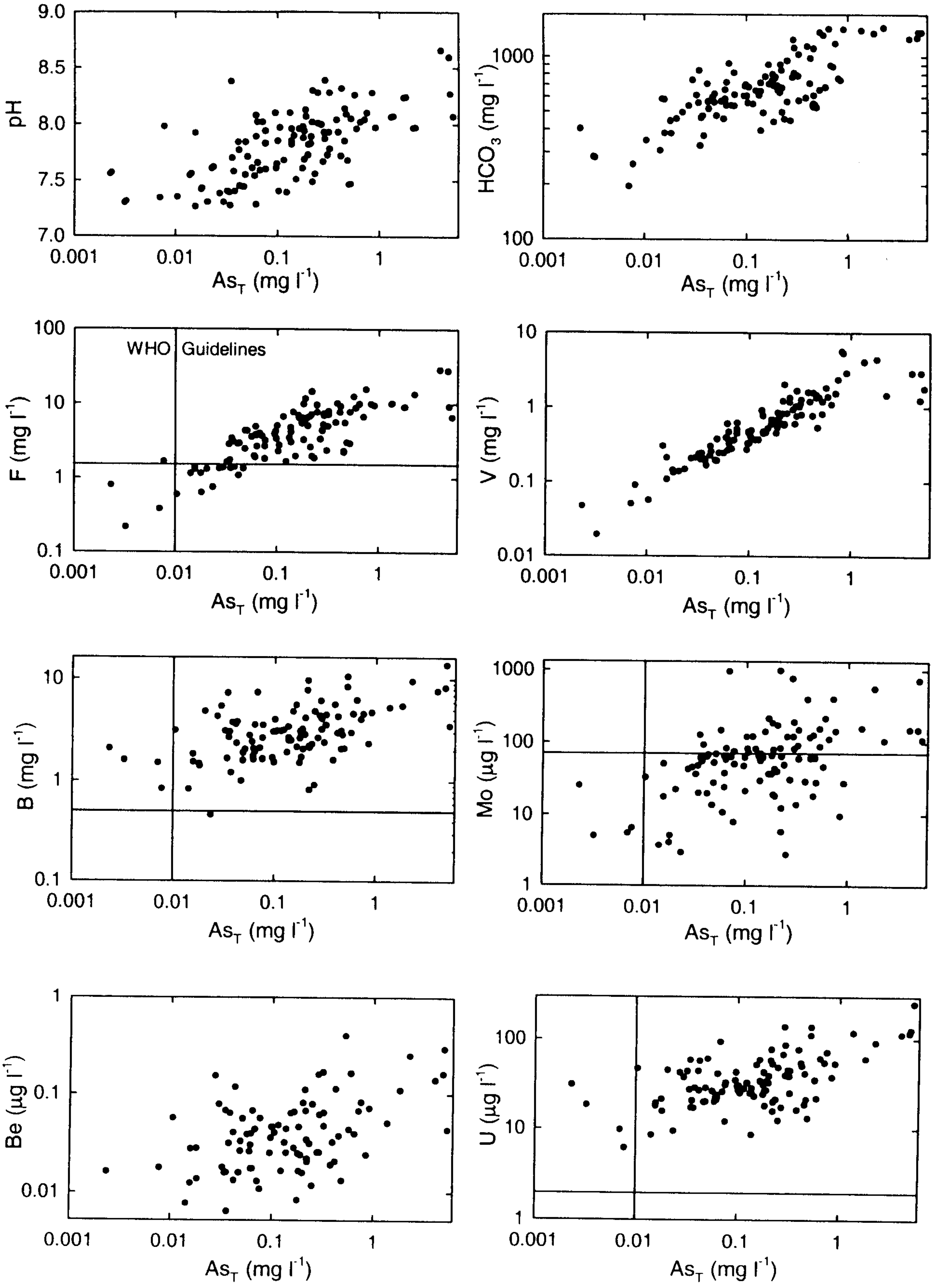

Figure 6.5 Variation of As_T concentrations with pH, HCO_3, F, V, B, Mo, Be and U in the Pampean groundwaters (two samples of surface water are also included)

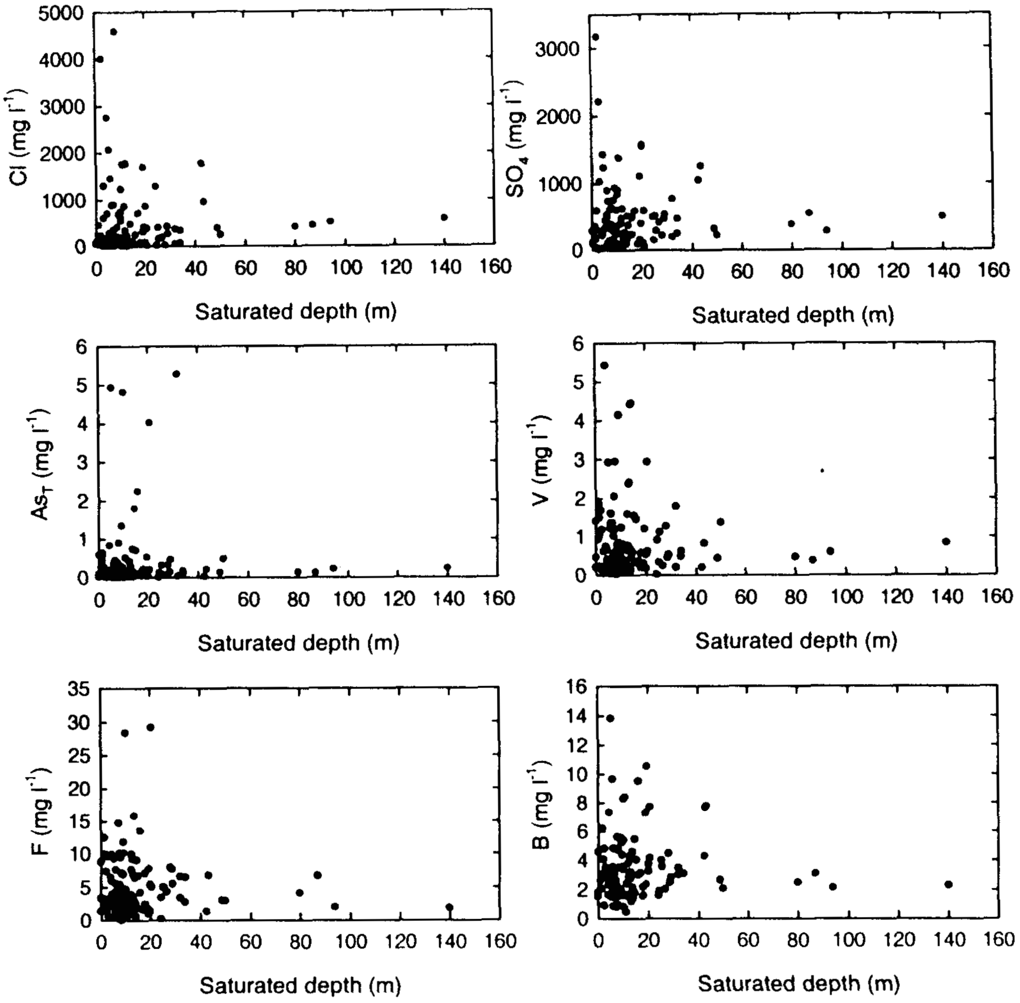

Figure 6.6 Variation of Cl, SO_4, As$_T$, V, F and B in the Pampean groundwaters with saturated depth (total well depth minus water level, in metres)

The fact that many of these constituents have assigned WHO drinking-water guidelines indicates that some health risk is attached to them from chronic exposure. The groundwaters are therefore potentially detrimental as potable water sources. However, since these ions are strongly correlated because of their similar hydrochemical behaviour, identification of sources with lowest As concentrations will coincidentally identify sources with the lowest concentrations of the other problem elements in this group. Arsenic shows no discernible correlation with groundwater salinity. However, of the low-As groundwaters investigated, it is unfortunate that many are relatively saline and hence also largely unsuitable for potable use. Of the samples investigated with As concentrations <50 µg l^{-1}, only 9 (32%) have SEC concentrations less than 2000 µS cm^{-1} and hence are of low salinity. These are also Na-HCO$_3$-dominated waters but have pH values close to neutral.

6.6 Other trace elements

6.6.1 Transition metals

Concentrations of many of the transition metals are relatively low. Nickel concentrations reach up to 19 µg l^{-1} (less than the WHO guideline value of 20 µg l^{-1} for drinking water). Chromium reaches up to only 20 µg l^{-1} despite its preferential mobility under oxidising conditions. Cobalt reaches a maximum of 1.3 µg l^{-1} and Cd occurs at up to 2 µg l^{-1} with most samples being less than 0.5 µg l^{-1}.

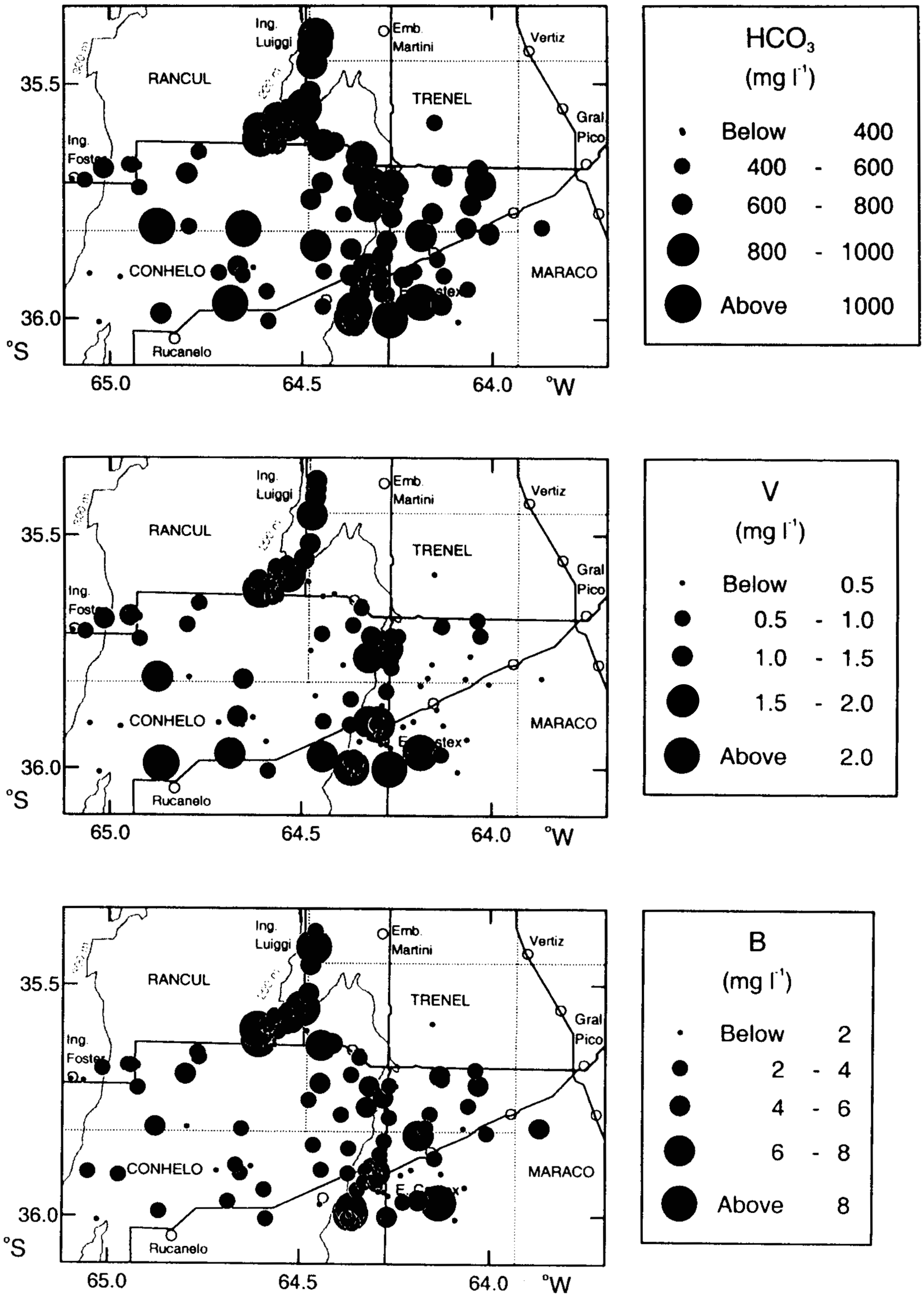

Figure 6.7 **Regional variation in HCO_3, V and B in groundwaters from La Pampa**

The low concentrations of many of the transition metals are believed to reflect the acidic composition of the loess sediments and ashes (dacitic and rhyolitic) which themselves have low concentrations of these elements, as well as the alkaline nature of the groundwaters.

Concentrations of Cu and Zn reach up to 89 μg l^{-1} and 1438 μg l^{-1} respectively. These maxima are relatively high but are not known to be detrimental to health. The WHO guideline value for Cu on health grounds is 2000 μg l^{-1}, much higher than the observed concentration range. No guideline value exists for Zn.

6.6.2 *Alkali metals*

Lithium, Rb and Cs concentrations reach up to 147 μg l^{-1}, 32 μg l^{-1} and 0.22 μg l^{-1} respectively. The concentrations are relatively high and reflect their likely abundance in the volcanic material of the host aquifer.

6.6.3 *Alkaline earth elements*

Strontium reaches up to 13 mg l^{-1} in the groundwaters. Celestite is undersaturated in the samples.

Barium concentrations are relatively low, having an observed range of 5–259 μg l^{-1}. The concentrations are much less than the WHO guideline value of 700 μg l^{-1} for drinking water. Concentrations are limited by barite solubility. Many of the groundwaters are saturated or oversaturated with respect to barite.

6.6.4 *Halogens*

Iodine concentrations range between 17–730 μg l^{-1} and are relatively high compared to world-average groundwater compositions. The sources potentially include carbonate minerals in the aquifer or organic matter in the surface soil horizons. Iodine in the groundwaters correlates positively with Mo and Cd (r^2 >0.7). Bromide concentrations are also high in most groundwaters, varying between 0.06–12 mg l^{-1}. Concentrations are highest in the more saline samples and Br correlates well with Cl.

6.6.5 *Rare earth elements (REE)*

Most of the groundwaters have REE concentrations below detection limits (which are highly variable due to differences in dilution factors used for analysis). In samples where the REE are detectable, these are usually dominated by the light REE (La, Ce, Pr, Nd) and often the middle and heavy REE are below detection limits. Shale-normalised (Sholkovitz, 1988) REE profiles for the few samples that have detectable concentrations are shown in Figure 6.8. Such plots are a means of comparing observed data with world-average shale values as an aid to identification of possible origins. The trends vary in

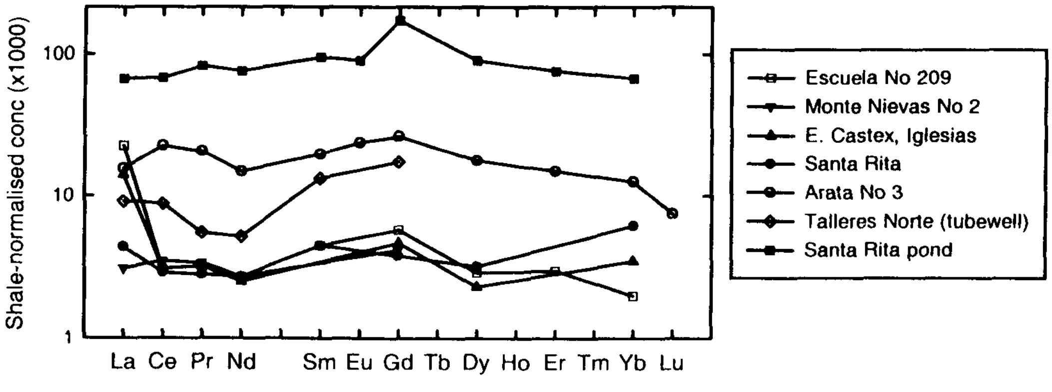

Figure 6.8 **Shale-normalised REE profiles for groundwaters with detectable concentrations**

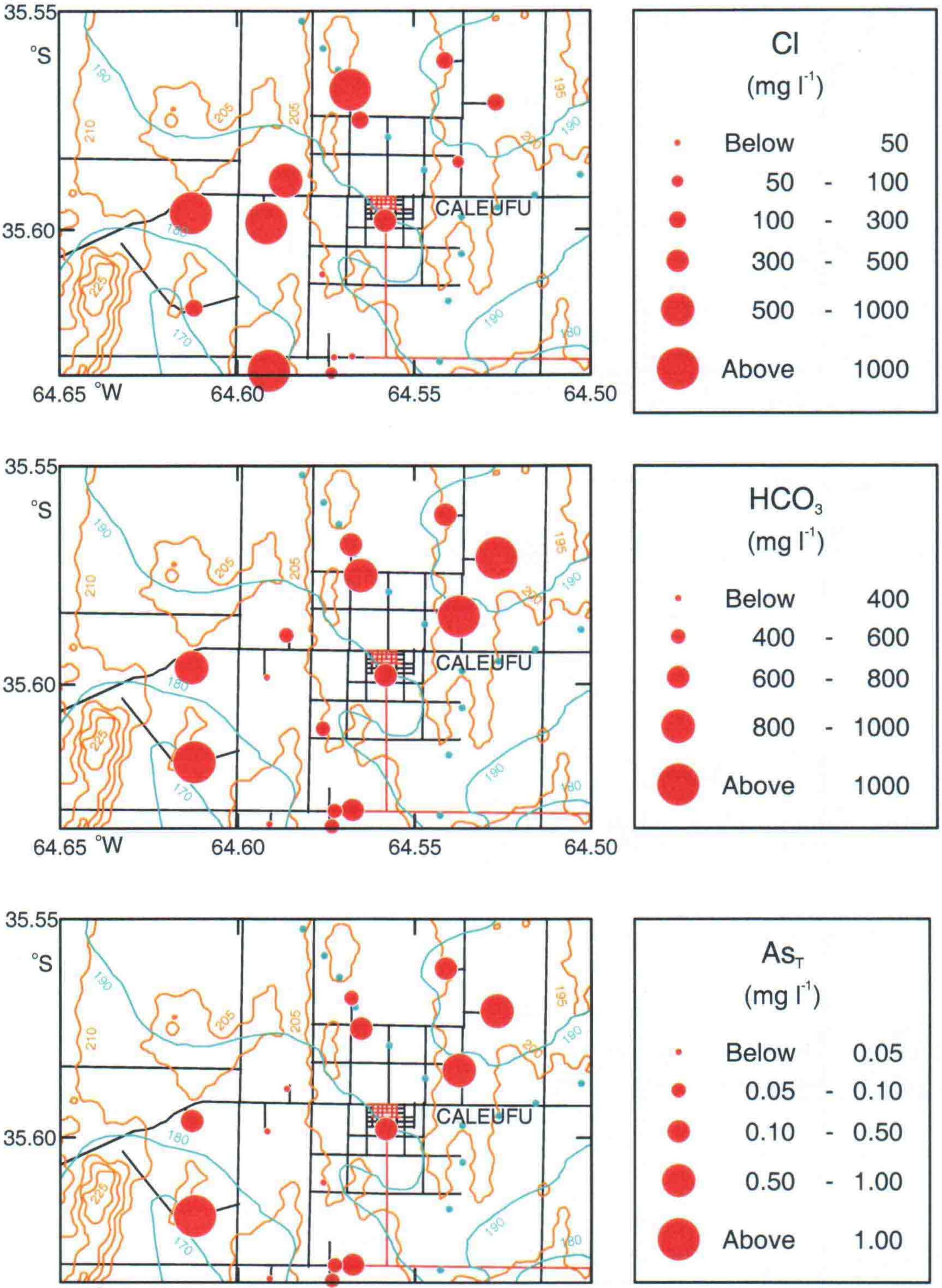

Figure 6.10 **Regional variation in Cl, HCO_3 and As_T in groundwaters from the Caleufu area, contours (m) in brown, water levels (m above OD) and groundwater divide in blue**

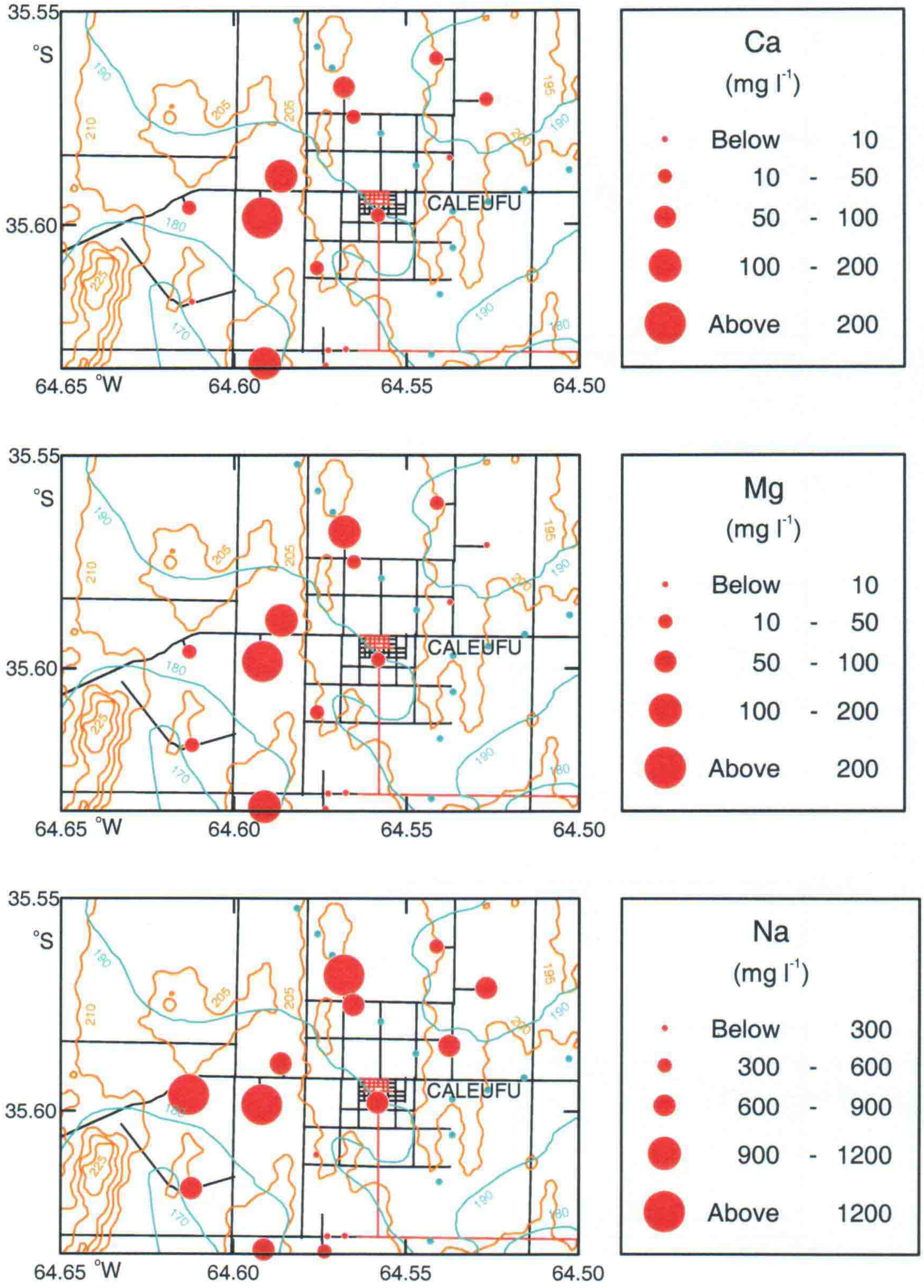

Figure 6.9 **Regional variation in Ca, Mg and Na in groundwaters from the Caleufu area, contours (m) in brown, water levels (m above OD) and groundwater divide in blue**

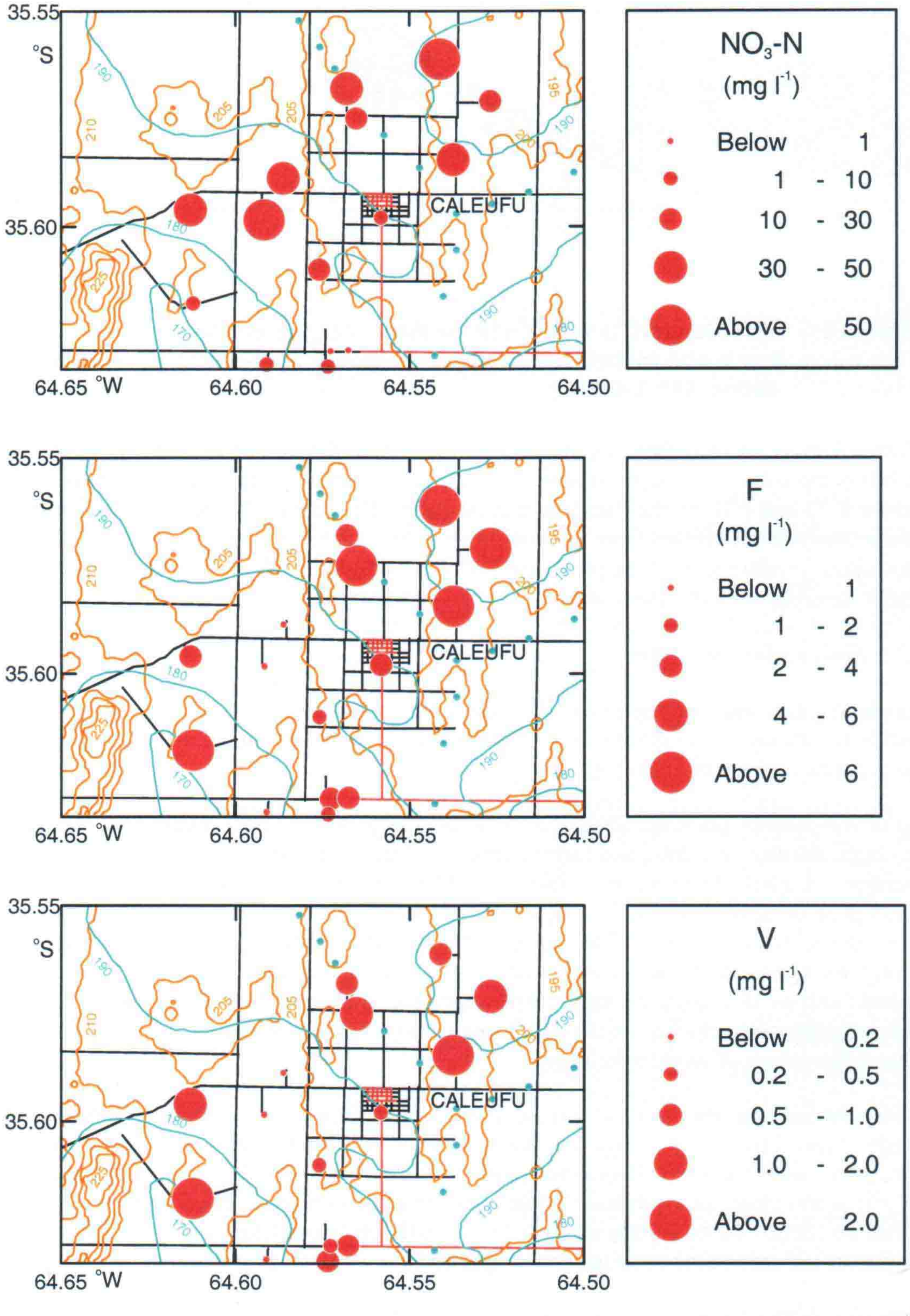

Figure 6.11 Regional variation in NO$_3$-N, F and V in groundwaters from the Caleufu area, contours (m) in brown, water levels (m above OD) and groundwater divide in blue

absolute concentrations but are generally flat relative to shale. None displays a negative Ce anomaly as is occasionally found in groundwaters (e.g. Smedley, 1991). The sample with the highest concentrations is Santa Rita pond (LP35) in which ΣREE is 12.7 μg l^{-1}. This sample was cloudy and has high concentrations of Fe and Al (1.5 mg l^{-1} and 2.3 mg l^{-1} respectively). The sample therefore probably contains colloidal particles of Fe and Al and the REE are thought to be associated with these rather than being in dissolved form.

Other samples with detectable REE concentrations have similar trends to that from Santa Rita pond and have slightly higher concentrations of Al in particular than other samples collected. It is therefore thought that these are also REE associated with the colloidal fraction. This is reasonable given the high pH of the Pampean groundwaters which should not favour stabilisation of detectable concentrations of REE in solution.

6.7 Local-scale chemical variations: Caleufu

The high degree of spatial variation in chemical compositions of the Pampean groundwaters is highlighted from more detailed sampling carried out in the Caleufu area of Rancul Department (ca. 20 km south of Ingeniero Luiggi; Figure 3.1). Selected determinands are plotted for the area in Figures 6.9–6.11, along with topographic and piezometric information (the latter from DDA data and maps). The maps cover an area of some 13 km x 8 km. Over the scale of just a few kilometres, salinity varies from relatively fresh to brackish groundwater (SEC values in the range 1340–15000 μS cm^{-1}). Well depths of these samples range between 7–56 m with no obvious chemical variation with depth on this local scale. Concentrations of As and other anions and oxyanions (F, HCO_3, V) are also highly spatially variable. The main observation is that the most saline samples have the lowest concentrations of these constituents as these are dominantly Na-Cl rather than Na-HCO_3 waters and have lower pH values than the HCO_3-dominant waters.

The plots in Figures 6.9–6.11 indicate the location of the local groundwater divide and piezometric levels. Although there is considerable variation, it appears that the highest As (and HCO_3, F, V) concentrations occur away from the groundwater divide, in the areas where groundwater levels are lowest (south-west and north-eastern areas). High concentrations also correlate with small degree of well penetration of the saturated aquifer (ie. where water is abstracted from close to the water table). These observations mirror those from the survey of the region as a whole (Section 6.4).

6.8 Isotopic compositions and groundwater residence time

Stable-isotopic compositions together with tritium and radiocarbon were analysed in selected groundwater samples to investigate groundwater residence times in the Pampean aquifer and to assess their likely geochemical evolution. Isotopic data are given in Appendix 1.7 and summarised with groundwater ^{14}C model ages in Table 6.4.

6.8.1 $\delta^{18}O$ and $\delta^{2}H$

Observed ratios of $\delta^{18}O$ in the groundwaters are in the range -6.4 to -3.8 ‰ and $\delta^{2}H$ in the range -36 to -23 ‰. The compositions do not show any distinct regional trend or trend with well depth, but as with the chemical data, display much variability on a local scale. The compositions show a very slight enrichment with increasing salinity but this is not marked. Ratios for $\delta^{18}O$ and $\delta^{2}H$ are -4.4 ‰ and -27 ‰ respectively in the most saline sample collected (Dorila, TDS 11,460 mg l^{-1}). This is not the most enriched composition and is not significantly more enriched than the mean values for these isotopes.

Two samples from the seasonal lakes (Santa Rita and the 'lake' next to Tamagnoni) gave extreme isotopic compositions of -7.1‰ and -2.3 ‰ respectively for $\delta^{18}O$ and of -41‰ and -16 ‰ respectively for $\delta^{2}H$. In the case of Santa Rita, the depleted values (most negative) are taken to be representative of

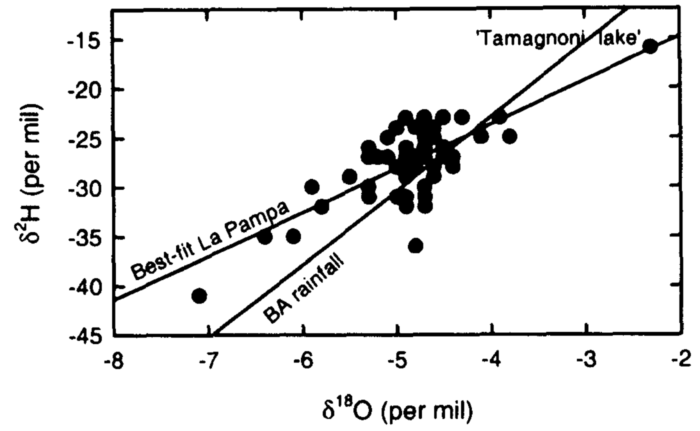

Figure 6.12 **Variation of $\delta^{18}O$ with $\delta^{2}H$ in the Pampean groundwaters. The best-fit regression line is also plotted for the data, alongside data for rainfall from Buenos Aires station (IAEA data)**

modern winter recharge without significant modification. In the case of the Tamagnoni lake, the more enriched composition is thought to have been caused by surface evaporation. Figure 6.12 shows the trend for $\delta^{18}O$ and $\delta^{2}H$ for the Pampean groundwaters. The best-fit line for the data has a shallower gradient than that for rainfall from Buenos Aires meteorological station (IAEA, 1999). The enriched composition therefore looks to be offset to higher $\delta^{18}O$ values than the curve for meteoric water which supports the suggestion that the water has undergone evaporation.

6.8.2 Radiocarbon and tritium

Radiocarbon data indicate measured ^{14}C activities ranging between 26 and 71 pmc (Table 6.4). Groundwater dating of the samples was attempted using the Fontes and Garnier (1979) model, using input parameters given in Table 6.4.

Most of the samples investigated appear to be modern in terms of ^{14}C model ages (negative model ages obtained using the Fontes and Garnier model). Some contain tritium and so are likely to include a component of post-1950s recharge (Table 6.4). However, many have no detectable tritium and are thought to be dominantly pre-1950s, although still modern in ^{14}C terms (order of decades likely). The only sample with a registrable ^{14}C model age is from Conhelo 4 (LP41; Table 6.4). Sensitivity analysis produces a range of model ages for this sample from modern up to 1300 years. This was the deepest analysed (well depth 140 m) and suggests that deeper groundwaters from the region may have slightly longer residence times. However, the sample also has measurable tritium (1.9 TU) and hence contains at least a component of modern recharge.

Correlations between the various isotopic compositions measured are generally poor. High-tritium (youngest) groundwaters generally have more depleted $\delta^{18}O$ compositions (Figure 6.13) and suggest that some climatic variations have taken place during recharge at different periods. The relationship with $\delta^{2}H$ is less clear, although some of the more enriched compositions also tend to be found in the low-tritium waters. There is little discernible correlation between tritium and $\delta^{13}C$ and ^{14}C shows no relationship with any of the other isotopes (Figure 6.12).

Values for $\delta^{18}O$ ranging between -6.4 ‰ and -4.7 ‰ and $\delta^{2}H$ between -36 ‰ and -24 ‰ are established from the radiocarbon data (Table 6.4) as being of young age. Lack of significant variation from these values with well depth in other samples analysed suggests that the age variation of the groundwaters abstracted from the aquifer is not great. In general, most of the groundwaters appear to be 'young' in ^{14}C terms (although low tritium concentrations in many suggest that these have residence times of the order of tens to hundreds of years).

Table 6.4 Collated isotopic data for groundwater samples from La Pampa

Sample	Field number	$\delta^{18}O$ ‰	$\delta^{2}H$ ‰	$\delta^{13}C$ ‰	Tritium TU	^{14}C pmc	^{14}C date years
970686	LP36	-5.3	-26	-9.1	8.7	63.1	Modern
970690	LP40	-6.1	-35	-9.8		47.4	Modern
970691	LP41	-4.7	-32	-9.1	1.9	26.4	Up to 1300
970692	LP42	-4.7	-27		2.5	53.0	Modern
970694	LP44	-5.0	-31	-12.2	0.0		
970697	LP47	-4.7	-25	-8.9	0.0	58.5	Modern
970776	LP59	-4.8	-24	-6.2	0.1	60.0	Modern
970781	LP64	-4.9	-28	-5.9	0.6	70.6	Modern
970788	LP71	-5.1	-27	-6.9	1.8	58.5	Modern
970795	LP78	-4.8	-36	-12.3	0.3	53.3	Modern
970797	LP80	-6.4	-35	-9.1	5.8	38.3	Modern

^{14}C model dates calculated taking activity of soil CO_2 as 103.7 % (Fontes and Garnier, 1979), $\delta^{13}C$ of soil CO_2 as -23 ‰ (Clark and Fritz, 1997), $\delta^{13}C$ of solid $CaCO_3$ as varying between 0 ‰ and -3.7 ‰ from literature carbonate values and measured values for calcrete, activity of solid $CaCO_3$ as 0% (ie. assuming carbonate in the aquifer to contain only dead carbon) and the isotopic fractionation factor between gaseous CO_2 and solid $CaCO_3$, ε, calculated at aquifer temperature from values given by Deines et al. (1974). Half life of ^{14}C is taken as 5730 years

6.8.3 $\delta^{13}C$

The observed range for $\delta^{13}C$ is between -12.8 and -4.0 ‰. Assuming that soil zone CO_2 has a $\delta^{13}C$ value in the range -23 to -25 ‰ (Fontes and Garnier, 1979) and carbonate minerals in the aquifer have values close to 0 ‰, evolution of groundwaters by carbonate reaction should drive the $\delta^{13}C$ isotopic compositions towards more enriched compositions. Indeed, three samples of calcrete from the aquifer gave $\delta^{13}C$ values of -1.1, -1.4 and -3.7 ‰ (Table 6.5). The most depleted groundwater samples analysed (-12 ‰) have undergone least carbonate reaction while the most enriched samples have apparently undergone considerable reaction. Observed $\delta^{13}C$ values show a weak positive correlation with HCO_3 (Figure 6.14) in support of the evidence for evolution of $\delta^{13}C$ by carbonate reaction. The correlation is presumably not strong because of the additional inputs of HCO_3 from silicate reaction.

The $\delta^{13}C$ compositions vary with well depth, with most enriched compositions being found in the shallowest groundwaters. This is probably because layers of calcrete are common in the top few metres of the aquifer in many parts and because relatively high pCO_2 values can be achieved at shallow depths from bacterial reactions in the soil and are able to drive carbonate dissolution. The groundwater sample with lowest ^{14}C activity and likely greatest aquifer residence time (Conhelo 4) has a relatively depleted $\delta^{13}C$ ratio of -9.1 ‰ (Table 6.4). This suggests that carbonate reaction has not been extensive in this sample and that $\delta^{13}C$ cannot be used as a residence-time indicator, but merely as a measure of degree of reaction.

6.8.4 $\delta^{34}S$

Data for $\delta^{34}S$ in selected groundwaters are given in Appendix 1.7 and plotted against SO_4 concentration in Figure 6.15. The values average 7.8 ‰ and show little variation (6.3–8.7 ‰), even given the large range of SO_4 concentrations (up to 3100 mg l^{-1}). Sulphur-isotopic compositions were measured to investigate the possibility that dissolved SO_4 (and As) were derived by oxidation of pyrite in the aquifer. Pyrite has not been identified in thin sections of the loess sediments but may feasibly be present as finely-disseminated grains. Sulphur-isotopic compositions of biogenic pyrite are highly variable but generally recognised to be relatively depleted (typical range -20 ‰ to 0 ‰; Clark and Fritz, 1997). The distinct range of $\delta^{34}S$ values in the Pampean groundwaters indicates that pyrite is

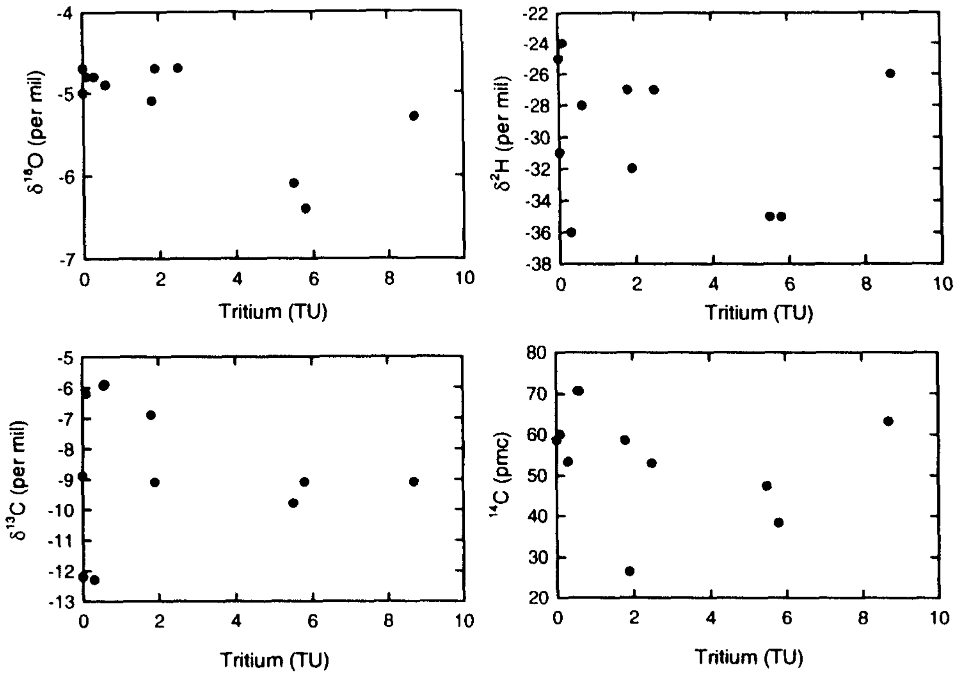

Figure 6.13 Variation in tritium concentration with stable isotopes and ^{14}C in groundwaters from La Pampa

unlikely to be involved in the production of SO_4 in the groundwaters and is hence also not likely to be a feasible source of As.

Evaporite minerals are the most likely alternative source of SO_4 in the groundwaters; salt encrustations are common around sites of evaporation (depressions) during dry seasons and some of the porewaters investigated are saturated with respect to gypsum. Sulphur-isotopic ratios were not measured in sulphate minerals from the study area. However, the range found for $\delta^{34}S$ in terrestrial evaporites, although large, (-15 ‰ to 10 ‰; Clark and Fritz, 1997), covers the range of values observed for SO_4 in the groundwaters. Little sulphur-isotopic fractionation is involved in dissolution or precipitation of gypsum (Clark and Fritz, 1997).

6.9 Porewater chemistry

Results of the chemical analysis of porewater samples collected from the two cored boreholes at Talleres Norte and Tamagnoni are given in Appendices 3.1–3.4 and chemical profiles are shown in Figures 6.16–6.20. Careful attempts were made during drilling to minimise the effects of cross-contamination of core porewaters by groundwater from overlying horizons. However, maintenance of sample integrity cannot in all cases be guaranteed and contamination may have occurred in some samples. In Talleres Norte borehole, possible contamination may have occurred in the topmost two samples (TN5, TN6) as well as samples TN22, TN25 and TN35. In Tamagnoni borehole, the topmost sample TN9 may have been affected, as well as sporadic samples from greater depth (TAM22–24, TAM26, TAM30, TAM32, TAM46, TAM48, TAM50) This is nonetheless thought to be relatively minor and not materially important to the overall interpretation of the chemical profiles.

6.9.1 Talleres Norte borehole

All porewater samples were recovered from the saturated zone. Analysis of moisture contents therefore gives an indication of the porosity of the sediments, which is variable between 22% and 40% but averages around 30% throughout the profile down to its base at 26.5 m depth.

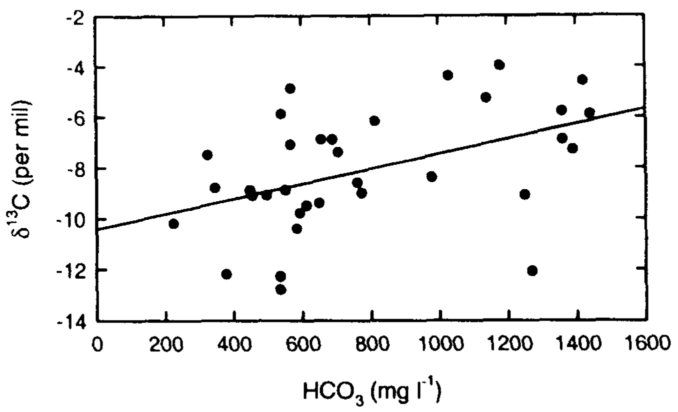

Figure 6.14 Variation in HCO_3 with $\delta^{13}C$ in groundwaters from La Pampa

Salinity of the porewaters is relatively low, with SEC values varying between around 600 µS cm^{-1} and 2000 µS cm^{-1} (Figure 6.16). Salinity increases gradually with depth, although the topmost sample also has relatively high salinity. This is shown by high SEC values as well as Na, Cl, SO_4, B, and Br concentrations. As noted above, the topmost sample may be unrepresentative but the deeper salinity profile is considered to be real. The porewater compositions compare well with those of pumped groundwaters from the site which reveal increasing salinity with depth, SEC values giving 1220 µS cm^{-1} at 12 m depth and 6760 µS cm^{-1} at 48 m, below the base of the cored profile.

Porewater pH varies relatively little in the porewaters, although is slightly higher (>8.5) betweeen 12–25 m depth. Calcium, Mg and Sr also vary little, although the topmost sample has much higher concentrations of these elements than those below (Figure 6.16). As with the pumped groundwaters, concentrations are low relative to Na.

By contrast, concentrations of NO_3-N decrease with depth, with a maximum of 9 mg l^{-1} close to the water table and values decreasing down to <0.2 mg l^{-1} from 16 m depth to the base of the borehole. The concentration in the pumped groundwaters from Talleres Norte was 2.9 mg l^{-1} at 48 m depth. Although this concentration is relatively low, the fact that it is higher than in the deepest part of the cored borehole suggests that a degree of drawdown of higher nitrate water from near the water table has occurred in the pumped borehole. The low NO_3-N concentrations of deeper porewaters is not thought to relate to NO_3-N reduction as the porewaters are largely oxidising. It is more likely that the low values reflect lack of pollution at depths greater than 16 m and historically efficient capture of atmospheric nitrogen by soils and plants.

Concentrations of Fe, Mn and Al are low in many of the Talleres Norte porewater samples but are relatively high in some samples from the middle section. The three elements are correlated which suggests that the affected samples have a significant colloidal component. Concentrations of Fe, Mn and Al in the pumped groundwaters from the site were found to be around 500 µg l^{-1}, 7 µg l^{-1} and 900 µg l^{-1} respectively. The Fe, Mn and Al concentrations in porewaters from the middle section reach up to 3.9 mg l^{-1}, 89 µg l^{-1} and 3.5 mg l^{-1} respectively. Concentrations of some of the trace elements (Figure 6.17), especially the REE, Y, Th and Co, show similarly spiky patterns which are probably due to association with colloidal material rather than the dissolved component of the porewaters.

Concentrations of F vary between 2.9–25.7 mg l^{-1} with the lowest values observed at around 9–10 m depth and highest values present from around 17 m depth to the base of the borehole. The porewaters are saturated with respect to fluorite in all sampes except those with lowest F concentrations at around the 10 m interval. Saturation with respect to fluorite ensures that concentrations of F are limited at around the 26 mg l^{-1} maximum. Concentrations of F in the pumped Talleres Norte groundwater samples are broadly comparable at 12 m depth (14.7 mg l^{-1}) but appear to be lower below the depth range of the cored borehole (being 6.8 mg l^{-1} at 48 m depth).

Table 6.5 **Carbon- and oxygen-isotopic ratios for samples of calcrete from the study area (all samples analysed in duplicate)**

Sample location	$\delta^{13}C$ ‰	$\delta^{18}O$ ‰	Description
Estancia la Sabina	-1.1	-2.3	Avg. ground and unground
Iglesias Evangelicus	-1.4	-3.0	Ground
Las Tres Hermanas	-3.7	-3.5	Ground

Concentrations of V are broadly comparable with those of F, with a maximum of 1.7 mg l^{-1} at 17.5 m depth. The As profile also shows some similarities with V and F, with a corresponding minimum at around 9–10 m depth and a maximum of 530 μg l^{-1} at 21 m. The profiles of As, V and F all show some correlation with that of HCO_3, as with samples from the regional survey. The concentrations also tend to be highest where pH values are above 8.5, although the correlation with pH is not so striking in the porewaters.

Concentrations of Ba are high in the topmost porewater sample but much lower and relatively uniform throughout the rest of the borehole. The shallow porewater is correspondingly saturated with respect to barite. Samples deeper than 15 m are also saturated with respect to barite as a result of higher SO_4 concentrations, but porewaters from the middle section of the profile are undersaturated (Figure 6.20).

Concentrations of B and U have some similarities, with generally increasing trends in both with depth with maxima at around 25 m. Molybdenum is generally low (<60 μg l^{-1}) throughout the profile but increases significantly, to >100 μg l^{-1} in the bottom four samples (lowermost 2 m of core).

6.9.2 Tamagnoni borehole

As noted in Section 5.2.1, the Tamagnoni borehole is located close to a localised depression which infills with water during the wet season and which undergoes evaporation during dry intervals. The site is therefore considered to be one of seasonal discharge of slow-moving groundwater and the locus of seasonal evaporative concentration of salts.

One of the most striking features of the Tamagnoni profile is the much enhanced salinity of the porewaters in the topmost 5 m of core (Figures 6.18–6.19). SEC values reach up to 10000 μS cm^{-1} at

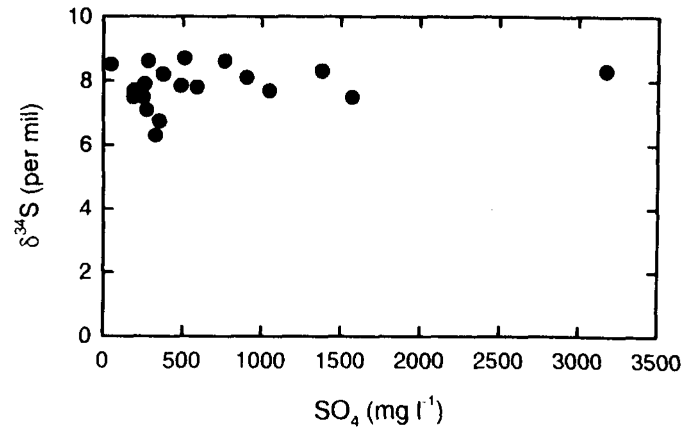

Figure 6.15 **Variation of $\delta^{34}S$ with SO_4 in groundwaters from La Pampa**

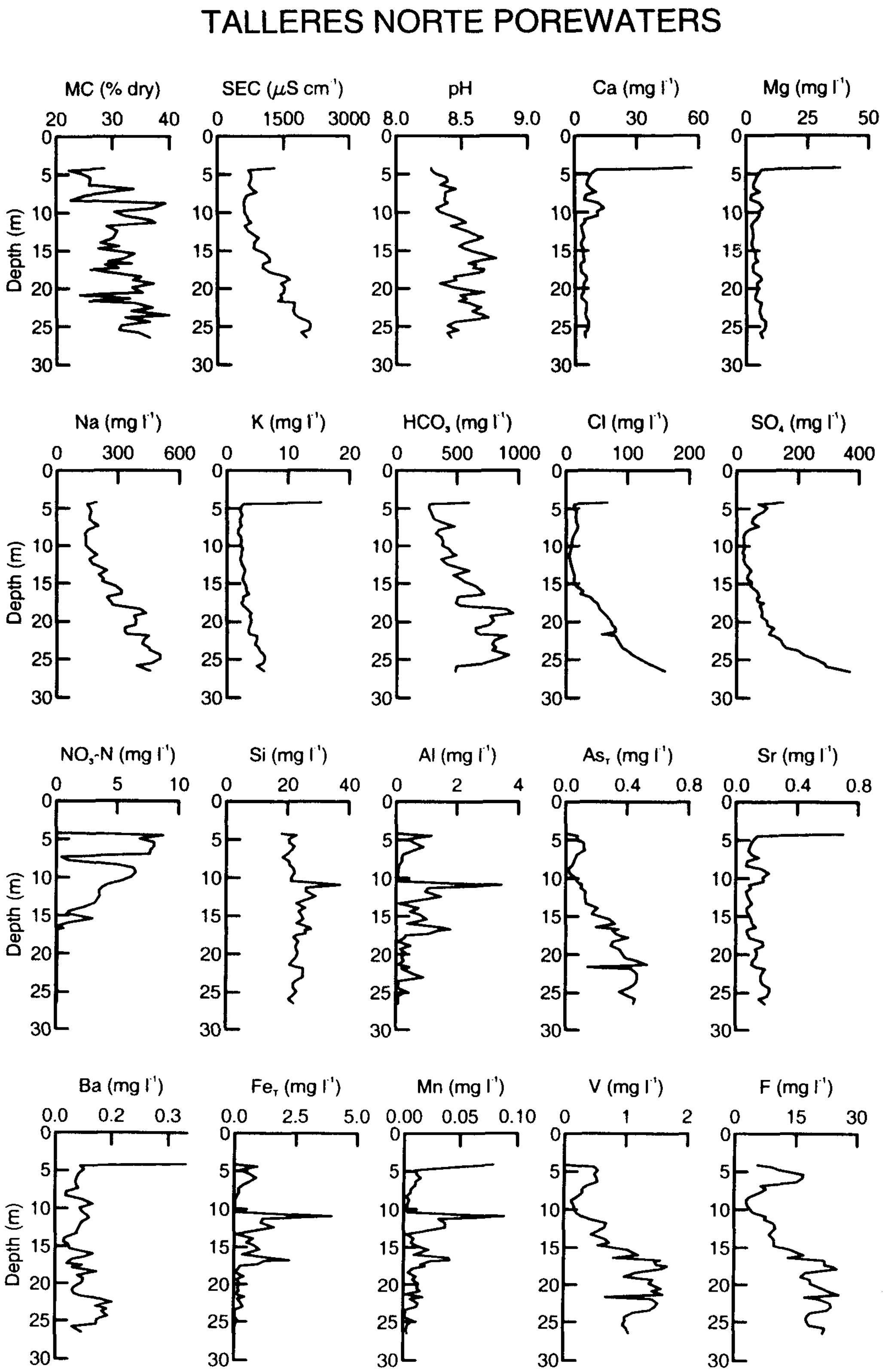

Figure 6.16 Porewater profiles for selected major and trace constituents in the Talleres Norte cored borehole

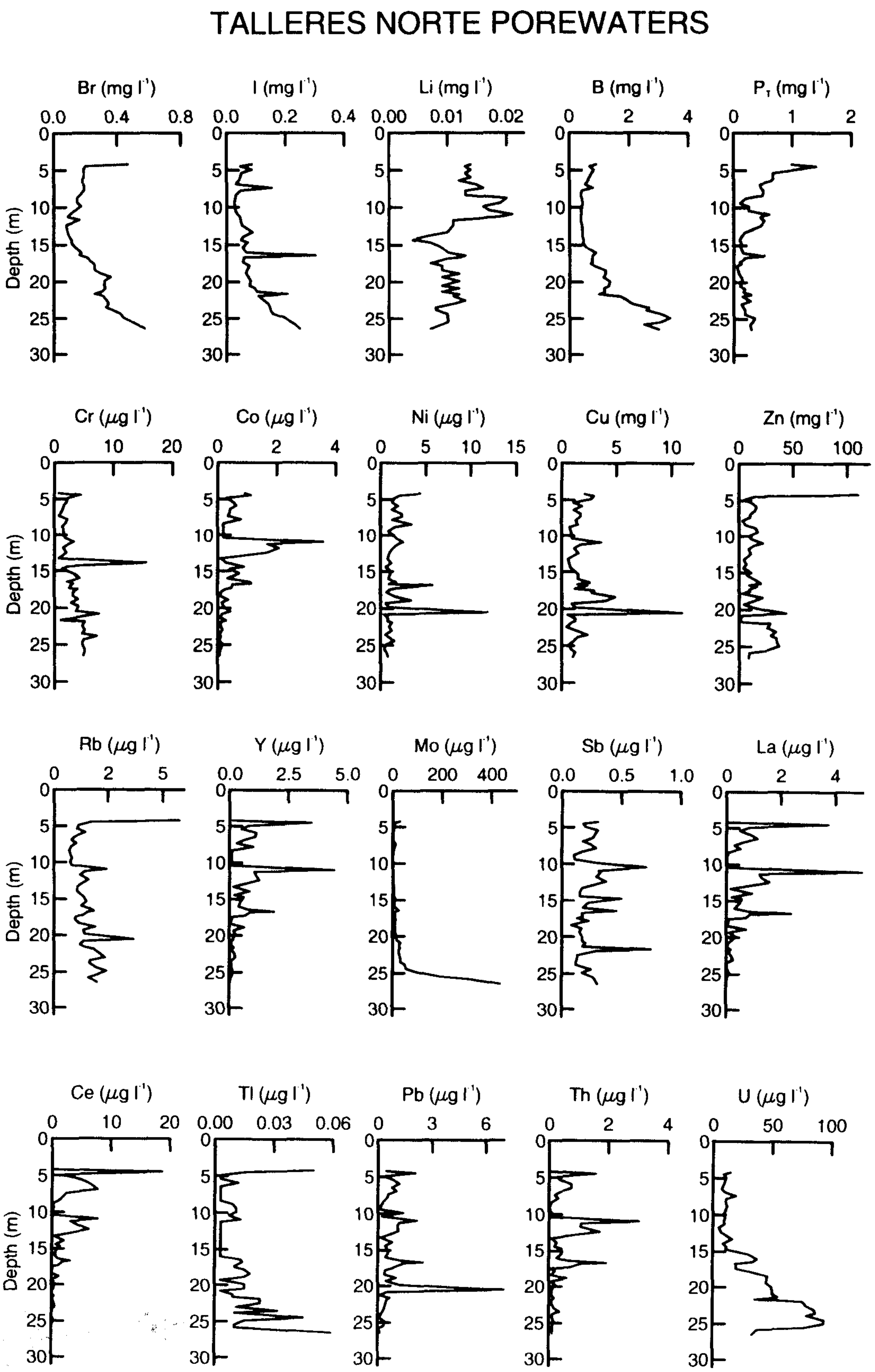

Figure 6.17 Porewater profiles for selected trace constituents in Talleres Norte cored borehole

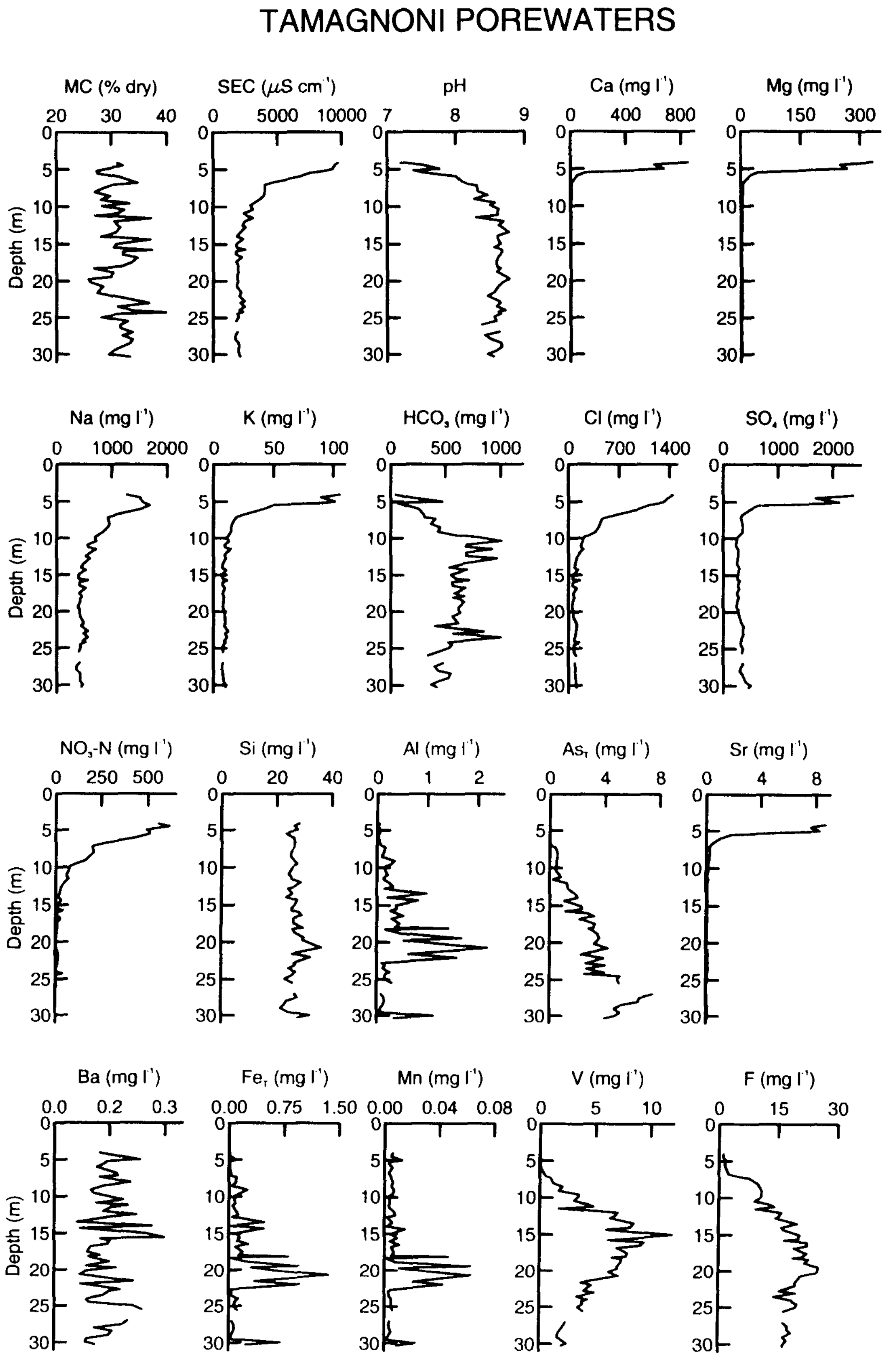

Figure 6.18 Porewater profiles for selected major and trace constituents in the Tamagnoni cored borehole

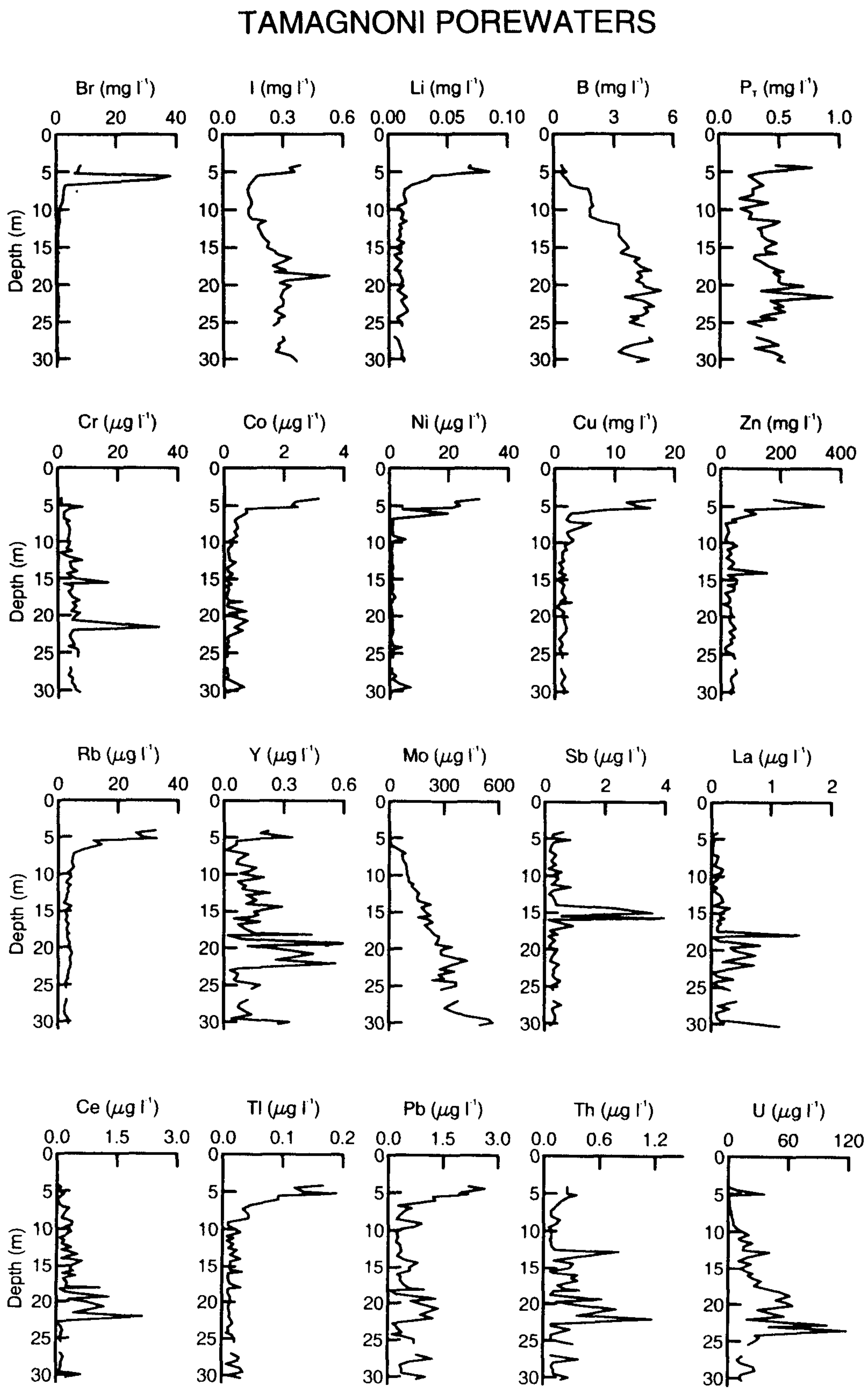

Figure 6.19 Porewater profiles for selected trace constituents in Tamagnoni cored borehole

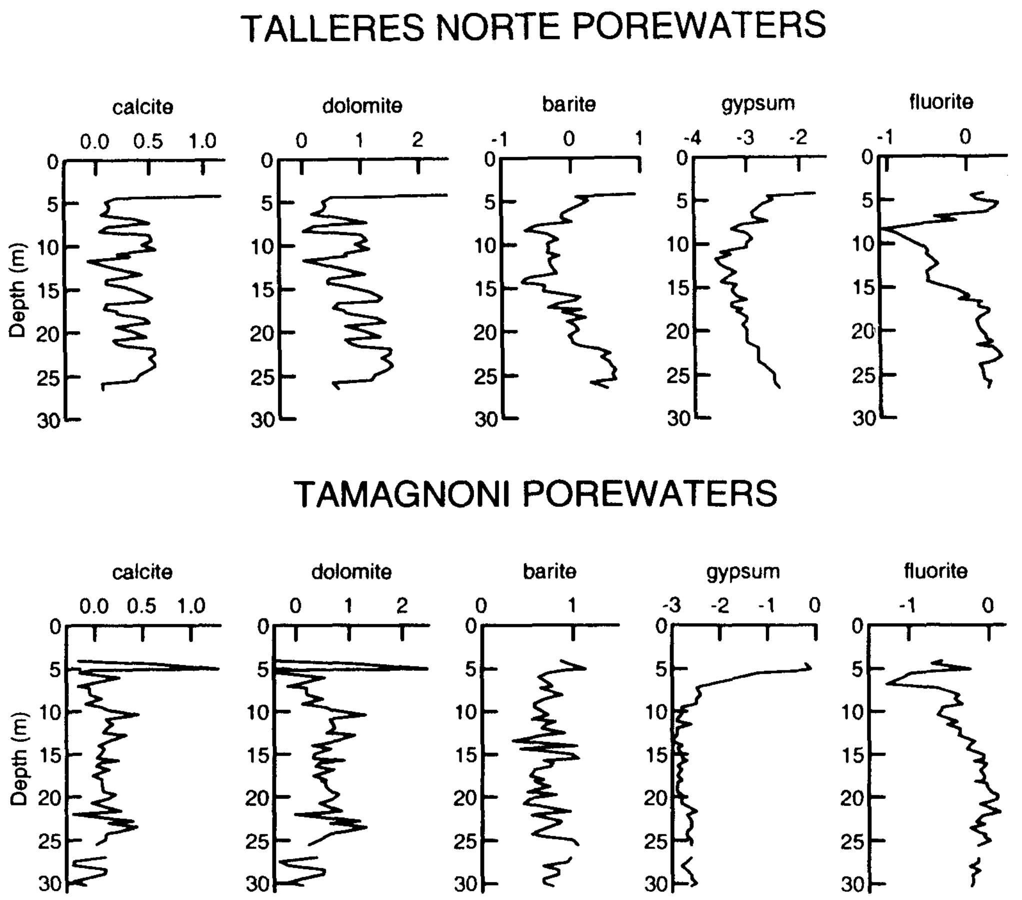

Figure 6.20 **Profiles of saturation indices (log values) for selected minerals in porewaters from the Talleres Norte and Tamagnoni cored boreholes**

the top of the profile and concentrations of most of the major elements (Na, Cl, Ca, Mg, K, SO_4, NO_3-N) as well as Sr, Li and Rb are correspondingly high. The enhanced concentrations are most likely to be the result of evaporative concentration of solutes in the zone of water-table fluctuation. Bailed samples taken from 5.5 m, 16 m and 30.5 m depth during drilling show broadly comparable salinity variations with depth.

Figure 6.20 indicates that the shallowest part of the profile has porewaters which are saturated with respect to gypsum as a result of the enhanced Ca and SO_4 concentrations (as well as supersaturated with respect to calcite and dolomite). Gypsum as well as carbonate minerals are likely to be important constituents of the salts forming around the depression when evaporation is most pronounced.

The evaporative process has led to extremes of many undesirable constituents but the concentrations of constituents considered to be detrimental to health are particularly notable. Nitrate (N) concentrations reach up to 620 mg l^{-1} at the top of the profile, a value 55 times the WHO guideline value for NO_3-N in drinking water. Although the Tamagnoni porewaters are not used for drinking water, the concentrations serve to illustrate the potential detrimental effects of evaporation on water quality and the potential problems arising from locating abstraction boreholes close to depressions which act as local groundwater-discharge centres in the region, at least periodically. The concentration of NO_3-N in a bailed sample from 5.5 m depth in the borehole during drilling was 308 mg l^{-1} (Appendix 1.2), although the concentration in the abstraction borehole at Tamagnoni used for potable supply was fortunately only 12 mg l^{-1} (though still above the WHO guideline value; Appendix 1.2).

Porewater pH varies mainly between 7–8 in the topmost saline portion of the profile but increases to around 8.6 from 10 m depth to the base of the borehole. Concentrations of HCO_3 show a similar trend, being less than 500 mg l^{-1} in the topmost part and close to 1000 mg l^{-1} in many samples below 10 m depth. The variations reflect the transition from Na-Cl dominant waters near surface to Na-HCO_3 waters below the major zone of evaporation.

As with the Talleres Norte core, moisture contents in the Tamagnoni samples (all saturated sediments) range between 26–40% with most being around 30%. This represents the average porosity of the cored sediments.

As with the Talleres Norte profile, some high concentrations of Fe, Mn, and Al occur in the porewaters at depths of 17–23 m (Figure 6.18). At the pH of the groundwaters, these are considered to be mainly colloidal fractions and are likely to be the reason why concentrations of REE, Y, and Th are correspondingly high at these depths. The colloidal fraction may give rise to increases in concentrations of other ions such as As, V and P but this is not considered to be the main control on these constituents as the profiles of these do not closely match those of Fe, Mn and Al.

Concentrations of As are low in the topmost (saline) section of the profile, but increase progressively with depth to a maximum of 7490 µg l^{-1} at 27 m depth and decrease slightly below this horizon to the base of the borehole (Appendix 3.2). It is notable that the highest concentration is more than ten times greater than the maximum observed in the Talleres Norte porewaters. The concentrations are also significantly higher than those found in the groundwater from the Tamagnoni abstraction borehole just a few metres away, although this was also very high at 1360 µg l^{-1}.

The high observed As concentrations are believed to reflect partly the fact that the area is a zone of periodic groundwater discharge, where groundwater flow is slow moving and flushing from the aquifer locally has been restricted. It is also notable that the highest concentrations of porewater As occur in a zone of the profile which was particularly dry (24–28 m depth; Appendix 2.1). Indeed, the maximum observed concentration occurred immediately below a clayey horizon so dry that insufficient water could be extracted for chemical analysis (hence the gap at 27 m in the Tamagnoni profile; Figures 6.18–6.20). This information suggests that groundwater movement is particularly restricted in this depth zone due to fine grain size. The dry clayey zone is also an area of enhanced mottling due to the presence of manganese-oxide coatings and cement. This combination of groundwater flow conditions and localised variation in mineralogy and lithology is believed to be responsible for the extremely high porewater-As concentrations in this part of the Tamagnoni profile. Mineralogy and lithological variations in the cored boreholes are discussed further in Section 7.

Porewater profiles for other anion and oxyanion species such as F, V, U, B and Mo show some similarities with that for As in that concentrations generally increase with depth, although the profiles of each do not correspond closely. The processes of release of these elements into the porewaters are believed to be broadly similar to those for As but differences between the elements are likely to reflect differing transport and retardation properties of the elements and resultant chromatographic separation of the elements over the vertical profile with time.

6.10 Discussion

Saline and high-pH groundwaters like those observed in La Pampa are typical features of arid and semi-arid regions where evaporative concentration of solutes may be an important process in the near-surface and limited recharge means that water-rock reactions can proceed to a relatively advanced stage without the dilution experienced in environments with higher amounts of recharge. Such groundwater provinces are well-documented for instance in large parts of the south-west USA as well as Mexico and Australia.

A notable analogue for the groundwater situation in La Pampa is the arid region of the San Joaquin Valley of California. In the Tulare Basin, a closed basin in the southern part of the Valley, shallow groundwaters (<7 m) commonly have high concentrations of major ions and many trace elements as a result of evaporative concentration, a feature confirmed by $\delta^{18}O$ and $\delta^{2}H$ trends (Fujii and Swain, 1995). The groundwaters often have high As concentrations (commonly under oxidising conditions, where As(V) is the dominant dissolved species) and many have associated high concentrations of B, Mo and U as well as Se. These groundwaters have high pH values and this is taken to be an important criterion for generating high concentrations of anions in solution. Processes controlling groundwater compositions in the Tulare Basin are believed to be very similar to those in La Pampa. Reducing conditions are also present in some parts of the aquifers, and these also experience As problems. In these however, the concentrations of Se, U and Mo are usually low (Fujii and Swain, 1995).

Arsenic concentrations in the Pampean groundwaters show a large range, spanning four orders of magnitude. However, most groundwater sources investigated in this study were found to be contaminated: 95 % above the WHO guideline value and 73 % above the Argentine standard. Sample collection was close to random and hence the exceedance statisitics are believed to be representative of the groundwaters from the region as a whole. The data indicate that the groundwaters are seriously contaminated with As, not only because of the percentage of samples exceeding guideline limits but also the absolute concentrations of many are high (53 % exceed 100 $\mu g\ l^{-1}$, 26 % exceed 300 $\mu g\ l^{-1}$ and 6.5 % exceed 1000 $\mu g\ l^{-1}$). For comparison, a recent survey of groundwaters from the arsenic-affected aquifers of Bangladesh found that around 35 % exceeded the WHO guideline value, while 25 % exceeded the Bangladesh national standard of 50 $\mu g\ l^{-1}$ (Kinniburgh and Smedley, 2000). The distribution of exceedances was patchy however, with some areas notably more contaminated than others.

The lack of distinct regional trends in chemical composition of the Pampean groundwaters is likely a reflection of the lack of distinctive geological variations in the aquifers. Although grain-size and texture are variable spatially on a local scale, the Pampean sediments are essentially similar across the whole region. Hence chemical variations are related dominantly to physical and hydrochemical factors rather than lithological variations.

The high degree of spatial variability in groundwater chemistry over short distances (typically a few kilometres) indicates restricted groundwater flow with poor mixing and homogenisation. This arises probably as a result of restricted recharge in the semi-arid climate of the region and limited permeability of the Pampean silts and fine sands.

Highest concentrations of As and other anions and oxyanions tend to be present in groundwaters from localised depressions which constitute zones of discharge during wet seasons. Such depressions are likely to be zones of restricted groundwater movement where flow is directed inwards towards the centre of the depression, although it is diluted seasonally by surface runoff which also collects in the depression. Fine-grained sediments may also be preferentially concentrated in the depressions due to aeolian reworking and may further restrict localised groundwater movement in the depressions. Restricted flow without significant flushing may be one reason for the accumulation of As and the other problem elements in solution in these areas.

High concentrations of As (and F, V, B, Mo, U) also tend to be found in the groundwaters abstracted from close to the water table. The mobilisation of the trace anions and oxyanions appears to be greatest where chemical reactions (carbonate, silicate) are occurring most actively.

No monitoring of groundwater chemistry was carried out during the project and no time-series data were obtained from other data sources for the groundwaters under investigation. Past temporal variations in chemistry and likely future trends are therefore unknown. However, since the high concentrations of As and other anions and oxyanions are found to be naturally derived and not thought to be significantly influenced by present abstraction, the likelihood is that water quality will not change considerably in future years in the present climatic conditions.

Correlations between the various residence-time indicators (especially isotopic compositions) are generally poor. The low tritium concentrations of many analysed groundwaters indicate that these have dominant components of pre-1950s recharge. However, ^{14}C model ages are usually low and indicative of essentially 'modern' groundwater. The deepest sample analysed (140 m) has the lowest concentration of modern carbon and therefore this groundwater is likely to have had a longer residence time in the aquifer. However, the fact that there is little discernible variation with well depth in $\delta^{18}O$ or $\delta^{2}H$ (for which more data are available), suggests that there is not a major variation in groundwater residence times across the aquifer. Few of the groundwaters can therefore be considered as palaeowaters. Although slow groundwater flow is indicated by low recharge, evaporation and considerable spatial variation in chemical compositions, the isotopic data suggest that there is at least a degree of active recharge which introduces some tritium and modern carbon to the aquifer.

7. SEDIMENT CHARACTERISATION

7.1 Lithology of sediment samples

Samples collected for mineralogical and chemical investigation are from archive material, road and quarry exposures, as well as the newly cored boreholes at Talleres Norte and Tamagnoni. The majority of samples consist of loess sediment of silt to fine sand grade. Most are brown in colour and many of those collected from shallow depths (1 m or less) in road cuttings are dark brown or blackish brown due to a higher concentrations of organic matter. Samples of volcanic ash (generally from discrete layers) are fine-grained, white and of rhyolitic composition. Descriptions of the samples collected are given in Appendices 2, 4, 5 and 6.

7.1.1 Cored sediments

Lithological logs for the cored boreholes at Talleres Norte and Tamagnoni are presented in Figures 7.1 and 7.2 respectively and summaries of sediment samples and drilling are given in Appendix 2.1.

Sediment recovered from Talleres Norte consists of dominantly silt, silty sand and fine sand although a few horizons comprise sediment of coarse sand and gravel grade (e.g. 5.4 m; 13.2–14.7 m depth; Figure 7.1). The sediments are generally brown (Plate 7.1) but as with samples collected from road cuttings, are dark-brown and more organic-rich in the topmost part of the profile. One thin layer of white sand (ca. 1 cm thick) occurs at 7.7 m depth (Plate 7.1) but this is a rare occurrence.

The Talleres Norte borehole shows much evidence of secondary precipitation of carbonate in the form of calcrete layers and irregular nodules of variable size. Layers of calcrete, interbedded with sediment, are particularly well-developed over the interval 1.5–4.2 m and led to drilling difficulties and poor core recovery from this interval. Calcrete layers are also noted at 7.9 m and 16.5 m depth. Calcrete concretions are abundant throughout the profile at greater than 5 m depth but are not developed at the top of the profile.

The sediments recovered from the Tamagnoni borehole have many similarities with those of Talleres Norte, although Tamagnoni sediments are generally finer grained. Silt and clayey silt is the dominant grain size (Plates 7.2–7.4) but several horizons of high-permeability sediment occur. Thin horizons of coarse sand occur at ca. 14.3 m and 21.6–22.8 m depth (Figure 7.2). The tendency for finer sediments in the Tamagnoni profile compared to Talleres Norte may be due to aeolian reworking of sediments and preferential deposition of fine materials in the low-lying depression in which the site is located.

As with Talleres Norte, the sediments are brown with darker brown material at the top of the profile, corresponding to the modern soil layer. Calcrete layers occur at 8.1–8.5 m and 28.1–28.2 m depth. At greater than 2.6 m depth, calcrete concretions of variable size are abundant throughout the profile. Some elongate ‘fingers’ of calcrete up to 10 cm long, possibly representing burrow infills, were recovered. Occurrence of black mottling is common throughout much of the Tamagnoni profile, but is particularly well-developed in the deeper section (below ca. 25 m). The mottling is the result of precipitation of black manganese oxide (Plates 7.2, 7.4).

No discrete layers of volcanic ash were found in either profile. This may have been due to lack of preservation of undisturbed core samples in the shallowest parts of the boreholes due to the use of the clear-out tool in the unsaturated zone. There is also the likelihood that the topmost parts of the profiles consist of made ground and hence have been disturbed recently.

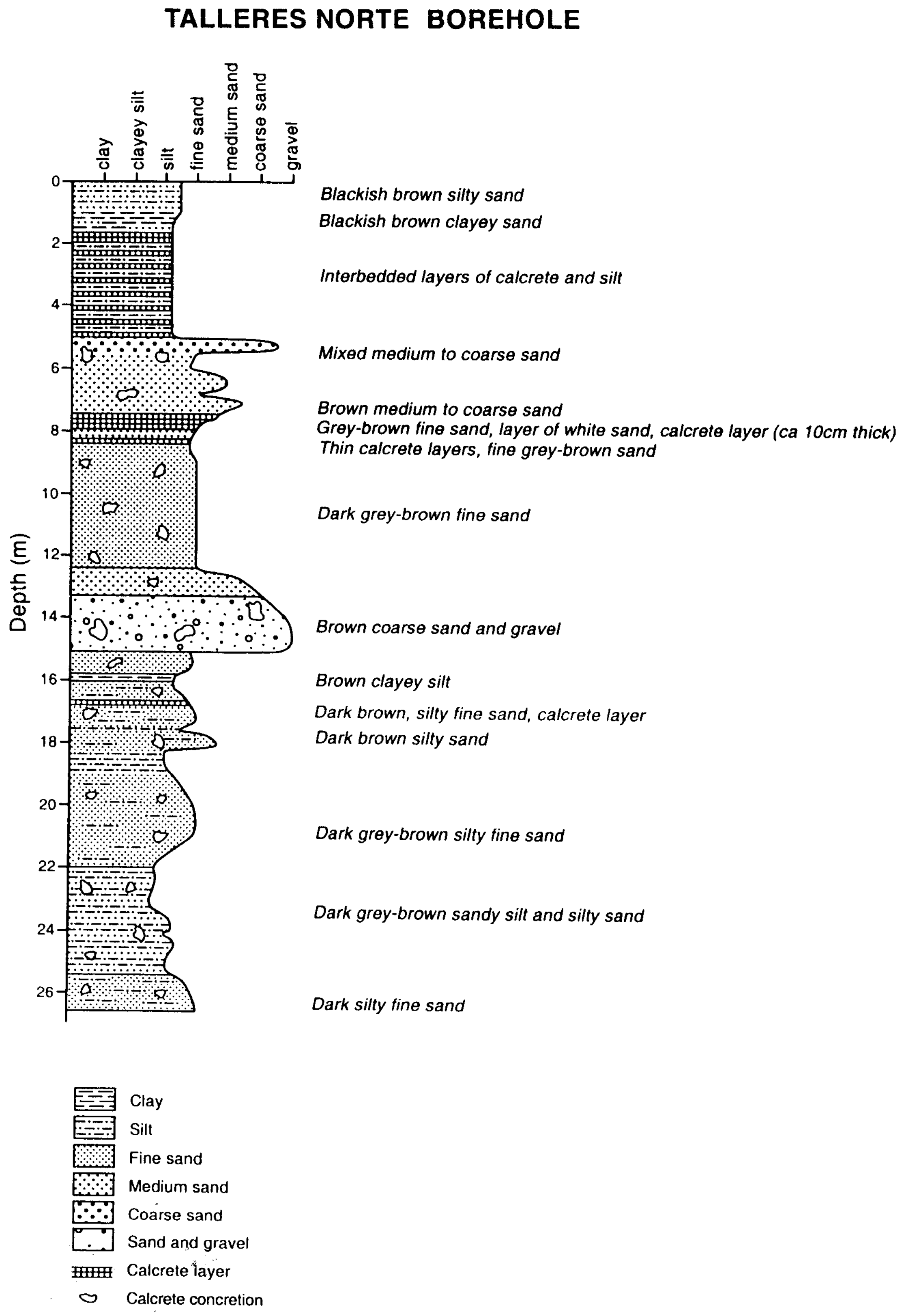

Figure 7.1 **Lithological log of Talleres Norte borehole, Eduardo Castex**

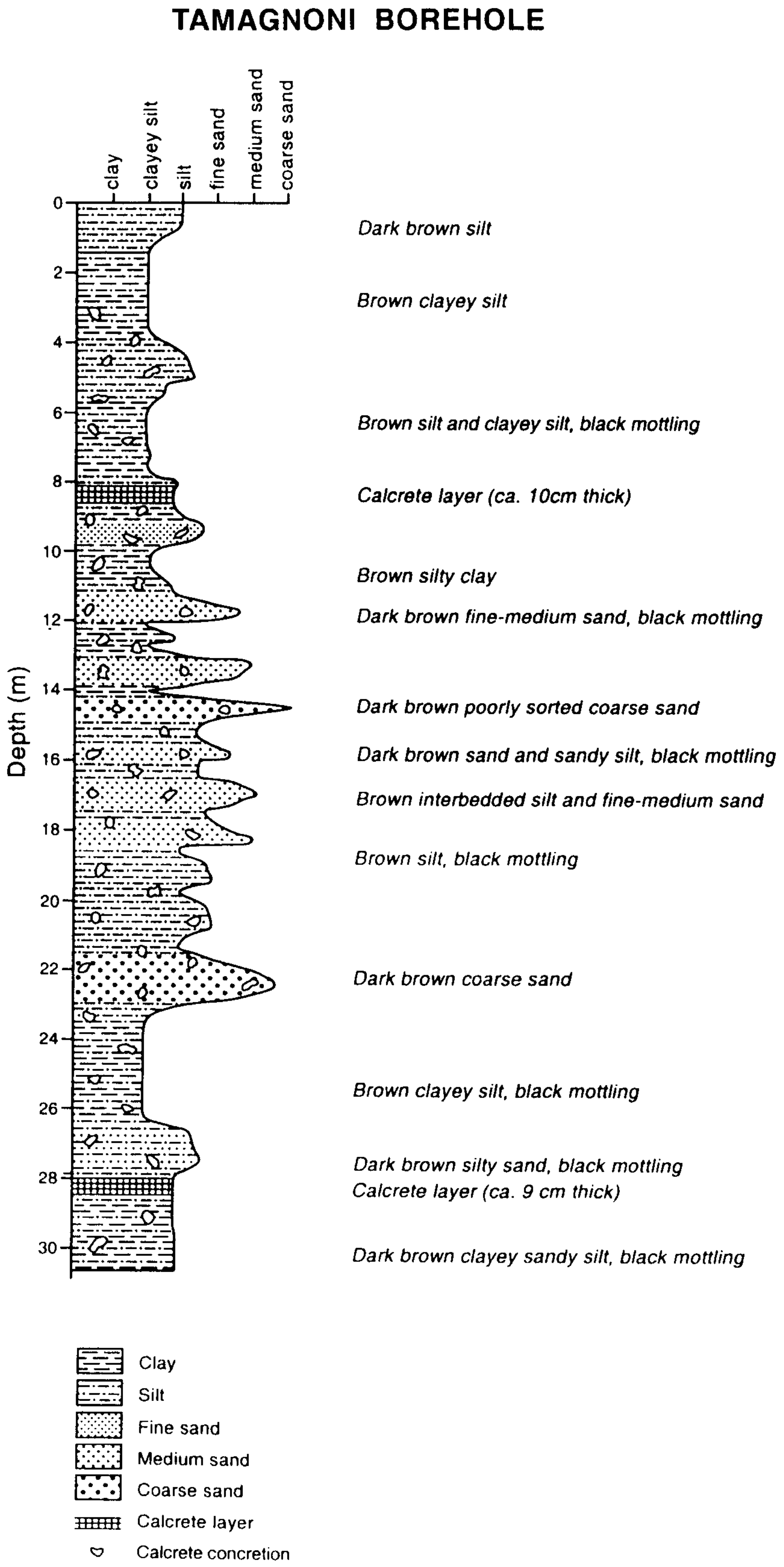

Figure 7.2 **Lithological log of Tamagnoni borehole, 10 km south of Eduardo Castex**

Plate 7.3 Tamagnoni core material (dry brown silt), sample depth: 27.5–28.0 m

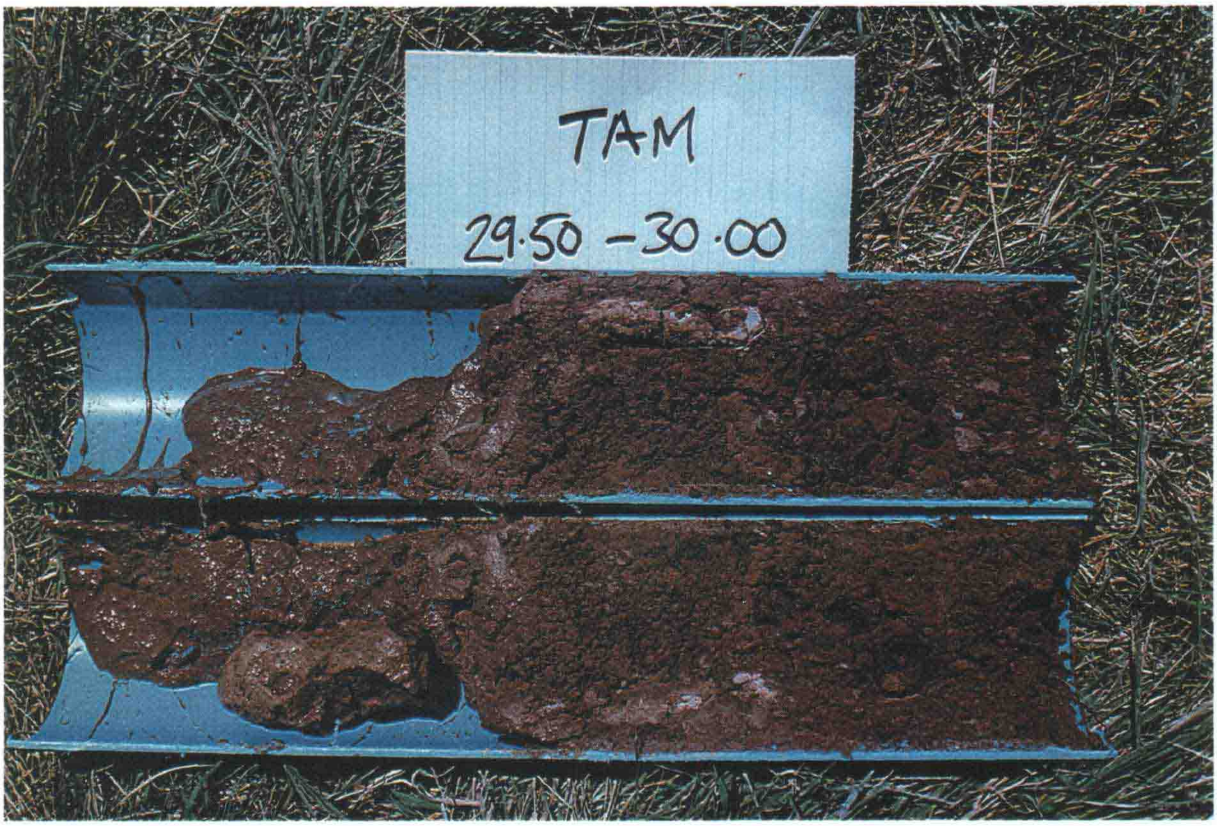

Plate 7.4 Tamagnoni core material (brown silt with white calcrete fingers and numerous black spots of manganese oxide); sample depth: 29.5–30.0 m

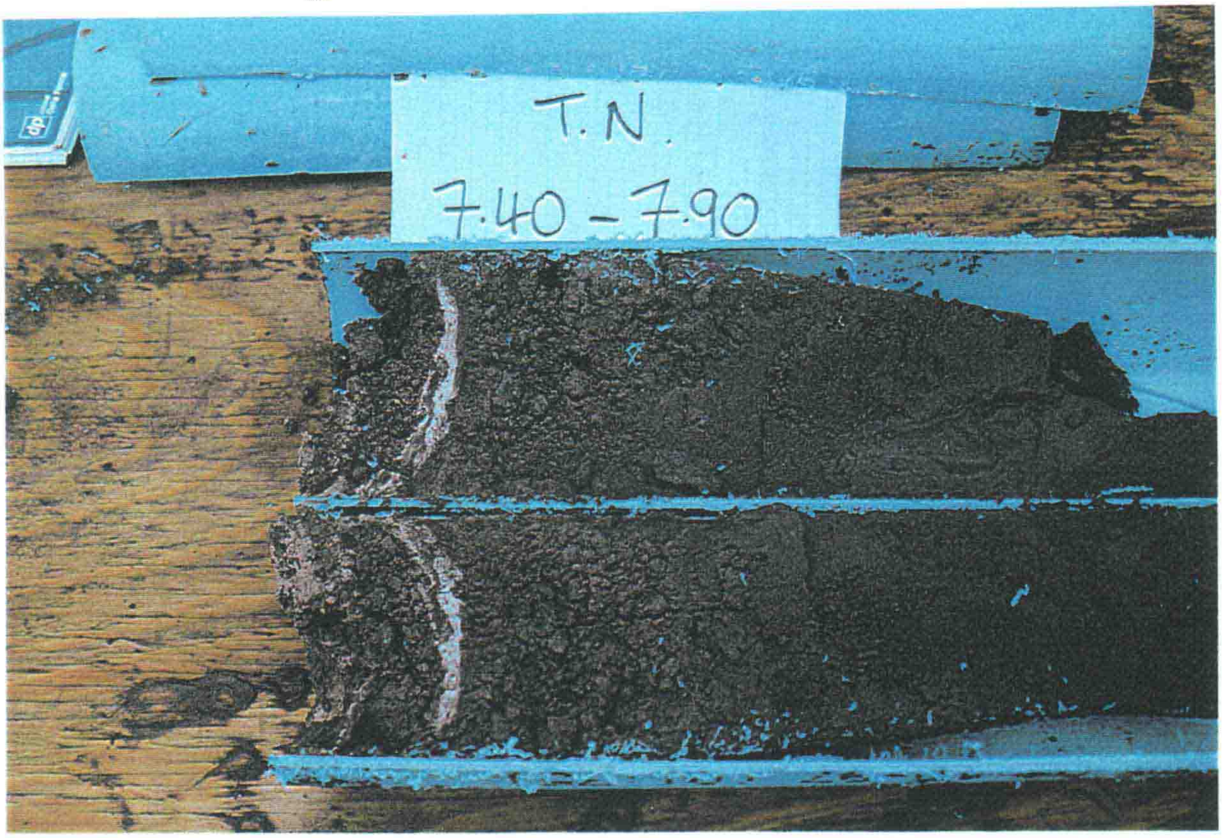

Plate 7.1 Talleres Norte core material (fine brown sand with some white sand), sample depth: 7.40–7.90 m

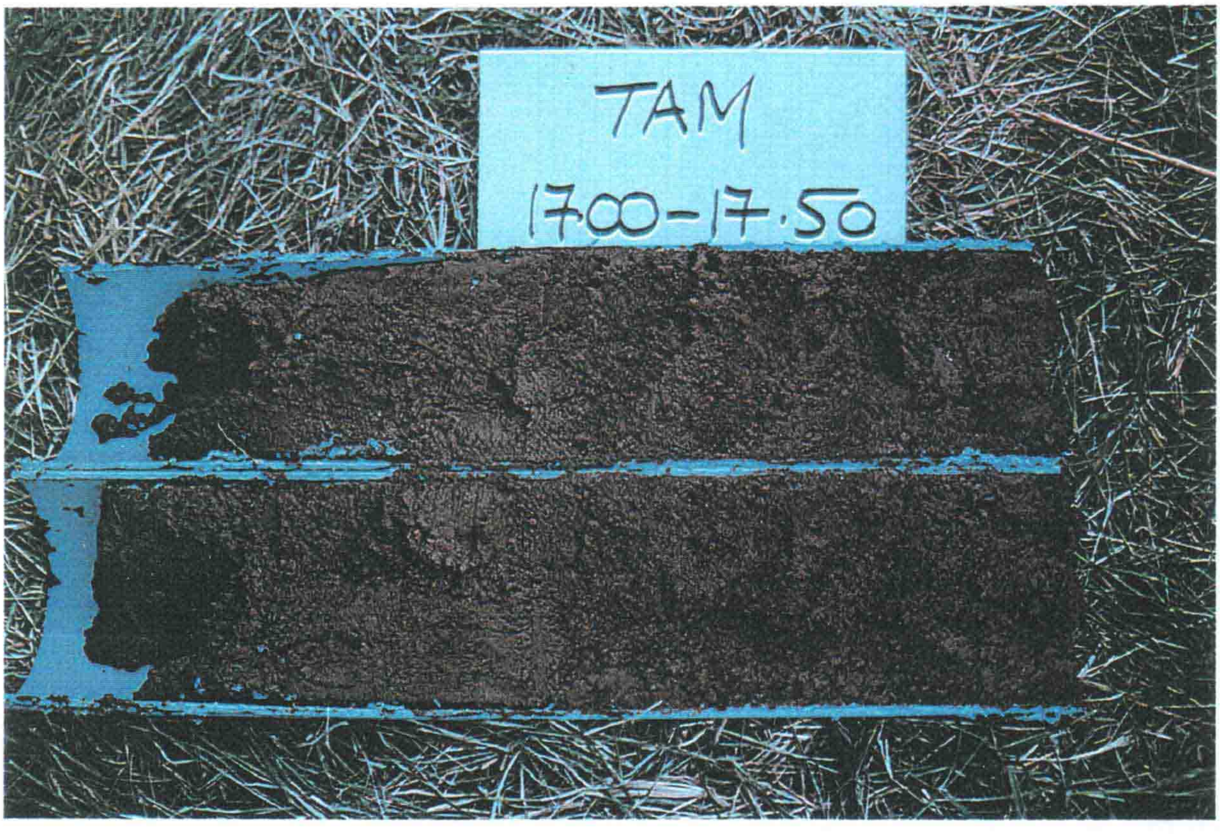

Plate 7.2 Tamagnoni core material (brown silt with some black manganese spots); sample depth: 17.0–17.5 m

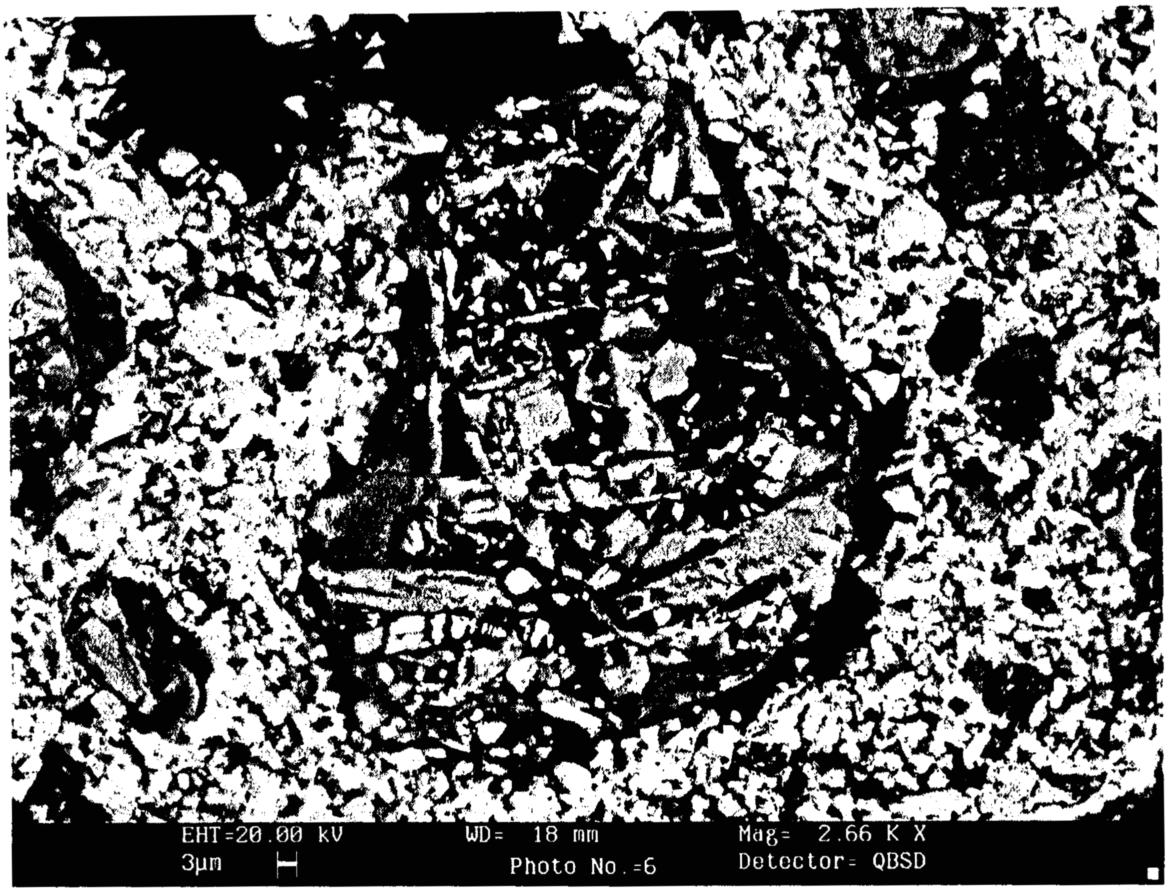

Plate7.5 Lithic volcanic clast comprising plagioclase laths and ferromagnesian minerals, altered and replaced by Fe oxide, ilmenite and chloritic clay. TN6, Talleres Norte borehole, 4.45-4.90 m

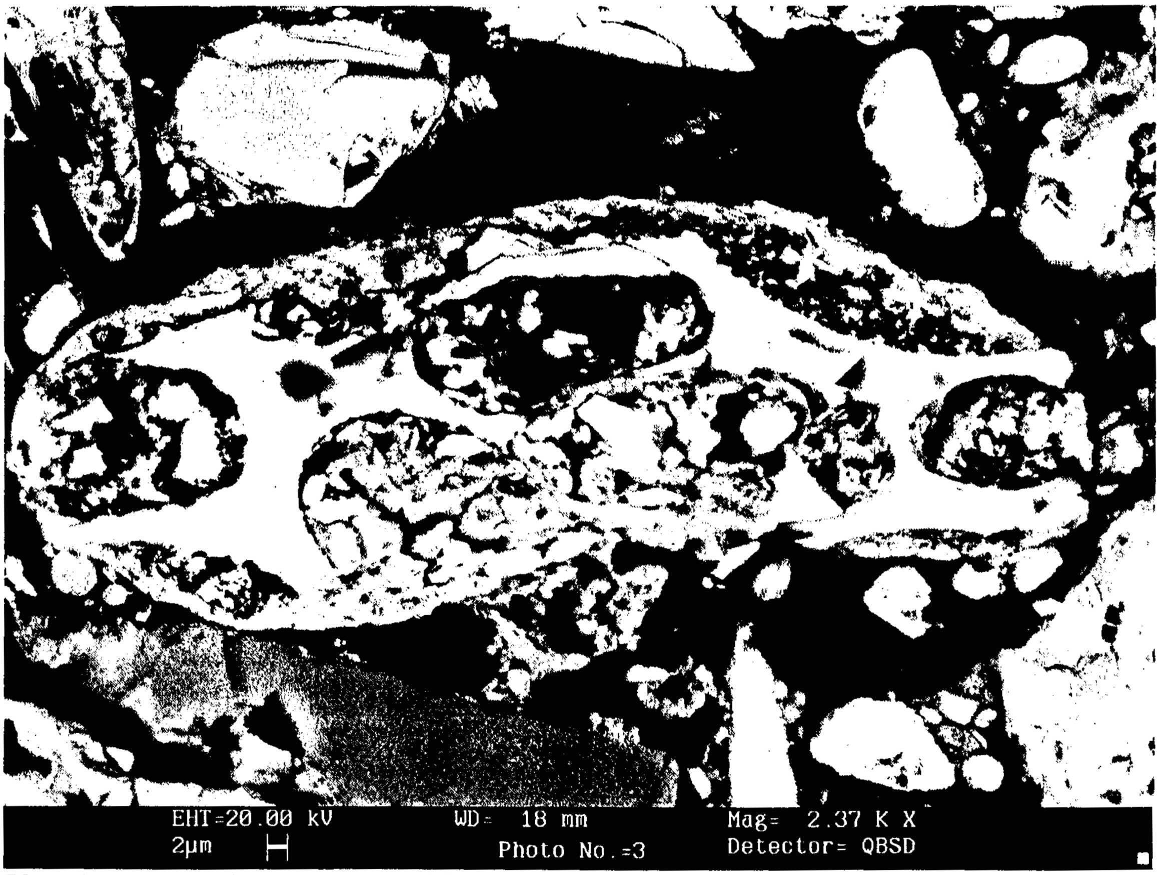

Plate 7.6 Pumice fragment with voids infilled by chloritic clay and Fe oxide. TN30, Talleres Norte borehole, 16.50-16.84 m

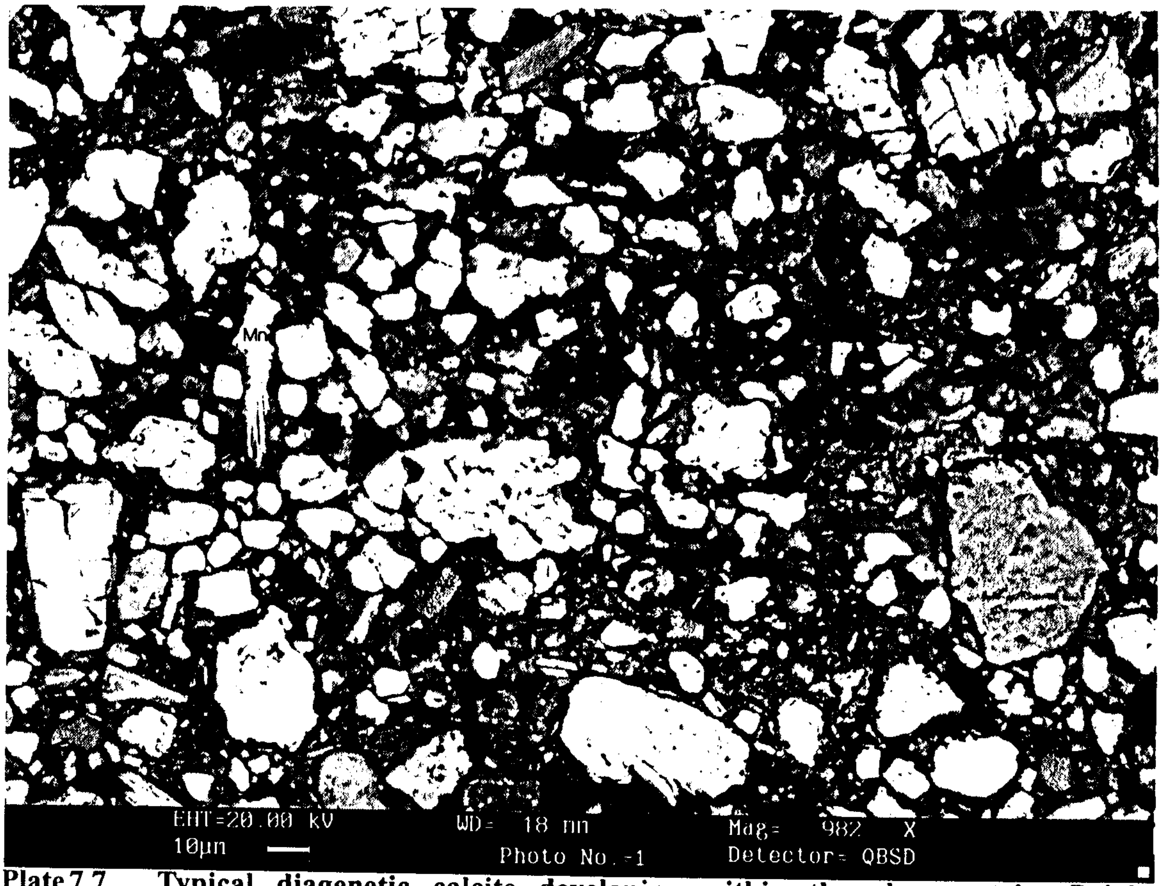

Plate 7.7 Typical diagenetic calcite developing within the clay matrix. Bright patch at centre left is rare Mn oxide ('Mn'). TAM58, Tamagnoni borehole, 26.50-27.00 m

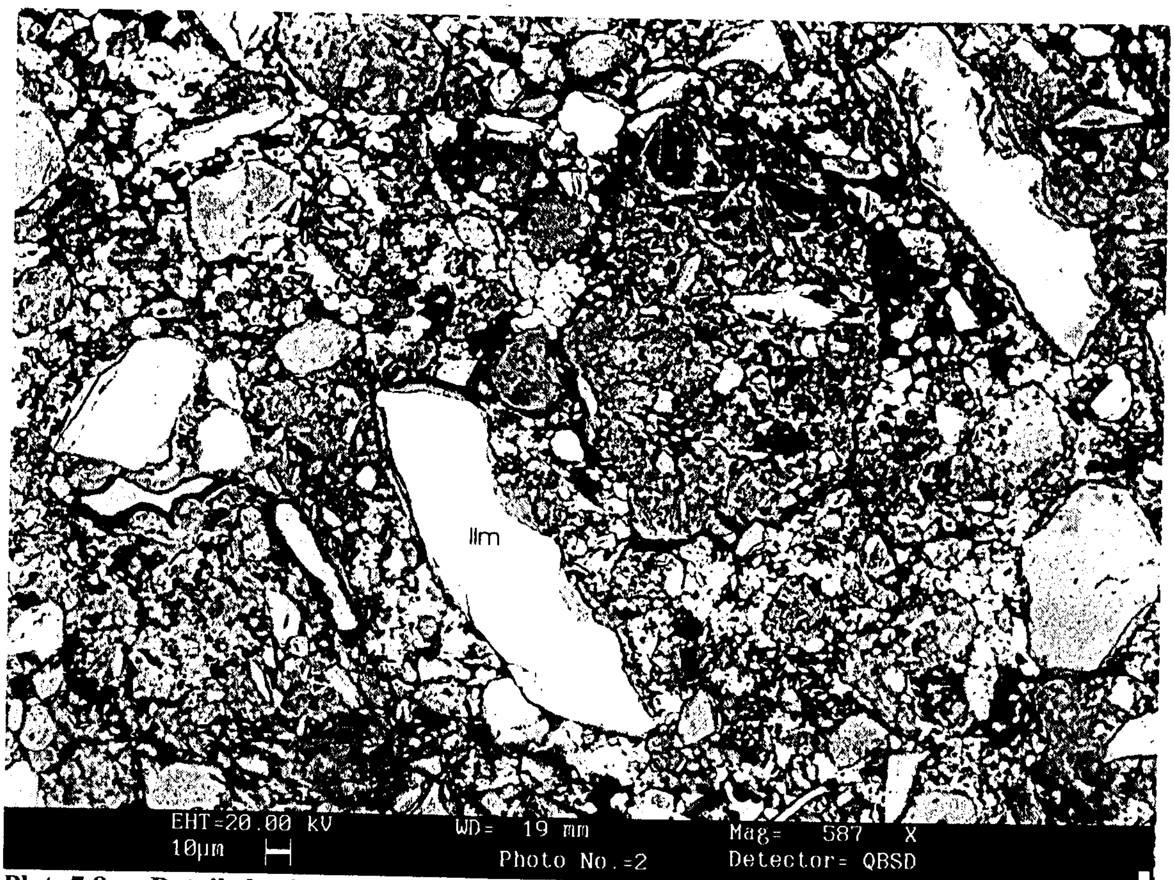

Plate 7.8 Detailed view of typical diagenetic calcite cement developing within the clay matrix. Note ilmenite grain ('Ilm', white) plus corroded grains of pumice and plagioclase. TAM44, Tamagnoni borehole, 19.70-20.15 m

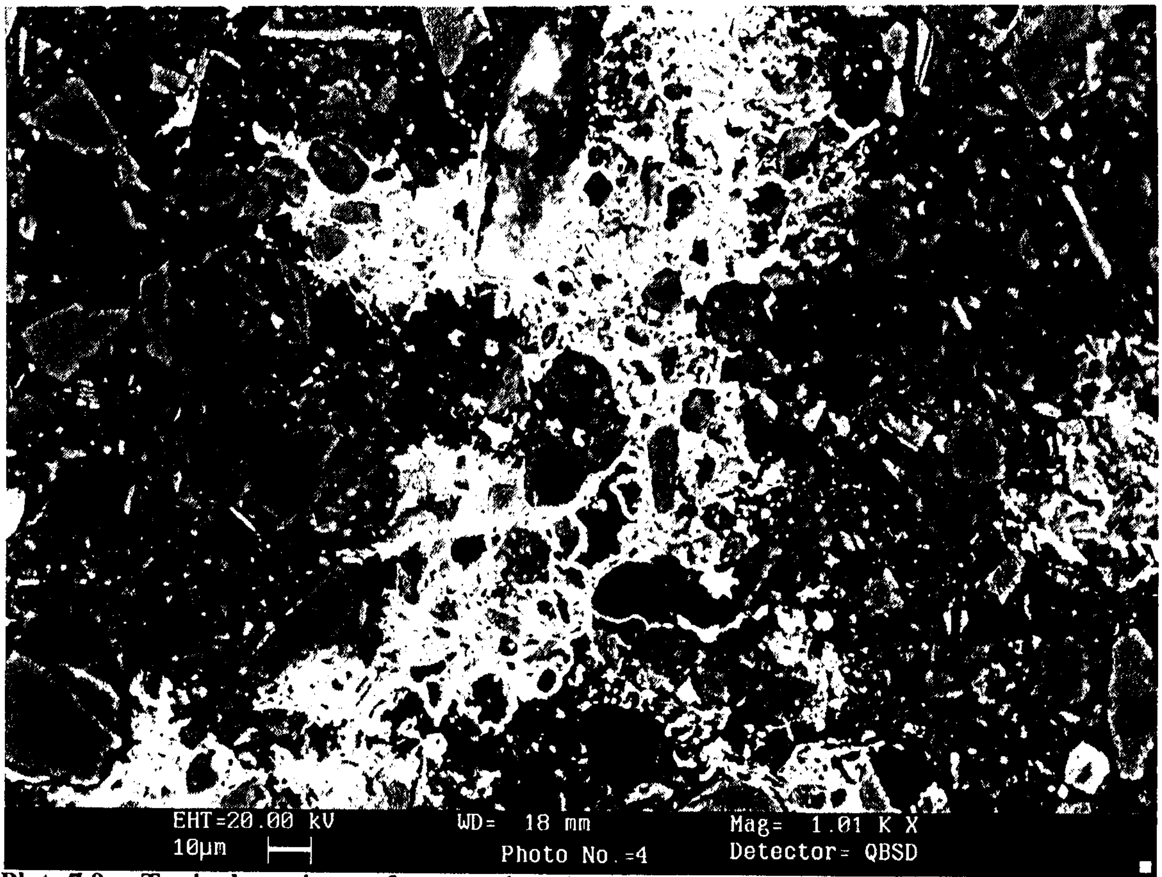

Plate 7.9 Typical view of pervasive Mn oxide development lining voids and partially replacing the clay matrix within aggregate particles. TAM64, Tamagnoni borehole, 29.50-29.95 m

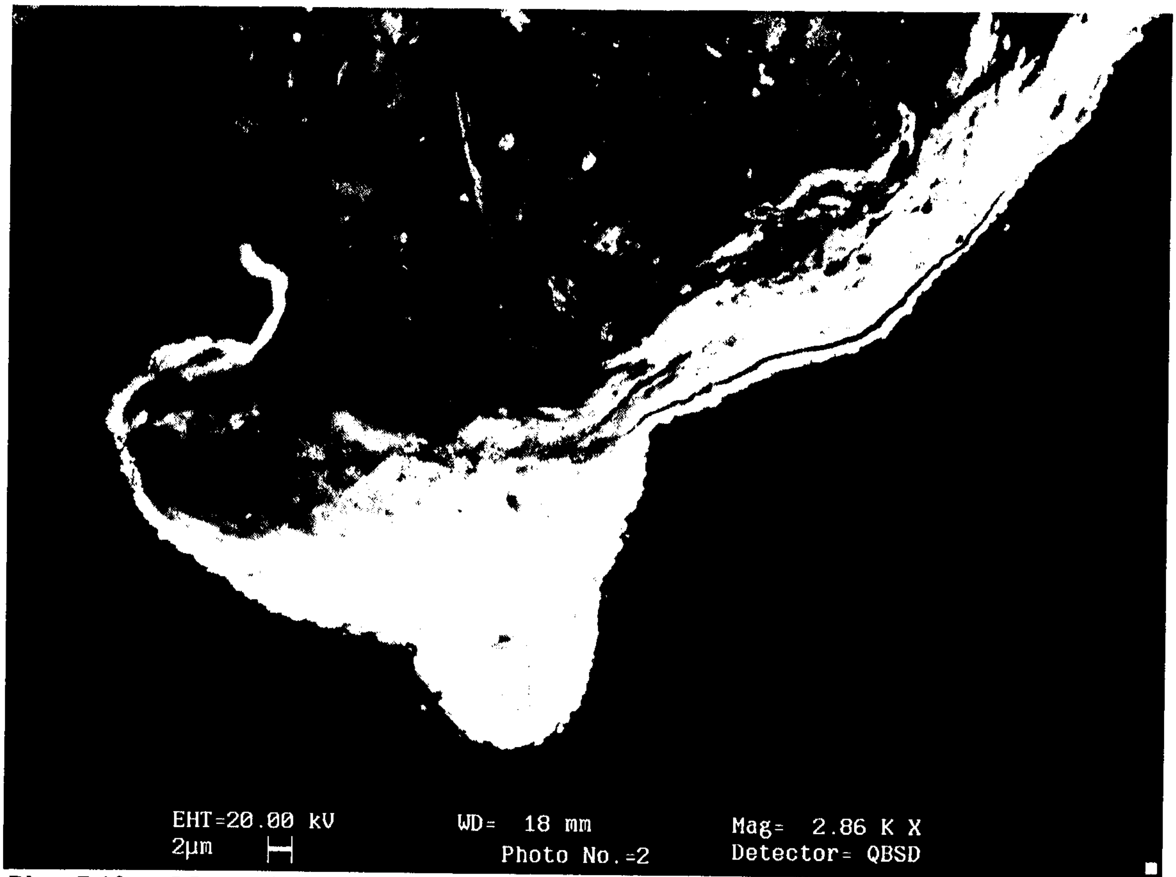

Plate 7.10 Mn oxide forming a coating on the external surface of aggregate particles. EDXA indicates this also contains variable amounts of Ba. TAM64, Tamagnoni borehole, 29.50-29.95 m

7.2 Petrography of cored sediments

Full details of the petrographic investigations carried out on selected sediments from the Talleres Norte and Tamagnoni drilled boreholes are given by Pearce (1998).

The samples examined by BSEM from the two boreholes have very similar mineralogies. All samples investigated comprise predominantly plagioclase with variable amounts of quartz, alkali feldspar, often severely altered ferromagnesian minerals, pumice fragments and heavy minerals. The heavy-mineral suite varies slightly between samples, ilmenite being the most abundant but with variable amounts of zircon, monazite, apatite and magnetite.

The ferromagnesian minerals are typically altered to a chloritic clay and Fe oxide, Ti oxide or mixed Fe,Ti oxide which occur as discrete alteration products and pore linings or are intimately mixed within the clay matrix. The major minerals are typically enclosed in a clay matrix. EDXA indicates that this clay matrix consists typically of an intimate mixture of silica, chloritic and illitic clays. The silica is likely to be derived from the dissolution of the pumice fragments.

Finely crystalline, subhedral to euhedral calcite occurs to varying extent in some samples. Although mainly confined to small irregular patches, occasionally more extensive, pervasive and expansive calcite is developed in some samples.

The deepest sample from the Tamagnoni borehole (TAM64, 29.50–29.95 m depth) contains significant Mn oxyhydroxide as coatings on the surfaces of particles and as a pervasive stain through the clay matrix. Typically this coating is 5-10 μm thick and contains a variable amount of Ba.

No discrete As minerals were identified in the thin sections.

7.2.1 Talleres Norte borehole

TN6 (4.45–4.90 m) comprises irregular, angular to subrounded fine gravel to silty aggregates with a mode of fine sand. The aggregates, developed possibly through soil-forming processes, are composed of angular clasts of major plagioclase, quartz and pumice fragments with minor ferromagnesian minerals, K-feldspar and Fe oxides. Grains are predominantly silt-sized with a maximum of fine sand-size. Rare biotite and muscovite flakes are also present. The plagioclase has variable compositions but albite is dominant. The ferromagnesian minerals are mainly clinopyroxene with minor olivine, amphibole and possibly epidote. Minor lithic fragments occur throughout the matrix and comprise plagioclase laths intergrown with pyroxene. The pyroxene has a composition close to diopside. The clasts are enclosed in a matrix-supported fabric of fine-grained ferruginous illitic clay. Occasional pumice fragments occur throughout. Trace phases include subangular to subrounded apatite and resistate iron oxides, possibly magnetite, plus rutile, ilmenite and monazite. Rare zircons also occur. The aggregate particles are not coated in iron oxide although this occurs finely intermixed within the clay matrix. Some of the aggregates comprise or are extensively cemented by fine-grained, crystalline subhedral to euhedral calcite in irregular patches. The plagioclase and pyroxene clasts are corroded to produce secondary voids which are subsequently partially infilled by authigenic Fe oxide and Fe,Ti-oxides (Plate 7.5). Barite occurs as a possible secondary alteration phase. The lithic fragments are altered to chloritic clay, Fe oxide and secondary Fe,Ti-oxides (Plate 7.6).

TN18 (5.40–5.90 m) comprises unconsolidated fine sand to silt-sized, subrounded to rounded grains which are moderately to very well sorted, except for a few very large coarse sand to gravel sized grains. These grains are of quartz, K-feldspar, plagioclase with minor pumice fragments, pyroxene and hornblende. Heavy minerals include ilmenite, rare zircon, apatite and monazite. Rare patches of chlorite and smectite are also present. Although rare, the pumice fragments and heavy mineral clasts appear largely fresh and unaltered.

TN30 (16.50–16.84 m) comprises aggregate particles of fine sand to silt sized, moderately well sorted grains, with minor clay grade matrix. The grains consist of plagioclase (variable from albite to anorthite), pyroxene, ilmenite, quartz and rare biotite. Minor rutile is also present. Rare vanadium-rich oxide particles occur as sub-micron particles finely disseminated throughout the matrix. Chromium-rich ilmenite and Fe-Cr-Ti oxides occur as possible alteration products of ferromagnesian minerals. Many of the feldspar and ferromagnesian minerals are at least partially corroded and altered. The resultant very minor secondary porosity is partially infilled by the clay matrix and iron oxides or ilmenite. EDXA indicates that the clay matrix has a chloritic composition. Secondary silica, possibly after alteration of pumice and volcanic glass infills some small voids. Very rare FeS phases, possibly pyrite or altered pyrite, occur as discrete isolated particles up to 3 µm across within the clay-rich matrix. Vesicles within the volcanic glass shards are infilled by clay with a chloritic chemistry and Fe oxides. The volcanic glass is typically partially altered.

TN40 (20.50–20.83 m) comprises aggregate particles of sand to silt-sized grains developed by soil-forming processes. The angular to well-rounded, moderately sorted grains consist of plagioclase, K-feldspar, quartz, ferromagnesian minerals and pumice fragments. Heavy minerals include zircon, ilmenite and chromium-rich ilmenite, zircon, apatite and monazite. Many of the aggregates are patchily cemented by fine-grained, micron-scale subhedral to euhedral calcite crystals forming a matrix-like cement. Silica is also developed in similar patches. Well-developed books of kaolinite (with individual plates up to 3 µm long) infill both primary and secondary porosity. Occasional well-rounded grains are completely replaced by secondary calcite and clay. Alkali feldspar grains are typically severely corroded to form skeletal grains with clay coatings. Rare biotite is also altered with splaying along basal cleavages which are subsequently lined with secondary Fe,Mn-hydroxides. The biotites are also partially replaced by chlorite.

TN50 (25.50–25.83 m) includes irregular aggregate particles of angular to moderately rounded grains of fine sand to silt. Grains consist of plagioclase, alkali feldspar and quartz, as well as minor pyroxene and rare pumice fragments. Some of the ferromagnesian minerals are altered to iron oxides with colloform habits. The pumice fragments are partially altered.

7.2.2 *Tamagnoni borehole*

TAM8 (4.10–4.45 m) includes irregular clasts up to gravel size, which consist of sub-angular to sub-rounded grains of plagioclase and K-feldspar, minor quartz, pumice fragments and biotite. The sand to silt-sized grains have a matrix-supported fabric. The clay matrix has a chloritic composition which also contains significant silica and illite. Isolated, micron-scale particles of iron oxide and ilmenite particles are disseminated throughout the clay matrix. The plagioclase is often partially corroded, with the secondary porosity infilled by the clay. Albite, is typically severely corroded. Heavy minerals include isolated particles of rare monazite, zircon, apatite and ilmenite. The ilmenite also occasionally contains Cr and Mn, either separately or, rarely, together. The ferromagnesian minerals (mainly pyroxene), are also severely corroded with iron hydroxide and chloritic clay alteration products. The clay matrix within many of the large aggregate particles contains open porosity, some of which is developed through the dissolution of pumice fragments. The porosity is partially infilled by micron-scale particles of secondary barite.

TAM14 (6.80–7.10 m) comprises irregular aggregate clasts consisting of sub-angular to sub-rounded plagioclase, K-feldspar and minor quartz in a chloritic, silica-rich clay matrix. Grains are of fine silt to fine sand. Ilmenite is a common accessory mineral as irregular to rounded clasts. Other heavy minerals include rare angular fragments of apatite. Much of the ferromagnesian material is altered to a chloritic clay. Occasional pumice fragments present have a Na,Ca aluminium silicate chemistry. Relict diopside or tremolite grains are highly corroded with local development of secondary porosity. Rare Mn oxides occur as discrete, isolated micron-scale particles. Occasional larger aggregate particles contain remnant lamination with laminae of fine sand in a clay matrix-supported fabric, silty laminae with common mica and abundant open porosity, and fine clay laminae. At least some of the porosity in the silty laminae may be due to extensive dissolution of the pumice fragments.

TAM24 (11.28–11.50 m) comprises irregular gravel-sized aggregate particles. These comprise a predominantly mixed feldspar assemblage of plagioclase and K-feldspar, with minor quartz, vesicular volcanic glass shards and minor ferromagnesian minerals (mainly pyroxene). The grains have a fine sand to silt grain size and are typically sub-angular to rounded. Rare heavy minerals include predominant ilmenite with rare zircon, monazite and apatite and very rare Fe-Cr-Ni oxides as micron-scale isolated particles. Occasional lithic igneous clasts are well-rounded with plagioclase laths in a matrix of probable ferromagnesian minerals (replaced by ilmenite and chlorite alteration products). The matrix comprises a mixed assemblage of silica-rich chloritic and illitic clay. Much of the pumice has been corroded to produce local secondary irregularly shaped voids. Plagioclase and ferromagnesian minerals are also partially corroded with secondary porosity infilled by clay. Occasional aggregate particles are cemented by euhedral micron-scale authigenic calcite crystals.

TAM34 (15.74–16.00 m) comprises irregular gravel-sized aggregate particles which are angular to sub-rounded, fine-sand to silt-sized, moderately to well sorted grains. Grains are predominantly albite and plagioclase with minor K-feldspar, quartz, biotite and some pumice. Quartz has a slightly higher concentration in this sample relative to shallower samples in the profile. No ferromagnesian minerals are present. Ilmenite is a common accessory phase, occurring as angular irregular isolated sand to silt-sized grains. Other minor phases include zircon, rutile, monazite and Ti-Fe(±Mn) oxides. The grains are enclosed in a clay matrix which EDXA indicates may be an intimate mixture of silica, chloritic and illitic clays. Biotite has been altered to Mg-rich chloritic clay. The finer feldspars are also corroded with the very minor secondary porosity infilled by the clay matrix. Occasional aggregate particles comprising sand- to silt-sized grains in a clay matrix are enclosed in a mica-rich clay matrix with only minor silt-sized detrital particles.

TAM44 (19.70–20.15 m) is composed of irregular gravel-sized peds which consist of aggregated angular to subrounded, fine sand to silt-sized, moderately to well sorted grains. Grains are predominantly albite, plagioclase and quartz with minor K-feldspar, biotite and some pumice. Quartz has a higher concentration in this sample relative to the shallower sediments. Rare relict ferromagnesian minerals, possibly pyroxene and amphibole, are typically severely corroded and altered. Plagioclase grains and pumice fragments are typically highly corroded, leaving local secondary voids throughout the aggregates. Ilmenite is a common accessory phase as angular irregular isolated sand to silt-sized grains. Other minor phases include zircon, rutile, monazite and apatite. The detrital grains are predominantly enclosed in a clay matrix which EDXA indicates is probably an intimate mixture of chloritic and illitic clay and silica. Some peds are cemented, both internally and externally, by expansive calcite cement comprising subhedral to euhedral crystals. Grains have become isolated within the cement which partially replaces the clay matrix. The calcite cement is patchily distributed throughout the aggregates (Plate 7.8).

TAM58 (26.50–27.00 m) consists of irregular clasts up to gravel size, which consist of sub-angular to sub-rounded, moderately to well sorted, fine sand to silt-sized grains. Grains are predominantly of plagioclase and K-feldspar, as well as minor quartz and biotite. No pumice is detectable. Minor lithic igneous clasts comprise plagioclase laths enclosed in ferromagnesian minerals which are typically altered and removed. Biotite is altered along basal cleavages to secondary chloritic clay. Detrital grains are less common in this sample. The clay matrix has a chloritic composition and contains significant amounts of silica and clay. Ilmenite (with variable amounts of Cr and Mn detected) is again a common accessory phase as angular, irregular isolated sand to silt-sized grains. Other trace phases include zircon, rutile, monazite and apatite. Minor authigenic calcite occurs as discrete euhedral to subhedral crystals (e.g. Plate 7.7) within the clay matrix. Rare Mn oxides occur throughout the matrix as isolated irregular patches up to 20 µm across (e.g. Plate 7.7), some of which appears to be associated with or has replaced ferromagnesian phases.

TAM64 (29.50–29.95 m) consists predominantly of fine silty detrital grains in a clay matrix with gravel-sized irregular aggregate particles. The moderately sorted, fine sand to silt sized, sub-angular to sub-rounded detrital grains are composed of plagioclase and K-feldspar, minor quartz and biotite. No pumice is visible. Minor lithic igneous clasts comprise plagioclase laths enclosed in ferromagnesian minerals which are typically altered and removed. Throughout the aggregates Mn oxides form as a pervasive cementing phase (Plate 7.9) in discrete, irregular patches up to hundreds of microns across and as extensive coatings on the external surfaces of the aggregates (Plate 7.10). They contain variable Ba concentrations. The coating develops up to around 10 µm thick and comprises a series of colloform layers which can extend for several millimetres across the surface of the aggregate soil particles.

7.3 Clay mineralogy

Results of XRD analysis of sediments from the Talleres Norte and Tamagnoni cores are summarised below. In both boreholes, the most abundant clay mineral is smectite, with illite present in smaller amounts. This contrasts with the clay mineralogy of loess sediments from neighbouring Córdoba, where illite was observed to dominate over smectite (Nicolli et al., 1989). Rare kaolinite is also developed as an alteration or weathering product. The clay minerals are typically poorly crystalline which is consistent with their likely derivation by recent alteration of feldspar, ferromagnesian minerals and volcanic glass. The predominance of smectite is in line with derivation by weathering of primary silicate minerals under relatively arid conditions (Appelo and Postma, 1993). As with the Córdoban sediments, volcanic glass is identified as an important constituent.

Table 7.1 **Description of the mineralogy of clays and associated minerals in Talleres Norte core material from XRD analysis**

Sample	Depth	Illite occurrence				Smectite crystallinity				Other minerals		
	m	s	r	a	va	p	r	c	vc	ch	ca	vg
TN5	4.2-4.5		X			X						
TN7	4.9-5.4	X				X						
TN12	7.6-7.8		X				X				X	
TN14	8.4-8.8					X						X
TN17	9.9-10.4					X						X
TN22	13.2-13.3		X			X						
TN24	14.0-14.4	X				X						?
TN27	15.4-16.0	X				X						
TN29	16.4-16.5	X					X					
TN32	17.3-17.5		X			X						
TN34	18.0-18.4	X				X						
TN36	19.0-19.3	X				X						
TN39	20.5-21.0						X					X
TN41	21.3-21.7	X					X					
TN43	21.9-22.5		X				X	X				
TN45	23.0-23.5		X				X					
TN47	23.8-24.5		X					X				
TN50	25.5-25.8	X						X				
TN51	26.0-26.5							X				

Illite	**Smectite crystallinity**	**Other minerals**
s: scarce	p: poor	ch: chlorite
r: regular	r: regular	ca: calcite
a: abundant	c: crystalline	vg: volcanic glass
va: very abundant	vc: very crystalline	

7.3.1 Talleres Norte

The most abundant clay mineral in the Talleres Norte core is smectite which occurs in all samples investigated and although often having poor crystallinity, this generally increases with depth (Table 7.1). Illite is less common but present in small concentrations throughout most of the investigated core.

Volcanic glass is the dominant clay-sized material found in samples TN14, TN17, TN24 and TN39 (depths 8.4–8.8 m, 9.9–10.4 m, 14.0–14.4 m and 20.5–21.0 m).

7.3.2 Tamagnoni

Clay minerals are apparently less abundant than in the Talleres Norte borehole and those present display generally low crystallinity. Of the clay minerals present, smectite is the most abundant and as with Talleres Norte, the crystallinity increases slightly with depth (Table 7.2). Smectite is notably more abundant and more crystalline in samples TAM35, TAM39, TAM56 and TAM58 (depths of 16.0–16.5 m, 18.0–18.11 m, 25.5–26.0 m, 26.5–27.0 m).

Illite is present in some samples, though in less abundance. Volcanic glass is observed in all samples but is the dominant clay-sized mineral in samples TAM2, TAM33, TAM35 and TAM41 (depths of 0.7–1.3 m, 15.5–15.7 m, 16.0–16.5 m, 18.3–18.8 m). Some samples in the profile contain amorphous material.

Table 7.2 Description of the mineralogy of clays and associated minerals in Tamagnoni core material from XRD analysis

Sample	Depth	Illite occurrence				Smectite crystallinity				Other minerals		
	m	s	r	a	va	p	r	c	vc	ch	ca	vg
TAM1	0.0-0.7					X						X
TAM2	0.7-1.3	X					X					X
TAM3	1.3-2.0	X					X			X		
TAM5	2.6-3.0	X					X					
TAM6	3.0-3.5	X				X						
TAM7	3.5-4.1	X					X					
TAM9	4.5-5.0	X					X			X		
TAM12	5.5-6.0	X				X				X		
TAM15	7.1-7.6		X				X			X	X	
TAM18	8.6-9.1		X			X					X	
TAM20	9.6-9.9	X				X						
TAM22	10.4-10.9		X				X			X		
TAM24	11.3-11.5		X			X						
TAM26	12.0-12.5	X				X						
TAM29	13.5-14.3	X					X					
TAM31	14.4-15.0	X				X						
TAM32	15.0-15.5					X						
TAM33	15.5-15.7	X				X						X
TAM35	16.5-16.8		X					X				
TAM37	16.8-17.5			X			X					
TAM39	18.0-18.1			X				X				
TAM41	18.3-18.8											X
TAM43	19.4-19.7		X			X						
TAM45	20.2-20.7	X					X					
TAM48+49	22.8-23.0		X			X						
TAM50	23.5-24.0						X					
TAM53	24.2-24.5	X				X						
TAM55	25.0-25.5	X				X						
TAM56	25.5-26.0	X							X			
TAM58	26.5-27.0	X							X			
TAM61	28.0-28.5		X					X				
TAM63	29.0-29.5	X				X						
TAM65	30.0-30.3		X					X				

Illite	**Smectite crystallinity**	**Other minerals**
s: scarce	p: poor	ch: chlorite
r: regular	r: regular	ca: calcite
a: abundant	c: crystalline	vg: volcanic glass
va: very abundant	vc: very crystalline	

7.4 Total-sediment chemistry of cored boreholes

Total chemical concentrations (analysed by XRF and TOC analyser) for sediment samples collected in the study are given in Appendices 4.1 and 4.2. Summary statistics for the loess sediments investigated are given in Table 7.3, along with analyses of loess samples given by Nicolli et al. (1989).

The Pampean loess sediments have concentrations of SiO_2 in the range 53–68%, Al_2O_3 in the range 10.8–16.7 % and Fe_2O_{3T} in the range 3.4–5.97 %, values at the lower end of these ranges corresponding to material with a high carbonate content. CaO ranges between 1.9–21.9 mg kg^{-1}. Average concentrations of the major constituents in the sediments are broadly similar to those of loess sediments analysed from Córdoba Province by Nicolli et al. (1989) although concentrations of Mn_3O_4 and Na_2O are slightly lower in La Pampa (Table 7.3).

Concentrations of As and U range to slightly higher values in the Córdoban loess (up to 37 mg kg^{-1} and 8 mg kg^{-1} respectively; Table 7.3). Average concentrations in loess from La Pampa are 8 mg kg^{-1} for As and 2.5 mg kg^{-1} for U. Nonetheless, the compositions suggest that the loess sediments from the two regions are from largely similar provenances and have undergone similar post-depositional processes. Similar ranges have been found for As (5.4–15.6 mg kg^{-1}) and U (1.5–4.6 mg kg^{-1}) in loess deposits from the provinces of Buenos Aires, Córdoba, San Luis and Santa Fe (Arribére et al., 1997). In these, V concentrations ranged between 74–189 mg kg^{-1} and compare well with the concentrations found in this study (70–174 mg kg^{-1}; Appendix 4.2).

The loess compositions differ slightly from loess sediments elsewhere. Loess silts in Missouri for example have higher concentrations of SiO_2 and lower Al_2O_3, Na_2O, CaO and Sr than Pampean loess, although concentrations of Fe_2O_3, K_2O and many trace elements are comparable (Ebens and Connor, 1980). The differences reflect the fact that Missouri loess is dominated by quartz and clay with minor amounts of dolomite, K-feldspar and plagioclase, in contrast to the Pampean sediments which are dominated by plagioclase with relatively minor amounts of quartz and K-feldspar, as well as presence of additional volcanic material (Section 7.2). Concentrations of As in Missouri loess lie in the range 5–15 mg kg^{-1} and are hence very similar to the Pampean samples.

Loess samples taken from the near surface (2 m depth or less) have higher concentrations of TOC than deeper samples, reflecting the proportion of recent organic matter in the modern soil horizons. Such shallow samples have TOC values of 0.15–0.94 % in contrast to samples collected from drilled cores (to 102 m depth) which have TOC values in the range 0.04–0.08 %.

The samples of volcanic ash are all rhyolitic with concentrations of Na_2O of 3.8–4.8 % and K_2O of 2.8–4.0 %. The ashes have higher concentrations of SiO_2, Na_2O, K_2O and Rb and lower concentrations of CaO, MgO, Fe_2O_3, TiO_2, Sr, Ni, Cr and Co than the loess sediments, as expected for material of

Table 7.3 **Statistical comparison of chemical data for loess samples (total-sediment analyses) from Córdoba (Nicolli et al., 1989) and La Pampa Provinces**

Constituent	Unit	Córdoba Min	Max	Mean	La Pampa Min	Max	Mean
SiO_2	wt %	59.4	64.1	61.3	39.25*	68.12	59.69
Al_2O_3	wt %	14.6	16.2	15.4	10.18*	16.72	15.03
Fe_2O_{3T}	wt %	4.04	5.55	4.83	3.35*	5.97	4.84
Mn_3O_4	wt %	0.07	0.79	0.50	0.06	0.15	0.10
MgO	wt %	1.55	2.33	1.87	0.88	2.8	1.85
CaO	wt %	3.43	5.51	4.45	1.92	21.97*	6.00
Na_2O	wt %	2.91	5.71	4.62	1.68	3.69	2.68
K_2O	wt %	2.23	2.43	2.33	1.32	2.78	2.23
TiO_2	wt %	0.64	0.77	0.70	0.51	0.85	0.71
P_2O5	wt %	0.15	0.18	0.17	0.08	0.24	0.15
LOI	wt %	3.28	5.63	4.45	1.83	18.28*	6.30
As	mg kg^{-1}	5.5	37.3	16.7	3	18	8
Se	mg kg^{-1}	1.1	2.3	1.5	1	1	1
U	mg kg^{-1}	1.3	8.0	3.0	0.9	5.1	2.5
Sb	mg kg^{-1}	0.25	0.88	0.55	1	1	1
Mo	mg kg^{-1}	2.2	5.2	3.4	1	5	3

*Lower values due to high carbonate component (higher values for CaO, LOI)

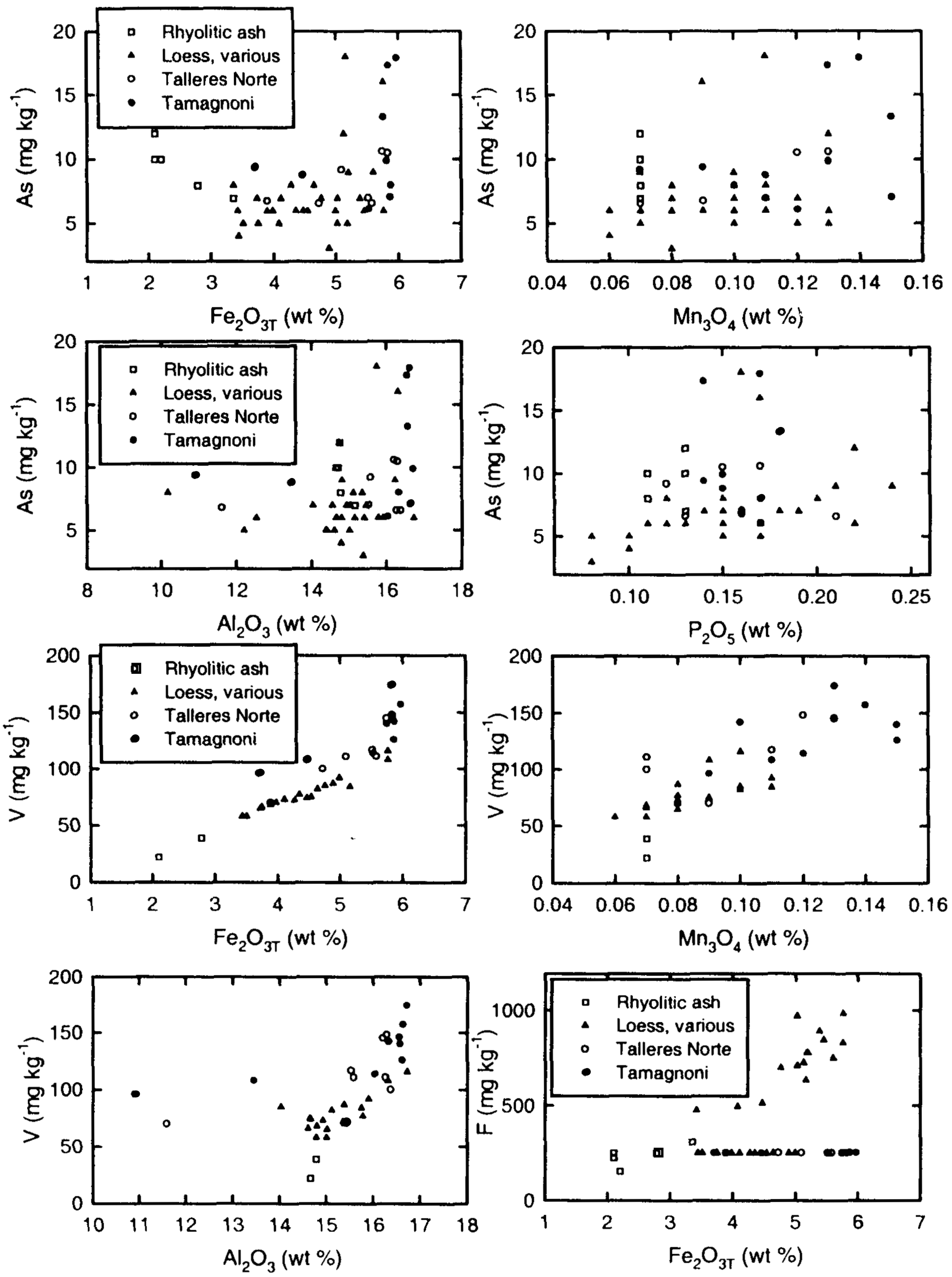

Figure 7.3 Variation of As, V and F with major oxides (Fe_2O_{3T}, Mn_3O_4, P_2O_5 and Al_2O_3) in the Pampean sediments (F has a high detection limit by this method, hence values below detection limit are plotted as 0.5 times the detection-limit value)

rhyolitic composition.

Variations between As and Fe_2O_{3T}, Mn_3O_4, Al_2O_3 and P_2O_5 are shown in Figure 7.3. Arsenic displays a weak positive correlation with Fe_2O_{3T}, although the rhyolitic ashes have relatively high As given the low concentrations of Fe_2O_{3T}. The weak correlation with Fe_2O_{3T} suggests that As is largely associated with Fe minerals although this is unlikely to be the case with the ashes, in which other minerals (such as aluminosilicates) may be more feasible sources. In the loess sediments, the Fe minerals retaining As may include magnetite, ilmenite, biotite, goethite and haematite as well as amorphous Fe oxides. It is not possible to distinguish between these from the major-oxide variations alone. The correlations between As and Mn_3O_4, Al_2O_3 and P_2O_5 are generally poor and do not show any clear associations to identify the main As mineral sources.

Variations of V and F show rather better correlations with Fe_2O_{3T} (Figure 7.3). As with As, the mineral associations are unclear, but it is considered that the most likely association is with Fe oxides. Positive correlations also exist between V and Mn_3O_4 and Al_2O_3 and suggest that Mn and Al oxides may also be potential sources for these elements.

7.4.1 *Talleres Norte and Tamagnoni samples*

The sediments analysed from the two cored boreholes have very similar major-element compositions, except in a few samples where a higher proportion of carbonate material is present (represented by lower SiO_2, Fe_2O_3 and higher CaO, LOI). TOC is typically in the range 0.04–0.07 % in all samples.

Concentrations of Mn_3O_4 increase with depth in Talleres Norte borehole (up to 0.13 %) and in Tamagnoni are relatively high (0.12–0.15 %) at 4.1–7.1 m depth and at 25-30 m depth (0.13–0.15 %). The horizons with highest Mn_3O_4 concentrations in Tamagnoni borehole correspond with the occurrence of black mottling observed in the sediment logs. There is no notable change in Fe_2O_3 with depth in the core sediments.

Concentrations of trace elements are also very similar in the two boreholes, although the carbonate-rich samples have lower concentrations of V (70–96 mg kg^{-1} compared to 100–174 mg kg^{-1}) and slightly lower Ba and Rb concentrations (Appendix 4.2).

Arsenic concentrations in the two profiles range between 7–18 mg kg^{-1}. Given the very high concentrations of As observed in the porewaters, especially at Tamagnoni, the measured results for total-sediment As concentration are noteworthy as they are not significantly above average concentrations in sediments (ca. 5–10 mg kg^{-1}; e.g. Webster, 1999). The average As concentration in sediments analysed from Talleres Norte is 8 mg kg^{-1}, and that for Tamagnoni is 11 mg kg^{-1}. The low concentrations support the observation from SEM investigation (Section 7.2) that no major As-rich mineral is present in the sediments. Nonetheless, the concentrations increase slightly with depth in each borehole and largely reflect the depth trends determined in the porewaters. The highest concentrations observed are from the deeper part of the Tamagnoni profile (25–30 m depth).

Despite the large differences in V observed in the porewaters from the two boreholes, total concentrations of sediment V are similar (excepting the carbonate-rich samples). Concentrations of U are uniformly low in both at 1–4 mg kg^{-1}. Fluorine concentrations are all less than 500 mg kg^{-1} and Mo and Se are 1 mg kg^{-1} or less throughout (Appendix 4.2).

7.5 Acid-ammonium-oxalate extracts

Ammonium oxalate (Tamm's Reagent) was chosen to selectively extract amorphous Fe oxide and associated trace elements from the sediments, without dissolving significant amounts of more crystalline oxide minerals such as haematite and goethite, although it is recognised that amorphous Al and Mn oxide will also dissolve (McKeague and Day, 1966; Brannon and Patrick, 1987). Other mineral phases such as magnetite and chlorite can also be partially leached by oxalate (Chou and Zhou, 1983; Kostka and Luther, 1994). Since both magnetite and chlorite have been identified in the sediments, it must be assumed that some of the oxalate-extractable element concentrations include additional components from these minerals. Nonetheless, the extract experiments give an upper limit to the amount of amorphous Fe as well as Mn and Al oxides present in the sediments and provide a useful measure for comparison since oxalate is a widely-used extract reagent in sediment investigations.

Results of the oxalate-extractable constituents in quarry and road cutting samples, augered samples and core samples (Talleres Norte and Tamagnoni) are given in Appendices 5.1 and 5.2. Results for Ca are not given because of precipitation of Ca oxalate and resultant low concentrations in the solutions.

Table 7.4 shows the proportions of oxalate-extractable element concentrations compared to the total concentrations (given by XRF analyses). The data indicate that Fe has been extracted from the sediments but that the proportion extracted is much less than the total Fe present (typically less than 5%). This indicates that a significant amount of Fe is present in other minerals, such as more structured iron oxides (e.g. goethite, haematite, ilmenite and in ferromagnesian minerals such as biotite and amphibole) which are not readily soluble in the oxalate solution. Nonetheless, a substantial amount of Fe is oxalate-extractable.

The data given in Table 7.4 also indicate that a significant amount of Mn has been extracted in the oxalate solutions, often more than 20% of the total available. It is assumed that these are mostly poorly ordered Mn(IV) oxides.

Oxalate-extractable Al concentrations are also large, ranging between ca. 250 and >2000 mg kg^{-1} (Appendix 5.1). Relatively high concentrations (ca. 630–1200 mg kg^{-1}) are found in the rhyolitic ashes. However, the oxalate-extractable Al concentrations are a very small proportion of the total Al present (typically 2% or less; Table 7.4). The Al mobilised is considered to be mainly from amorphous Al oxides, but a minor amount of silicate leaching (e.g. clays) may also have taken place. The small proportion of Al dissolved in oxalate reflects the high Al concentrations in these acid-volcanic rich silts and sands, where feldspar and clays are dominant mineral components.

The ranges of oxalate-extractable As concentrations are 0.3–1.3 mg kg^{-1} in quarry and road cutting samples, 0.7–6.8 mg kg^{-1} in augered samples and 0.6–10 mg kg^{-1} in cored sediments (Appendix 5.1). Rhyolitic ashes have concentrations of around 1 mg kg^{-1}. Table 7.4 shows that the proportions of oxalate-extractable As have a wide range between 4–56% of the total available. The higher oxalate-extractable concentrations tend to be present in sediments associated with high groundwater-As concentrations (especially Santa Rita and Tamagnoni).

Oxalate-extractable V concentrations range between 1–81 mg kg^{-1}, being 2–15 mg kg^{-1} in quarry and road cutting samples, 7–23 mg kg^{-1} in augered samples and 5–76 mg kg^{-1} in the cored sediments. As with As, the higher concentrations tend to be found in areas of high groundwater-V concentrations. Oxalate-extractable V concentrations represent 2–48% of the total available V (Table 7.4).

7.5.1 Cored sediments

Talleres Norte profiles

Profiles of oxalate-extractable concentrations for selected constituents are shown for the Talleres Norte and Tamagnoni cored boreholes in Figures 7.4 and 7.5.

In Talleres Norte, concentrations of Mg and Na increase with depth up to a maximum of around 3000 mg kg^{-1} and 2500 mg kg^{-1} respectively. The increases broadly reflect the increases in porewater concentrations of these elements with depth. The variations do not show any clear relationship with sediment lithology. Concentrations of oxalate-extractable S are highest in the shallowest parts of the profile (<5 m depth) and may be linked to the organic fraction in the sediments.

Concentrations of Al as well as Si, F and Ba are variable but do not show any clear trend with depth or lithology. As discussed above, Al is likely to be largely derived from Al oxide. However, this together with Si, F and Ba may also to have been sorbed onto Fe-oxide surfaces. Some may also have been derived from dissolution of chlorite and other silicate phases.

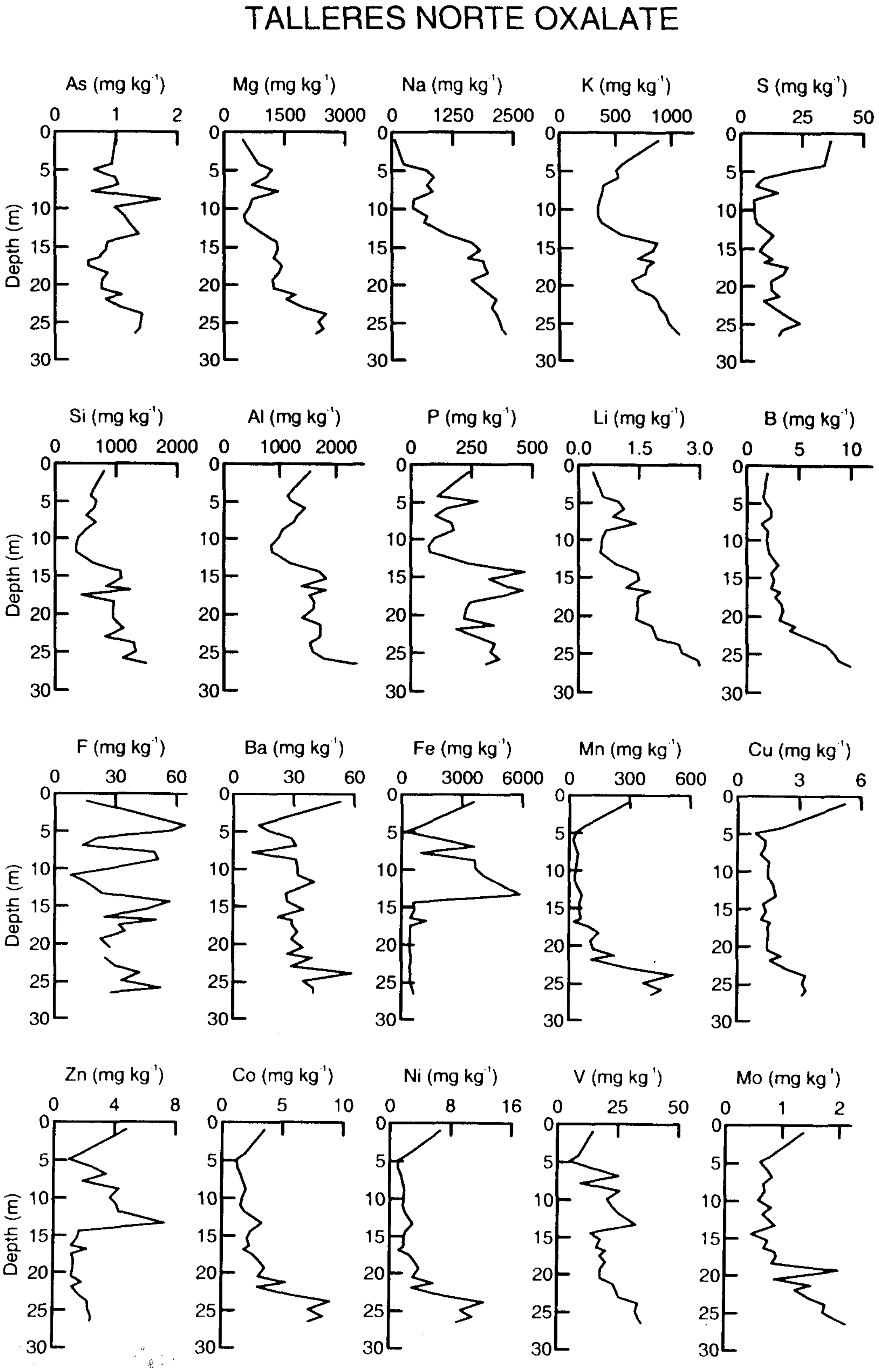

Figure 7.4 **Profiles for oxalate-extractable element concentrations in Talleres Norte borehole**

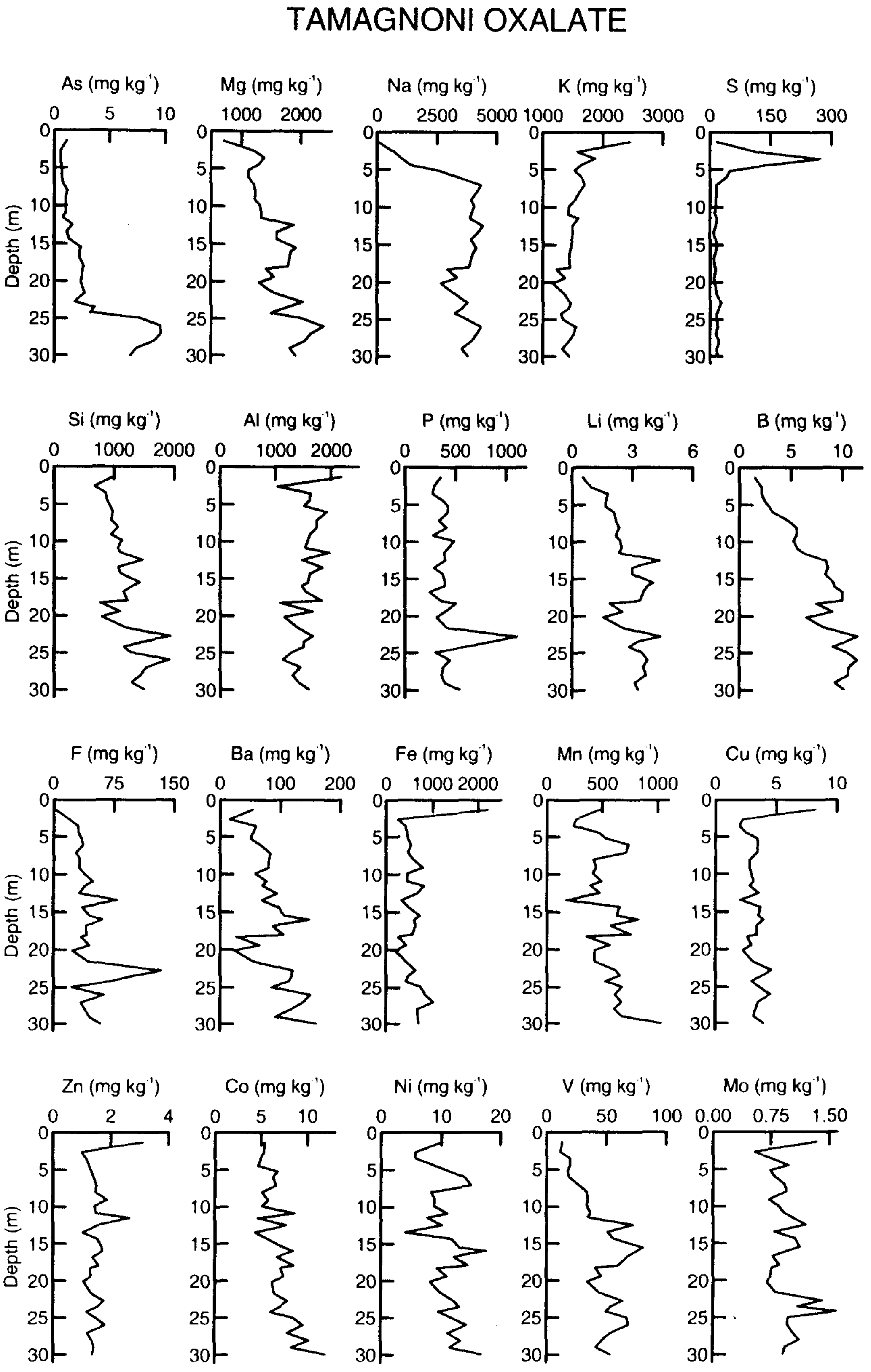

Figure 7.5 **Profiles for oxalate-extractable element concentrations in Tamagnoni borehole**

Table 7.4 **Proportions of selected determinands in oxalate and hydroxylamine extracts relative to total concentrations (%) in La Pampa sediments.**

Locality	Depth	Fe	Mn	Al	As	V	Fe	Mn	As	V
		%	%	%	%	%	%	%	%	%
	range (m)	-------- oxalate data ---------					-- hydroxylamine data --			
Quarry and road cutting samples										
?Tertiary, Toay cutting	1-2	0.8	37	1.7	11	13	nd	nd	nd	nd
?Quatern'y, Toay cutting	<1	2.0	20	0.9	20	7.0	nd	nd	nd	nd
4 km N Conhelo, above*	Nr surface	3.7	28	1.0	10	8.7	nd	nd	nd	nd
4 km N of Conhelo, ash	Nr surface	12	61	1.5	13	48	nd	nd	nd	nd
4 km N Conhelo, below	Nr surface	1.0	4	0.3	4	2.1	nd	nd	nd	nd
14 km E. Castex, above	Nr surface	2.7	17	0.5	13	6.1	nd	nd	nd	nd
14 km E. Castex, ash	Nr surface	6.0	34	0.8	13	16	nd	nd	nd	nd
14 km E Castex, below	Nr surface	3.8	27	0.8	16	8.3	nd	nd	nd	nd
LPS9, Caleufu	0.5-0.7	2.1	13	0.7	12	5.8	nd	nd	nd	nd
LPS10, Caleufu	1.3-1.5	3.7	31	1.3	13	8.5	nd	nd	nd	nd
LPS11, Caleufu	2-2.2	2.8	26	1.6	12	7.8	nd	nd	nd	nd
LPS12, La Maruja	1	1.7	18	0.9	10	5.2	nd	nd	nd	nd
Augered samples							nd	nd	nd	nd
Santa Rita	1-1.4	1.2	36	1.4	42	18	nd	nd	nd	nd
La Invernada	0.2-1	1.4	40	1.3	12	10	nd	nd	nd	nd
La Invernada	1-2	0.6	45	1.1	15	17	nd	nd	nd	nd
Piorno	1-1.4	2.4	45	1.3	21	17	nd	nd	nd	nd
Talleres Norte, E. Castex	0-0.25	3.8	32	1.8	12	10	nd	nd	nd	nd
Cored boreholes										
TN6	4.45-4.90	1.0	5	1.9	10	7	0.12	18	6.8	3
TN8	5.40-5.90	5.2	4	1.8	11	14	0.02	18	2.4	19
TN18	10.40-10.89	12	6	1.0	17	23	0.04	3	1.9	2
TN30	16.50-16.84	3.1	5	2.1	8	18	0.01	3	10	6
TN40	21.00-21.33	1.2	29	2.1	16	20	0.003	29	6.1	8
TN46	23.50-23.83	1.1	55	1.8	14	23	0.10	14	5.9	12
TN50	25.50-25.83	1.4	53	2.1	13	23	0.04	41	6.9	10
TAM8	4.10-4.45	1.1	54	1.9	10	17	0.06	57	7.1	8
TAM14	6.80-7.10	1.1	66	2.0	12	22	0.10	42	6.8	11
TAM24	11.28-11.50	2.0	54	2.3	10	25	0.07	46	7.2	14
TAM34	15.74-16.00	1.4	88	1.7	23	44	0.06	48	18	30
TAM40	18.11-18.30	1.0	55	1.9	27	42	0.09	61	11	27
TAM44	19.70-20.15	0.6	54	1.6	27	31	0.31	47	13	20
TAM56	25.38-25.50	2.0	61	1.3	53	44	0.04	43	26	26
TAM58	26.50-27.00	2.5	72	1.7	56	37	0.01	39	23	21
TAM64	29.50-29.95	1.7	95	1.8	52	38	0.02	41	23	19
Mean		2.7	39	1.4	18	19	0.07	34	11	15

*For more sediment details, see Appendix 5.1

Oxalate-extractable P concentrations vary with depth but have a maximum (up to 470 mg kg^{-1}) at around 14–17 m depth. The concentrations represent a significant proportion of the total P present (13–56%) in the sediments. Much of the P present may have been sorbed onto Fe-oxide surfaces. However, it is also likely that the P derives partly by dissolution of apatite. Calcium oxalate is highly insoluble and results in removal of Ca from the oxalate solution. Resultant reduction of the Ca^{2+} activity can therefore potentially drive dissolution of apatite.

Concentrations of Li, B, K, Mo, Co and Ni show a general increase with depth. In contrast, concentrations of Fe are highest over the depth range 0–13 m and decrease to around 400–500 mg kg^{-1} at deeper levels. The profile for Zn closely reflects that for Fe. Vanadium also shows some similarity to the Fe trend in the shallow parts of the borehole but unlike Fe, increases to high concentrations (up to 30 mg kg^{-1}) at the base of the borehole.

Concentrations of Mn are relatively high (up to 300 mg kg^{-1}) at the top of the Talleres Norte borehole, are lowest in the interval 5–15 m depth, and increase progressively at greater than 15 m. The Mn profile has some similarities with those of Li, B, Mo, Co and Ni (Figure 7.4). The trends suggest that some of the trace elements appear to be associated with the Mn-oxide fraction. Table 7.4 shows that up to 55% of the total Mn in Talleres Norte sediment is oxalate-extractable. The data suggest that amorphous Fe oxide dominates in the shallow part of the Talleres Norte boreholes, but that the amount of Mn oxide present increases with depth.

Concentrations of As vary slightly throughout the Talleres Norte profile but do not show any significant trend with depth, being mostly around 1 mg kg^{-1} (Figure 7.4), or 8–17% of the total As present (Table 7.4). The oxalate-extractable As concentrations are substantially lower than the oxalate-extractable P concentrations. Closer comparisons between the two and similar depth trends might be expected if both were present dominantly as sorbed ions on amorphous Fe oxide. The apparent excess of P further supports the suggestion that oxalate has dissolved some apatite.

Tamagnoni profiles

Profiles for Tamagnoni (Figure 7.5) indicate a slight increase in Mg and Na with depth. These trends are significantly different from those for Mg and Na in the extracted porewaters. Oxalate-extractable Na concentrations in particular are significantly lower at depths less than 7 m in the borehole. The reason for these divergent trends is not clear but may relate to ion exchange involving clay minerals in the sediments.

As with Talleres Norte, concentrations of total S are highest at shallow levels, reaching a maximum (273 mg kg^{-1}) at 3.0–3.5 m depth, possibly linked to organic matter. Oxalate-extractable Si, Al and P shows little variation with depth or lithology but as with Talleres Norte, much of this is likely to be associated with Fe oxide and Al oxide, although some minor silicate material may also have been dissolved.

Iron shows a marked peak at the top of the Tamagnoni profile (up to 2200 mg kg^{-1} in the shallowest sample measured). Below this, Fe concentrations are typically around 500 mg kg^{-1} and vary little with depth or lithology. These concentrations are significantly less than the oxalate-extractable Fe at the top of Talleres Norte borehole (<13 m depth) but comparable to the concentration range found in the deeper profile at Talleres Norte. Trends for Cu and Zn follow the Fe trend closely (Figure 7.5).

As with Talleres Norte, a significant amount of Mn (up to 95 %; Table 7.4) has been extracted in the Tamagnoni oxalate solutions. Manganese increases slightly with depth. Concentrations are higher than in Talleres Norte throughout the profile and reach up to 1000 mg kg^{-1} in the lower part of the borehole.

Oxalate-extractable P concentrations vary little with depth (300–400 mg kg^{-1}), apart from a discrete peak (1100 mg kg^{-1}) at 23.0–23.5 m depth. The concentrations represent around 50–70% of the total P present. As with Talleres Norte, it is likely that some of the P derives by dissolution of apatite by oxalate, although some may have been desorbed from oxide surfaces.

Concentrations of As increase with depth in Tamagnoni borehole, with a pronounced peak of up to 10 mg kg^{-1} at 24–30 m depth (Figure 7.5). Oxalate-extractable As concentrations are higher in the lower part of Tamagnoni than in any of the other sediments investigated (Appendix 5.1), amounting to in excess of 50 % of the total As present (Table 7.4). The depth trend does not follow closely that of any other determinand in the oxalate extracts. The highest concentrations correlate broadly with the occurrence of finer-grained sediments (clayey silts) near the base of the borehole. The peak also coincides with the highest As concentrations found in the porewaters. From the trends it is not clear whether the oxalate-extractable As is associated with Fe oxides or with other phases (such as Mn oxide). As with Talleres Norte and indeed sediments in general, the amounts of oxalate-extractable As are substantially lower than oxalate-extractable P concentrations.

Of the other constituents which form anions and oxyanions in solution, there is significantly more oxalate-extractable F and V in Tamagnoni than Talleres Norte, though ranges for B and Mo are comparable.

Comparisons between the two profiles

Since porewater As concentrations in the Talleres Norte and Tamagnoni profiles are relatively high, some of the As derived in the extract fractions is likely to be derived directly from the original porewater. Assuming that the average porewater volume is 30% (from dry-weight moisture-content measurements, Appendix 3.1), and sediment crystal density is close to quartz at 2.65 g cm^{-3}, amounts of As derived from porewater can be up to 0.07 mg kg^{-1} in sediments from Talleres Norte and up to 1.3 mg kg^{-1} (TAM58, 26.5–27.0 m depth) in the Tamagnoni borehole. Whilst in Tamagnoni, this is a significant amount of As, it is still relatively small compared to the total As extracted by oxalate and hydroxylamine at the corresponding depths. The measurements therefore indicate that the As extracted by oxalate and hydroxylamine is derived significantly from the sediments (principally Fe and Mn oxides) and not simply from porewater.

Figure 7.6 shows the variation in concentrations of oxalate-extractable As with Fe, Mn and Al, considered to be dominantly from amorphous oxide phases. These are compared with the ranges from parts of the alluvial aquifers of Bangladesh (BGS/MML, 1999).

Trends for Fe and As are notably different between Talleres Norte and Tamagnoni. Talleres Norte sediments have much higher oxalate-extractable Fe (up to 6000 mg kg^{-1}) and there is a slight positive correlation between the oxalate-extractable As and Fe concentrations in this profile. Concentrations from Talleres Norte are broadly comparable to those found in sediments containing high-As groundwaters from the Chapai Nawabganj (CN1) area of Bangladesh but much higher than those in sediments containing low-As groundwaters (CN2, Figure 7.6; BGS/MML, 1999).

Concentrations of oxalate-extractable Fe in the Tamagnoni sediments are at the low end of the range observed for Bangladesh sediments from high-As aquifers (CN1, Figure 7.6) and suggest that they have much smaller amounts of amorphous Fe(III) oxide than in the As-affected Bangladesh aquifers.

Figure 7.6 highlights the different ranges of oxalate-extractable Mn concentrations between the Talleres Norte and Tamagnoni profiles. Concentrations are much higher in Tamagnoni and these samples show a weak positive correlation with oxalate-extractable As. Concentrations of Mn are also higher than oxalate-extractable Fe concentrations. Tamagnoni Mn concentrations are also considerably higher than values obtained from high-As aquifers in Bangladesh (Figure 7.6) and suggest that Mn oxide is a much more prevalent mineral in Tamagnoni and may be an important mineral source of As.

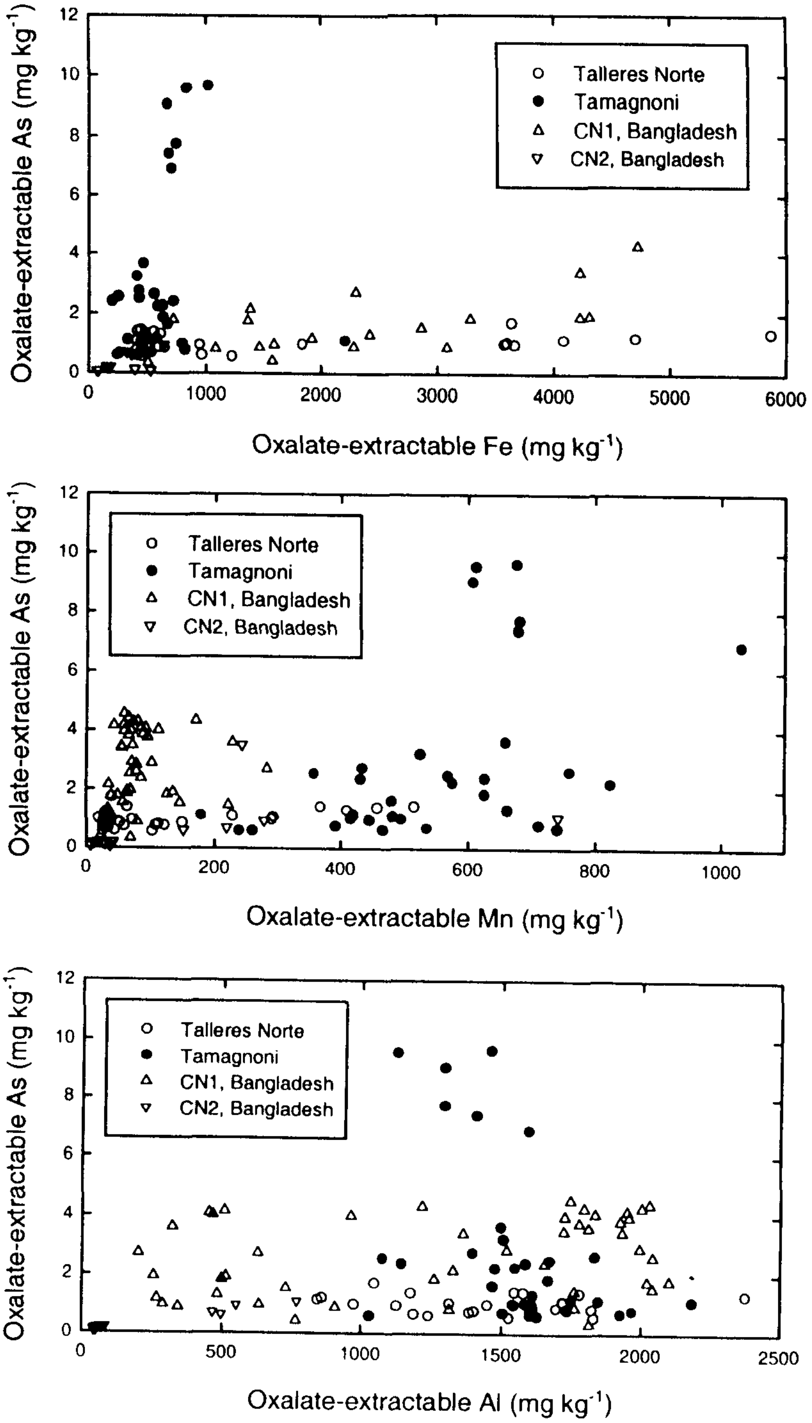

Figure 7.6 Variation in concentrations of oxalate-extractable Fe, Mn and Al with oxalate-extractable As in sediments from the Talleres Norte and Tamagnoni boreholes, compared to sediments from a high-groundwater-As area (CN1) and low-groundwater-As area (CN2) in Chapai Nawabganj District, Bangladesh

Oxalate-extractable Mn concentrations in sediments from Talleres Norte are also at the high end of the range for Mn concentrations from As-rich aquifers in Bangladesh (CN1, Figure 7.6), despite being much lower than Tamagnoni values. The data indicate that amorphous Mn is more prevalent in the Pampean sediments than the Bangladesh alluvial sediments.

Oxalate-extractable Al concentrations have a similar range in the Talleres Norte and Tamagnoni profiles. On a mole basis, the concentrations are much higher than oxalate-extractable Fe in

Tamagnoni sediments. They are also broadly comparable with oxalate-extractable-Al concentrations in the As-rich aquifers from Bangladesh (CN1; Figure 7.6).

The presence of high concentrations of Mn as well as Si and Al in the oxalate extracts indicates that significant amounts of amorphous oxide minerals, as well as possibly magnetite, chlorite and other silicates, have been dissolved. While the reagent gives a good overall assessment of trace-element associations with poorly-ordered oxide minerals, more selective reagents would be of additional value for assessing specific trace-element associations. Ascorbate for example (pH 8; Kostka and Luther, 1994) may have been useful for specific assessment of amorphous Fe(III) oxide concentrations. Hydroxylamine hydrochloride is recognised as a more specific reagent for Mn (IV) oxide (Chou, 1972).

7.6 Hydroxylamine-hydrochloride extracts of cored sediments

Petrographic investigations of the sediment profiles indicated the presence of Mn oxide in some horizons, particularly the deeper parts of Tamagnoni borehole where the mineral has been found as a pervasive cement. Hydroxylamine hydrochloride was therefore chosen as a more specific extract reagent for assessing the associations between trace elements and Mn oxide (Chou, 1972). Chemical data for the hydroxylamine extracts are given in Appendices 6.1 and 6.2. Profiles for selected elements are given in Figures 7.7 and 7.8.

The highest hydroxylamine-extractable concentrations observed in either profile are for Ca (up to 5 wt %) and indicate that the reagent (being acidic, pH 2) has also extracted some carbonate from the sediments.

As expected, concentrations of Fe are significantly lower than for the oxalate extracts (hydroxylamine-extractable Fe being typically <50 mg kg^{-1}) and indicate that relatively little Fe oxide has been extracted in the procedure. Silicon and Al are also present in the hydroxylamine extracts, indicating the release of some additional mineral phases such as Al oxide and silicate minerals. However, the amounts are significantly less than in the oxalate extracts (typically 50% less) and suggest that less of this material has been extracted. Concentrations of hydroxylamine-extractable Mn are slightly lower than oxalate-extractable concentrations in each borehole. This may be because hydroxylamine has been selective for Mn oxide whilst the oxalate may include some Mn oxide as well as Mn from other minerals (including Fe minerals).

Talleres Norte

Profiles for Mg and Na closely reflect those found in the oxalate extracts for these sediments. Concentrations of Ca are highest in sediments from around 4–8 m depth, in the depth range where bands of calcrete are best-developed.

Hydroxylamine-extractable Mn increases steadily throughout the borehole, reaching a maximum of around 400 mg kg^{-1} at the bottom of the borehole (Figure 7.7). Hydroxylamine-extractable Fe is high (87 mg kg^{-1}) at the topmost part of the borehole, but is low although variable throughout the rest of the profile.

Hydroxylamine-extractable As varies between 0.02–0.7 mg kg^{-1} in Talleres Norte and generally increases with depth. The concentrations are around half the oxalate-extractable As concentrations.

The trend for V roughly follows that for As (with the exception of a spurious V peak, 21 mg kg^{-1} at ca. 5.5 m depth). Trends for the other elements do not show any clear association with depth or lithology (Figure 7.7).

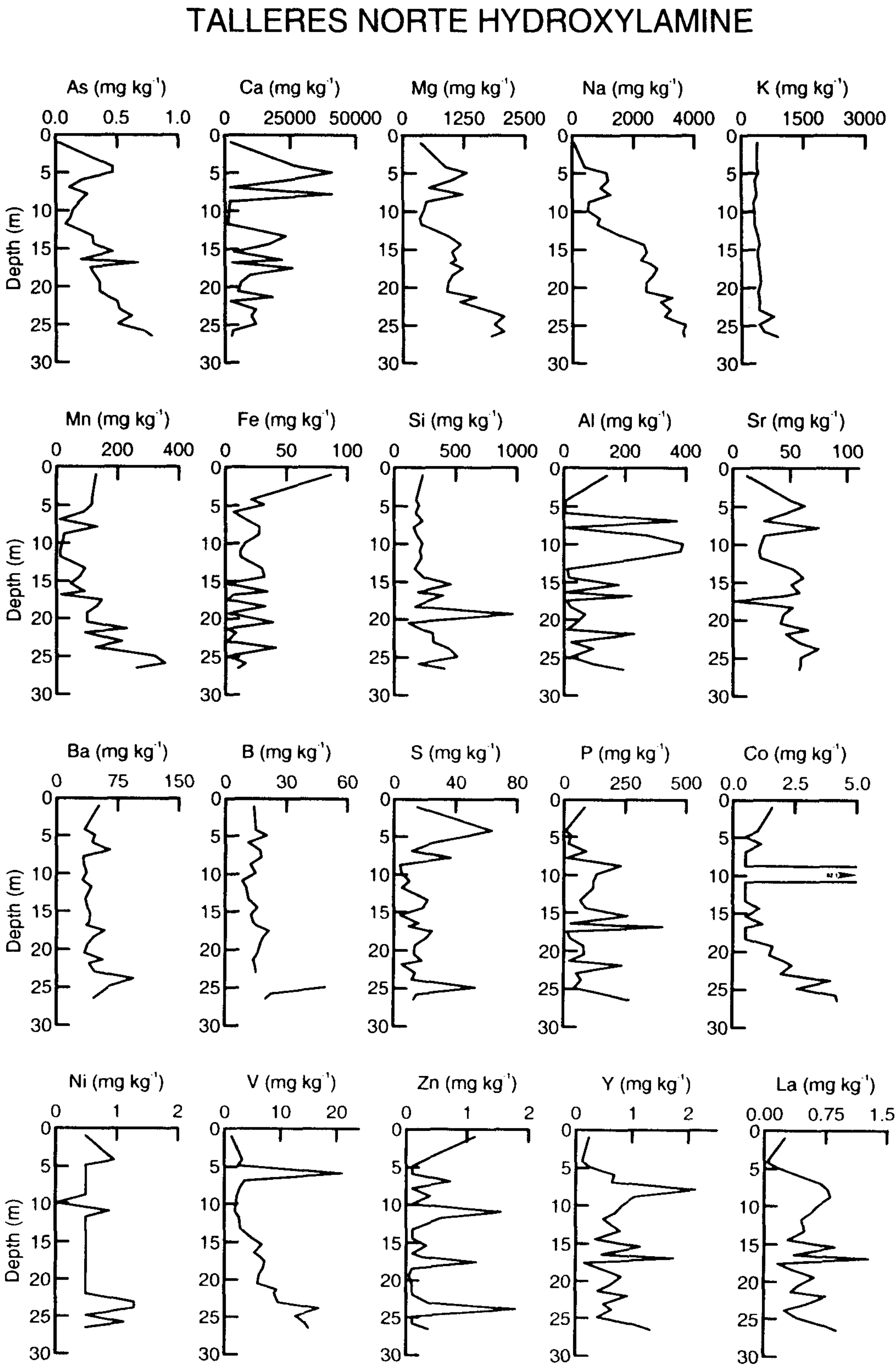

Figure 7.7 Profiles of hydroxylamine-extractable element concentrations in sediments from Talleres Norte borehole

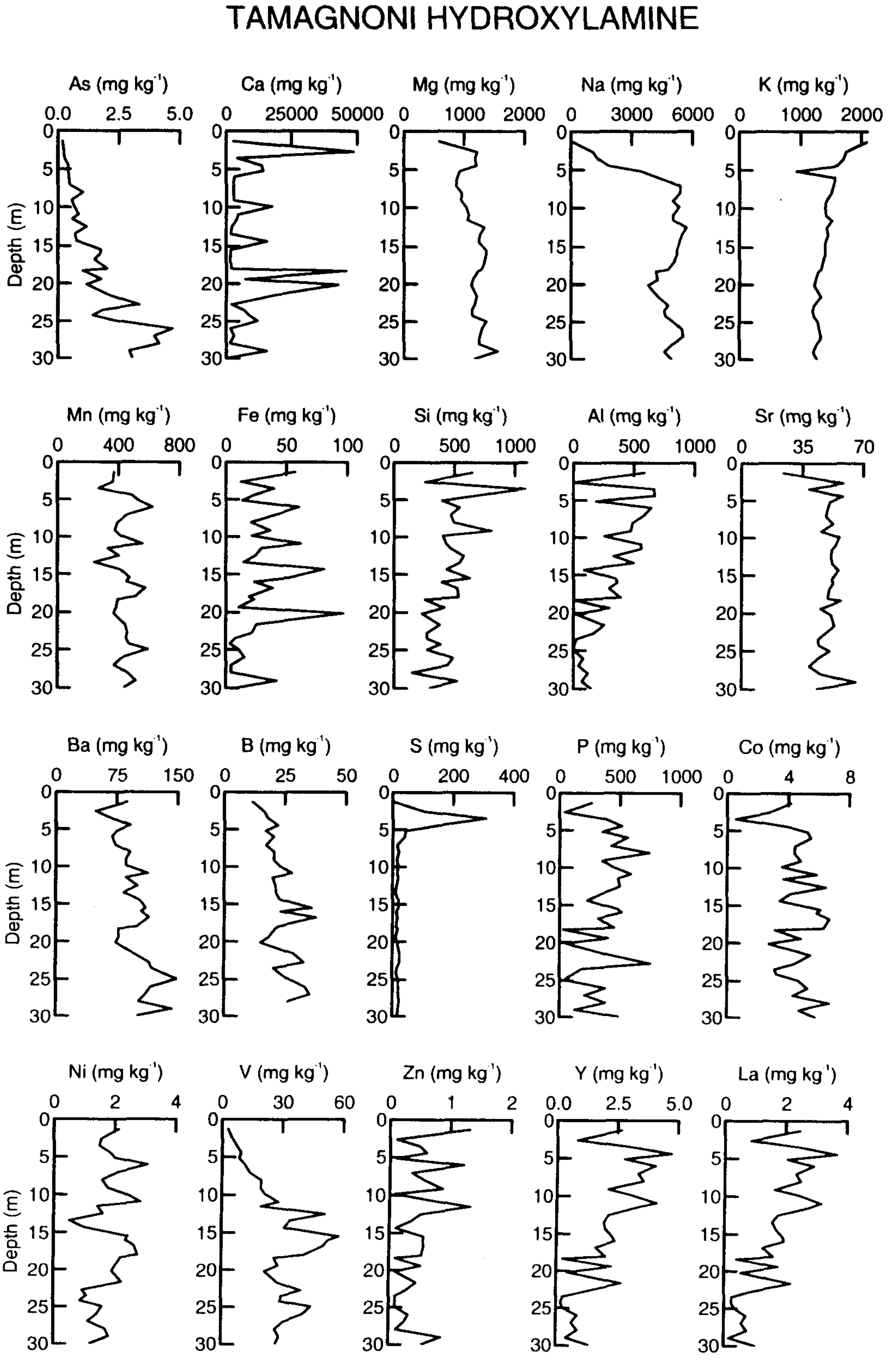

Figure 7.8 Profiles of hydroxylamine-extractable element concentrations in sediments from Tamagnoni borehole

Profiles of Mg and Na largely coincide with the oxalate-extractable trends. Calcium concentrations are variable throughout the profile and do not have any obvious relationship with horizons of calcrete. As with the oxalate profile, S has a marked peak of comparable magnitude (up to 300 mg kg^{-1}) at 3.0–3.5 m depth (Figure 7.8). The concentration is uniformly low throughout the rest of the profile. Although not positively identified petrographically, it is possible that the peak reflects presence of gypsum in the topmost part of the profile as porewaters at the water table in the profile are saturated with respect to this mineral (Figure 6.20) and hydroxylamine-extractable Ca concentrations are also high at the top part of the borehole.

Hydroxylamine-extractable Mn varies slightly with depth, but is mainly around 400 mg kg^{-1} throughout the Tamagnoni profile. Values are broadly comparable with oxalate-extractable concentrations of Mn and the trends with depth are also similar.

Hydroxylamine-extractable Al concentrations have a relatively large variation (2–60 mg kg^{-1}) but generally decrease with increasing depth. The source is likely to be an Al oxide in particular. Profiles of Y and La broadly follow the Al trend (Figure 7.8).

Concentrations of hydroxylamine-extractable As increase with depth, reaching up to 5 mg kg^{-1} near the bottom of the profile. As with Talleres Norte, the amounts are roughly half those of the oxalate-extractable fractions. Concentrations of V largely increase with depth and have some correlation with As (Figure 7.8). Concentrations of other trace elements have little notable change with depth in the Tamagnoni profile.

Figure 7.9 shows the relationship between hydroxylamine-extractable Mn and As in both the Talleres Norte and Tamagnoni profiles. The plot demonstrates the clear distinction in Mn between the two profiles, Tamagnoni being much higher, as well as the much higher concentrations of hydroxylamine-extractable As in Tamagnoni. The relationship suggests that much of the As in the Tamagnoni sediments is associated with Mn oxide (either within the structure or adsorbed). The data contrast strongly with a batch of five samples extracted at the same time as the Pampean samples from sediments from a high-groundwater arsenic area in Bangladesh (Chapai Nawabganj). These samples all had <0.02 mg kg^{-1} of hydroxylamine-extractable As despite having total As concentrations in the same range. Unlike La Pampa, As in the Bangladesh sediments therefore does not appear to be significantly associated with Mn oxides.

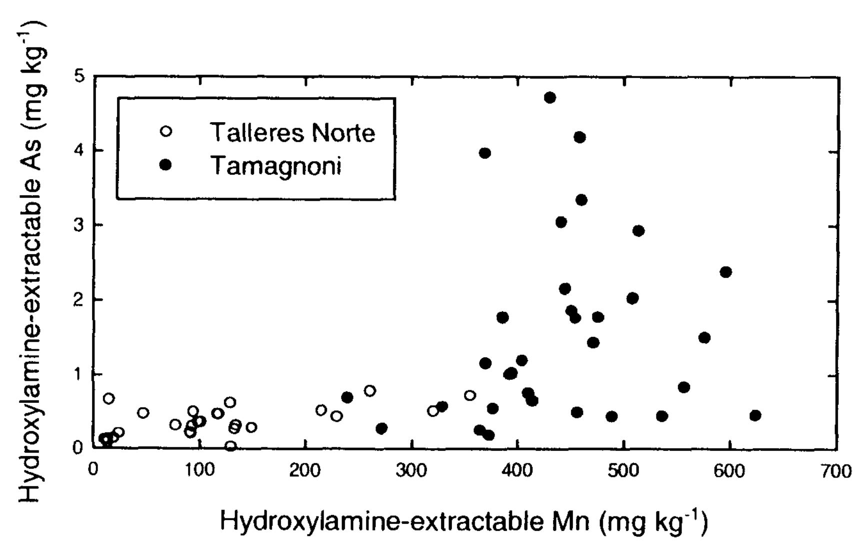

Figure 7.9 **Variation of hydroxylamine-extractable Mn with hydroxylamine-extractable As concentrations in the Talleres Norte and Tamagnoni profiles**

7.7 Discussion: arsenic associations in the sediments

It has been shown that the Pampean sediments are dominated by brown to dark brown silts with a high proportion of sodic plagioclase, together with quartz, K-feldspar, ferromagnesian minerals, pumice and some altered glass fragments and heavy minerals (ilmenite, magnetite, zircon, monazite and apatite). The ferromagnesian minerals (e.g. biotite) are often highly altered and replaced by chloritic clay, Fe oxide and Mn oxide. The clay minerals are dominated by smectite with subordinate illite and are largely poorly crystalline. Precipitation of secondary calcium carbonate has been prominent in the form of calcrete nodules, cements and discrete layers ('tosca'). Cements of Fe and Mn oxides are also formed in places. It is clear that the sediments have been highly reworked and altered since deposition and, in the case of volcanogenic products, since eruption.

Arsenic and other trace elements may therefore have undergone a significant degree of recycling during the processes of alteration and diagenesis. Nicolli et al. (1989) postulated that the source of arsenic in groundwaters from neighbouring Córdoba Province was the volcanic glass from the loess deposits which weathered and released arsenic and other trace elements. These authors gave the range of As concentrations for volcanic glass separated from Córdoban sediments as 6.8–10.4 mg kg^{-1}. This is slightly higher than the average for volcanic glasses from silicic volcanic rocks given by Onishi and Sandell (1955; 5.9 ± 0.9 mg kg^{-1}). This may indeed be one of the primary sources of As in the sediments, especially since highly unstable in the weathering environment and potentially prone to rapid devitrification. However, several other minerals present in the loess deposits are also likely to have arsenic concentrations in the range of a few mg kg^{-1} and provided they are susceptible to alteration, are also likely sources of arsenic. Indeed, primary Fe oxides (e.g. magnetite, ilmenite) typically have significantly more As than the silicate minerals (Section 2.4). As discussed above, secondary oxides (Fe, Mn, Al) have especially high capacities for As sorption and hence high concentrations of As derived from the primary minerals following alteration. It is therefore considered that the secondary minerals, particularly the oxide minerals, are the key phases controlling mobilisation of As and other anions/oxyanions in the Pampean aquifer. Hence sorption/desorption reactions are considered critical to the mobilisation of these elements.

The oxalate- and hydroxylamine-extract data indicate that some of the As and other anion species in the sediments are associated with amorphous Fe, Mn and Al oxides. The data produced show the limitations of using such methods to test the associations of trace elements because of the lack of selectivity. Although the hydroxylamine reagent appears to be relatively selective for Mn oxide, oxalate is clearly a more general extract reagent for amorphous and poorly-ordered oxides of Fe, Mn and Al, as well as partially dissolving magnetite, chlorite and other silicate minerals. Nonetheless, the data give some appreciation of the relative contributions of the different mineral phases.

The combined evidence from oxalate and hydroxylamine data suggests an increasing concentration of amorphous Mn oxide and concomitant decreasing concentration of amorphous Fe oxide with increasing depth in the profiles, particularly that of Talleres Norte. Presence of As in both the extract fractions and correlations with Mn in particular suggest that a significant proportion of the As is sorbed to amorphous oxides of Mn as well as Fe and Al.

The fact that not all the As was extracted using these reagents (typically <50% was mobilised) indicates that other more crystalline phases also retain As. These are likely to include goethite, haematite and ilmenite among the oxide minerals, as well as biotite.

7.7.1 Arsenic partitioning and transport

If the oxalate-extractable As concentrations are taken as representative of the As associated with amorphous oxides (dominantly Fe oxide), a sorption isotherm for As on amorphous Fe oxide can be constructed using oxalate data and groundwater As concentrations. Figure 7.10 shows such a sorption isotherm for the Pampean sediments, constructed using dissolved As in porewater against sorbed As estimated from the acid-oxalate extracts (minus the porewater As component which can be significant in the samples with highest As concentrations near the bottom of Tamagnoni borehole, up to ca. 1.3 mg kg^{-1}).

The oxalate-extractable As concentrations used to construct the isotherm include not only 'sorbed' As associated with the amorphous Fe oxides, but also As dissolved from these minerals, as well as from Mn and Al oxide, magnetite, chlorite and other silicate phases. The oxalate-extractable concentrations must therefore be an upper estimate of the amounts of sorbed As, but nonetheless give a useful approximation.

Figure 7.10 indicates a general positive correlation for Tamagnoni, though the Talleres Norte data produce a broad scatter, at lower concentrations. The 'isotherm' is close to linear. The As present in both solution and sorbed is taken to be dominantly arsenate (As(V)) because of the predominance of this species in the Pampean groundwaters. The correlation has been fitted with a linear regression and gives a slope (or distribution coefficient, K_d) of 1.1 l kg^{-1}. This small K_d value indicates that the retardation of As(V) on the Tamagnoni sediments is likely to be small, which follows from the large amount of As observed in the porewaters compared to the relatively small concentrations found in the solid phase. The value obtained is at the low end of the range of K_ds for arsenate sorption onto sediments given in the literature. Baes and Sharp (1983) collated literature data for K_d values for a number of elements and reported values of between 1.9 and 18.0 l kg^{-1} (median 6.7 l kg^{-1}, 37 samples) for arsenate in soils and clays. Davis et al. (1997) found K_d values for As of 1300 l kg^{-1} and 2900 l kg^{-1} for sediments from two inter-tidal cores, the As being principally associated with ferric oxides and hydroxides.

For the Tamagnoni profile, an approximate retardation factor (R) can be calculated using the equation $R = 1+(\rho_b/\varepsilon)K_d$, where ρ_b is bulk density (g cm^{-3}) and ε the porosity (Appelo and Postma, 1993). Using an ε value of 0.3 (30%, from moisture-content values), ρ_b of 1.86 g cm^{-3} and K_d of 1.1 l kg^{-1}, this gives a value for R of around 8 and suggests that in the Tamagnoni part of the aquifer, As transport in groundwater is only around 8 times slower than groundwater flow velocity. This again is likely to represent an upper estimate.

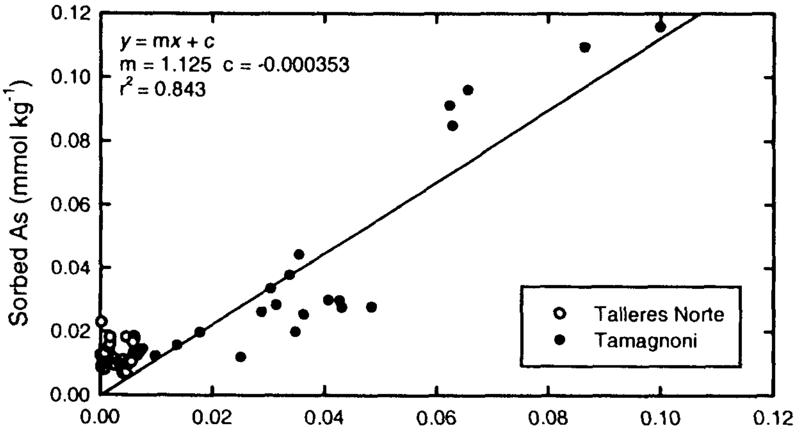

Figure 7.10 **Sorption isotherm for As using data from Tamagnoni borehole and fitted using a linear regression equation. Data for Talleres Norte are also given for comparison, but are not included in the regression calculation. Dissolved As is the porewater As concentration; sorbed As is As measured from the oxalate extraction minus the As component from the porewater, calculated using porosity from the sediment moisture-content data and assuming crystal density of 2.65 g cm^{-3}**

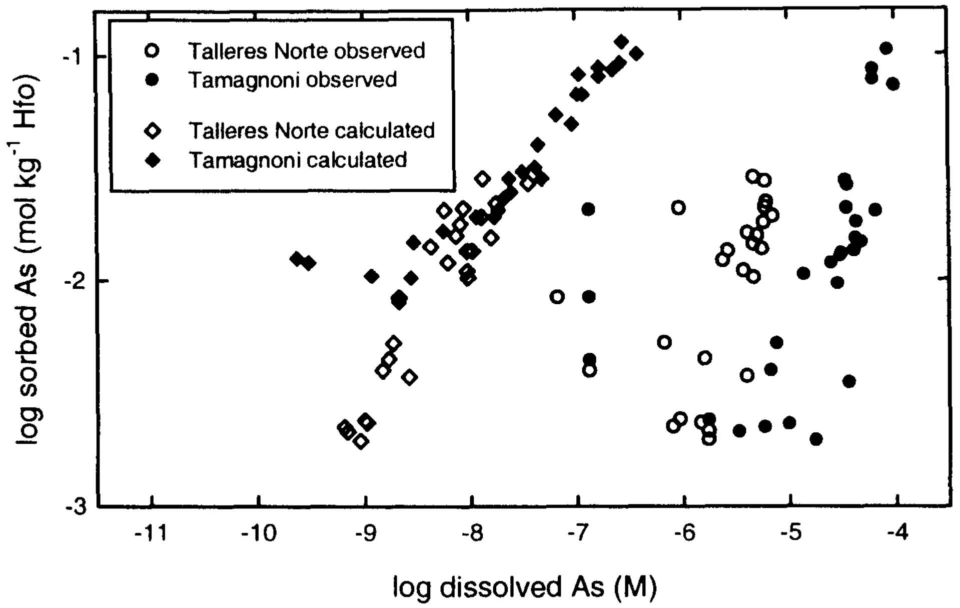

Figure 7.11 **Isotherm plots for As in the Talleres Norte and Tamagnoni boreholes showing observed values (dissolved concentrations in porewaters, sorbed from oxalate-extractable As data minus the porewater As component) compared to values calculated from equilibrium sorption of arsenate onto Hfo using PHREEQC and the diffuse double-layer model (DLM) of Dzombak and Morel (1990). Hfo concentrations are taken from oxalate-extractable Fe**

The derived K_d and retardation values for Tamagnoni are of direct relevance for the modelling of As mobilisation in aquifers using solute-transport models. The low retardation factor is considered to be caused by the high pH of the groundwaters (laboratory-measured pH values in the porewaters were 8.3 or higher; Appendix 3.1), the predominance of As in the (V) oxidation state and the high concentration of competitors. As noted in Section 6, the high pH values are controlled by extensive silicate reaction (particularly feldspar weathering which involves take-up of protons) and calcite/dolomite precipitation which involves loss of CO_2. Predominance of As as As(V) in the groundwater will also be accentuated in the presence of Mn(IV) oxide as this is a well-documented oxidising agent for As(III) and other trace-element species (e.g. Kuhn and Sigg, 1993).

Figure 7.11 shows a sorption isotherm plot for the Talleres Norte and Tamagnoni As data compared to predicted trends from equilibrium sorption of arsenate onto Hfo. The observed data are the porewater As concentrations for each profile against sorbed As concentration, taken as the oxalate-extractable As concentration minus the porewater As component (calculated as for Figure 7.10) and recalculated to kg Hfo assuming all oxalate-extractable Fe is present as Hfo. Predicted dissolved and sorbed concentrations are calculated using PHREEQC and the diffuse double-layer model (DLM) of Dzombak and Morel (1990). Values were calculated using the porewater pH, As and Na concentrations and assuming an Hfo concentration equivalent to the oxalate-extractable Fe value for each sample.

Trends given in Figure 7.11 indicate that the predicted dissolved As concentrations from the model are much lower (by three orders of magnitude) than the measured As concentrations in the porewaters. Even though the oxalate-extractable Fe concentrations are low in the cored boreholes, if this is taken to be Hfo, the model predicts that sufficient Hfo is present for near-complete sorption of As (arsenate) onto the Hfo surfaces. The most likely cause of the discrepancy is that oxalate-extractable Fe concentrations are a significant overestimate of the amount of Hfo available in the system because they include other minerals. More crystalline Fe oxides present have capacity to sorb As but lower surface areas render them less efficient as sorption surfaces than Hfo. The model has also not taken into account potential competition from other anions, particularly phosphate which has porewater concentrations of typically 0.5 mg l^{-1} (as P_T) and relatively high oxalate-extractable concentrations (100–1000 mg kg^{-1}, although some of this is likely to be from apatite).

The modelled results indicate either that oxalate-extractable Fe concentrations are a poor indicator of the concentrations of amorphous Fe oxide present in the sediments (likely, from the above discussion), and/or that the simple application of the DLM model to natural iron oxides significantly overestimates the amount of As expected to be sorbed. This is either because, under the natural conditions found in Argentina, anion competition greatly reduces sorption of As or because the surface properties of natural Hfo are significantly different from synthetic Hfo. These possibilities are the focus of much current research.

8. OPTIONS FOR MITIGATION

8.1 Groundwater-quality situation

It is clear from the results of the hydrogeochemical surveys of the Pampean groundwaters that the groundwater has many serious quality problems with potentially detrimental consequences for human and animal health. From the regional survey, very few samples had acceptable concentrations of As. Only 27% of samples analysed had As concentrations less than the Argentine standard of 50 µg l^{-1} and only 5% less than the WHO guideline value of 10 µg l^{-1}. Additional problems due to high salinity, F, B, NO_3-N, Mo, U and a number of other constituents make the majority of groundwaters in the area unacceptable for potable supply. It is therefore critical that moves to mitigate the water-quality problems be implemented in order to safeguard public health. However, given the climatic and hydrogeological conditions in La Pampa, solutions to the problem are not easily found.

The scale of the water-quality problems in the Pampean groundwaters has been summarised here using a scoring system defined on the basis of As, F, Na and NO_3-N to encompass the range of inorganic quality problems encountered. This 'contamination index' has been defined using the following criteria:

As	10–50 µg l^{-1}	1
	50–200 µg l^{-1}	2
	200–1000 µg l^{-1}	3
	>1000 µg l^{-1}	4
F	1.5–5 mg l^{-1}	1
	5–10 mg l^{-1}	2
	10–20 mg l^{-1}	3
	>20 mg l^{-1}	4
Na	200–1000 mg l^{-1}	1
	>1000 mg l^{-1}	2
NO_3-N	>11.3 mg l^{-1}	1

The scores for each parameter have been added and summarised in a histogram in Figure 8.1. High scores indicate the worst chemical quality. Only a score of zero would indicate a water source with overall good inorganic quality suitable for drinking. The results indicate the severity and scope of the problems in the Pampean groundwaters. The modal index score is 7 and scores up to 12 are observed. None of the sampled sources had a value of zero. Mitigation measures need to take adequate account of the many parameters which are potentially detrimental and/or undesirable.

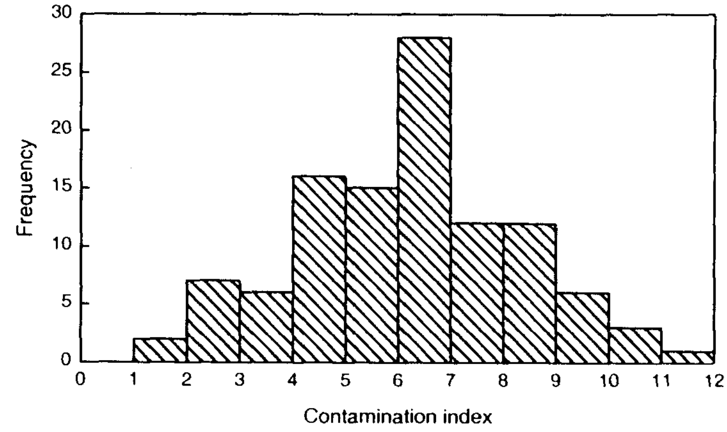

Figure 8.1 **'Contamination index' defined using the parameters As, F, Na (as index of salinity) and NO_3-N in the Pampean groundwaters**

Table 8.1 Summary of the range of mitigation options for La Pampa and their practical viability

Mitigation option	Viability
Surface water	No sustainable supplies available, not an option
Rainwater harvesting	Semi-arid climate means limited rainwater supply, and seasonal. Nonetheless, is likely to provide a suitable supply of water for some rural areas, at least for parts of the year
Groundwater treatment	*Urban scale:* Requires sophisticated and expensive treatmemt methods such as reverse osmosis or activated alumina. Reverse osmosis is the currently used method in most urban areas *Domestic/rural scale:* Treatment using coagulation/filtration (e.g. alum) will provide some improvement, but efficacy may be compromised by high salinity (and pH)
Borehole siting	Suitable for installation of new boreholes. Existing boreholes could be deepened to provide some amelioration. The improvements are likely to be limited as few groundwaters of acceptable quality are known to exist in the region, even given optimal siting

8.2 Potential mitigation strategies

A logical mitigation step would be distinction of available water supplies according to their intended use. Better quality is required for potable supply than for agricultural, industrial and other domestic uses. However, irrigation using brackish water has potentially serious implications for crop productivity and irrigation with water containing high concentrations of toxic elements including As, B, F and U has unknown, but potentially detrimental, consequences for plant uptake and accumulation in food supplies.

For potable supply, the range of potential mitigation options for La Pampa include:

i. use of surface water;

ii. rainwater harvesting;

iii. treatment of existing groundwater;

iv. optimisation of borehole siting.

Each of these options is discussed further below.

8.2.1 Surface water

There are no sources of permanent surface water in the northern part of La Pampa. The nearest rivers are the Rio Salado, some 140 km west of Ingeniero Foster and the Rio Colorado which demarkates the southern border of La Pampa, over 300 km south of Eduardo Castex. Use of surface water is therefore not a viable option for La Pampa.

8.2.2 Rainwater harvesting

Although the Pampean climate is semi-arid, storage of seasonal rainfall could be a potential option for provision of potable water supply, at least for part of the year. This option is practised in many parts of the world where either limited availability or poor quality of groundwater are a problem. Rainwater harvesting is a traditional method used in parts of southern Asia for example, and is being tried currently in Bangladesh as a mitigation measure against groundwater-As problems. Rainwater is also used commonly in parts of Australia, where climatic conditions are also arid or semi-arid. Here, rainwater is collected from roofs and stored typically in suitably protected containers or storage ponds. Despite limited rainfall, many of these are able to provide permanent supplies of water for potable domestic use. Storage of rainwater in La Pampa could be either in lined ponds or large covered containers. Since from average rainfall figures (Section 4), all months except May to September have more than 40 mm of rainfall, storage capacity would only need to be sufficient to cater for these dry months.

The potential benefits of rainwater harvesting in terms of water quality are obvious and the technology relatively simple. The method should therefore be worthy of investigation for the Pampean situation.

8.2.3 Groundwater treatment

As there is no permanent surface water in northern La Pampa and rainwater harvesting is not practised, groundwater currently constitutes the only major source for potable and agricultural supply. Mitigation of the groundwater quality is complicated by the fact that As is only one of a number of chemical constituents that give rise to potential health or acceptability problems. One of the most serious problems for humans, livestock and irrigation is high salinity which, as shown in Section 6, can be extreme in many of the shallow groundwaters affected by evaporation (e.g. Dorila, sample LP5, TDS value of 11400 mg l^{-1}). Water salinity cannot easily be reduced without expensive and centralised treatment methods.

Figure 8.2 shows the relationship between As in the groundwaters and Na and F. As also described in Section 6, As correlates positively with F as well as many other anion and oxyanion constituents. Therefore, groundwaters with problematic concentrations of As are also problematic from the point of view of many other of these constituents. Even the samples with low As concentrations often have unacceptably high salinity, as evidenced by the high Na concentrations in Figure 8.2.

Treatment of groundwaters to remove other potentially detrimental ions present, including As, F, V, B, NO_3-N, U, Mo and P (and probably also Se, though this was not measured in the present study) also ideally requires sophisticated methods for effective removal. Some low-technology methods can also provide a degree of improvement at domestic level. In the urban areas of La Pampa, treatment to remove dissolved inorganic constituents, including reduction in salinity, is typically achieved by reverse osmosis. This form of treatment has not been available for the remote rural areas where typically one well or borehole serves as the potable supply for a family ranch. In these areas, groundwaters are currently used without prior treatment.

A list of tested treatment methods for removal of As from drinking water is given in Table 8.2.

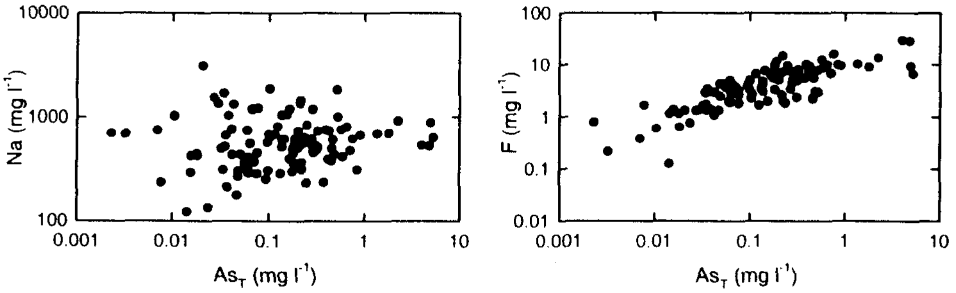

Figure 8.2 **Variations of Na and F with As in the Pampean groundwaters. High As is accompanied by high F (and other oxyanion species), low As waters often have salinity problems indicated here by Na**

Methods include co-precipitation (alum coagulation, iron coagulation, lime softening), adsorption methods (activated alumina, ion exchange) or membrane techniques (reverse osmosis, electrodialysis). In all these methods, removal is most efficiently carried out when As is present as As(V). This is the case in the Pampean groundwaters. In other areas however, where As is present substantially as the reduced form, As(III), oxidation can be achieved by addition of oxidants such as chlorine, ferric chloride, potassium permanganate or ozone.

In some of the reducing high-As aquifers (e.g. Bangladesh) where groundwaters often have coincident high concentrations of Fe, there exists the possibility to remove the As (and other trace elements) at least partially by passive aeration and sedimentation. This is not applicable in the oxidising groundwaters of La Pampa and other parts of Argentina which have generally low dissolved Fe concentrations. In this case, co-precipitation of As with Fe will require addition of Fe salts to the water.

Treatment of groundwaters using coagulation/filtration methods is often effective for removal of As and some other constituents (Table 8.2). Indeed, treatment of river waters in neighbouring Córdoba Province to remove high concentrations of As and V is carried out in central treatment plants using alum (Lerda and Prosperi, 1996). This method may be effective on a smaller (domestic) scale in La Pampa, although its efficacy will be dependent on a number of factors, including pH, TDS and initial As concentration. The alum method also suffers from the inherent problems of residual aluminium and sulphate in the treated water and from problems with disposal of contaminated sludge. Nonetheless, these problems are likely to be minor relative to the potential health risks from use of untreated water.

Coagulation/filtration using iron salts may be an alternative option at domestic level. Use of ferric sulphate has been reported to be more effective than alum (US-EPA, 1999), though is likely to be a more expensive option.

Activated alumina may also be a suitable method for groundwater treatment in La Pampa, although efficiency of removal of As is impaired in the presence of high concentrations of other ions, such as Se, F, Cl and SO_4 (Table 8.2). The method is expensive relative to coagulation methods but may have some applicability for the Pampean situation.

Ion-exchange methods are also effective for the removal of As and some other elements, though again competition from other constituents for binding sites on the resin may impair As removal efficacy. Use of ion-exchange columns rather than as a batch process should help to improve efficiency and decrease regeneration frequency (US-EPA, 1999).

Reverse osmosis is currently an effective method for removal of As, F and TDS in public-supply waters in urban areas of La Pampa, though is not used on a smaller, rural scale. US-EPA (1999) described a small-scale reverse-osmosis (RO) plant being tested in New Mexico, USA for removal of As and F from water to supply a rural community of around 200 people. The RO unit removed 86% of the total As.

The techniques outlined above indicate the range of problems encountered with these approaches. Nonetheless, given the widespread occurrence of poor-quality groundwater in La Pampa, groundwater treatment constitutes one of the most important remediation options available for the region and requires further development, particularly in the rural areas, to ensure provision of safe drinking water.

8.2.4 Borehole siting

As noted above, the majority of groundwaters sampled in northern La Pampa are of unacceptable quality for drinking-water use. However, it has been seen that large variations in chemical quality occur in the aquifers, both spatially and with depth. Although few parts of the aquifer appear to yield

Table 8.2 Water treatment methods for removal of As and some other inorganic constituents (after US-EPA, 1999)

Treatment Method	Applicability	Advantages	Disadvantages
Coagulation/filtration: Using alum or ferric sulphate	Efficiency impaired at high or low pH. Alum less efficient than ferric sulphate	Well-established method; also used for removal of other constituents e.g. F, V. Low cost, simple chemicals	Disposal of toxic sludge often a problem. With alum, may have high residual Al and SO_4. Need trained operators
Using naturally dissolved Fe, Mn (passive sedimentation)	Not suitable for La Pampa due to low natural concentrations	Low cost	May not be efficient if Fe, Mn concentrations are too low
Lime softening	Operates at pH >10.5	Low-technology, simple chemicals	Requires pH adjustment after treatment
Activated alumina	Good for treatment of water with high solute concentrations (e.g. La Pampa). Relatively expensive technology; may require regular replacement	Highly selective towards As(V). Well-known, commercially available. No sludge problem	Requires monitoring of breakthrough. High concentrations of Se, F, Cl, SO_4 compete for adsorption sites and so decrease efficiency. High selectivitiy for As(V) results in potential regeneration problems, and reduced efficiency with time. Disposal of waste brine may be a problem. Requires pH readjustment. High technology
Ion exchange	Most effective if used in a column system. Waters with high TDS may require pre-treatment before ion exchange	Efficient in removal of As and probably other oxyanions	SO_4, high salinity, Se, F, NO_3-N compete with As and can affect run length. Disposal of waste brine may be a problem. Suspended solids and Fe precipitates can cause clogging of columns. High technology
Reverse osmosis	Currently used for urban water supply in La Pampa	Efficient removal of As and other ions (TDS, F)	Disposal of reject brine may be a problem. High running costs. High-technology operation and maintenance. Reajustment of water-quality required
Electrodialysis		Efficient As removal. Easier to operate than reverse osmosis	More expensive and potentially less efficient than reverse osmosis. High-technology

good-quality groundwater, there may be some benefit gained from siting of boreholes in optimal locations.

The most saline groundwaters are mainly present in the shallow parts the aquifers, particularly in low-lying depressions which undergo seasonal flooding and evaporation. Ideally, such zones are best avoided when considering new sites for borehole drilling in water-supply programmes.

The good correlations observed between As and many of the other elements of potential health concern (F, B, V, U, Be and Mo, possibly also Se) indicate that the groundwaters in the region having the lowest As concentrations are also likely to be of better quality with respect to these other problem elements. Highest concentrations of these have also been found in low-lying depressions where groundwater flow is likely to be sluggish and has no easy exit from the catchment. Borehole siting should clearly aim to avoid such depressions.

Lower concentrations of As at greater depths below the zone of water-table fluctuation (Section 6) also suggest that some degree of mitigation of water-quality problems can be afforded by completing boreholes in deeper parts of the Pampean aquifer.

Good correlations between the anion and oxyanion elements and both groundwater alkalinity (HCO_3) and pH are a useful yardstick in detecting poor-quality waters as both alkalinity and pH are readily measurable in the field. This provides the potential to predict As concentrations from measurement of these parameters during drilling and before borehole completion. Measurement of As using commercially-available field-test kits would also aid identification of potential problems, although currently available models struggle to measure As at concentrations of 50 μg l^{-1} and are probably only reliable at concentrations in the region of 100 μg l^{-1} or higher. Development of field-test kits is a rapidly growing area at present and new models under development (e.g. the 'Arsenator', Karl-Franzens University of Graz, Austria) show considerable promise in detecting As reliably at lower concentrations (down to around 5 μg l^{-1}).

It is likely that borehole-siting considerations can only provide limited amelioration of the water-quality problems because of the observation that, even with optimal siting, the majority of groundwaters sampled are of unacceptable quality for potable use.

8.3 Wider strategy for groundwater-quality mitigation

It is clear that a very extensive area of the arid and semi-arid zones of Argentina is potentially affected by the water-quality problems demonstrated in La Pampa. Estimates are that similar groundwaters occupy aquifers of the Chaco-Pampean Plain over around 1 million km^2 and that up to 5 million people nationally may be drinking groundwater with >50 μg l^{-1} (Nicolli et al., 1989; Nicolli and Merino, 2000). However, the distribution and scale of the problems are still poorly defined and need further investigation. Obtaining such data requires instigation of large-scale randomised groundwater surveys with testing of key elements, particularly measures of salinity (SEC, Na or Cl), As and F and mapping of results. Laboratory measurements are clearly preferable, but rapid investigations may be facilitated by the use in particular of As field-test kits (such as the 'Arsenator', see above). Alongside further groundwater testing, public awareness campaigns would also help to disseminate the potential health concerns from drinking water and to highlight the need for mitigation measures.

9. CONCLUSIONS AND RECOMMENDATIONS

Hydrogeochemical investigations in northern La Pampa have established that severe groundwater-quality problems exist in groundwaters from the Quaternary loess deposits with respect to many inorganic constituents. Particular problems highlighted are high salinity and high concentrations of potentially detrimental elements such as As, F, NO_3-N, SO_4, B, Mo and U (as well as other elements not known to have health consequences such as V and P). Studies from hydrogeologically similar aquifers elsewhere suggest that Se is also likely to be a problem in the groundwaters, though Se has not been determined in this study. Although As is only one of a number of undesirable constituents, it ranks as one of the most serious because of its high toxicity at relatively low concentrations. Our survey indicated that 95 % of groundwater samples collected (108 samples from both potable and agricultural supply sources) exceeded the WHO guideline value for As in drinking water (10 $\mu g\ l^{-1}$) and 73 % were above the Argentine standard (50 $\mu g\ l^{-1}$). Indeed, many are significantly above these guidelines. Concentrations were found in pumped groundwaters at up to 5.3 $mg\ l^{-1}$. The water quality of northern La Pampa is believed to be representative of a large area of the Chaco-Pampean Plain (around 10^6 km^2) and potentially affecting several million people.

The groundwaters from the area are oxidising with high concentrations of dissolved oxygen and high redox potentials. Arsenic dissolved in the waters is dominantly present as As(V). The groundwaters also have variable but often high alkalinity (HCO_3) and pH values. The pH values are high as a result of silicate and carbonate reactions under closed conditions, facilitated particularly by the arid climatic conditions and limited recharge to the Pampean aquifers. Concentrations of As, F, V and B and to a lesser extent Mo and Be, correlate positively with pH and alkalinity (HCO_3).

Concentrations of As and other anions and oxyanions (e.g. HCO_3, F, V, Mo, B) appear to be particularly increased near to small-scale depressions which act as centres of groundwater discharge, at least seasonally. Concentrations of these are also relatively high in many groundwaters close to the water table.

Groundwater chemistry shows a high degree of spatial variability which indicates a lack of groundwater homogenisation and mixing. This is probably aided by fine grain size and poor permeability as well as limited recharge in the arid climatic conditions. However, isotopic evidence indicates that a degree of active groundwater flow is taking place in the aquifer (at least at shallow depths) as there is little evidence for occurrence of palaeowaters and some groundwaters contain tritium.

Porewaters extracted from the cored boreholes also demonstrate this particularly well. One borehole drilled close to a topographic depression (Tamagnoni) has saline waters at the shallowest depth, indicative of evaporation. Concentrations of As increase with depth in the borehole, to a maximum of 7490 $\mu g\ l^{-1}$ at 26 m depth. The concentrations are almost ten times greater than porewaters extracted from a borehole not adjacent to a depression. Fine grain size of the sediments also appears to have some control on generation of high-As porewaters.

Sediments from the study area have concentrations of As close to world average values. Arsenic in the sediments appears to be associated with total Fe. The proportion of As present in readily extractable form (by acid oxalate and hydroxyalamine hydrochloride) is relatively high and suggests that much of the As is labile and associated with amorphous Fe and Mn oxides. Both Fe and Mn oxides are recognised as abundant mineral phases in the sediments. Varying conditions of pH and redox are therefore of great importance in determining mobilisation of As and the other anionic species. Concentrations of V, B, U, F, Mo and Se in the loess sediments are similarly unremarkable and mobilisation processes similar to those involving As are considered to apply.

Mobilisation of As and the other anion and oxyanion species in solution is thought to be a function of desorption (in the case of As as arsenate) from iron and manganese oxides in the aquifer under high pH conditions. Presence of high concentrations of HCO_3 may further enhance the desorption process because of competition for sorption sites on the oxide surfaces.

It is believed that the combination of oxidising conditions, high groundwater-pHs, young aquifer sediments and slow groundwater flow (limited opportunity for flushing of the aquifers) have all been instrumental in generating the As problems (and other anion/oxyanion problems) in the Pampean groundwaters.

Comparison of the hydrogeochemical data from La Pampa with data from other As-affected aquifers worldwide indicates that As can be mobile across a wide range of redox conditions. In problem aquifers such as the alluvial and deltaic plains of the Bengal Basin (Bangladesh and West Bengal), Inner Mongolia and the Danube Basin (Hungary), As release occurs under highly reducing conditions, usually in association with sulphate reduction. In Argentina as well as Chile, parts of Mexico and western USA, As release in groundwaters occurs under oxidising conditions when groundwater pH is particularly high (>8). The evidence suggests that other areas in the world where young sediments have accumulated in alluvial, deltaic or aeolian environments, where groundwater flow is slow and where aquifer conditions are either highly reducing or oxidising with high pH may also be at risk. Such problem areas should become recognised as awareness of potential problems from groundwater As grows and more groundwater testing takes place in potentially vulnerable aquifers.

The main recommendations arising from the research results are outlined below.

i. In view of the severity of contamination of Pampean groundwaters with arsenic and other potentially toxic constituents, rapid instigation of mitigation measures for drinking water needs to be carried out. The most applicable of these measures is likely to be groundwater treatment (e.g. by coagulation/filtration or reverse osmosis) but rainwater harvesting may be a useful additional water source, at least for parts of the year. There is some scope for improved groundwater quality through optimised borehole siting (increasing abstraction depths and siting away from topographical depressions), though this is likely to be limited because of the overwhelming dominance of poor-quality groundwater in the aquifers, irrespective of groundwater location.

ii. Public-awareness campaigns need to be promoted in order to highlight the quality problems and stress the need for use of good-quality water for drinking purposes.

iii. Surveys of groundwater quality in the Chaco-Pampean Plain need to be carried out on a large scale to assess the scale of the problems from arsenic and other elements and to enable better development of provincial or national mitigation strategies. The constituents most in need of testing are arsenic and fluoride, although measures of salinity (e.g. sodium, electrical conductivity) are also desirable given the high salinity of many of the groundwaters in the region. Results also require mapping to identify any spatial patterns and allow prioritisation of mitigation measures.

10. REFERENCES

Acharyya, S. K. 1997. Arsenic in groundwater – geological overview. *In:* Consultation on arsenic in drinking water and resulting arsenic toxicity in India and Bangladesh, Proceedings WHO conference, New Delhi, May 1997, 12 pp.

Adyalkar, P. G., Ghosh., P. C. and Mehta, B. C. 1981. On the salinity of groundwater in South 24 Parganas District, West Bengal, India. In: *Quality of Groundwater,* Proc. Intl Symposium, Noordwijkerhout, the Netherlands, March 1981, eds: van Duijvenbooden, W., Glasbergen, P. and van Lelyveld, H. *Studies in Environmental Science,* Volume 17, 63-67.

AIP Steering Committee 1991. Arsenic Pollution in Groundwater in West Bengal. Report of Arsenic Investigation Project to the National Drinking Water Mission, Delhi, India, 58 pp.

Albores, A., Cebrián, M. E., Tellez, I. and Valdez, B. 1979. Estudio comparativo de hidrarsenicismo crónico en dos comunidades rurales de la Región Lagunera de México. Bol. of. Sanit. Panam., 86, 196-205.

Amasa, S. K. 1975. Arsenic pollution at Obuasi goldmine, town and surrounding countryside. *Environ. Health Persp.* **12,** 131-135.

Anderson, R. K., Thompson, M. and Culbard, E. 1984. Selective reduction of arsenic species by continuous hydride generation. Part I. Reaction media. *Analyst.* **111,** 1143-1152.

Appelo, C. A. J. and Postma, D. 1993. *Geochemistry, Groundwater and Pollution,* A.A. Balkema, Rotterdam, 536 pp.

Arehart, G. B., Chryssoulis, S. L. and Kesler, S. E. 1993. Gold and arsenic in iron sulfides from sediment-hosted disseminated gold deposits – implications for depositional processes. *Econ. Geol.& Bull. Soc. Econ. Geologists,* **88,** 171-185.

Argüello, R. A., Cenget, D. D. and Tello, E. E. 1938. Cancer y arsenicismo regional endémico en Córdoba. *Argent. Rev. Dermatosyphilol.,* **22,** 461-487.

Arribére, M. A., Cohen, I. M., Ferpozzi, L. H., Kestelman, V. A., Casa, V. A. and Ribeiro Guevera, S. 1997. Neutron activation analysis of soils and loess deposits, for the investigation of the origin of the natural arsenic-contamination in the Argentine Pampa. *Radiochim. Acta,* **78,** 187-191.

Auge, M. P. 1986. Hydrodynamic behaviour of the Puelche aquifer in Matanza River basin. Groundwater, 24, No.5, pp 636-642.

Azcue, J. M. and Nriagu, J. O. 1995. Impact of abandoned mine tailings on the arsenic concentrations in Moira Lake, Ontario. *J. Geochem. Expl.,* **52,** 81-89.

Baes, C. F. and Sharp, R. D. 1983. A proposal for estimation of soil leaching and leaching constants for use in assessment models. *J. Environ. Qual.,* **12,** 17-28.

Bannert, D. 1974. Hydrogeological investigations in the Pampa of Argentina. Federal Geological Survey, SR No 330, Federal Republic of Germany.

Baur, W. H. and Onishi, B.-M. H. 1969. Arsenic. *In:* K.H. Wedepohl [Ed] *Handbook of Geochemistry.* Springer-Verlag, Berlin, 33-A-1-33-0-5.

Besuschio, S. C., Desanzo, A. C., Perez, A. and Croci, M. 1980. Epidemiological associations between arsenic and cancer in Argentina. *Biol. Trace Element Res.,* **2,** 41-55.

BGS/MML 1999. Groundwater studies for arsenic contamination in Bangladesh. Phase I: Rapid Investigation Phase. BGS/MML Technical Report to DFID, Six Volumes.

Biagini, R., Rivero, M., Salvador, M. and Córdoba, S. 1978. Hidroarsenicismo crónico y cancer de pulmón. *Arch. Argent. Dermatol.*, **48**, 151-158.

Bowell, R. J. 1992. Supergene gold mineralogy at Ashanti, Ghana: implications for the supergene behaviour of gold. *Min. Mag.* **56**, 545-560.

Bowell, R. J. 1993. Mineralogy and geochemistry of tropical rain forest soils: Ashanti, Ghana. *Chem. Geol.* **106**, 345-358.

Bowell, R. J. 1994. Sorption of arsenic by iron oxides and oxyhydroxides in soils. *Appl. Geochemistry*, **9**, 279-286.

Boyle, R. W. and Jonasson, I. R. 1973. The geochemistry of As and its use as an indicator element in geochemical prospecting. *J. Geochem. Explor.*, **2**, 251-296.

Boyle, D. R., Turner, R. J. W. and Hall., G. E. M. 1998. Anomalous arsenic concentrations in groundwaters of an island community, Bowen Island, British Columbia. *Environ. Geochem. Health*, **20**, 199-212.

Brannon, J. M. and Patrick, W. H. 1987. Fixation, transformation, and mobilization of arsenic in sediments. *Env. Sci. Technol.*, **21**, 450-459.

Brookins, D. G. 1988. *Eh-pH Diagrams for Geochemistry*. Springer-Verlag, 176 pp.

Cáceres, L., Gruttner, V. E. and Contreras, R. 1992. Water recycling in arid regions: Chilean case. *Ambio*, **21**, 138-144.

Cebrián, M. E., Albores, A., Aguilar, M. and Blakely, E. 1983. Chronic arsenic poisoning in the north of Mexico. *Hum. Toxicol.*, **2**, 121-133.

Cebrián, M. E., Albores, A., García-Vargas., G, Del Razo, L. M. and Ostrosky-Wegman, P. 1994. Chronic arsenic poisoning in humans: the case of Mexico. In: *Arsenic in the Environment, Part II: Human Health and Ecosystem Effects*, ed: Nriagu, J.O., 93-107, Wiley, New York.

CGWB 1999. *High Incidence of Arsenic in Ground Water in West Bengal*. Central Ground Water Board report, India, 142 pp.

Chappell, W. R., Beck, B. D., Brown, K. G., Chaney, R., Cothern, C. R., Irgolic, K. J., North, D. W., Thornton, I. and Tsongas, T. A. 1997. Inorganic arsenic: a need and an opportunity to improve risk assessment. *Environ. Health Persp.*, **105**, 1060-1067.

Chen, C. J., Chuang, Y. C., Lin, T. M. and Wu, H. Y. 1985. Malignant neoplasms among residents of a blackfoot disease-endemic area in Taiwan: high-arsenic artesian well water and cancers. *Cancer Res.*, **45**, 5895-5899.

Chen, S-L., Dzeng, S. R., Yang, M-H., Chiu, K-H., Shieh, G-M. and Wai, C. M. 1994. Arsenic species in groundwaters of the Blackfoot Disease area, Taiwan. *Environ. Sci. Technol.*, **28**, 877-881.

Chen, S.-L., Yeh, S. J., Yang, M. H. and Lin, T. H. 1995. Trace element concentration and arsenic speciation in the well water of a Taiwan area with endemic blackfoot disease. *Biol. Trace Elem. Res.*, **48**, 263-274.

Cherry, J. A., Shaikh, A. U., Tallman, D. E. and Nicholson, R. V. Arsenic species as an indicator of redox conditions in groundwater. *J. Hydrology*, **43**, 373-392.

Chiou, H. Y., Hsue, Y. M., Liaw, K. F., Horng, S. F., Chiang, M. H., Pa, Y. S., Lin, J. S. N., Huang, C. H., and Chen, C. J. 1995. Incidence of internal cancers and ingested arsenic – a seven-year follow-up study in Taiwan. *Cancer Res.*, **55**, 1296-1300.

Chou, T. T. 1972. Selective dissolution of manganese oxides from soils and sediments with acidified hydroxylamine hydrochloride. *Soil Sci. Soc. Amer. Proc.*, **36**, 764-768.

Chou, T. T. and Zhou, L. 1983. Extraction techniques for selective dissolution of amorphous iron oxides from soils and sediments. *Soil Sci. Soc. Am.. J.* **47**, 225-232.

Círculo Médico del Rosario 1917. Sobre la nueva enfermedad descubierta en Bell-Ville. Rev. Médica del Rosario, Rosario, Argentina, VII, 485.

Clapperton, C. 1983. The glaciation of the Andes. *Quat. Sci. Rev.*, **2**, 83-155.

Clapperton, C. 1990. Quaternary glaciations in the southern hemisphere: an overview. *Quat. Sci. Rev.*, **9**, 299-304.

Clark, I. and Fritz, P. 1997. *Environmental Isotopes in Hydrogeology*. Lewis Publishers, 328 pp.

Clewell, H. J., Gentry, P. R., Barton, H. A., Shipp, A. M., Yager, J. W. and Andersen, M. E. 1999. Requirements for a biologically realistic cancer risk assessment for inorganic arsenic. *Internl. J. Toxicol.*, **18**, 131-147.

Criaud, A. and Fouillac, C. 1989. The distribution of arsenic(III) and arsenic(V) in geothermal waters: examples from the Massif Central of France, the Island of Dominica in the Leeward Isl;ands of the Caribbean, the Valles Caldera of New Mexico, USA and southwest Bulgaria. *Chem. Geol.*, **76**, 259-269.

CSME 1997. Geology and geochemistry of arsenic occurrences in groundwater of six districts of West Bengal. Report of the Centre for Study of Man & Environment, Calcutta.

Cullen, W. R. and Reimer, K. J. 1989. Arsenic speciation in the environment. *Chem. Reviews*, **89**, 713-764.

Das, D., Chatterjee, A., Mandal., B. K., Samanta, G., Chakraborti, D. and Chanda, B. 1995. Arsenic in groundwater in six districts of West Bengal, India: the biggest arsenic calamity in the world. Part 2. Arsenic concentration in drinking water, hair, nails, urine, skin-scale and liver tissue (biopsy) of the affected people. *Analyst*, **120**, 917-924.

Davis, A., de Curnou, P. and Eary, L. E. 1997. Discriminating between sources of arsenic in the sediments of a tidal waterway, Tacoma, Washington. *Environ. Sci. Technol.*, **31**, 1985-1991.

DDA 1983. Water-level and quality map series for La Pampa, Plan Norte (Zona II). Diréccion de Recursos Hidricos, Estudio Hidrogeologico Régional, Diréccion de Aguas, Santa Rosa, Argentina.

Deines, P., Langmuir, D. and Harmon, R. S. 1974. Stable carbon isotope ratios and the existence of a gas phase in the evolution of carbonate ground waters. *Geochim. Cosmochim. Acta*, **38**, 1147-1164.

Del Razo, L. M., Arellano, M. A. and Cebrián, M. E. 1990. The oxidation states of arsenic in well-water from a chronic arsenicism area of northern Mexico. *Envl. Pollution*, **64**, 143-153.

Del Razo, L. M., Hernández, J. L., García-Vargas, G. G., Ostrosky-Wegman, P., Cortinas de Nava, C. and Cebrián, M. E. 1994. Urinary excretion of arsenic species in a human population chronically exposed to arsenic via drinking water. A pilot study. Chapter 9 In: *Arsenic Exposure and Health*, eds: Chappell, W. R., Abernathy, C. O. and Cothern, C. R. 91-100.

Dhar, R. K., Biswas, B. Kr., Samanta, G., Mandal, B. Kr., Chakraborti, D., Roy, S., Jafar, A., Islam, A., Ara, G., Kabir, S., Khan, A. W., Ahmed, S. A. and Hadi, S. A. 1997. Groundwater arsenic calamity in Bangladesh. *Current Science*, **73**, 48-59.

Driehaus, W. and Jekel, M. 1992. Determination of As(III) and total inorganic arsenic by on-line pretreatment in hydride generation atomic absorption spectrometry. *Fres. J. Anal. Chem.*, **343**, 352-356.

Driehaus, W., Seith, R. and Jekel, M. 1995. Oxidation of arsenate(III) with manganese oxides in water treatment. *Water Res.*, **29**, 297-305.

Dudas, M. J. 1984. Enriched levels of arsenic in post-active acid sulfate soils in Alberta. *Soil Sci. Soc.Amer. J.*, **48**, 1451-1452.

Dulout, F. N., Grillo, C. A., Seoane, A. I., Maderna, C. R., Nilsson, R., Vahter, M., Darroudi, F. and Natarajan, A. T. 1996. Chromosomal aberrations in peripheral blood lymphocytes from native Andean women and children from Northwestern Argentian exposed to arsenic in drinking water. *Mut. Res.*, **370**, 151-158.

Dzombak, D. A. and Morel, F. M. M. 1990. *Surface Complexation Modeling: Hydrous Ferric Oxide.* Wiley, 393pp.

Ebens, R. J. and Connor, J. J. 1980. Geochemistry of loess and carbonate residuum. *USGS Professional Paper 954-G*, 32 pp.

Elorriaga, E. E. and Tullio, J. O. 2000. Estructuras del subsuelo y su influenca en la morfología en el norte de la Provincia de La Pampa. Actas X Congreso Latinamericano de Geología y VI Congreso Nacional de Geología Económica, Volume III, pp 499-506.

Faust, S. D., Winka, A. J. and Belton, T. 1987. An assessment of chemical and biological significance of arsenical species in the Maurice River Drainage Basin (N. J.). Part 1: Distribution in water and river and lake sediments. *J. Env. Sci. Health*, **A22**, 209-237.

Ferguson, J. F. and Gavis, J. 1972. A review of the arsenic cycle in natural waters. *Water Res.* **6**, 1259-1274.

Ficklin, W. H. and Callender, E. 1989. Arsenic geochemistry of rapidly accumulating sediments, Lake Oahe, South Dakota. *In:* U. S. Geological Survey Water Resources Investigations Report 88-4220; U.S. Geological Survey Toxic Substances Hydrology Program – Proceedings of the Technical Meeting, Phoenix, Arizona, September 26-30, 1988. *Eds:* Mallard, G. E. and Ragone, S. E, pp 217-222.

Fontaine, J. A. 1994. Regulating arsenic in Nevada drinking water supplies past problems, future challenges. Chapter 28, In: *Arsenic Exposure and Health*, eds: Chappell, W. R., Abernathy, C. O. and Cothern, C. R. 285-288.

Fontes, J-C. and Garnier, J-M. 1979. Determination of the initial ^{14}C activity of the total dissolved carbon:

a review of the existing models and a new approach. *Water Resour. Res.*, **15**, 399-413.

Freeze, R. A. and Cherry, J. A., 1979. *Groundwater.* Prentice Hall, 604 pp.

Fujii, R. and Swain, W. C. 1995. Areal distribution of selected trace elements, salinity, and major ions in shallow ground water, Tulare Basin, southern San Joaquin Valley, California. USGS Water-Resources Investigations Report 95-4048, 67 pp.

Goldberg, S. 1986. Chemical modeling of arsenate adsorption on aluminum and iron oxide minerals. *Soil Sci. Soc. Am. J.* **50**, 1154-1157.

Gorby, M. S. 1994. Arsenic in human medicine. In: *Arsenic in the Environment, Part II: Human Health and Ecosystem Effects*, ed: Nriagu, J. O., 1-16, Wiley, New York.

Grimes, D. J., Ficklin, W. H., Meier, A. L. and McHugh, J. B. 1995. Anomalous gold, antimony, arsenic, and tungsten in ground water and alluvium around disseminated gold deposits along the Getchell Trend, Humboldt County, Nevada. *J. Geochem. Expl.*, **52**, 351-371.

Guo, H. R., Chen, C. J. and Greene, H. L. 1994. Arsenic in drinking water and cancers: a brief descriptive review of Taiwan studies. Chapter 13, In: *Arsenic Exposure and Health*, eds: Chappell, W. R., Abernathy, C. O. and Cothern, C. R. 129-138.

Hernández, M. A. and González, N. 1999. Impact of rising piezometric levels on Greater Buenos Aires due to partial changing of water services infrastructure. *Proc. XXVII IAH Congress on Groundwater in the Urban Environment*, Nottingham, UK, 21-27 September. Volume 1: Problems, Processes and Management. Eds. J Chilton et al.

Hopenhayn-Rich, C., Biggs, M. L., Fuchs, A., Bergoglio, R., Tello, E. E., Nicolli, H. and Smith, A. H. 1996. Bladder cancer mortality associated with arsenic in drinking water in Argentina. *Epidemiol.*, **7**, 117-124.

Karcher, S., Cáceres, L., Jekel, M. and Contreras, R. 1999. Arsenic removal from water supplies in northern Chile using ferric chloride coagulation. *J. Ciwem.*, **13**, 164-169.

Kinniburgh, D. G. and Jackson, M. L. 1981. Cation adsorption by hydrous metal oxides and clay. Chapter 3, In: *Adsorption of Inorganics at Solid-Liquid Interfaces.* eds: Anderson, M. A. and Rubin, A. J., Ann Arbor Science, Michigan, USA, pp 91-160.

Kinniburgh, D. G. Jackson, M. L. and Syers, J. K. 1976. Adsorption of alkaline earth, transition, and heavy metal cations by hydrous oxide gels of iron and aluminum. *Soil Sci. Soc. Am. J.* **40**, 796-799.

Kinniburgh, D. G. and Smedley, P. L. 2000. *Groundwater Studies of Arsenic Contamination in Bangladesh.* Report of DPHE/BGS, In press.

Komnitsas, K. , Xenidis, A. and Adam, K. 1995. Oxidation of pyrite and arsenopyrite in sulphidic soils in Lavrion. *Minerals Eng.*, **8**, 1443-1454.

Kostka, J. E. and Luther, G. W. III, 1994. Partitioning and speciation of solid phase iron in saltmarsh sediments. *Geochim. Cosmochim. Acta*, **58**, 1701-1710.

Kröhling, D. M. 1999. Upper Quaternary geology of the lower Carcarañá Basin, North Pampa, Argentina. *Quat. Interml.*, **57/58**, 135-148.

Kuhn, A. and Sigg, L. 1993. Arsenic cycling in eutrophic Lake Greifen, Switzerland – influence of seasonal redox processes. *Limnol. Oceanogr.*, **38**, 1052-1059.

Kuo, T-L. 1968. Arsenic content of artesian well water in endemic area of chronic arsenic poisoning. *Repts. Inst. Pathol. Natl. Taiwan Univ.*, **20**, 7-13.

Lerda, D. E. and Prosperi, C. H. 1996. Water mutagenicity and toxicology in Rio Tercero (Cordoba, Argentina). *Water Res.*, **30**, 819-824.

Livesey, N. T. and Huang, P. M. 1981. Adsorption of arsenate by soils and its relation to selected chemical properties and anions. *Soil Sci.*, **131**, 88-94.

Lo, M-C., Hsen, Y-C. and Lin, K-K. 1977. Second report on the investigation of arsenic content in underground water in Taiwan. Taichung, Taiwan: Taiwan Provincial Institute of Environmental Sanitation.

Logan, W. S. and Rudolph, D. L. 1997. Microdepression-focused recharge in a coastal wetland, La Plata, Argentina. *J. Hydrol.*, **194**, 221-238.

Luo, Z. D., Zhang, Y. M., Ma, L., Zhang, G. Y., He, X., Wilson, R., Byrd, D. M., Griffiths, J. G., Lai, S., He, L., Grumski, K. and Lamm, S. H. 1997. Chronic arsenicism and cancer in Inner Mongolia – consequences of well-water arsenic levels greater than 50 $\mu g\ l^{-1}$. In: *Arsenic Exposure and Health Effects*, eds: Abernathy, C. O., Calderon, R. L. and Chappell, W. R., 55-68.

Ma, H. Z., Xia, Y. J., Wu, K. G., Sun, T. Z. and Mumford, J. L. 1999. Arsenic exposure and health effects in Bayingnormen, Inner Mongolia. In: *Arsenic Exposure and Health Effects. Proc.* Third Intl Conference on Arsenic Exposure and Health Effects, San Diego, 1998, eds: Chappell, W. R., Abernathy, C. O. and Calderon, R. L. Elsevier, Amsterdam, pp 127-131.

Manning, B. A. and Goldberg, S. 1996. Modeling competetive adsorption of arsenate with phosphate and molbdate on oxide minerals. *Soil Sci. Soc. Am. J.*, **60**, 121-131.

Mathers, S. J. and Zalasiewicz, J. A. 1993. A guide to the sedimentology of unconsolidated sedimentary aquifers. *British Geological Survey Technical Report* WC/93/32.

McKeague, J. A. and Day, J. H. 1966. Dithionite- and oxalate-extractable Fe and Al as aids in differentiating various classes of soils. *Can. J. Soil Sci.*, **46**, 13-22.

Michelena, R. O. and Irurtia, C. B. 1995. Susceptibility of soil to wind erosion in La Pampa Province, Argentina. *Arid Soil Res. Rehabil.*, **9**, 227-234.

Mok, W. M. and Wai, C. M. 1989. Distribution and mobilization of arsenic species in the creeks around the Blackbird mining district, Idaho. *Water Res.*, 23, 7-13.

Mok, W. M. and Wai, C. M. 1990. Distribution and mobilization of arsenic species in the Coeur D'Alene River, Idaho. *Environ. Sci. Technol.* 24, 102-108.

Mok, W. M. and Wai, C. M. 1994. Mobilization of arsenic in contaminated river waters. In: *Arsenic in the Environment, Part I: Cycling and Characterization*, ed: Nriagu, J. O., 99-118, Wiley, New York, 99-118.

Nag, J. K., Balaram, V., Rubio, R., Alberti, J. and Das, A. K. 1996. Inorganic arsenic species in groundwater: a case study from Purbasthali (Burdwan), India. *J. Trace Elements Med. Biol.*, **10**, 20-24.

Nicolli, H. B. and Merino, M. H. 2000. High contents of F, As and Se in groundwater of the Carcarañá river basin, Argentine Pampean Plain, *Environ. Geol.*, In press.

Nicolli, H. B., Suriano, J. M., Gómez Peral, M. A., Ferpozzi, L. H. and Baleani, O. A. 1989.

Groundwater contamination with arsenic and other trace elements in an area of the Pampa, Province of Córdoba, Argentina. *Environ. Geol. Water Sci.*, 14, 3-16.

Nimick, D. A., Moore, J. N., Dalby, C. E. and Savka, M. W. 1998. The fate of geothermal arsenic in the Madison and Missouri Rivers, Montana and Wyoming. *Water Res. Research*, **34**, 3051-3067.

Niu, S., Cao, S. and Shen, E. 1997. The status of arsenic poisoing in China. In: *Arsenic Exposure and Health Effects*, eds: Abernathy, C. O., Calderon, R. L. and Chappell, W. R., 78-83.

O'Brien, R., Keller, C. K. and Smith, J. L. 1996. Multiple tracers of shallow ground-water flow and recharge in hilly loess. *Groundwater*, **34**, No 4.

Onishi, H. and Sandell, E. B. 1955. Geochemistry of arsenic. *Geochim. Cosmochim. Acta*, **7**, 1-33.

Pearce, J. 1998. A petrographic study of potential arsenic sources in loess deposits from the Pampa Region, Argentina. BGS Technical Report, WG/98/34R, 17 pp.

Peterson, M. L. and Carpenter, R. 1986. Arsenic distributions in porewaters and sediments of Puget Sound, Lake Washington, the Washington coast and Saanich Inlet, B. C. *Geochim. Cosmochim. Acta*. **50**, 353-369.

Pichler, T., Veizer, J. and Hall, G. E. M. 1999. Natural input of arsenic into a coral reef ecosystem by hydrothermal fluids and its removal by Fe(III) oxyhydroxides. *Env. Sci. Technol.*, **33**, 1373-1378.

POA 1999. Joint Plan of Action to Address Arsenic Contamination of Drinking Water. Government of West Bengal and UNICEF. Public Health Engineering Department, Government of West Bengal.

Pye, K. 1995. The nature, origin and accumulation of loess. *Quat. Sci. Rev.*, **14**, 653-667.

Rabassa, J. and de Francesco, F. 1986. The loess of central and western Buenos Aires Pampas, Argentina. *Loess Lett* (Leicester, Waterloo), Issue 16, 36-37.

Robertson, F. N. 1989. Arsenic in ground-water under oxidising conditions , south-west United States. *Environ. Geochem. Health*, **11**, 171-185.

Robinson, B., Outred, H., Brooks, R. and Kirkman, J. 1995. The distribution and fate of arsenic in the Wakato River system, North Island, New Zealand. *Chem. Spec. & Bioavail.*, **7**, 89-96.

Sayago, J M. 1995. The Argentine neotropical loess: a review. *Quat. Sci. Rev.*, 14, 755-766.

Sholkovitz, E. R. 1988. Rare earth elements in the sediments of the North Atlantic Ocean, Amazon Delta, and East China Sea: reinterpretation of terrigenous input patterns to the oceans. *Am. J. Sci.*, **288**, 236-281.

Smedley, P. L. 1991. The geochemistry of rare earth elements in groundwater from the Carnmenellis area, southwest England. *Geochim. Cosmochim. Acta*, **55**, 2767-2779.

Smedley, P L, Edmunds, W M and Pelig-Ba, K B. 1996a. Mobility of arsenic in groundwater in the Obuasi area of Ghana. In: *Environ. Geochem. Health*, eds: Appleton, JD, Fuge, R & McCall, G J H., *Geol. Soc. Special Publ. No 113*, 163-181.

Smedley, P. L. 1996b. Arsenic in rural groundwater in Ghana. *J. Afr. Earth Sci.*, **22**, 459-470.

Smedley, P. L., Luo, Z-D., Zhang, G-Y. and Zhang, M-Y. 2000. Arsenic and fluoride problems in groundwaters from the Huhhot Basin, Inner Mongolia. *Appl. Geochem.*, In prep.

Smith, A., Goycolea, M., Haque, R. and Biggs, M. L. 1998. Marked increase in bladder and lung cancer mortality in a region of Northern Chile due to arsenic in drinking water. *Am. J. Epidemiol.*, **147**, 660-669.

Smith, A., Hopenhayn-Rich, C., Bates, M., Goeden, H., Hertz-Picciotto, I., Duggan, H., Wood, R., Kosnett, M. and Smith, M. 1992. Cancer risks from arsenic in drinking water. *Environ. Health Persp.*, **97**, 259-267.

Stone, A. T. 1987. Microbial metabolites and the reductive dissolution on manganese oxides: oxalate and pyruvate. *Geochim. Cosmochim. Acta*, **51**, 919-925.

Stumm, W. and Morgan, J. J. 1981. *Aquatic Chemistry*. Wiley, 583 pp.

Sun, G. F., Dai, G. J., Li, F. J., Yamauchi, H., Yoshida, T. and Aikawa, H. 1999. The present situation of chronic arsenism and research in China. In: *Arsenic Exposure and Health Effects*. Proc. Third Intl. Conference of Arsenic Exposure and Health Effects, San Diego, 1998, eds: Chappell, W. R., Abernathy, C. O. and Calderon, R. L. Elsevier, Amsterdam, pp 123-126.

Takamatsu, T., Kawashima, M. and Koyama, M. 1985. The role of Mn^{2+}-rich hydrous manganese oxide in the accumulation of arsenic in lake sediments. *Water Res.*, **19**, 1029-1032.

Teruggi, M. E. 1957. The nature and origin of Argentine loess. *J. Sed. Petrol.*, **27**, 322-332.

Thornton, I. and Farago, M. 1997. The geochemistry of arsenic. In: *Arsenic Exposure and Health Effects*, eds: Abernathy, C. O., Calderon, R. L. and Chappell, W. R., 1-16.

Tonni, E. P., Cione, A. L. and Figini, A. J. 1999. Predominance of arid climates indicated by mammals in the pampas of Argentina during the Late Pleistocene and Holocene. *Palaeogeog. Palaeoclimatol. Palaeoecol.*, **147**, 257-281.

Trafford, J. M. 1986. Investigations into the storage of groundwater containing trace levels of arsenic, prior to analysis by hydride generation combined with ICP-AES. *British Geological Survey Technical Report 86/8.*

Tseng, W-P., Chu, H-M., How, S-H., Fong, J-M., Lin, C-S. and Yeh, S. 1968. Prevalence of skin cancer in an endemic area of chronic arsenicism in Taiwan. *J. Nat. Cancer Inst.*, **40**, 453-463.

Umitsu, M. 1993. Late Quaternary sedimentary environments and landforms in the Ganges delta. *Sed. Geol.*, **83**, 177-186.

United Nations, 1976. Ground water in the western hemisphere. *Natural Resources, Water Series* No.4.

US-EPA, 1999. Arsenic in drinking water: treatment technologies. Report of the United States Environmental Protection Agency, Office of Water, 3 pp.

Varsányi, I., Fodré, Z. and Bartha, A. 1991. Arsenic in drinking water and mortality in the southern Great Plain, Hungary. *Environ. Geochem. Health*, **13**, 14-22.

Vahter, M., Concha, G., Nermell, B., Nilsson, R., Dulout, F. and Natarajan, A. T. 1995. A unique metabolism of inorganic arsenic in native Andean women. *Eur. J. Pharmacol. (Environ. Toxicol. Pharmacol.)*, **293**, 455-462

Verhoef, A. and Fettes, R. A. 1991. Preliminary review of revised FAO radiation and temperature methods. Report 16, Department of Hydrology, Soil Physics and Hydraulics, Wageningen Agricultural University, Wageningen, The Netherlands.

Wang, G. 1984. Arsenic poisoning from drinking water in Xinjiang. *Chin. J. Prevent. Med.*, **18**, 105-107.

Wang, L and Huang, J. 1994. Chronic arsenism from drinking water in some areas of Xinjiang, China. In: *Arsenic in the Environment, Part II: Human Health and Ecosystem Effects*, ed: Nriagu, J. O., 159-172, Wiley, New York.

Wauchope, R. D. 1975. Fixation of arsenical herbicides, phosphate and arsenate in alluvial soils. *J. Environ. Quality*, **4**, 355-358.

Webster, J. G. 1999. Arsenic. In: *Encyclopaedia of Geochemistry*, eds: Marshall, C. P. and Fairbridge, R. W., Chapman and Hall, 21-22.

Welch, A. H. and Lico, M. S. 1998. Factors controlling As and U in shallow ground water, southern Carson Desert, Nevada. *Appl. Geochem.*, **13**, 521-539.

Welch, A. H., Lico, M. S. and Hughes, J. L. 1988. Arsenic in ground water of the western United States. Ground Water, 26, 333-347.

Welch, A.H., Helsel, D. R., Focazio, M. J. and Watkins, S. A. 1999. Arsenic in ground water supplies of the United States. In: *Arsenic Exposure and Health Effects*, eds: Chappell, W. R. Abernathy, C. O. and Calderon, R. L., Elsevier, pp 9-17.

WHO 1993. *Guidelines for Drinking-Water Quality. Volume 1: Recommendations*. Second edition. World Health Organization, Geneva.

WHO 1998. *Guidelines for Drinking-Water Quality. Addendum to Volume 1: Recommendations.* Second Edition, World Health Organization, Geneva.

Wilkie, J. A. and Hering, J. G. 1996. Adsorption of arsenic onto hydrous ferric oxide: effects of adsorbate/adsorbent ratios and co-ocurring solutes. *Colloids and Surfaces, A: Phys. Eng. Aspects*, **107**, 97-110.

Wilkie, J. A. and Hering, J. G. 1998. Rapid oxidation of geothermal arsenic(III) in streamwaters of the eastern Sierra Nevada. *Environ. Sci. Technol.*, **32**, 657-662.

Williams, M., Fordyce, F., Paijitprapapon, A. and Charoenchaisri, P. 1996. Arsenic contamination in surface drainage and groundwater in part of the southest Asian tin belt, Nakhon Si Thammarat Province, southern Thailand. *Environ. Geol.*, **27**, 16-33.

Williams, M. 1997. Mining-related arsenic hazards: Thailand case-study. Summary Report. *British Geological Survey Technical Report*, WC/97/49, 36 pp.

Wilson, F. H. and Hawkins, D. B. 1978. Arsenic in streams, stream sediments and ground water, Fairbanks area, Alaska. *Environ. Geol.*, **2**, 195-202.

Wu, M. M., Kuo, T. L., Hwang, Y. H. and Chen, C. J. 1989. Dose-response relation between arsenic concentration in well water and mortality from cancers and vascular disease. *Am. J. Epidemiol*, **130**, 1123-1132.

Wyatt, C. J., Fimbres, C., Romo, L., Méndez, R. O. and Grijalva, M. 1998. Incidence of heavy metal contamination in water supplies in northern Mexico. *Environ. Res. Section A*, **76**, 114-119.

Yokoyama, T., Takahashi, Y. and Tarutani, T. 1993. Simulataneous determination of arsenic and arsenious acids in geothermal water. *Chem. Geol.*, **103**, 103-111

Zaldivar, R. 1974. Arsenic contamination of drinking water and foodstuffs causing endemic chronic poisoning. *Beitr. Pathol.*, **151**, 384-400.

Zárate, M. and Blasi, A. 1993. Late Pleistocene-Holocene eolian deposits of the Southern Buenos Aires Province, Argentina: A preliminary model. *Quat. Internl.*, **17**, 15-20.

Zárate, M. A. and Fasano, J. L. 1989. The Plio-Pleistocene Record of the Central Eastern Pampas, Buenos-Aires Province, Argentina – the Chapadmalal case-study. *Palaeogeog. Palaeoclimatol. Palaeoecol.*, **72**, 27-52.

Zhai, C., Dai, G., Zhang, Z., Gao, H. and Li, G. 1998. An environmental epidemiological study of endemic arsenic poisoning in Inner Mongolia. In: *Abstracts from Proc. Third Intl. Conference of Arsenic Exposure and Health Effects*, San Diego, 1998, p154.

APPENDIX 1.1 Details of groundwater (and surface water) samples collected from La Pampa and on-site measurements

Sample	Locality	Field No	APA No	Well depth	Water level	Elev'n	Latitude		Longitude		Date sampled	Temp	pH	Eh	DO	SEC
				m	m	m	°S	'	°W	'		°C		mV	mg l⁻¹	µS cm⁻¹
962071	Escuela No 209	LP1		6	3.56	192	35	46.090	64	16.290	25-Oct-96	18.3	8.28		6.9	981
962072	Rostagno	LP2	126	49	39	212	35	37.537	64	24.902	25-Oct-96	27.2	7.30		4.0	7270
962073	Monte Nievas No 2	LP3		13		175	35	52.493	64	8.743	25-Oct-96	19.3	7.61	492	5.4	1830
962074	Metileo	LP4		30.4	5.25	151	35	49.231	64	0.583	26-Oct-96	19.9	7.85	384	5.3	3340
962075	Dorila	LP5		6	3.5		35	48.457	63	52.353	26-Oct-96	19.8	7.30	275	4.9	17520
962076	Trenel No 4	LP6		32		178	35	42.128	64	7.583	26-Oct-96	20.8	7.70	411	4.6	3600
962077	Estancia Los Olivos	LP7	93	15	7.2	180	35	34.967	64	9.067	26-Oct-96	20.3	7.89	359	5.8	1310
962078	Garcia (Rosales)	LP8		12	3.5	178	35	46.670	64	9.477	26-Oct-96	18.3	7.28	355	2.3	2630
962079	E Castex Iglesias Evangelica	LP9		14	5	187	35	54.476	64	18.186	27-Oct-96	18.9	8.07	439	6.4	1550
962080	E Castex (Don Arturo)	LP10		80			36	0.871	64	21.616	27-Oct-96	23.1	7.82	395	6.6	3220
962081	E Castex, E de Soria	LP11		48.5	44		36	0.323	64	22.293	27-Oct-96	19.2	7.40	252	5.5	12400
962082	E Castex, Santa Rita	LP12		30	19.8	189	35	59.623	64	21.996	27-Oct-96	18.3	8.60	318	6.6	2130
962083	E Castex, La Invernada	LP13		20	5.5	164	35	57.932	64	11.232	27-Oct-96	18.8	8.24	321	4.4	2990
962084	Monte Nievas (Uterman)	LP14	34	26	8	162	35	56.251	64	3.959	27-Oct-96	18.9	7.55	254	6.7	1430
962085	Arata No 3	LP15		34.1		214	35	39.227	64	20.629	28-Oct-96	21.0	7.88	415	5.2	2070
962086	Escuela No 136	LP16		74	55	214	35	37.854	64	26.750	28-Oct-96	25.6	7.27	244	2.6	9010
962087	Ing Luiggi No 8	LP17	7	28		188	35	23.844	64	27.737	28-Oct-96	20.1	8.28	392	8.2	2200
962088	Pichi Huinca No 2	LP18		108	59.24	242	35	39.300	64	45.992	28-Oct-96	21.8	7.96	311	4.1	2850
962089	La Maruja No 4	LP19		140	90	282	35	40.329	64	56.973	28-Oct-96	29.0	7.68	389	5.4	2160
962090	Ing Foster Pozo	LP20		131	125	312	35	42.240	65	6.006	28-Oct-96	26.4	7.98	360	6.5	1150
962091	Caleufu No 5	LP21		34		203	35	35.971	64	33.504	28-Oct-96	20.8	7.97	343	6.5	3200
962092	La Pichona	LP22		36.5	28	204	35	53.969	64	26.594	29-Oct-96	21.3	7.78	445	7.4	3680
962093	Don Luis	LP23	16	110	100	213	35	54.123	64	43.220	29-Oct-96	26.5	7.69	363	5.7	3000
962094	Nicola	LP24	43	84.7	73.3	215	35	56.527	64	35.723	29-Oct-96	24.6	7.54	324	5.5	4240
962095	Conhelo	LP25	27	110	100	223	35	53.461	64	37.794	29-Oct-96	26.4	7.56	367	6.5	939
962096	Caleufu (Mazaferro Hnos)	LP26		38.6	32	194	35	48.541	64	39.333	29-Oct-96	21.4	8.14	408	6.9	1980
962097	Pichi Huinca (T Reche)	LP27	42	96	90	261	35	48.355	64	47.765	29-Oct-96	25.1	7.42	218	3.8	2530
962098	La Maruja (Barales)	LP28	54	36.5	34.5	254	35	48.328	64	52.689	29-Oct-96	19.9	8.39	306	7.9	1870
962099	Eduardo Castex, Talleres Norte	LP29		48	4.65	187	35	54.300	64	18.067	30-Oct-96	20.4	7.83	406	6.7	6760
962100	Eduardo Castex, Talleres Norte	LP30		12	4.65	187	35	54.300	64	18.067	30-Oct-96	18.3	8.30		7.4	1220
962101	Eduardo Castex	LP31	4	6.1	4.77		35	54.012	64	19.550	30-Oct-96	17.2	8.26	321	4.4	3420
962102	Eduardo Castex (Jote Herrero)	LP32	70	16	3.7	194	35	50.185	64	16.679	30-Oct-96	18.4	7.94	333	8.1	1570

APPENDIX 1.1 cont'd...

Sample	Locality	Field No	APA No	Well depth	Water level	Elev'n	Latitude		Longitude		Date sampled	Temp	pH	Eh	DO	SEC
				m	m	m	°S	'	°W	'		°C		mV	mg l^{-1}	µS cm^{-1}
962103	Eduardo Castex (Macagno)	LP33	111	28	16.2	198	35	57.374	64	16.076	30-Oct-96	20.3	7.26	412	3.2	2570
962104	Eduardo Castex	LP34	29	20	6.63	188	35	56.920	64	16.726	30-Oct-96	18.3	7.58	323	7.4	1150
970685	Eduardo Castex, Santa Rita Pond	LP35		0	0	189	35	59.830	64	22.142	23-Apr-97		7.74		7.4	219
970686	Eduardo Castex, Santa Rita	LP36		30	9.35	189	35	59.851	64	22.188	23-Apr-97	18.7	8.66	402	7.1	1990
970687	Establ Las Chacras	LP37			14.1	189	35	58.871	64	21.798	23-Apr-97	20.0	7.93	420	5.4	4950
970688	El Porvenir (Sciaretta)	LP38		15.1		197	35	56.557	64	20.892	23-Apr-97	18.7	7.66	411	8.1	2420
970689	Estab Maria Paula	LP39	8	12		193	35	55.601	64	19.767	24-Apr-97	17.5	7.45	326	4.9	7590
970690	Epifanio	LP40		49		211	35	58.480	64	26.795	24-Apr-97	20.6	8.04	280	6.3	1000
970691	Conhelo 4	LP41		140		221	36	0.304	64	35.365	24-Apr-97	26.3	7.56	265	6.5	3560
970692	Estab El Tigre	LP42		106	74	200	35	58.112	64	41.401	24-Apr-97	21.5	8.07	306	5.7	2740
970693	Estancia La Sabina	LP43		29.5	25.3	243	35	59.345	64	52.085	25-Apr-97	17.8	8.28	409	5.8	1260
970694	Estancia La Maruja Puesto 10	LP44		95		281	36	0.495	65	1.750	25-Apr-97	22.9	7.43	226	6.1	3100
970695	La Legua	LP45		53		281	35	54.239	65	3.277	25-Apr-97	21.4	8.38	359	9.9	2710
970696	Estancia Don Carlos	LP46		65		260	35	54.673	64	58.401	25-Apr-97	22.7	7.40		7.2	5880
970697	Eduardo Castex No 1	LP47		87		185	35	55.391	64	18.237	26-Apr-97	20.8	7.68	393	6.3	3590
970698	Eduardo Castex No 12	LP48		38.8	12.1	192	35	55.793	64	17.986	26-Apr-97	19.8	7.71	242	6.4	2190
970699	Eduardo Castex, Quinte de Piorno	LP49		9.8	5.73	195	35	56.847	64	17.490	26-Apr-97	18.0	7.39	320	6.8	1730
970700	Eduardo Castex (M Tamagnoni)	LP50		14	4.8	170	35	59.919	64	16.033	26-Apr-97	18.6	8.07	359	3.8	2580
970701	Lake next to Tamagnoni	LP51		0	0	160	36	0.465	64	16.616	26-Apr-97	15.8	8.08		8.2	197
970702	Eduardo Castex (Omar Piorno)	LP52		11	9.15	183	35	58.174	64	13.630	26-Apr-97	18.5	7.40	276	2.1	2550
970703	Establ Fuentes	LP53	49	20	4	189	35	51.989	64	17.351	27-Apr-97	18.1	7.61	425	3.1	3000
970704	Establ Las Toscas	LP54	46	28	14.2	204	35	51.154	64	22.322	27-Apr-97	18.8	7.96	393	7.6	1760
970705	La Gloria	LP55		60.1	53.1	212	35	50.733	64	27.883	27-Apr-97	21.2	7.83	250	5.2	2100
970706	Establ Enrigue Villalba	LP56		82	39.5	211	34	48.386	64	26.334	27-Apr-97	23.2	7.38	266	0.8	7830
970707	Establ Winschel Hermanos	LP57		29.1	20.8	213	35	46.748	64	23.542	27-Apr-97	19.2	8.02	318	6.2	1830
970708	Establ El Cencerro (Barbero)	LP58		19.3	4.1	201	35	45.734	64	19.479	27-Apr-97	19.4	8.04	315	7.6	2010
970776	Arata No 2	LP59		34	21	211	35	39.369	64	20.593	28-Apr-97	21.4	7.87	416	5.9	2070
970777	Establ Los Tauras	LP60	16	17.4	13.1	207	35	41.625	64	21.990	28-Apr-97	20.1	7.98	392	8.5	2180
970778	La Ocasión	LP61		72.9	66.0	213	35	42.716	64	26.867	28-Apr-97	24.1	7.51	327	4.7	5240
970779	Establ Las Mercedes	LP62		89.5	72.5	215	35	44.847	64	28.627	28-Apr-97	23.4	7.39	333	5.1	4620
970780	Establ La Pebeta (Viglione Hnos)	LP63		13.2	5.65	195	35	43.020	64	19.022	28-Apr-97	18.7	7.93	283	5.4	2990
970781	Caleufu No 2	LP64		42	27.8	208	35	37.709	64	34.471	29-Apr-97	21.0	8.02	433	7.1	1350
970782	Caleufu (R Destouches)	LP65				207	35	36.585	64	34.627	29-Apr-97	18.9	7.92	425	7.5	1370
970783	Caleufu (F Coronel E Hijos)	LP66		26.9	18.8	208	35	35.867	64	35.545	29-Apr-97	20.0	6.99	282	2.4	15000

APPENDIX 1.1 cont'd...

Sample	Locality	Field No	APA No	Well depth	Water level	Elev'n	Latitude		Longitude		Date sampled	Temp	pH	Eh	DO	SEC
				m	m	m	°S	'	°W	'		°C		mV	mg l^{-1}	$\mu S\ cm^{-1}$
970784	Caleufu, El Destino	LP67		18.6	12.3	206	35	35.198	64	35.243	29-Apr-97	21.0	7.57	259	6.1	4290
970785	Caleufu (Groppo)	LP68		14	8	204	35	34.416	64	33.932	29-Apr-97	17.9	8.01	308	4.6	3390
970786	Caleufu, B Assone Lote 6	LP69		7.1	5.4	198	35	34.230	64	31.622	29-Apr-97	18.9	8.02	270	7.4	2980
970787	Caleufu, molino 2km NE Caleufu	LP70		11.6	3.55	197	35	35.019	64	32.282	29-Apr-97	16.7	7.97	258	2.2	2510
970788	Trenel No 2	LP71		30	9.4	178	35	41.756	64	7.870	30-Apr-97	19.2	7.82	431	7.7	3570
970789	Trenel (J Peinado)	LP72		10		154	35	40.990	64	2.378	30-Apr-97	18.4	7.85	433	6.1	4870
970790	H Massa	LP73		13	4	154	35	42.898	64	1.881	30-Apr-97	18.2	7.96	354	5.9	5230
970791	Simonetti Hermanos	LP74		14	4	161	35	45.589	64	3.439	30-Apr-97	18.6	7.84	380	5.0	3080
970792	Estancia Cnia, Trenel (Feninger)	LP75		18	12	163	35	48.492	64	4.232	30-Apr-97	18.9	7.84	246	5.1	1300
970793	A Lovera	LP76	23	13.7	10.7	182	35	48.406	64	10.158	30-Apr-97	19.2	7.35	281	5.3	5660
970794	F Fuchs	LP77		10.5	6	178	35	49.474	64	11.227	30-Apr-97	18.2	7.59	296	5.0	5390
970795	Ing Foster, Establ Las Margaritas	LP78		130	120.5	300	35	42.398	65	3.974	01-May-97	27.0	7.94	131	6.6	1350
970796	Establ La Costera (Barale)	LP79		130	128.6	301	35	40.843	65	1.042	01-May-97	29.1	7.85	154	3.9	1790
970797	La Maruja No 2	LP80		94		280	35	40.395	64	56.554	01-May-97	26.7	7.49		5.5	2910
970798	La Marina (La Nelioa)	LP81		90	61	273	35	43.342	64	55.458	01-May-97	22.5	8.09	162	7.7	2640
970799	Establ Los Dos Pinos (Ferroro)	LP82		61	51.3	247	35	41.560	64	48.060	01-May-97	23.1	7.67	217	8.2	2740
970800	Pichi Huinca No 3	LP83		65	64	245	35	38.774	64	46.204	01-May-97	23.8	8.00	168	9.7	3040
970801	Eduardo Castex No 9	LP84		51	22.3	186	35	55.293	64	17.810	02-May-97	20.3	7.90	386	6.4	2980
970802	Rolando	LP85		38	18	197	35	54.463	64	22.385	02-May-97	18.7	8.13	318	5.6	2610
970803	Establ La Loma (Gaiottino)	LP86		85.4	66.3	212	35	54.472	64	39.468	02-May-97	25.4	7.77	211	5.7	2250
970804	Las Torcacitas (Heinz)	LP87		91	84	217	35	53.360	64	40.255	02-May-97	24.9	7.73	300	9.2	2590
970805	Caleufu No 3	LP88		42	17.5	207	35	37.691	64	34.131	03-May-97	20.7	8.10	459		1340
970806	Caleufu No 1	LP89		42	27.3	209	35	37.931	64	34.697	03-May-97	20.9	8.08	361	6.7	1580
970807	Caleufu Establ El Caldén	LP90		56	31.8	212	35	37.927	64	35.403	03-May-97	21.6	7.31	236	3.9	4960
970808	Caleufu Establ El Ontoño	LP91		28	22.7	207	35	37.029	64	36.692	03-May-97	19.8	8.27	320	7.2	3910
970809	Caleufu Establ La Pichincha	LP92		23.8	18	207	35	35.739	64	36.854	03-May-97	19.0	7.89	344	4.8	6600
970810	Galcerán	LP93		12	9	204	35	33.996	64	34.135	03-May-97	19.0	7.60	357	5.0	5860
970811	Caleufu (M Bauduco)	LP94		12	8	201	35	33.621	64	32.450	03-May-97	16.1	7.73	353	6.5	2100
970812	Blanco	LP95		16.6	4.2	192	35	47.150	64	15.896	04-May-97	18.9	7.72	442	8.5	1810
970813	Molino 7 km S of El Cruce	LP96		16	2.35	189	35	44.549	64	16.819	04-May-97	17.8	8.10	348	4.2	2610
970814	Estancia Los Olmos	LP97		12	4.2	193	35	43.069	64	14.764	04-May-97	18.8	7.61	294	7.3	1860
970815	José Gariglio	LP98		24	6.01	197	35	42.966	64	15.877	04-May-97	18.9	8.02	238	8.2	1470
970816	Estancia Las Tres Hermanas	LP99		28.4	16.0	209	35	35.893	64	29.017	05-May-97	17.9	8.10	287	7.6	1130
970817	El Peral	LP100		18.5	2.4	192	35	33.009	64	29.677	05-May-97	19.0	7.97	315	6.6	4070

APPENDIX 1.1 cont'd...

Sample	Locality	Field No	APA No	Well depth	Water level	Elev'n	Latitude		Longitude		Date sampled	Temp	pH	Eh	DO	SEC
				m	m	m	°S	'	°W	'		°C		mV	mg l^{-1}	µS cm^{-1}
970818	Estancia La Leonor	LP101				191	35	31.049	64	28.689	05-May-97	19.0	7.96	264	8.9	1830
970819	Campo Arduino	LP102		17.1	4.5	187	35	27.364	64	28.396	05-May-97	22.0	8.32	300	5.3	2740
970820	Establ Don Fidel	LP103		25	5.5	189	35	25.021	64	27.864	05-May-97	18.4	8.05	322	3.9	4050
970821	Ing. Luiggi No 3 (Municipalidad)	LP104		40	14.5	193	35	22.917	64	27.657	05-May-97	19.9	7.93	283	5.7	2100
970822	Establ La Querencía (Armitano)	LP105				181	35	54.658	64	13.981	06-May-97	18.0	7.65	478	7.6	1530
970823	Estancia La Dulce	LP106		12	4.3	167	35	54.482	64	7.705	06-May-97	17.6	7.44	343	6.7	1170
970824	Establ La Rebollada	LP107		18.5	13.1	163	36	0.452	64	5.457	06-May-97	18.9	7.34	293	5.1	6700
970825	Estancia Jagüel Grande	LP108		15	4.25	160	35	58.242	64	8.057	06-May-97	18.5	7.47	381	2.4	8320
970826	Establ El Amanecer (Ferrero)	LP109		13	2.1	176	35	53.941	64	12.390	06-May-97	18.2	7.62	346	6.5	773
971630	Across lake from Tamagnoni	LP110				160	36	0.05	64	16.030	10-May-97	22.0	8.65			2160
Talleres Norte, Tamagnoni samples																
971631	E Castex, Talleres Norte	LP30R		12	3.02	185	35	54.300	64	18.067	14-May-97	19.2	7.90			1370
971632	E Castex, Talleres Norte	LP29R		48	3.0	185	35	54.300	64	18.067	14-May-97	20.5	7.75			5650
971629	Tamagnoni	LP50R		14		170	35	59.919	64	16.033	11-May-97	19.4	8.23			2930
971625	Tamagnoni depth sample	LP111		5.5	3.5	170	35	59.917	64	15.950	06-May-97	19.6	7.28			6560
971626	Tamagnoni depth sample	LP112		16	3.5	170	35	59.917	64	15.950	08-May-97	24.6	8.54			3160
971627	Tamagnoni depth sample	LP113		30.5	3.5	170	35	59.917	64	15.950	10-May-97	24.7	8.36			3660
971628	Talleres Norte depth sample	LP114		26.5	4	185	35	54.90	64	17.767	11-May-97	21.0	8.01			1020

Temp: temperature; elev'n: elevation (above OD); SEC: specific electrical conductance; DO: dissolved oxygen

APA No: DDA (formerly APA) borehole reference number

APPENDIX 1.2 Major-element data for groundwater (and surface water) samples from La Pampa (BGS data)

Sample	Locality	Ca mg l^{-1}	Mg mg l^{-1}	Na mg l^{-1}	K mg l^{-1}	Cl mg l^{-1}	SO_4 mg l^{-1}	HCO_3 mg l^{-1}	NO_3-N mg l^{-1}	NO_2-N mg l^{-1}	NH_4.N mg l^{-1}	Total hardness $CaCO_3$	DOC mg l^{-1}	pCO_2 log atm
962071	Escuela No 209	3.69	3.55	231	3.9	8.5	6.8	566	0.8	0.003	0.02	23.8		-2.59
962072	Rostagno	57.9	64.3	1340	29.2	1240	904	741	17.2	0.004	<0.01	409		-1.49
962073	Monte Nievas No 2	29.8	18.3	363	5.9	103	253	567	7.2	0.003	<0.01	150		-1.93
962074	Metileo	17.9	24.0	685	12.2	405	512	610	1.5	0.010	<0.01	143	3.2	-2.15
962075	Dorila	266	368	3100	70.6	4000	3170	455	7.5	0.010	<0.01	2177		-1.81
962076	Trenel No 4	39.9	46.0	667	13.1	370	767	462	1.2	0.004	<0.01	289	1.1	-2.12
962077	Estancia Los Olivos	10.8	6.42	292	3.3	61.3	98.5	585	1.6	0.003	<0.01	53.4		-2.18
962078	Garcia (Rosales)	80.6	52.7	412	13.7	205	161	656	73	0.02	<0.01	418		-1.55
962079	E Castex Iglesias Evangelica	7.07	6.1	360	5.5	38	84.9	773	1.8	0.004	<0.01	42.7	5.6	-2.25
962080	E Castex (Don Arturo)	36	45.0	613	19.0	418	376	717	11.8	0.003	<0.01	275	1.8	-2.03
962081	E Castex, E de Soria	203	278	1850	56.6	2750	1430	558	14.3	0.012	<0.01	1650		-1.80
962082	E Castex, Santa Rita	1.55	2.35	526	10.6	12.5	33.4	1270	5.2	0.026	<0.01	13.5		-2.60
962083	E Castex, La Invernada	4.15	7.97	695	15.9	70	376	1340	4.3	0.020	<0.01	43.1	4.7	-2.21
962084	Monte Nievas (Uterman)	43.2	18.9	267	6.8	75	83.9	561	30.6	0.008	<0.01	186		-1.87
962085	Arata No 3	8.4	12.2	451	9.6	70	249	799	1.2	0.011	<0.01	71.1	4.7	-2.04
962086	Escuela No 136	54.1	66.2	1680	30.2	1690	1100	836	16.3	0.007	0.01	407		-1.43
962087	Ing Luiggi No 8	3.7	8.62	508	7.3	20	219	1030	2.2	0.017	<0.01	44.7	4.8	-2.34
962088	Pichi Huinca No 2	18.1	21.8	519	13.6	400	322	394	3.4	0.008	<0.01	135		-2.43
962089	La Maruja No 4	15	16.5	437	14.3	245	222	527	9.1	0.007	<0.01	105		-1.97
962090	Ing Foster Pozo	10.3	7.71	224	10.7	150	98	258	2.2	<0.003	<0.01	57.4		-2.59
962091	Caleufu No 5	12.1	14.7	655	14.6	340	483	680	1.8	0.009	0.02	90.7	2.4	-2.21
962092	La Pichona	27.1	43	745	18.0	410	773	575	3.4	0.003	<0.01	244		-2.10
962093	Don Luis	27.2	39.9	539	15.9	550	251	441	3.6	<0.003	<0.01	232		-2.09
962094	Nicola	46.4	72.3	756	31.1	870	403	455	18.9	0.014	<0.01	413		-1.95
962095	Conhelo	35.8	27.6	120	17.1	94	82.6	306	5.5	0.004	<0.01	203		-2.09
962096	Caleufu (Mazaferro Hnos)	4.15	4.76	493	16.7	20	53.9	1110	28.7	0.017	<0.01	29.9	5.8	-2.16
962097	Pichi Huinca (T Reche)	51.5	50.5	438	15.5	260	499	444	3.0	<0.003	0.01	336		-1.82
962098	La Maruja (Barales)	2.01	2.97	449	6.1	15	28.2	1120	5.6	0.010	0.01	17.2		-2.42
962099	Eduardo Castex, Talleres Norte	25.6	53.8	1430	25.7	970	1340	635	2.9	0.007	<0.01	285		-2.14
962100	Eduardo Castex, Talleres Norte	4.57	2.64	299	3.3	10.5	33.8	674	3.4	0.007	<0.01	22.3		-2.55
962101	Eduardo Castex	10.7	14.9	761	13.6	120	160	1310	83	0.025	0.01	88.0		-2.25
962102	Eduardo Castex (Jote Herrero)	10.2	13.6	354	7.2	62.5	122	691	4.3	<0.003	<0.01	81.4		-2.17

APPENDIX 1.2 cont'd...

Sample	Locality	Ca mg l^{-1}	Mg mg l^{-1}	Na mg l^{-1}	K mg l^{-1}	Cl mg l^{-1}	SO_4 mg l^{-1}	HCO_3 mg l^{-1}	NO_3-N mg l^{-1}	NO_2-N mg l^{-1}	NH_4.N mg l^{-1}	Total hardness $CaCO_3$	DOC mg l^{-1}	pCO_2 log atm
962103	Eduardo Castex (Macagno)	98.7	54.4	422	8.5	340	481	380	4.9	<0.003	0.10	470		-1.76
962104	Eduardo Castex	29.6	16.4	211	4.0	33.5	89.2	473	11.6	0.006	<0.01	141		-1.97
970685	Eduardo Castex, Santa Rita Pond	21.9	2.93	1.3	13.2	1.74	2	92.4	0.7	0.308	<0.02	66.7		-2.13
970686	Eduardo Castex, Santa Rita	2.22	2.4	534	11.6	16.9	50	1250	14.8	0.029	<0.02	15.4	5.6	-2.63
970687	Establ Las Chacras	11.4	25.4	1180	21.4	626	776	1240	6.8	0.011	<0.02	133		-1.94
970688	El Porvenir (Sciaretta)	36.6	22.3	559	7.6	254	347	720	22.6	<0.005	<0.02	183		-1.89
970689	Estab Maria Paula	252	161	1320	16.0	1780	622	518	144	0.035	<0.02	1291		-1.88
970690	Epifanio	6.09	7.07	235	10.2	10.1	34.5	594	7.1	<0.005	<0.02	44.3		-2.32
970691	Conhelo 4	41.7	46.3	641	25.2	580	487	456	12.2	<0.005	<0.02	294		-1.95
970692	Estab El Tigre	4.18	6.06	636	9.6	55.4	192	1360	16.5	<0.005	<0.02	35.4	7.2	-2.01
970693	Estancia La Sabina	2.28	2.08	310	4.7	10.2	28.4	742	2.4	0.021	<0.02	14.2	<0.1	-2.48
970694	Estancia La Maruja Puesto 10	102	96.2	427	21.3	484	513	379	22.7	<0.005	<0.02	650		-1.93
970695	La Legua	38.3	42.6	521	18.4	352	605	326	3.3	<0.005	<0.02	271		-2.96
970696	Estancia Don Carlos	116	131	1030	25.6	864	1570	368	4.9	<0.005	<0.02	828		-1.93
970697	Eduardo Castex No 1	26.6	29.7	686	11.6	444	537	551	6.1	<0.005	<0.02	189		-2.02
970698	Eduardo Castex No 12	26.4	20.5	437	8.5	188	411	474	1.0	<0.005	<0.02	150		-2.11
970699	Eduardo Castex, Quinte de Piorno	76.6	29.9	310	6.9	90	284	557	29.3	<0.005	<0.02	314		-1.73
970700	Eduardo Castex (M Tamagnoni)	5.43	8.25	692	14.8	68.6	285	1390	12.1	0.015	<0.02	47.5		-2.02
970701	Lake next to Tamagnoni	18.7	5.12	5.9	24.6	3.67	2.3	118	<0.5	<0.005	0.05	67.7		-3.07
970702	Eduardo Castex (Omar Piorno)	68.3	55.9	499	9.6	230	591	613	9.3	<0.005	<0.02	400		-1.70
970703	Establ Fuentes	41.2	38.3	576	10.1	244	485	688	21	0.022	<0.02	260		-1.86
970704	Establ Las Toscas	10.6	12.5	400	8.2	84.3	167	707	12.2	<0.005	<0.02	77.9		-2.18
970705	La Gloria	20	27.6	453	15.2	93	323	812	5.4	<0.005	<0.02	163	3.7	-1.99
970706	Establ Enrigue Villalba	128	164	1520	36.4	1780	1050	536	92	0.166	<0.02	994		-1.76
970707	Establ Winschel Hermanos	24	28.5	371	9.4	123	283	540	16.3	<0.005	0.14	177		-2.37
970708	Establ El Cencerro (Barbero)	8.35	15.3	477	10.7	87.8	228	880	7.1	<0.005	<0.02	83.8		-2.17
970776	Arata No 2	7.4	11.8	468	9.7	102	261	813	1.58	<0.005	<0.02	67.0		-2.02
970777	Establ Los Tauras	12.3	19.9	490	11.1	146	242	737	30.7	<0.005	<0.02	113		-2.19
970778	La Ocasión	33.8	59	1060	25.9	906	739	775	16.9	0.007	<0.02	327	2.2	-1.70
970779	Establ Las Mercedes	42.2	68.5	817	25.6	713	581	650	26.6	0.008	<0.02	387		-1.65
970780	Establ La Pebeta (Viglione Hnos)	13.8	12.0	752	8.7	151	390	1140	40.9	0.008	<0.02	83.8		-1.96
970781	Caleufu No 2	8.35	9.63	291	8.8	34.4	194	541	0.66	<0.005	<0.02	60.4		-2.34
970782	Caleufu (R Destouches)	11.6	12.2	292	10.6	39.3	97.3	580	27.2	<0.005	<0.02	79.1		-2.22
970783	Caleufu (F Coronel E Hijos)	599	521	2090	58.6	4580	626	226	59.5	0.014	<0.02	3637		-1.82

APPENDIX 1.2 cont'd...

Sample	Locality	Ca mg l-1	Mg mg l-1	Na mg l-1	K mg l-1	Cl mg l-1	SO_4 mg l-1	HCO_3 mg l-1	NO_3-N mg l-1	NO_2-N mg l-1	NH_4.N mg l-1	Total hardness $CaCO_3$	DOC mg l-1	pCO_2 log atm
970784	Caleufu, El Destino	137	124	700	23.6	889	732	402	31.5	0.011	<0.02	852		-2.07
970785	Caleufu (Groppo)	21.3	25.4	833	10.7	131	898	950	17.3	0.049	<0.02	158		-2.14
970786	Caleufu, B Assone Lote 6	12.1	8.16	802	11.3	156	306	1420	28.9	<0.005	<0.02	63.8		-1.96
970787	Caleufu, molino 2km NE Caleufu	5.83	4.84	672	10.2	63.8	138	1410	33.8	0.169	<0.02	34.5		-1.92
970788	Trenel No 2	17.5	31.1	739	14.6	385	588	655	32.9	0.008	<0.02	172		-2.10
970789	Trenel (J Peinado)	32.8	28.2	1050	9.5	751	840	646	9.28	<0.005	<0.02	198		-2.15
970790	H Massa	15.0	26.6	1200	12.9	691	934	902	43.1	0.014	<0.02	147		-2.12
970791	Simonetti Hermanos	38.2	24.2	766	7.4	625	361	707	18	<0.005	<0.02	195		-2.09
970792	Estancia Cnia, Trenel (Feninger)	6.3	6.89	304	5.0	70.5	93.2	624	0.76	<0.005	<0.02	44.1		-2.11
970793	A Lovera	271	144	1020	19.3	610	2210	346	32.4	<0.005	<0.02	1268		-1.94
970794	F Fuchs	53.4	74.8	1190	20.2	713	1230	913	31.9	<0.005	<0.02	441		-1.75
970795	Ing Foster, Establ Las Margaritas	8.63	7.93	285	9.5	85.1	98.5	537	3.3	<0.005	<0.02	54.1		-2.23
970796	Establ La Costera (Barale)	9.45	9.64	380	12.9	135	187	613	3.97	<0.005	<0.02	63.2		-2.07
970797	La Maruja No 2	30.5	37.0	546	19.8	513	274	497	11.8	<0.005	<0.02	228		-1.83
970798	La Marina (La Nelioa)	16.8	14.5	609	12.2	262	537	547	9.01	<0.005	<0.02	102		-2.42
970799	Establ Los Dos Pinos (Ferroro)	20.8	30.0	616	13.8	196	598	769	3.98	<0.005	<0.02	175		-1.85
970800	Pichi Huinca No 3	20.8	25.1	559	14.7	458	352	448	5.34	<0.005	<0.02	155		-2.41
970801	Eduardo Castex No 9	21.0	23.9	615	10.7	428	472	493	1.42	<0.005	<0.02	151		-2.29
970802	Rolando	7.74	11.4	623	12.1	79.2	108	760	80.4	0.021	nd	66.2	1.9	-2.16
970803	Establ La Loma (Gaiottino)	14.4	17.2	434	12.4	306	144	566	6.89	<0.005	nd	107		-2.05
970804	Las Torcacitas (Heinz)	14.6	21.2	531	14.3	338	138	790	7.46	<0.005	nd	124		-1.88
970805	Caleufu No 3	5.52	6.26	287	8.3	16.9	144	613	<0.23	<0.005	nd	39.5	2.4	-2.37
970806	Caleufu No 1	7.22	6.78	322	8.7	54.3	223	568	1.09	<0.005	nd	45.9		-2.38
970807	Caleufu Establ El Caldén	169	145	691	29.6	1290	494	281	7.46	<0.005	nd	1018		-1.96
970808	Caleufu Establ El Ontoño	4.23	11.4	882	14.4	281	439	1360	8.59	0.008	nd	57.4	4.1	-2.24
970809	Caleufu Establ La Pichincha	25.9	46.3	1440	26.3	1460	527	905	38.9	0.013	nd	255	4.1	-2.05
970810	Galcerán	93.4	126	1220	27.4	1310	1030	617	44.1	<0.005	nd	751		-1.93
970811	Caleufu (M Bauduco)	33.1	17.1	507	10.3	156	220	693	70.3	<0.005	nd	153		-1.99
970812	Blanco	21.4	14.5	394	6.4	76.9	212	714	7.91	<0.005	nd	113		-1.94
970813	Molino 7 km S of El Cruce	24.1	22.9	616	12.6	113	190	1180	45.9	0.008	nd	154		-2.13
970814	Estancia Los Olmos	75.6	50.9	299	6.8	110	95.9	705	55.5	<0.005	nd	398	1.3	-1.84
970815	José Gariglio	9.00	5.61	365	5.1	29.9	86.1	839	1.89	<0.005	nd	45.5		-2.17
970816	Estancia Las Tres Hermanas	8.75	5.76	253	3.9	12.1	71	607	1.89	<0.005	nd	45.5		-2.39
970817	El Peral	32.8	28.5	916	20.9	248	230	1440	135	0.080	nd	199		-1.91

APPENDIX 1.2 cont'd...

Sample	Locality	Ca	Mg	Na	K	Cl	SO_4	HCO_3	NO_3-N	NO_2-N	NH_4.N	Total hardness	DOC	pCO_2
		mg l^{-1}	mg l^{-1}	mg l^{-1}	mg l^{-1}	mg l^{-1}	mg l^{-1}	mg l^{-1}	mg l^{-1}	mg l^{-1}	mg l^{-1}	$CaCO_3$	mg l^{-1}	log atm
970818	Estancia La Leonor	9.8	11.7	416	11.9	81.1	283	680	3.17	<0.005	nd	72.6		-2.20
970819	Campo Arduino	5.69	7.96	738	10.2	234	254	979	64.5	0.006	nd	46.9		-2.41
970820	Establ Don Fidel	7.78	15.0	1000	10	409	392	1360	58.4	0.008	nd	81.1		-2.02
970821	Ing. Luiggi No 3 (Municipalidad)	11.5	17.1	485	11.7	161	285	784	4.24	<0.005	nd	99.0		-2.11
970822	Establ La Querencía (Armitano)	32.1	20.2	306	4.4	58.9	108	701	16.4	<0.005	nd	163	4.2	-1.88
970823	Estancia La Dulce	57.9	38.9	176	9.7	40.7	72.5	597	11.6	<0.005	nd	304	5.7	-1.74
970824	Establ La Rebollada	286	288	748	18.1	2070	329	195	6.7	0.014	nd	1898	2.1	-2.20
970825	Estancia Jagüel Grande	65	114	1820	30.6	1760	1380	657	12.4	0.014	nd	631	2.4	-1.78
970826	Establ El Amanecer (Ferrero)	33.5	21.2	135	4.9	15.9	36.8	494	0.98	<0.005	nd	171	5.4	-1.99
971630	Across lake from Tamagnoni	2.15	2.01	546	11.4	25.2	53.3	1230	13.4	0.012	<0.01	13.6	nd	-2.65
Talleres Norte, Tamagnoni samples														
971631	E Castex, Talleres Norte	11.5	7.31	311	2.8	36.5	50.7	683	3.2	0.014	<0.01	58.8	nd	-2.13
971632	E Castex, Talleres Norte	19.9	43.1	1280	22.3	900	1110	707	2	0.006	<0.01	227	nd	-2.00
971629	Tamagnoni	5.46	7.91	707	15.1	77	277	1350	16.3	0.020	<0.01	46.2	nd	-2.19
971625	Tamagnoni depth sample	57.9	30.9	1460	43.6	705	468	1090	308	0.083	<0.01	272	nd	-1.35
971626	Tamagnoni depth sample	3.84	4.65	738	14.4	148	231	1170	45.4	0.133	<0.01	28.7	nd	-2.55
971627	Tamagnoni depth sample	10.6	9.75	857	20.8	224	313	1200	81.9	0.448	<0.01	66.6	nd	-2.36
971628	Talleres Norte depth sample	17.5	13	206	4.8	15.8	64	574	9.4	0.004	<0.01	97.1	nd	-2.30

APPENDIX 1.3 Trace-element data for groundwater (and surface water) samples from La Pampa (BGS data, F data also from INGEOQUI)

Sample	Locality	Si mg l^{-1}	Al mg l^{-1}	P mg l^{-1}	B mg l^{-1}	V mg l^{-1}	Sr µg l^{-1}	Ba µg l^{-1}	Fe µg l^{-1}	Mn µg l^{-1}	As$_T$ µg l^{-1}	As(III) µg l^{-1}	F$_{(IN)}$ mg l^{-1}	F$_{(BGS)}$ mg l^{-1}	Br µg l^{-1}	I µg l^{-1}
962071	Escuela No 209	28.8	0.24	<0.2	0.91	1.18	78	14	193	2	249	6	9.64	9.6	55	45
962072	Rostagno	33.7	0.07	<0.2	5.40	0.211	1480	24	232	13	30	<4	1.38	1.6	2480	223
962073	Monte Nievas No 2	29.6	0.16	<0.2	2.77	0.242	541	99	415	4	56	<4	3.56	3.7	427	200
962074	Metileo	28.8	<0.04	<0.2	3.99	0.333	710	21	8	<1	101	<4	5.02	5.6	994	195
962075	Dorila	24.2	0.10	0.3	4.80	0.138	9980	22	44	3	21	<4	1.31	2.0	9740	179
962076	Trenel No 4	29.9	<0.04	<0.2	3.02	0.204	989	30	7	<1	36	<4	3.4	3.6	986	249
962077	Estancia Los Olivos	31.2	<0.04	<0.2	1.62	0.266	200	41	1160	9	62	<4	4.89	4.6	288	86
962078	Garcia (Rosales)	29.8	<0.04	0.2	2.06	0.377	1150	175	42	<1	62	<4	3.78	3.7	2360	150
962079	E Castex Iglesias Evangelica	28.8	0.22	<0.2	2.05	0.851	207	40	176	2	191	5	11.8	10.1	180	121
962080	E Castex (Don Arturo)	31.8	0.10	<0.2	2.48	0.471	1060	24	179	4	137	<4	4.13	4.2	876	129
962081	E Castex, E de Soria	30.2	0.10	<0.2	3.02	0.413	6620	24	599	12	103	<4	2.28	3.4	5350	105
962082	E Castex, Santa Rita	26.8	0.23	0.3	8.30	1.25	183	22	618	3	4810	73	28.4	25.0	71	180
962083	E Castex, La Invernada	27.0	0.20	0.4	5.47	4.44	219	53	412	3	1800	46	9.01	8.2	327	430
962084	Monte Nievas (Uterman)	30.0	<0.04	<0.2	1.58	0.192	558	120	89	1	48	<4	2.46	2.7	327	74
962085	Arata No 3	31.0	0.14	0.2	3.07	0.626	239	38	52	<1	180	76	6.43	6.2	302	264
962086	Escuela No 136	32.5	0.05	0.3	7.28	0.242	1600	18	226	9	34	<4	1.74	2.4	3080	208
962087	Ing Luiggi No 8	28.6	<0.04	<0.2	4.46	1.28	267	22	10	<1	324	12	7.92	7.5	188	86
962088	Pichi Huinca No 2	25.9	<0.04	<0.2	2.66	0.449	480	24	82	50	137	5	3.03	3.9	1300	127
962089	La Maruja No 4	39.2	<0.04	<0.2	2.08	1.38	414	37	18	<1	485	13	3.01	3.2	409	78
962090	Ing Foster Pozo	21.1	0.07	<0.2	0.83	0.090	189	58	132	10	8	<4	1.67	1.9	306	20
962091	Caleufu No 5	28.3	<0.04	<0.2	3.03	0.486	733	27	<6	<1	105	<4	2.76	2.9	890	101
962092	La Pichona	29.0	<0.04	<0.2	3.47	0.797	1070	26	219	4	324	6	7.09	6.5	1440	176
962093	Don Luis	29.8	<0.04	<0.2	1.66	0.453	660	38	276	7	184	<4	3.28	3.3	964	76
962094	Nicola	33.7	<0.04	<0.2	2.33	0.393	1460	25	55	1	60	<4	1.97	2.3	1530	59
962095	Conhelo	36.7	<0.04	<0.2	0.81	0.301	593	62	78	2	14	<4	1.14	1.3	251	18
962096	Caleufu (Mazaferro Hnos)	29.2	<0.04	<0.2	3.03	1.37	135	21	72	<1	456	12	2.22	2.2	180	104
962097	Pichi Huinca (T Reche)	34.2	0.10	<0.2	1.45	0.143	995	31	422	11	18	<4	1.15	1.2	1120	17
962098	La Maruja (Barales)	28.7	0.13	<0.2	4.03	1.69	66	11	170	3	293	8	7.37	6.2	94	163
962099	Eduardo Castex, Talleres Norte	28.2	0.72	0.3	8.12	0.825	2020	30	522	9	212	11	6.75	7.4	2470	390
962100	Eduardo Castex, Talleres Norte	28.4	0.99	<0.2	0.83	2.05	97	30	575	9	221	11	14.7	13.5	113	76
962101	Eduardo Castex	26.2	0.11	0.6	2.97	1.86	615	98	137	4	570	13	12.5	12.2	659	209
962102	Eduardo Castex (Jote Herrero)	30.2	0.08	<0.2	2.83	0.652	291	57	88	2	184	7	9.94	9.8	280	142
962103	Eduardo Castex (Macagno)	34.6	<0.04	<0.2	1.54	0.108	1300	24	41	14	16	<4	1.29	1.8	1500	80

APPENDIX 1.3 cont'd...

Sample	Locality	Si mg l^{-1}	Al mg l^{-1}	P mg l^{-1}	B mg l^{-1}	V mg l^{-1}	Sr µg l^{-1}	Ba µg l^{-1}	Fe µg l^{-1}	Mn µg l^{-1}	As$_T$ µg l^{-1}	As(III) µg l^{-1}	F$_{(IN)}$ mg l^{-1}	F$_{(BGS)}$ mg l^{-1}	Br µg l^{-1}	I µg l^{-1}
962104	Eduardo Castex	33.0	<0.04	<0.2	1.20	0.194	464	55	81	<1	37	<4	3.08	3.1	171	86
970685	Eduardo Castex, Santa Rita Pond	9.8	2.29	0.6	0.02	0.009	117	56	1460	63	<4	<3			26	5
970686	Eduardo Castex, Santa Rita	24.0	0.11	0.4	7.69	2.93	230	26	62	2	4010	65	29.2	26.0	149	141
970687	Establ Las Chacras	28.0	<0.04	0.3	6.11	1.04	970	31	123	5	286	28	5.21		1400	243
970688	El Porvenir (Sciaretta)	30.1	<0.04	<0.2	3.54	0.324	721	64	32	2	64	<3	3.73		900	143
970689	Estab Maria Paula	27.2	<0.04	0.2	3.78	0.256	3670	72	41	5	43	<3	2.92		2300	110
970690	Epifanio	29.6	<0.04	<0.2	1.61	1.62	225	30	59	1	380	11	5.56		63	82
970691	Conhelo 4	34.6	<0.04	<0.2	2.29	0.834	1240	17	54	8	234	6	1.84		880	135
970692	Estab El Tigre	29.6	<0.04	0.4	3.48	1.79	187	34	149	4	5280	86	6.57	7.4	231	280
970693	Estancia La Sabina	31.0	0.09	<0.2	2.33	5.43	66	5	32	2	842	17	9.9		74	96
970694	Estancia La Maruja Puesto 10	34.7	<0.04	<0.2	1.40	0.132	2120	36	128	3	18	<3	0.634		1090	21
970695	La Legua	25.1	<0.04	<0.2	2.66	0.204	1290	11	14	<1	35	<3	1.35		1420	82
970696	Estancia Don Carlos	31.3	<0.04	<0.2	3.73	0.166	3330	14	311	8	38	<3	1.39		2400	143
970697	Eduardo Castex No 1	28.5	<0.04	<0.2	3.08	0.371	750	29	394	1	116	3	6.65		1250	174
970698	Eduardo Castex No 12	29.2	<0.04	<0.2	2.03	0.243	542	83	52	7	51	<3	4.3		670	122
970699	Eduardo Castex, Qte. de Piorno	28.9	<0.04	0.2	1.66	0.199	775	41	86	3	34	<3	2.85		630	113
970700	Eduardo Castex (M Tamagnoni)	27.2	0.06	0.4	5.25	4.15	278	50	49	<1	1360	30	10.1		273	229
970701	Lake next to Tamagnoni	13.9	<0.04	1.0	0.07	0.012	138	28	59	31	14	<3	0.125	0.15	215	27
970702	Eduardo Castex (Omar Piorno)	31.0	<0.04	<0.2	3.06	0.237	1280	22	10	<1	32	<3	1.63		720	82
970703	Establ Fuentes	31.0	<0.04	0.3	3.02	0.331	745	36	14	2	97	4	4.21		890	249
970704	Establ Las Toscas	30.9	<0.04	<0.2	2.15	0.683	279	47	21	<1	166	5	6.38		480	111
970705	La Gloria	33.9	<0.04	<0.2	2.63	0.445	576	19	283	11	76	4	2.66	3.0	280	119
970706	Establ Enrigue Villalba	32.8	<0.04	0.4	4.28	0.205	3100	35	30	79	27	<3	1.33		3600	137
970707	Establ Winschel Hermanos	31.4	<0.04	<0.2	2.09	0.365	510	20	236	11	71	<3	3.62		630	111
970708	Establ El Cencerro (Barbero)	28.3	<0.04	0.4	4.05	1.56	418	36	25	<1	710	28	6.67		400	420
970776	Arata No 2	29.8	<0.00	0.2	3.19	0.764	232	39	<6	<1	292	8	6.88		340	248
970777	Establ Los Tauras	29.7	<0.04	<0.2	2.61	0.674	358	69	47	<1	178	13	6		830	156
970778	La Ocasión	32.7	<0.04	0.3	4.80	0.521	1110	15	188	14	153	<4	1.96		1670	277
970779	Establ Las Mercedes	32.5	<0.04	0.3	3.14	0.371	1270	22	23	2	123	<4	1.66		1470	197
970780	Establ La Pebeta (Viglione)	28.3	<0.04	0.5	5.62	1.20	361	36	121	2	394	14	10.1	10.2	642	590
970781	Caleufu No 2	29.2	<0.04	<0.2	1.91	0.464	273	40	<6	<1	63	<4	2.64		167	117
970782	Caleufu (R Destouches)	29.4	<0.04	<0.2	1.82	0.210	386	61	33	<1	16	<4	1.38		196	87
970783	Caleufu (F Coronel E Hijos)	30.5	0.09	<0.2	1.91	0.029	13000	132	143	12	<4	<4	0.034		11600	40
970784	Caleufu, El Destino	27.5	<0.04	<0.2	2.06	0.047	3880	36	148	26	<4.0	<4	0.796		2520	59
970785	Caleufu (Groppo)	25.4	0.04	0.4	4.81	1.36	1090	28	45	8	250	6	7.62	7.5	760	130

APPENDIX 1.3 cont'd...

Sample	Locality	Si mg l^{-1}	Al mg l^{-1}	P mg l^{-1}	B mg l^{-1}	V mg l^{-1}	Sr µg l^{-1}	Ba µg l^{-1}	Fe µg l^{-1}	Mn µg l^{-1}	As$_T$ µg l^{-1}	As(III) µg l^{-1}	F$_{(IN)}$ mg l^{-1}	F$_{(BGS)}$ mg l^{-1}	Br µg l^{-1}	I µg l^{-1}
970786	Caleufu, B Assone Lote 6	26.0	<0.04	0.4	6.20	1.10	464	64	19	<1	646	14	9.94		720	264
970787	Caleufu molino 2km NE Caleufu	24.6	0.06	0.5	4.72	2.95	242	58	134	4	904	15	9.45		330	199
970788	Trenel No 2	27.9	<0.04	0.3	4.14	0.615	640	22	<6	<1	202	6	5.03		980	268
970789	Trenel (J Peinado)	26.5	<0.04	0.2	3.39	0.772	928	38	17	<1	136	<4	4.73		1710	160
970790	H Massa	27.0	<0.04	0.3	5.56	0.593	863	21	10	<1	164	6	6.94		2440	360
970791	Simonetti Hermanos	28.8	<0.04	<0.2	3.57	0.224	835	53	76	3	41	<4	2.89		1490	181
970792	Estancia Cnia, Trenel (Feninger)	31.5	<0.04	<0.2	1.87	0.374	260	39	55	<1	49	<4	4.3		176	102
970793	A Lovera	28.6	<0.04	0.3	3.11	0.057	3160	16	53	6	10.4	<4	0.594	0.79	1500	201
970794	F Fuchs	28.0	<0.04	0.7	7.33	0.277	1560	23	174	2	67	<4	3.94	4.15	1700	700
970795	Ing Foster, Establ Las Margaritas	35.1	<0.04	<0.2	1.64	0.502	207	47	95	2	76	<4	1.81		155	30
970796	Establ La Costera (Barale)	37.5	<0.04	<0.2	2.06	1.49	244	46	29	2	454	11	2.31		220	91
970797	La Maruja No 2	34.7	<0.04	<0.2	2.12	0.596	770	58	<6	<1	222	5	1.96		790	60
970798	La Marina (La Nelioa)	30.1	<0.04	<0.2	2.82	0.532	441	19	15	<1	468	10	5.51		940	45
970799	Establ Los Dos Pinos (Ferroro)	32.0	<0.04	<0.2	4.37	0.604	700	14	12	<1	280	11	4.33		510	181
970800	Pichi Huinca No 3	30.5	<0.04	<0.2	2.64	0.937	537	28	43	<1	268	6	3.35		1330	88
970801	Eduardo Castex No 9	28.7	<0.04	<0.2	2.49	0.459	587	31	17	2	145	<4	7.65		920	108
970802	Rolando	27.1	<0.04	0.2	3.23	0.537	675	118	99	1	189	7	5.4		338	74
970803	Establ La Loma (Gaiottino)	35.7	<0.04	<0.2	2.33	0.301	302	33	578	7	42	<4	1.08		600	36
970804	Las Torcacitas (Heinz)	34.1	<0.04	<0.2	2.38	1.03	490	43	221	11	310	7	2.35		530	57
970805	Caleufu No 3	28.6	<0.04	<0.2	1.90	0.913	207	28	125	4	133	4	3.44	3.7	72	99
970806	Caleufu No 1	29.5	<0.04	<0.2	1.74	0.600	212	36	34	<1	61	<4	1.89		195	101
970807	Caleufu Establ El Caldén	33.4	<0.04	<0.2	1.59	0.019	2550	41	170	7	<4	<4	0.216		3000	30
970808	Caleufu Establ El Ontoño	27.0	0.08	0.7	13.80	2.93	354	26	11	<1	4930	105	9.28		670	730
970809	Caleufu Establ La Pichincha	26.8	<0.04	0.3	9.66	1.22	1970	30	96	10	214	8	2.61	2.72	3500	150
970810	Galcerán	27.3	<0.04	0.2	3.50	0.616	5910	30	25	2	76	<4	3.18		3300	120
970811	Caleufu (M Bauduco)	22.1	<0.04	<0.2	2.85	0.754	735	116	31	<1	200	6	6.44		970	93
970812	Blanco	30.6	<0.04	<0.2	2.96	0.771	374	45	23	<1	418	12	7.63		310	179
970813	Molino 7 km S of El Cruce	28.1	0.04	0.4	4.58	2.41	597	46	55	2	750	28	15.8		430	400
970814	Estancia Los Olmos	30.7	<0.04	<0.2	1.51	0.621	1070	89	15	<1	177	5	5.41		590	80
970815	José Gariglio	29.9	<0.04	<0.2	2.20	0.578	167	32	43	14	220	5	7.1		146	120
970816	Estancia Las Tres Hermanas	32.5	<0.04	<0.2	1.68	0.271	160	63	73	3	95	<4	3.9		114	85
970817	El Peral	27.2	<0.04	0.6	9.53	1.47	13300	259	136	1	2248	33	13.5	12.9	900	310
970818	Estancia La Leonor	28.5	<0.04	<0.2	4.57	1.41	589	27	38	<1	594	18	8.76		352	74
970819	Campo Arduino	25.6	<0.04	0.2	4.28	1.59	357	56	377	5	424	9	9.24		1700	167
970820	Establ Don Fidel	25.5	<0.04	0.4	10.50	1.20	637	62	20	<1	524	13	7.73		1110	366

APPENDIX 1.3 cont'd...

Sample	Locality	Si mg l^{-1}	Al mg l^{-1}	P mg l^{-1}	B mg l^{-1}	V mg l^{-1}	Sr µg l^{-1}	Ba µg l^{-1}	Fe µg l^{-1}	Mn µg l^{-1}	As$_T$ µg l^{-1}	As(III) µg l^{-1}	F$_{(IN)}$ mg l^{-1}	F$_{(BGS)}$ mg l^{-1}	Br µg l^{-1}	I µg l^{-1}
970821	Ing. Luiggi No 3 (Municipalidad)	28.2	<0.04	<0.2	3.54	1.12	602	33	15	<1	318	8	4.95		460	36
970822	Establ La Querencía (Armitano)	28.5	<0.04	<0.2	1.52	0.466	502	76	<6	<1	99	<4	3.38		343	90
970823	Estancia La Dulce	23.7	<0.04	<0.2	1.00	0.195	780	90	27	2	47	<4	1.34		242	40
970824	Establ La Rebollada	30.4	<0.04	<0.2	1.50	0.051	5230	74	13	39	7.0	<4	0.382	0.88	5100	40
970825	Estancia Jagüel Grande	28.5	<0.04	0.4	8.40	0.812	2910	16	9	1	520	11	2.92		3700	325
970826	Establ El Amanecer (Ferrero)	28.2	<0.04	<0.2	0.46	0.147	567	80	32	<1	24	<4	0.751		140	24
971630	Across lake from Tamagnoni	27.3	<0.04	0.3	6.69	1.36	82.1	53	58	1	950	63	14.6		120	180
971631	E Castex, Talleres Norte	25.9	<0.04	<0.2	0.80	2.01	171	40	<6	<1	210	12	13.1		143	78
971632	E Castex, Talleres Norte	26.6	<0.04	0.4	7.94	0.927	1690	25	21	<1	230	18	7.65		1920	369
971629	Tamagnoni	27.3	0.06	0.4	5.14	4.11	291	55	79	3	1200	136	9.4		280	214
971625	Tamagnoni depth sample	25.5	<0.04	0.3	1.40	0.112	1320	153	8	79	30	<4	1.2		3700	127
971626	Tamagnoni depth sample	21.6	0.09	0.4	3.42	2.32	181	65	81	26	460	45	8.69		600	147
971627	Tamagnoni depth sample	15.6	0.63	0.3	3.56	0.224	330	85	492	153	60	<4	7.41		1200	185
971628	Talleres Norte depth sample	20.3	0.05	<0.2	1.04	0.150	250	85	44	30	<20	<4	5.76		190	45

APPENDIX 1.4 Trace-element data for groundwater (and surface water) samples from La Pampa (ICP-MS analyses, BGS data)

Sample	Locality	Li µg l^{-1}	Be µg l^{-1}	Al µg l^{-1}	Cr µg l^{-1}	Mn µg l^{-1}	Co µg l^{-1}	Ni µg l^{-1}	Cu µg l^{-1}	Zn µg l^{-1}	Ga µg l^{-1}	Ge µg l^{-1}	Rb µg l^{-1}	Y µg l^{-1}	Mo µg l^{-1}
962071	Escuela No 209	5.7	0.012	330	1.08	3.05	0.08	<0.15	22	51	0.072	0.02	1.8	0.119	2.7
962072	Rostagno	55.7	0.078	112	4.26	14.9	0.34	2.04	57	156	0.069	<0.12	12.9	0.090	46
962073	Monte Nievas No 2	26.8	0.039	240	2.60	4.83	0.21	1.43	21	35	0.031	<0.04	2.9	0.111	148
962074	Metileo	17.6	0.046	16	5.03	0.32	0.07	<0.45	1.2	11	<0.025	<0.05	4.7	0.040	120
962075	Dorila	147.4	<0.24	200	9.41	2.49	0.97	18.7	17.5	61	<2.197	<2.44	31.6	22.5	<1.0
962076	Trenel No 4	30.8	<0.04	8.8	5.50	0.77	0.17	9.59	2.0	44	<0.034	<0.07	5.4	0.055	62
962077	Estancia Los Olivos	17.1	0.018	22	2.09	9.88	0.26	0.69	10.6	38	<0.008	0.04	1.5	0.030	38
962078	Garcia (Rosales)	43.8	0.039	13.6	1.66	0.95	0.60	4.28	5.9	32	<0.025	<0.05	5.1	0.136	24
962079	E Castex Iglesias Evangelica	13.2	0.024	254	1.49	2.42	0.11	<0.15	12.8	27	0.044	0.03	2.6	0.108	18
962080	E Castex (Don Arturo)	29.8	0.044	151	1.51	3.95	0.23	1.27	14.7	142	<0.025	<0.05	9.7	0.093	57
962081	E Castex, E de Soria	98.1	<0.12	110	4.43	12.7	1.16	11.1	29	239	<0.102	<0.21	26.3	0.364	83
962082	E Castex, Santa Rita	6.0	0.162	248	1.04	3.41	0.11	<0.30	15.2	27	0.058	0.16	3.4	0.088	151
962083	E Castex, La Invernada	21.7	0.110	160	4.48	3.26	0.11	<0.45	14.1	25	0.030	<0.05	5.7	0.098	564
962084	Monte Nievas (Uterman)	24.5	0.026	27.7	1.81	1.30	0.22	2.18	4.9	40	0.010	0.03	2.8	0.055	28
962085	Arata No 3	13.0	0.025	209	2.48	0.66	0.06	<0.30	2.2	12	0.054	<0.04	4.0	0.035	187
962086	Escuela No 136	53.2	<0.09	55	1.86	9.77	0.32	<1.34	5.5	60	<0.076	<0.16	12.7	0.067	20
962087	Ing Luiggi No 8	16.1	0.064	36	6.84	0.17	0.04	<0.30	1.0	14	<0.017	0.05	3.0	0.016	150
962088	Pichi Huinca No 2	19.7	<0.03	10.5	6.21	51.8	0.10	<0.45	0.9	69	<0.025	<0.05	5.6	0.018	71
962089	La Maruja No 4	17.7	<0.02	8.1	2.22	0.52	0.05	<0.30	0.7	25	<0.017	0.12	6.0	0.015	28
962090	Ing Foster Pozo	20.8	0.018	27	1.82	1.76	0.05	0.33	3.7	113	0.011	<0.02	3.3	0.029	6.5
962091	Caleufu No 5	15.0	0.040	7.3	4.92	0.14	0.07	<0.45	1.3	11	<0.025	<0.05	4.8	0.020	74
962092	La Pichona	30.9	0.047	14.5	3.56	4.30	0.16	0.66	26	273	<0.034	<0.07	6.6	0.030	61
962093	Don Luis	17.4	<0.03	21	2.35	5.95	0.16	0.88	7.7	312	<0.025	0.11	6.3	0.036	19
962094	Nicola	50.0	<0.04	14.9	2.67	0.91	0.29	2.00	2.9	53	<0.034	<0.07	13.0	0.060	11
962095	Conhelo	24.6	<0.01	9.9	5.17	1.74	0.15	1.65	3.9	299	<0.008	0.02	7.2	0.024	3.7
962096	Caleufu (Mazaferro Hnos)	11.1	0.037	14.4	1.80	0.80	0.05	<0.30	3.0	68	<0.017	<0.04	6.4	0.010	127
962097	Pichi Huinca (T Reche)	32.6	0.028	14.7	1.57	11.5	0.27	2.52	4.1	149	<0.017	0.13	6.1	0.044	4.0
962098	La Maruja (Barales)	12.1	0.061	87	1.54	2.23	0.05	<0.30	6.6	86	0.028	<0.04	2.4	0.052	83
962099	Eduardo Castex, Talleres Norte	16.5	0.110	638	8.30	7.83	0.28	<1.04	8.1	156	0.125	<0.12	10.4	0.277	991
962100	Eduardo Castex, Talleres Norte	9.1	0.022	991	1.37	6.50	0.21	0.34	6.0	59	0.179	0.04	2.1	0.246	5.8
962101	Eduardo Castex	10.0	0.044	105	3.43	4.09	0.37	0.71	21	375	<0.025	<0.05	4.8	0.102	47
962102	Eduardo Castex (Jote Herrero)	8.7	0.046	57	1.52	1.53	0.07	0.35	9.0	102	0.014	0.05	2.9	0.045	80
962103	Eduardo Castex (Macagno)	45.8	0.028	16.3	3.54	14.3	0.46	5.14	10.8	241	<0.017	<0.04	3.8	0.070	18

APPENDIX 1.4 cont'd...

Sample	Locality	Li μg l^{-1}	Be μg l^{-1}	Al μg l^{-1}	Cr μg l^{-1}	Mn μg l^{-1}	Co μg l^{-1}	Ni μg l^{-1}	Cu μg l^{-1}	Zn μg l^{-1}	Ga μg l^{-1}	Ge μg l^{-1}	Rb μg l^{-1}	Y μg l^{-1}	Mo μg l^{-1}
962104	Eduardo Castex	23.1	0.031	13.9	1.72	1.38	0.13	1.38	4.7	67	<0.008	0.08	1.8	0.036	56
970685	Eduardo Castex, Santa Rita Pond	4.4	0.092	2111	0.84	72.0	1.24	3.59	6.4	11	0.681	<0.15	7.3	2.078	1.0
970686	Eduardo Castex, Santa Rita	6.6	0.140	98	0.60	2.12	0.13	0.40	7.0	76	<0.035	0.18	3.6	0.125	152
970687	Establ Las Chacras	30.6	0.158	37	4.82	5.06	0.15	1.80	8.7	179	<0.087	0.18	8.3	0.043	122
970688	El Porvenir (Sciaretta)	34.9	0.067	12.0	2.03	1.09	0.13	0.95	28	183	<0.035	0.16	3.3	0.069	83
970689	Estab Maria Paula	85.8	<0.13	34	1.01	3.55	0.76	6.85	30	133	<0.139	<0.21	7.0	0.223	68
970690	Epifanio	13.5	0.019	17.9	0.73	1.21	0.04	0.17	3.2	54	<0.017	0.07	3.3	0.024	29
970691	Conhelo 4	47.0	<0.07	16.2	1.61	7.67	0.12	1.58	2.2	26	<0.070	0.14	11.0	0.034	50
970692	Estab El Tigre	9.7	<0.05	47	1.07	4.12	0.11	0.58	7.1	58	<0.052	0.08	3.5	0.111	110
970693	Estancia La Sabina	10.2	0.024	6.9	0.43	1.42	0.04	0.90	3.1	19	<0.017	0.07	1.8	0.008	10
970694	Estancia La Maruja Puesto 10	44.3	<0.05	24	0.81	2.10	0.16	2.65	5.9	143	<0.052	0.18	8.5	0.042	5.1
970695	La Legua	46.6	<0.05	10.1	2.91	0.25	0.08	1.19	1.7	18	<0.052	0.19	7.9	0.030	128
970696	Estancia Don Carlos	64.8	<0.10	19	2.61	6.13	0.30	2.88	5.4	72	<0.104	0.18	9.4	0.053	93
970697	Eduardo Castex No 1	15.6	<0.07	9.5	5.23	0.16	0.09	0.61	1.8	21	<0.070	<0.11	4.9	0.034	122
970698	Eduardo Castex No 12	79.6	0.056	30	1.23	3.85	0.70	5.78	27	92	<0.035	0.13	7.5	0.190	70
970699	Eduardo Castex, Qte. de Piorno	32.6	<0.03	23	1.42	3.01	0.22	1.75	44	138	<0.035	0.12	3.2	0.062	48
970700	Eduardo Castex (M Tamagnoni)	20.8	0.051	18	2.20	0.90	0.13	<0.27	4.8	43	<0.052	0.12	5.3	<0.007	158
970701	Lake next to Tamagnoni	1.3	<0.02	13.0	<0.07	25.5	0.50	1.12	2.0	4	<0.017	<0.03	4.2	0.063	7.4
970702	Eduardo Castex (Omar Piorno)	30.3	<0.05	7.5	0.98	0.41	0.11	0.89	2.9	34	<0.052	0.09	3.2	0.056	37
970703	Establ Fuentes	34.6	<0.05	10.1	3.13	1.79	0.16	0.89	16.6	37	<0.052	0.14	4.0	0.034	63
970704	Establ Las Toscas	13.6	0.065	27	1.82	0.61	0.07	0.83	6.1	76	<0.035	0.05	4.1	0.057	38
970705	La Gloria	27.0	0.056	11.0	1.28	10.5	0.09	0.82	20	109	<0.035	0.24	6.3	0.028	75
970706	Establ Enrigue Villalba	58.9	0.152	31	1.09	77.6	0.72	4.38	11.7	1438	<0.139	<0.21	15.5	0.118	43
970707	Establ Winschel Hermanos	23.3	<0.03	13.4	1.15	10.6	0.20	1.03	6.2	75	<0.035	0.10	4.6	0.015	64
970708	Establ El Cencerro (Barbero)	12.7	0.067	9.7	2.72	0.86	0.03	0.23	7.0	45	<0.035	0.08	4.4	0.034	407
970776	Arata No 2	15.2	<0.03	7.9	2.61	<0.08	0.02	<0.18	0.5	10	<0.035	<0.05	4.3	0.014	194
970777	Establ Los Tauras	15.6	<0.03	8.1	1.57	1.03	0.07	0.34	17.1	48	<0.035	0.09	4.8	0.024	66
970778	La Ocasión	51.5	<0.08	252	2.63	15.2	0.17	1.22	32	294	<0.087	<0.13	12.1	0.022	142
970779	Establ Las Mercedes	48.7	<0.08	30	2.14	1.83	0.16	1.16	1.7	58	<0.087	<0.13	11.8	0.025	82
970780	Establ La Pebeta (Viglione)	24.8	<0.05	6.4	4.08	2.04	0.13	0.38	14.8	120	<0.052	0.11	3.5	0.034	400
970781	Caleufu No 2	17.7	0.017	2.9	1.96	0.08	0.02	0.18	0.4	3	<0.017	0.11	3.7	<0.002	59
970782	Caleufu (R Destouches)	17.5	<0.02	3.2	0.78	0.41	0.05	0.32	11.2	206	<0.017	0.05	3.8	0.009	51
970783	Caleufu (F Coronel E Hijos)	99.2	<0.25	10.1	2.67	9.58	1.07	13.0	32	111	<0.261	0.45	27.2	0.141	8.3
970784	Caleufu, El Destino	50.0	<0.07	10.7	0.43	25.3	0.51	4.40	12.1	227	<0.070	<0.11	10.2	0.075	25
970785	Caleufu (Groppo)	26.1	0.079	9.4	3.37	6.91	0.24	0.60	9.2	51	<0.055	<0.08	4.5	0.043	122

APPENDIX 1.4 cont'd...

Sample	Locality	Li µg l^{-1}	Be µg l^{-1}	Al µg l^{-1}	Cr µg l^{-1}	Mn µg l^{-1}	Co µg l^{-1}	Ni µg l^{-1}	Cu µg l^{-1}	Zn µg l^{-1}	Ga µg l^{-1}	Ge µg l^{-1}	Rb µg l^{-1}	Y µg l^{-1}	Mo µg l^{-1}
970786	Caleufu, B Assone Lote 6	20.8	<0.05	11.6	3.23	0.15	0.06	<0.27	7.8	31	<0.052	0.14	5.0	0.044	112
970787	Caleufu, molino 2km NECaleufu	19.7	0.072	14.2	0.62	3.92	0.20	0.64	18.9	345	<0.052	0.11	4.7	0.056	28
970788	Trenel No 2	27.4	0.081	15.0	4.68	<0.15	0.04	0.37	0.7	38	<0.070	0.18	6.6	0.020	174
970789	Trenel (J Peinado)	34.0	<0.08	47	5.67	0.51	0.08	1.13	10.9	52	<0.087	0.13	4.1	0.023	30
970790	H Massa	30.6	<0.08	18.8	6.76	0.48	0.20	0.79	8.4	47	<0.087	<0.13	5.3	0.040	217
970791	Simonetti Hermanos	40.3	<0.05	21	3.46	3.16	0.16	1.00	89	825	<0.052	0.14	3.6	0.065	64
970792	Estancia Cnia, Trenel (Feninger)	23.7	0.033	3.8	1.62	0.82	0.04	0.18	40	59	<0.017	0.05	2.0	0.033	53
970793	A Lovera	80.7	<0.10	30	3.90	5.16	0.41	5.03	14.8	71	<0.104	<0.16	8.7	0.055	33
970794	F Fuchs	40.7	<0.08	13.1	5.00	1.97	0.13	1.09	41	247	<0.087	0.24	8.1	0.079	961
970795	Ing Foster, Est Las Margaritas	10.0	<0.02	3.0	2.27	1.84	0.02	0.19	5.0	292	<0.017	0.13	3.5	0.009	7.9
970796	Establ La Costera (Barale)	11.4	<0.03	33	1.03	1.68	0.02	0.33	10.6	42	<0.035	0.26	4.4	0.029	18
970797	La Maruja No 2	27.4	<0.05	9.0	1.63	0.43	0.05	0.37	0.9	11	<0.052	0.20	8.2	0.015	12
970798	La Marina (La Nelioa)	20.8	<0.05	12.2	20.37	1.70	<0.09	0.61	3.5	36	<0.412	<0.46	5.1	<0.18	62
970799	Establ Los Dos Pinos (Ferroro)	34.2	<0.05	10.1	3.16	0.41	<0.09	0.84	2.3	26	<0.412	<0.46	6.3	<0.18	771
970800	Pichi Huinca No 3	30.9	<0.05	14.7	5.97	1.90	<0.09	1.06	2.3	72	<0.412	<0.46	7.9	<0.18	31
970801	Eduardo Castex No 9	12.0	<0.05	18.4	3.10	1.46	<0.09	0.62	0.8	21	<0.412	<0.46	4.5	<0.18	63
970802	Rolando	16.2	<0.05	10.6	1.66	1.21	0.22	0.72	17.9	83	<0.412	<0.46	4.5	<0.18	44
970803	Establ La Loma (Gaiottino)	19.2	<0.03	6.9	2.25	7.19	0.09	0.74	4.5	401	<0.275	<0.31	4.7	<0.12	20
970804	Las Torcacitas (Heinz)	15.4	<0.05	8.1	2.16	10.2	0.11	1.11	8.3	307	<0.412	<0.46	6.0	<0.18	14
970805	Caleufu No 3	12.5	0.032	4.4	2.06	3.88	<0.03	0.27	0.4	13	<0.137	<0.15	3.2	<0.06	65
970806	Caleufu No 1	20.0	0.030	16.5	2.76	0.61	<0.03	0.61	0.8	4	<0.137	<0.15	3.8	<0.06	65
970807	Caleufu Establ El Caldén	79.6	<0.08	7.8	3.02	6.36	0.33	11.3	6.1	37	<0.687	<0.76	14.3	<0.30	5
970808	Caleufu Establ El Ontoño	11.9	0.294	14.8	2.30	<0.21	<0.12	0.52	2.4	7	<0.549	<0.61	5.1	<0.24	733
970809	Caleufu Establ La Pichincha	45.3	<0.11	12.6	2.60	8.47	0.25	2.95	11.9	72	<0.961	<1.07	9.5	<0.42	84
970810	Galcerán	51.7	<0.09	110	3.95	0.51	0.29	3.83	11.6	100	<0.824	<0.92	12.9	<0.36	51
970811	Caleufu (M Bauduco)	36.1	<0.03	19.1	2.67	1.10	0.20	1.58	17.9	47	<0.275	<0.31	5.5	<0.12	40
970812	Blanco	27.2	<0.03	12.9	2.70	0.48	0.06	1.12	5.3	27	<0.275	<0.31	3.0	<0.12	119
970813	Molino 7 km S of El Cruce	20.0	0.083	68	7.29	1.75	0.16	1.74	5.5	90	<0.412	<0.46	5.1	<0.18	145
970814	Estancia Los Olmos	26.5	<0.03	11.6	1.03	0.55	0.28	3.57	6.1	26	<0.275	<0.31	3.1	<0.12	37
970815	José Gariglio	23.0	0.034	5.6	1.72	13.0	0.07	0.53	4.5	29	<0.137	<0.15	2.7	<0.06	65
970816	Estancia Las Tres Hermanas	25.0	0.025	7.4	1.07	2.81	0.09	0.61	12.3	43	<0.137	<0.15	1.9	<0.06	48
970817	El Peral	30.0	0.248	38	4.10	1.38	1.28	3.96	21	33	<0.549	<0.61	8.9	0.51	106
970818	Estancia La Leonor	31.6	0.163	42	7.40	0.83	<0.06	1.02	6.7	52	<0.275	<0.31	5.2	<0.12	219
970819	Campo Arduino	39.2	0.113	20	3.49	4.82	0.44	1.28	73	104	<0.412	<0.46	5.4	<0.18	61
970820	Establ Don Fidel	47.3	0.399	20	3.99	1.07	0.18	0.74	8.3	50	<0.549	<0.61	5.0	<0.24	89

APPENDIX 1.4 cont'd...

Sample	Locality	Li μg l^{-1}	Be μg l^{-1}	Al μg l^{-1}	Cr μg l^{-1}	Mn μg l^{-1}	Co μg l^{-1}	Ni μg l^{-1}	Cu μg l^{-1}	Zn μg l^{-1}	Ga μg l^{-1}	Ge μg l^{-1}	Rb μg l^{-1}	Y μg l^{-1}	Mo μg l^{-1}
970821	Ing. Luiggi No 3 (Mun'palidad)	33.8	0.167	15.6	6.34	0.34	0.06	0.91	9.3	20	<0.275	<0.31	5.7	<0.12	92
970822	Establ La Querencía (Armitano)	36.9	0.046	6.9	1.81	0.22	0.13	1.64	3.1	31	<0.137	<0.15	2.3	<0.06	21
970823	Estancia La Dulce	41.7	0.016	5.7	0.40	1.67	0.28	3.48	8.3	153	<0.137	<0.15	4.7	0.084	14
970824	Establ La Rebollada	90.8	<0.11	26	1.25	43.1	0.84	16.8	5.2	242	<0.961	<1.07	11.1	<0.42	5.5
970825	Estancia Jagüel Grande	71.0	<0.12	30	2.98	0.73	<0.24	3.64	9.1	40	<1.099	<1.22	13.1	<0.47	156
970826	Establ El Amanecer (Ferrero)	26.1	<0.02	5.8	1.01	0.99	0.12	1.73	25	82	<0.137	<0.15	2.1	<0.06	2.9

APPENDIX 1.5 Trace-element data for groundwater (and surface water) samples from La Pampa (ICP-MS analyses, BGS data)

Sample	Locality	Cd µg l^{-1}	Sb µg l^{-1}	Cs µg l^{-1}	Ba µg l^{-1}	Tl µg l^{-1}	Pb µg l^{-1}	As µg l^{-1}	Ag µg l^{-1}	Th µg l^{-1}	U µg l^{-1}
962071	Escuela No 209	0.06	0.12	0.045	19	<0.01	0.75	258	<0.04	0.10	12
962072	Rostagno	<0.19	<0.37	0.191	34	<0.07	0.49	45	<0.28	<0.03	37
962073	Monte Nievas No 2	0.40	0.12	0.046	125	<0.02	0.59	63	<0.08	0.078	26
962074	Metileo	0.27	<0.16	0.047	27	<0.03	1.00	114	<0.12	0.056	27
962075	Dorila	<0.61	<11	<2.3	26	<2.38	<7	48		<1.6	45
962076	Trenel No 4	<0.11	<0.21	0.059	39	<0.04	0.50	44	<0.16	<0.02	21
962077	Estancia Los Olivos	0.09	0.11	0.018	53	<0.01	0.26	64	<0.04	0.039	24
962078	Garcia (Rosales)	<0.08	<0.16	0.036	223	<0.03	0.35	74	<0.12	<0.01	21
962079	E Castex Iglesias Evangelica	0.05	0.14	0.035	50	<0.01	0.20	208	<0.04	0.077	34
962080	E Castex (Don Arturo)	0.11	<0.16	0.065	31	<0.03	0.36	160	<0.12	0.028	28
962081	E Castex, E de Soria	<0.32	<0.64	0.217	33	0.14	1.02	153	<0.48	0.24	30
962082	E Castex, Santa Rita	0.44	0.24	0.054	27	<0.02	0.53	4873	<0.08	0.10	117
962083	E Castex, La Invernada	1.63	<0.16	0.055	66	<0.03	0.21	2223	<0.12	0.037	60
962084	Monte Nievas (Uterman)	0.09	0.07	0.017	158	<0.01	0.22	51	<0.04	0.036	20
962085	Arata No 3	0.57	<0.11	0.032	46	<0.02	1.40	506	<0.08	0.45	42
962086	Escuela No 136	<0.24	<0.48	0.086	24	<0.09	0.40	61	<0.36	<0.039	58
962087	Ing Luiggi No 8	0.50	0.13	0.025	28	<0.02	0.22	379	<0.08	0.059	44
962088	Pichi Huinca No 2	0.15	<0.16	0.041	30	<0.03	0.31	146	<0.12	0.030	9
962089	La Maruja No 4	0.09	<0.11	0.048	46	<0.02	0.15	505	<0.08	<0.01	13
962090	Ing Foster Pozo	<0.03	<0.05	0.018	72	<0.01	0.78	10	<0.04	0.013	6
962091	Caleufu No 5	0.23	<0.16	0.047	31	<0.03	0.16	112	<0.12	<0.01	25
962092	La Pichona	<0.11	<0.21	0.044	33	<0.04	0.48	330	<0.16	0.018	25
962093	Don Luis	<0.08	<0.16	0.055	47	<0.03	0.63	198	<0.12	<0.01	18
962094	Nicola	<0.11	<0.21	0.086	32	<0.04	0.35	70	<0.16	<0.02	20
962095	Conhelo	0.05	0.08	0.036	76	<0.01	0.27	18	<0.04	<0.004	9
962096	Caleufu (Mazaferro Hnos)	0.31	<0.11	0.037	25	<0.02	0.31	519	<0.08	0.009	41
962097	Pichi Huinca (T Reche)	<0.05	<0.11	0.057	39	<0.02	0.41	25	<0.08	0.035	21
962098	La Maruja (Barales)	0.21	0.11	0.046	13	<0.02	0.48	343	<0.08	0.038	86
962099	Eduardo Castex, Talleres Norte	2.70	<0.37	0.144	37	<0.07	1.64	228	<0.28	0.100	58
962100	Eduardo Castex, Talleres Norte	<0.03	0.23	0.102	33	<0.01	0.83	103	<0.04	0.006	16
962101	Eduardo Castex	0.54	0.20	0.045	119	<0.03	4.55	583	<0.12	0.041	35
962102	Eduardo Castex (Jote Herrero)	0.37	0.09	0.019	72	<0.01	1.30	200	<0.04	0.041	26
962103	Eduardo Castex (Macagno)	<0.05	<0.11	0.023	30	<0.02	0.77	23	<0.08	<0.01	19

APPENDIX 1.5 cont'd…

Sample	Locality	Cd $\mu g\ l^{-1}$	Sb $\mu g\ l^{-1}$	Cs $\mu g\ l^{-1}$	Ba $\mu g\ l^{-1}$	Tl $\mu g\ l^{-1}$	Pb $\mu g\ l^{-1}$	As $\mu g\ l^{-1}$	Ag $\mu g\ l^{-1}$	Th $\mu g\ l^{-1}$	U $\mu g\ l^{-1}$
962104	Eduardo Castex	0.10	0.10	0.011	68	<0.01	0.49	38	0.04	0.027	17
970685	Eduardo Castex, Santa Rita Pond	0.09	<0.69	0.187	58	<0.15	1.55	2	<0.06	0.055	0.27
970686	Eduardo Castex, Santa Rita	0.30	<0.88	0.076	27	0.035	0.66	4142	<0.08	0.38	113
970687	Establ Las Chacras	0.25	<2.2	0.076	33	0.097	1.26	294	<0.19	<0.36	138
970688	El Porvenir (Sciaretta)	0.14	<0.9	0.023	70	0.033	0.58	65	<0.08	<0.14	41
970689	Estab Maria Paula	<0.17	<3.5	0.072	80	0.080	1.62	49	<0.30	<0.58	57
970690	Epifanio	0.09	<0.44	0.024	30	0.004	0.10	400	<0.04	<0.07	16
970691	Conhelo 4	0.09	<1.8	0.026	19	0.026	1.23	240	<0.15	<0.29	21
970692	Estab El Tigre	0.18	<1.3	0.021	37	0.025	0.79	5297	<0.11	<0.22	248
970693	Estancia La Sabina	<0.02	<0.44	0.006	6	0.008	0.14	792	<0.04	<0.07	37
970694	Estancia La Maruja Puesto 10	0.13	<1.3	<0.017	36	0.041	0.66	19	<0.11	<0.22	16
970695	La Legua	0.30	<1.3	0.037	11	0.029	0.42	41	<0.11	<0.22	17
970696	Estancia Don Carlos	0.18	<2.6	0.053	14	0.057	0.66	53	<0.23	<0.43	29
970697	Eduardo Castex No 1	0.13	<1.8	<0.023	31	0.021	0.45	124	<0.15	<0.29	28
970698	Eduardo Castex No 12	0.17	<0.9	0.039	82	0.018	0.74	55	<0.08	<0.14	60
970699	Eduardo Castex, Qte. de Piorno	0.08	<0.9	0.012	42	0.019	0.14	36	<0.08	<0.14	27
970700	Eduardo Castex (M Tamagnoni)	0.14	<1.3	0.034	52	0.020	0.39	1315	<0.11	<0.22	118
970701	Lake next to Tamagnoni	0.05	<0.4	<0.006	28	0.015	0.03	8	<0.04	<0.07	0.39
970702	Eduardo Castex (Omar Piorno)	<0.06	<1.3	<0.017	23	0.016	0.45	32	<0.11	<0.22	43
970703	Establ Fuentes	0.23	<1.3	0.017	38	0.030	0.42	93	<0.11	<0.22	42
970704	Establ Las Toscas	0.14	<0.9	0.018	49	0.025	0.90	156	<0.08	0.21	34
970705	La Gloria	0.08	<0.9	0.015	21	0.017	0.52	75	<0.08	<0.14	31
970706	Establ Enrigue Villalba	0.45	<3.5	0.065	41	0.049	3.14	38	<0.30	<0.58	42
970707	Establ Winschel Hermanos	0.24	<0.9	0.027	21	0.012	0.10	71	<0.08	<0.14	26
970708	Establ El Cencerro (Barbero)	0.46	<0.9	0.016	39	<0.008	0.12	656	<0.08	<0.14	54
970776	Arata No 2	0.16	<0.9	<0.011	38	<0.008	0.21	297	<0.08	<0.14	39
970777	Establ Los Tauras	0.07	<0.9	0.031	72	0.013	0.31	174	<0.08	<0.14	31
970778	La Ocasión	0.16	<2.2	<0.029	18	0.019	13.8	172	<0.19	<0.36	51
970779	Establ Las Mercedes	0.16	<2.2	0.049	22	0.036	0.50	134	<0.19	<0.36	32
970780	Establ La Pebeta (Viglione)	0.45	<1.3	<0.017	36	0.031	0.68	408	<0.11	0.27	76
970781	Caleufu No 2	0.03	<0.44	0.021	41	0.009	0.03	65	<0.04	<0.07	22
970782	Caleufu (R Destouches)	0.03	<0.44	0.011	61	0.010	0.21	16	<0.04	<0.07	18
970783	Caleufu (F Coronel E Hijos)	<0.32	<6.6	<0.09	142	0.126	2.02	32	<0.56	<1.08	17
970784	Caleufu, El Destino	0.23	<1.8	0.043	38	0.046	0.53	10	<0.15	<0.29	31
970785	Caleufu (Groppo)	0.19	<1.4	0.027	28	0.038	0.37	231	<0.11	<0.22	48

APPENDIX 1.5 cont'd...

Sample	Locality	Cd µg l^{-1}	Sb µg l^{-1}	Cs µg l^{-1}	Ba µg l^{-1}	Tl µg l^{-1}	Pb µg l^{-1}	As µg l^{-1}	Ag µg l^{-1}	Th µg l^{-1}	U µg l^{-1}
970786	Caleufu, B Assone Lote 6	0.20	<1.3	0.018	68	0.018	0.41	664	<0.11	<0.22	61
970787	Caleufu, molino 2km NECaleufu	0.12	<1.3	0.034	59	0.031	0.79	926	<0.11	<0.22	53
970788	Trenel No 2	0.19	<1.8	0.028	25	0.026	0.42	206	<0.15	<0.29	38
970789	Trenel (J Peinado)	<0.11	<2.2	<0.03	42	0.048	0.64	141	<0.19	<0.36	26
970790	H Massa	0.22	<2.2	<0.03	22	0.064	4.23	165	<0.19	<0.36	58
970791	Simonetti Hermanos	0.50	<1.3	<0.02	55	0.027	0.93	45	<0.11	<0.22	44
970792	Estancia Cnia, Trenel (Feninger)	0.05	<0.44	<0.01	39	0.009	0.35	51	<0.04	<0.07	28
970793	A Lovera	<0.13	<2.6	0.05	17	0.047	0.53	16	<0.23	<0.43	46
970794	F Fuchs	1.17	<2.2	<0.03	25	0.033	0.71	77	<0.19	<0.36	93
970795	Ing Foster, Establ Las Margaritas	<0.02	<0.44	0.01	47	0.012	0.56	73	<0.04	<0.07	12
970796	Establ La Costera (Barale)	<0.04	0.92	<0.01	46	<0.008	0.56	464	<0.08	<0.14	19
970797	La Maruja No 2	<0.06	<1.3	0.04	60	0.013	0.50	229	<0.11	<0.22	20
970798	La Marina (La Nelioa)	0.24	<2.1	<0.4	21	<0.45	<1.3	476	<0.18	0.12	21
970799	Establ Los Dos Pinos (Ferroro)	1.13	<2.1	<0.4	16	<0.45	<1.3	274	<0.18	0.042	67
970800	Pichi Huinca No 3	<0.11	<2.1	<0.4	35	<0.45	<1.3	282	<0.18	0.060	17
970801	Eduardo Castex No 9	<0.11	<2.1	<0.4	34	<0.45	<1.3	144	<0.18	0.047	23
970802	Rolando	<0.11	<2.1	<0.4	133	<0.45	<1.3	205	<0.18	0.025	27
970803	Establ La Loma (Gaiottino)	<0.08	<1.4	<0.3	36	<0.30	<0.89	44	<0.12	0.022	27
970804	Las Torcacitas (Heinz)	<0.11	<2.1	<0.4	46	<0.45	<1.3	325	<0.18	0.014	45
970805	Caleufu No 3	0.10	<0.7	<0.1	31	<0.15	<0.45	129	<0.06	0.010	25
970806	Caleufu No 1	0.10	<0.7	<0.1	41	<0.15	<0.45	62	<0.06	0.008	22
970807	Caleufu Establ El Caldén	<0.19	<3.4	<0.7	47	<0.75	<2.2	11	<0.30	0.004	18
970808	Caleufu Establ El Ontoño	1.54	<2.7	<0.6	28	<0.60	<1.8	4534	<0.24	0.18	126
970809	Caleufu Establ La Pichincha	<0.27	<4.8	<1.0	33	<1.04	<3.1	219	<0.42	0.044	77
970810	Galcerán	0.25	<4.1	<0.9	37	<0.89	<2.7	84	<0.36	0.055	32
970811	Caleufu (M Bauduco)	0.11	<1.4	<0.3	129	<0.30	<0.89	202	<0.12	0.052	32
970812	Blanco	0.15	<1.4	<0.3	50	<0.30	<0.89	377	<0.12	0.052	54
970813	Molino 7 km S of El Cruce	0.34	<2.1	<0.4	52	<0.45	<1.3	798	<0.18	0.027	71
970814	Estancia Los Olmos	<0.08	<1.4	<0.3	99	<0.30	<0.89	188	<0.12	0.009	24
970815	José Gariglio	0.11	<0.7	<0.15	36	<0.15	<0.45	225	<0.06	0.024	52
970816	Estancia Las Tres Hermanas	0.05	<0.7	<0.15	66	<0.15	<0.45	98	<0.06	0.016	35
970817	El Peral	0.29	<2.7	<0.6	297	<0.60	<1.8	2213	<0.24	0.040	91
970818	Estancia La Leonor	0.40	<1.4	<0.3	30	<0.30	<0.89	616	<0.12	0.100	22
970819	Campo Arduino	<0.11	<2.1	<0.4	64	<0.45	<1.34	446	<0.18	0.060	50
970820	Establ Don Fidel	0.27	<2.7	<0.6	70	<0.60	<1.8	527	<0.24	0.032	137

APPENDIX 1.5 cont'd...

Sample	Locality	Cd µg l^{-1}	Sb µg l^{-1}	Cs µg l^{-1}	Ba µg l^{-1}	Tl µg l^{-1}	Pb µg l^{-1}	As µg l^{-1}	Ag µg l^{-1}	Th µg l^{-1}	U µg l^{-1}
970821	Ing. Luiggi No 3 (Mun'palidad)	0.14	<1.4	<0.3	39	<0.30	<0.89	339	<0.12	0.026	38
970822	Establ La Querencía (Armitano)	0.07	<0.7	<0.15	90	<0.15	<0.45	104	<0.06	0.009	30
970823	Estancia La Dulce	0.16	<0.7	<0.15	106	<0.15	<0.45	54	<0.06	0.003	20
970824	Establ La Rebollada	<0.27	<4.8	<1.0	91	<1.0	<3.12	23	<0.42	0.020	10
970825	Estancia Jagüel Grande	0.62	<5.5	<1.2	19	<1.2	<3.56	523	<0.48	0.024	111
970826	Establ El Amanecer (Ferrero)	<0.04	<0.7	<0.15	87	<0.15	<0.45	25	<0.06	0.005	9

APPENDIX 1.6 Rare-earth element data for groundwater (and surface water) samples from La Pampa (ICP-MS analyses)

Sample	Locality	La μg l^{-1}	Ce μg l^{-1}	Pr μg l^{-1}	Nd μg l^{-1}	Eu μg l^{-1}	Sm μg l^{-1}	Gd μg l^{-1}	Tb μg l^{-1}	Dy μg l^{-1}	Ho μg l^{-1}	Er μg l^{-1}	Tm μg l^{-1}	Yb μg l^{-1}	Lu μg l^{-1}
962071	Escuela No 209	0.73	0.23	0.025	0.090	<0.004	0.026	0.030	0.004	0.016	0.003	0.010	<0.002	0.006	<0.002
962072	Rostagno	0.24	0.16	<0.028	<0.066	<0.030	<0.055	<0.067	<0.019	<0.047	<0.012	<0.049	<0.015	<0.039	<0.012
962073	Monte Nievas No 2	0.10	0.25	0.027	0.089	<0.008	<0.016	0.022	<0.005	<0.013	<0.004	<0.014	<0.004	<0.011	<0.003
962074	Metileo	<0.01	<0.011	<0.012	<0.028	<0.013	<0.024	<0.029	<0.008	<0.020	<0.005	<0.021	<0.006	<0.017	<0.005
962075	Dorila	<0.73	<0.985	<0.75	<0.760	<0.931	<1.052	<0.961	<0.862	<0.822	<0.754	<0.909	<0.905	<0.814	<0.818
962076	Trenel No 4	<0.02	<0.015	<0.016	<0.038	<0.017	<0.031	<0.038	<0.011	<0.027	<0.007	<0.028	<0.008	<0.022	<0.007
962077	Estancia Los Olivos	0.074	0.033	0.005	<0.009	<0.004	<0.008	<0.010	<0.003	<0.007	<0.002	<0.007	<0.002	0.008	<0.002
962078	Garcia (Rosales)	0.061	<0.011	<0.012	<0.028	<0.013	<0.024	<0.029	<0.008	<0.020	<0.005	<0.021	<0.006	<0.017	<0.005
962079	E Castex Iglesias Evangelica	0.45	0.22	0.025	0.082	<0.004	<0.008	0.024	0.004	0.013	0.002	<0.007	<0.002	0.011	<0.002
962080	E Castex (Don Arturo)	0.11	0.16	0.012	0.069	<0.013	<0.024	<0.029	0.008	<0.020	<0.005	<0.021	<0.006	<0.017	<0.005
962081	E Castex, E de Soria	0.19	0.12	<0.047	<0.113	<0.051	<0.094	<0.115	<0.033	<0.081	<0.021	<0.084	<0.025	<0.067	<0.021
962082	E Castex, Santa Rita	0.14	0.21	0.022	0.088	<0.008	0.025	0.020	0.006	0.018	<0.004	<0.014	<0.004	0.019	<0.003
962083	E Castex, La Invernada	0.14	0.19	0.031	0.043	<0.013	<0.024	<0.029	<0.008	<0.020	<0.005	<0.021	<0.006	<0.017	<0.005
962084	Monte Nievas (Uterman)	0.16	0.025	<0.004	0.010	<0.004	<0.008	<0.010	<0.003	<0.007	<0.002	<0.007	<0.002	<0.006	<0.002
962085	Arata No 3	0.50	1.65	0.16	0.49	0.030	0.113	0.137	0.015	0.098	0.011	0.051	0.008	0.039	0.004
962086	Escuela No 136	0.42	<0.034	<0.036	<0.085	<0.038	<0.071	<0.086	<0.025	<0.061	<0.016	<0.063	<0.019	<0.050	<0.016
962087	Ing Luiggi No 8	0.22	0.015	<0.008	<0.019	<0.008	0.018	<0.019	<0.005	<0.013	<0.004	<0.014	<0.004	<0.011	<0.003
962088	Pichi Huinca No 2	0.10	<0.011	<0.012	<0.028	<0.013	<0.024	<0.029	<0.008	<0.020	<0.005	<0.021	<0.006	<0.017	<0.005
962089	La Maruja No 4	0.012	<0.008	<0.008	<0.019	<0.008	<0.016	<0.019	<0.005	<0.013	<0.004	<0.014	<0.004	<0.011	<0.003
962090	Ing Foster Pozo	0.023	0.038	<0.004	0.013	<0.004	<0.008	<0.010	<0.003	<0.007	<0.002	<0.007	<0.002	<0.006	<0.002
962091	Caleufu No 5	<0.01	<0.011	<0.012	<0.028	<0.013	<0.024	<0.029	<0.008	<0.020	<0.005	<0.021	<0.006	<0.017	<0.005
962092	La Pichona	0.034	0.024	<0.016	<0.038	<0.017	<0.031	<0.038	<0.011	<0.027	<0.007	<0.028	<0.008	<0.022	<0.007
962093	Don Luis	<0.01	0.013	<0.012	<0.028	<0.013	<0.024	<0.029	<0.008	<0.020	<0.005	<0.021	<0.006	<0.017	<0.005
962094	Nicola	0.032	<0.015	<0.016	<0.038	<0.017	<0.031	<0.038	<0.011	<0.027	<0.007	<0.028	<0.008	<0.022	<0.007
962095	Conhelo	0.014	0.014	<0.004	<0.009	<0.004	<0.008	<0.010	<0.003	<0.007	<0.002	<0.007	<0.002	<0.006	<0.002
962096	Caleufu (Mazaferro Hnos)	0.011	0.019	<0.008	<0.019	<0.008	<0.016	<0.019	<0.005	<0.013	<0.004	<0.014	<0.004	<0.011	<0.003
962097	Pichi Huinca (T Reche)	0.042	0.014	<0.008	<0.019	<0.008	<0.016	<0.019	<0.005	<0.013	<0.004	<0.014	<0.004	<0.011	<0.003
962098	La Maruja (Barales)	0.054	0.11	0.015	<0.019	<0.008	<0.016	<0.019	<0.005	<0.013	<0.004	<0.014	<0.004	<0.011	<0.003
962099	Eduardo Castex, Talleres Norte	0.29	0.64	0.043	0.17	<0.030	0.076	0.090	<0.019	<0.047	<0.012	<0.049	<0.015	<0.039	<0.012
962100	Eduardo Castex, Talleres Norte	6.43	0.019	<0.004	<0.009	<0.004	<0.008	<0.010	<0.003	0.007	<0.002	<0.007	<0.002	<0.006	<0.002
962101	Eduardo Castex	0.064	0.14	<0.012	<0.028	<0.013	<0.024	<0.029	<0.008	<0.020	<0.005	<0.021	<0.006	<0.017	<0.005
962102	Eduardo Castex (Jote Herrero)	0.036	0.068	0.007	0.014	<0.004	<0.008	<0.010	<0.003	<0.007	<0.002	<0.007	<0.002	<0.006	<0.002
962103	Eduardo Castex (Macagno)	0.010	0.021	<0.008	<0.019	<0.008	<0.016	<0.019	<0.005	<0.013	<0.004	<0.014	<0.004	<0.011	<0.003

APPENDIX 1.6 cont'd...

Sample	Locality	La µg l^{-1}	Ce µg l^{-1}	Pr µg l^{-1}	Nd µg l^{-1}	Eu µg l^{-1}	Sm µg l^{-1}	Gd µg l^{-1}	Tb µg l^{-1}	Dy µg l^{-1}	Ho µg l^{-1}	Er µg l^{-1}	Tm µg l^{-1}	Yb µg l^{-1}	Lu µg l^{-1}
962104	Eduardo Castex	0.015	0.009	<0.004	<0.009	<0.004	<0.008	<0.010	<0.003	<0.007	<0.002	<0.007	<0.002	<0.006	<0.002
970685	Eduardo Castex, Santa Rita Pond	2.14	4.96	0.65	2.50	0.111	0.54	0.88	0.09	0.50	0.068	0.26	<0.057	0.21	<0.051
970686	Eduardo Castex, Santa Rita	<0.11	0.24	<0.063	<0.11	<0.065	<0.07	<0.06	<0.08	<0.09	<0.06	<0.08	<0.06	<0.06	<0.08
970687	Establ Las Chacras	<0.27	<0.56	<0.16	<0.27	<0.163	<0.19	<0.15	<0.19	<0.23	<0.16	<0.19	<0.16	<0.15	<0.19
970688	El Porvenir (Sciaretta)	<0.11	<0.22	<0.063	<0.11	<0.065	<0.07	<0.06	<0.08	<0.09	<0.06	<0.08	<0.06	<0.06	<0.08
970689	Estab Maria Paula	<0.43	<0.89	<0.25	<0.42	<0.260	<0.30	<0.24	<0.30	<0.36	<0.25	<0.31	<0.25	<0.24	<0.30
970690	Epifanio	<0.05	<0.11	<0.032	<0.05	<0.033	<0.04	<0.03	<0.04	<0.05	<0.03	<0.04	<0.03	<0.03	<0.04
970691	Conhelo 4	<0.22	<0.45	<0.13	<0.21	<0.130	<0.15	<0.12	<0.15	<0.18	<0.13	<0.16	<0.13	<0.12	<0.15
970692	Estab El Tigre	<0.16	<0.33	<0.095	<0.16	<0.098	<0.11	<0.09	<0.11	<0.14	<0.09	<0.12	<0.09	<0.09	<0.11
970693	Estancia La Sabina	<0.05	<0.11	<0.032	<0.05	<0.033	<0.04	<0.03	<0.04	<0.05	<0.03	<0.04	<0.03	<0.03	<0.04
970694	Estancia La Maruja Puesto 10	<0.16	<0.33	<0.095	<0.16	<0.098	<0.11	<0.09	<0.11	<0.14	<0.09	<0.12	<0.09	<0.09	<0.11
970695	La Legua	<0.16	<0.33	<0.095	<0.16	<0.098	<0.11	<0.09	<0.11	<0.14	<0.09	<0.12	<0.09	<0.09	<0.11
970696	Estancia Don Carlos	<0.33	<0.67	<0.19	<0.32	<0.195	<0.22	<0.18	<0.23	<0.27	<0.19	<0.23	<0.19	<0.18	<0.23
970697	Eduardo Castex No 1	<0.22	<0.45	<0.13	<0.21	<0.130	<0.15	<0.12	<0.15	<0.18	<0.13	<0.16	<0.13	<0.12	<0.15
970698	Eduardo Castex No 12	<0.11	<0.22	<0.063	<0.11	<0.065	<0.07	<0.06	<0.08	<0.09	<0.06	<0.08	<0.06	<0.06	<0.08
970699	Eduardo Castex, Qte. de Piorno	<0.11	<0.22	<0.063	<0.11	<0.065	<0.07	<0.06	<0.08	<0.09	<0.06	<0.08	<0.06	<0.06	<0.08
970700	Eduardo Castex (M Tamagnoni)	<0.16	<0.33	<0.095	<0.16	<0.098	<0.11	<0.09	<0.11	<0.14	<0.09	<0.12	<0.09	<0.09	<0.11
970701	Lake next to Tamagnoni	0.060	<0.11	<0.032	<0.05	<0.033	<0.04	<0.03	<0.04	<0.05	<0.03	<0.04	<0.03	<0.03	<0.04
970702	Eduardo Castex (Omar Piorno)	<0.16	<0.33	<0.095	<0.16	<0.098	<0.11	<0.09	<0.11	<0.14	<0.09	<0.12	<0.09	<0.09	<0.11
970703	Establ Fuentes	<0.16	<0.33	<0.095	<0.16	<0.098	<0.11	<0.09	<0.11	<0.14	<0.09	<0.12	<0.09	<0.09	<0.11
970704	Establ Las Toscas	<0.11	<0.22	<0.063	<0.11	<0.065	<0.07	<0.06	<0.08	<0.09	<0.06	<0.08	<0.06	<0.06	<0.08
970705	La Gloria	<0.11	<0.22	<0.063	<0.11	<0.065	<0.07	<0.06	<0.08	<0.09	<0.06	<0.08	<0.06	<0.06	<0.08
970706	Establ Enrigue Villalba	<0.43	<0.89	<0.25	<0.42	<0.260	<0.30	<0.24	<0.30	<0.36	<0.25	<0.31	<0.25	<0.24	<0.30
970707	Establ Winschel Hermanos	<0.11	<0.22	<0.063	<0.11	<0.065	<0.07	<0.06	<0.08	<0.09	<0.06	<0.08	<0.06	<0.06	<0.08
970708	Establ El Cencerro (Barbero)	<0.11	<0.22	<0.063	<0.11	<0.065	<0.07	<0.06	<0.08	<0.09	<0.06	<0.08	<0.06	<0.06	<0.08
970776	Arata No 2	<0.11	<0.22	<0.063	<0.11	<0.065	<0.07	<0.06	<0.08	<0.09	<0.06	<0.08	<0.06	<0.06	<0.08
970777	Establ Los Tauras	<0.11	<0.22	<0.063	<0.11	<0.065	<0.07	<0.06	<0.08	<0.09	<0.06	<0.08	<0.06	<0.06	<0.08
970778	La Ocasión	<0.27	<0.56	<0.16	<0.27	<0.16	<0.19	<0.15	<0.19	<0.23	<0.16	<0.19	<0.16	<0.15	<0.19
970779	Establ Las Mercedes	<0.27	<0.56	<0.16	<0.27	<0.16	<0.19	<0.15	<0.19	<0.23	<0.16	<0.19	<0.16	<0.15	<0.19
970780	Establ La Pebeta (Viglione Hnos)	<0.16	<0.33	<0.09	<0.16	<0.10	<0.11	<0.09	<0.11	<0.14	<0.09	<0.12	<0.09	<0.09	<0.11
970781	Caleufu No 2	<0.05	<0.11	<0.032	<0.05	<0.03	<0.04	<0.03	<0.04	<0.05	<0.03	<0.04	<0.03	<0.03	<0.04
970782	Caleufu (R Destouches)	<0.05	<0.11	<0.032	<0.05	<0.03	<0.04	<0.03	<0.04	<0.05	<0.03	<0.04	<0.03	<0.03	<0.04
970783	Caleufu (F Coronel E Hijos)	<0.81	<1.7	<0.47	<0.80	<0.49	<0.56	<0.44	<0.57	<0.68	<0.47	<0.58	<0.47	<0.46	<0.57
970784	Caleufu, El Destino	<0.22	<0.45	<0.13	<0.21	<0.13	<0.15	<0.12	<0.15	<0.18	<0.13	<0.16	<0.13	<0.12	<0.15
970785	Caleufu (Groppo)	<0.16	<0.33	<0.095	<0.16	<0.10	<0.11	<0.09	<0.11	<0.14	<0.09	<0.12	<0.09	<0.09	<0.11

APPENDIX 1.6 cont'd...

Sample	Locality	La μg l^{-1}	Ce μg l^{-1}	Pr μg l^{-1}	Nd μg l^{-1}	Eu μg l^{-1}	Sm μg l^{-1}	Gd μg l^{-1}	Tb μg l^{-1}	Dy μg l^{-1}	Ho μg l^{-1}	Er μg l^{-1}	Tm μg l^{-1}	Yb μg l^{-1}	Lu μg l^{-1}
970786	Caleufu, B Assone Lote 6	<0.16	<0.33	<0.095	<0.16	<0.10	<0.11	<0.09	<0.11	<0.14	<0.09	<0.12	<0.09	<0.09	<0.11
970787	Caleufu, molino 2km NE Caleufu	<0.16	<0.33	<0.095	<0.16	<0.10	<0.11	<0.09	<0.11	<0.14	<0.09	<0.12	<0.09	<0.09	<0.11
970788	Trenel No 2	<0.22	<0.45	<0.13	<0.21	<0.13	<0.15	<0.12	<0.15	<0.18	<0.13	<0.16	<0.13	<0.12	<0.15
970789	Trenel (J Peinado)	<0.27	<0.56	<0.16	<0.27	<0.16	<0.19	<0.15	<0.19	<0.23	<0.16	<0.19	<0.16	<0.15	<0.19
970790	H Massa	<0.27	<0.56	<0.16	<0.27	<0.16	<0.19	<0.15	<0.19	<0.23	<0.16	<0.19	<0.16	<0.15	<0.19
970791	Simonetti Hermanos	<0.16	<0.33	<0.09	<0.16	<0.10	<0.11	<0.09	<0.11	<0.14	<0.09	<0.12	<0.09	<0.09	<0.11
970792	Estancia Cnia, Trenel (Feninger)	<0.05	<0.11	<0.032	<0.05	<0.03	<0.04	<0.03	<0.04	<0.05	<0.03	<0.04	<0.03	<0.03	<0.04
970793	A Lovera	<0.33	<0.67	<0.19	<0.32	<0.20	<0.22	<0.18	<0.23	<0.27	<0.19	<0.23	<0.19	<0.18	<0.23
970794	F Fuchs	<0.27	<0.56	<0.16	<0.27	<0.16	<0.19	<0.15	<0.19	<0.23	<0.16	<0.19	<0.16	<0.15	<0.19
970795	Ing Foster, Establ Las Margaritas	<0.05	<0.11	<0.032	<0.05	<0.03	<0.04	<0.03	<0.04	<0.05	<0.03	<0.04	<0.03	<0.03	<0.04
970796	Establ La Costera (Barale)	<0.11	<0.22	<0.06	<0.11	<0.07	<0.07	<0.06	<0.08	<0.09	<0.06	<0.08	<0.06	<0.06	<0.08
970797	La Maruja No 2	<0.16	<0.33	<0.095	<0.16	<0.10	<0.11	<0.09	<0.11	<0.14	<0.09	<0.12	<0.09	<0.09	<0.11
970798	La Marina (La Nelioa)	<0.14	<0.18	<0.14	<0.14	<0.17	<0.20	<0.18	<0.16	<0.15	<0.14	<0.17	<0.17	<0.15	<0.15
970799	Establ Los Dos Pinos (Ferroro)	<0.14	<0.18	<0.14	<0.14	<0.17	<0.20	<0.18	<0.16	<0.15	<0.14	<0.17	<0.17	<0.15	<0.15
970800	Pichi Huinca No 3	<0.14	<0.18	<0.14	<0.14	<0.17	<0.20	<0.18	<0.16	<0.15	<0.14	<0.17	<0.17	<0.15	<0.15
970801	Eduardo Castex No 9	<0.14	<0.18	<0.14	<0.14	<0.17	<0.20	<0.18	<0.16	<0.15	<0.14	<0.17	<0.17	<0.15	<0.15
970802	Rolando	<0.14	<0.18	<0.14	<0.14	<0.17	<0.20	<0.18	<0.16	<0.15	<0.14	<0.17	<0.17	<0.15	<0.15
970803	Establ La Loma (Gaiottino)	<0.09	<0.12	<0.094	<0.09	<0.12	<0.13	<0.12	<0.11	<0.10	<0.09	<0.11	<0.11	<0.10	<0.10
970804	Las Torcacitas (Heinz)	<0.14	<0.18	<0.14	<0.14	<0.17	<0.20	<0.18	<0.16	<0.15	<0.14	<0.17	<0.17	<0.15	<0.15
970805	Caleufu No 3	<0.05	<0.062	<0.05	<0.05	<0.06	<0.07	<0.06	<0.05	<0.05	<0.05	<0.06	<0.06	<0.05	<0.05
970806	Caleufu No 1	<0.05	<0.062	<0.05	<0.05	<0.06	<0.07	<0.06	<0.05	<0.05	<0.05	<0.06	<0.06	<0.05	<0.05
970807	Caleufu Establ El Caldén	<0.23	<0.31	<0.23	<0.24	<0.29	<0.33	<0.30	<0.27	<0.26	<0.24	<0.28	<0.28	<0.25	<0.26
970808	Caleufu Establ El Ontoño	<0.18	<0.25	<0.19	<0.19	<0.23	<0.26	<0.24	<0.22	<0.21	<0.19	<0.23	<0.23	<0.20	<0.20
970809	Caleufu Establ La Pichincha	<0.32	<0.43	<0.33	<0.33	<0.41	<0.46	<0.42	<0.38	<0.36	<0.33	<0.40	<0.40	<0.36	<0.36
970810	Galcerán	<0.27	<0.37	<0.28	<0.28	<0.35	<0.39	<0.36	<0.32	<0.31	<0.28	<0.34	<0.34	<0.31	<0.31
970811	Caleufu (M Bauduco)	<0.09	<0.12	<0.094	<0.09	<0.12	<0.13	<0.12	<0.11	<0.10	<0.09	<0.11	<0.11	<0.10	<0.10
970812	Blanco	<0.09	<0.12	<0.094	<0.09	<0.12	<0.13	<0.12	<0.11	<0.10	<0.09	<0.11	<0.11	<0.10	<0.10
970813	Molino 7 km S of El Cruce	<0.14	<0.18	<0.14	<0.14	<0.17	<0.20	<0.18	<0.16	<0.15	<0.14	<0.17	<0.17	<0.15	<0.15
970814	Estancia Los Olmos	<0.09	<0.12	<0.094	<0.09	<0.12	<0.13	<0.12	<0.11	<0.10	<0.09	<0.11	<0.11	<0.10	<0.10
970815	José Gariglio	<0.05	<0.062	<0.047	<0.05	<0.06	<0.07	<0.06	<0.05	<0.05	<0.05	<0.06	<0.06	<0.05	<0.05
970816	Estancia Las Tres Hermanas	<0.05	<0.062	<0.047	<0.05	<0.06	<0.07	<0.06	<0.05	<0.05	<0.05	<0.06	<0.06	<0.05	<0.05
970817	El Peral	<0.18	<0.25	<0.19	<0.19	<0.23	<0.26	<0.24	<0.22	<0.21	<0.19	<0.23	<0.23	<0.20	<0.20
970818	Estancia La Leonor	<0.09	<0.12	<0.094	<0.09	<0.12	<0.13	<0.12	<0.11	<0.10	<0.09	<0.11	<0.11	<0.10	<0.10
970819	Campo Arduino	<0.14	<0.18	<0.14	<0.14	<0.17	<0.20	<0.18	<0.16	<0.15	<0.14	<0.17	<0.17	<0.15	<0.15
970820	Establ Don Fidel	<0.18	<0.25	<0.19	<0.19	<0.23	<0.26	<0.24	<0.22	<0.21	<0.19	<0.23	<0.23	<0.20	<0.20

APPENDIX 1.6 cont'd...

Sample	Locality	La µg l^{-1}	Ce µg l^{-1}	Pr µg l^{-1}	Nd µg l^{-1}	Eu µg l^{-1}	Sm µg l^{-1}	Gd µg l^{-1}	Tb µg l^{-1}	Dy µg l^{-1}	Ho µg l^{-1}	Er µg l^{-1}	Tm µg l^{-1}	Yb µg l^{-1}	Lu µg l^{-1}
970821	Ing. Luiggi No 3 (Municipalidad)	<0.09	<0.12	<0.09	<0.09	<0.12	<0.13	<0.12	<0.11	<0.10	<0.09	<0.11	<0.11	<0.10	<0.10
970822	Establ La Querencía (Armitano)	<0.05	<0.06	<0.05	<0.05	<0.06	<0.07	<0.06	<0.05	<0.05	<0.05	<0.06	<0.06	<0.051	<0.05
970823	Estancia La Dulce	<0.05	<0.06	<0.05	<0.05	<0.06	<0.07	<0.06	<0.05	<0.05	<0.05	<0.06	<0.06	<0.051	<0.05
970824	Establ La Rebollada	<0.32	<0.43	<0.33	<0.33	<0.41	<0.46	<0.42	<0.38	<0.36	<0.33	<0.40	<0.40	<0.36	<0.36
970825	Estancia Jagüel Grande	<0.36	<0.49	<0.37	<0.38	<0.47	<0.53	<0.48	<0.43	<0.41	<0.38	<0.45	<0.45	<0.41	<0.41
970826	Establ El Amanecer (Ferrero)	<0.05	<0.06	<0.05	<0.05	<0.06	<0.07	<0.06	<0.05	<0.05	<0.05	<0.06	<0.06	<0.05	<0.05

APPENDIX 1.7 Isotopic data for groundwater (and surface water) samples from La Pampa and calculated log saturation indices of selected minerals

Sample	Locality	$\delta^{18}O$ ‰	$\delta^{2}H$ ‰	$\delta^{13}C$ ‰	$\delta^{34}S$ ‰	^{3}H TU	^{14}C pmc	calcite	dolomite	barite	gypsum	fluorite	quartz	celestite	gibbsite
962071	Escuela No 209	-5.8	-32	-7.1				-0.03	0.19	-1.47	-4.0	-0.28	0.75	-4.0	1.6
962072	Rostagno	-5.9	-30		+8.1			0.12	0.65	0.06	-1.3	-1.19	0.71	-1.1	1.7
962073	Monte Nievas No 2	-5.0	-24		+7.5			0.12	0.31	0.66	-1.7	-0.36	0.76	-1.8	2.1
962074	Metileo	-4.8	-28		+8.7			0.08	0.57	0.10	-1.8	-0.35	0.74	-1.5	0.6
962075	Dorila	-4.4	-27		+8.3			0.26	0.95	0.27	-0.4	-0.60	0.69	-0.1	2.2
962076	Trenel No 4	-4.9	-23		+8.6			0.14	0.63	0.33	-1.3	-0.45	0.74	-1.2	0.4
962077	Estancia Los Olivos	-4.9	-27	-10.4				0.05	0.17	-0.00	-2.5	-0.54	0.76	-2.5	0.7
962078	Garcia (Rosales)	-5.0	-28					0.26	0.60	0.68	-1.6	0.03	0.78	-1.7	1.0
962079	E Castex Iglesias Evangelica	-4.8	-24	-9.0				0.12	0.45	-0.07	-2.8	-0.05	0.75	-2.6	1.7
962080	E Castex (Don Arturo)	-4.9	-26		+8.2			0.49	1.39	-0.00	-1.6	-0.34	0.73	-1.5	1.5
962081	E Castex, E de Soria	-4.7	-24					0.44	1.30	0.19	-0.7	-0.09	0.79	-0.5	1.9
962082	E Castex, Santa Rita	-5.5	-29	-12.1				0.08	0.62	-0.78	-4.0	-0.02	0.71	-3.1	1.2
962083	E Castex, La Invernada	-4.8	-27		+8.2			0.13	0.83	0.44	-2.6	-0.64	0.72	-2.1	1.3
962084	Monte Nievas (Uterman)							0.28	0.46	0.38	-2.0	-0.40	0.77	-2.2	1.2
962085	Arata No 3							-0.01	0.44	0.20	-2.3	-0.50	0.75	-2.2	1.7
962086	Escuela No 136							0.05	0.54	-0.02	-1.3	-0.89	0.72	-1.1	1.4
962087	Ing Luiggi No 8	-4.9	-29	-4.4				0.10	0.86	-0.08	-2.8	-0.71	0.72	-2.2	0.6
962088	Pichi Huinca No 2	-4.9	-31					0.09	0.58	0.04	-1.9	-0.61	0.66	-1.8	0.2
962089	La Maruja No 4							-0.01	0.41	0.01	-2.1	-0.91	0.74	-2.0	0.1
962090	Ing Foster Pozo							-0.12	0.00	0.08	-2.5	-1.36	0.50	-2.5	0.4
962091	Caleufu No 5							0.09	0.57	0.19	-2.0	-1.09	0.72	-1.5	0.1
962092	La Pichona							0.14	0.77	0.25	-1.5	-0.12	0.72	-1.2	0.6
962093	Don Luis							0.12	0.77	0.04	-1.9	-0.66	0.65	-1.8	0.6
962094	Nicola							0.13	0.79	-0.04	-1.6	-0.82	0.74	-1.3	0.7
962095	Conhelo							0.09	0.43	0.01	-2.0	-1.17	0.74	-2.1	0.4
962096	Caleufu (Mazaferro Hnos)							0.11	0.59	-0.64	-3.3	-1.69	0.72	-3.0	0.2
962097	Pichi Huinca (T Reche)							0.08	0.49	0.19	-1.3	-1.28	0.74	-1.3	0.8
962098	La Maruja (Barales)							0.01	0.50	-1.14	-3.9	-1.08	0.72	-3.6	0.9
962099	Eduardo Castex, Talleres Norte							0.08	0.78	0.38	-1.5	-0.15	0.73	-0.9	2.2
962100	Eduardo Castex, Talleres Norte							0.12	0.26	-0.51	-3.3	0.06	0.75	-3.3	2.1
962101	Eduardo Castex							0.56	1.52	0.43	-2.5	0.16	0.73	-2.0	1.2
962102	Eduardo Castex (Jote Herrero)							0.09	0.57	0.21	-2.5	0.08	0.78	-2.3	1.2

APPENDIX 1.7 cont'd...

Sample	Locality	$\delta^{18}O$ ‰	δ^2H ‰	$\delta^{13}C$ ‰	$\delta^{34}S$ ‰	^3H TU	^{14}C pmc	calcite	dolomite	barite	gypsum	fluorite	quartz	celestite	gibbsite
962103	Eduardo Castex (Macagno)							0.07	0.17	0.13	-1.1	-0.58	0.81	-1.3	1.2
962104	Eduardo Castex							0.09	0.17	0.13	-2.1	-0.40	0.82	-2.2	1.0
970685	Eduardo Castex, Santa Rita Pond	-7.1	-41					-1.16	-2.84	-1.33	-3.6	nd	0.19	-4.2	3.4
970686	Eduardo Castex, Santa Rita	-5.3	-26	-9.1	+8.5	8.7	63.1	0.33	1.08	-0.68	-3.7	0.04	0.55	-2.9	0.4
970687	Establ Las Chacras	-4.7	-31					0.17	0.98	0.30	-2.0	-0.73	0.73	-1.3	0.9
970688	El Porvenir (Sciaretta)	-4.5	-27					0.30	0.66	0.52	-1.6	-0.32	0.78	-1.6	0.8
970689	Estab Maria Paula	-4.7	-25					0.62	1.31	0.52	-0.8	0.04	0.76	-1.0	1.5
970690	Epifanio	-6.1	-35	-9.8		5.5	47.4	-0.00	0.35	-0.52	-3.1	-0.59	0.73	-2.9	0.5
970691	Conhelo 4	-4.7	-32	-9.1	+7.9	1.9	26.4	0.13	0.66	-0.13	-1.5	-1.04	0.72	-1.3	0.6
970692	Estab El Tigre	-4.7	-27		+7.5	2.5	53.0	0.06	0.60	-0.01	-2.8	-0.71	0.72	-2.4	0.8
970693	Estancia La Sabina	-4.7	-30					-0.17	-0.12	-1.35	-3.7	-0.51	0.79	-3.5	-0.0
970694	Estancia La Maruja Puesto 10	-5.0	-31	-12.2		0.0		0.27	0.83	0.24	-1.1	-1.57	0.78	-1.1	1.1
970695	La Legua	-4.4	-28	-7.5				0.67	1.69	-0.15	-1.4	-1.28	0.64	-1.2	-0.2
970696	Estancia Don Carlos	-4.6	-24		+7.5			0.11	0.59	0.03	-0.8	-1.02	0.74	-0.6	1.0
970697	Eduardo Castex No 1	-4.7	-25	-8.9		0.0	58.6	0.05	0.44	0.23	-1.6	-0.04	0.72	-1.5	0.5
970698	Eduardo Castex No 12	-4.7	-26					0.06	0.28	0.69	-1.6	-0.34	0.75	-1.6	1.1
970699	Eduardo Castex, Qte. de Piorno							0.28	0.40	0.30	-1.3	-0.18	0.77	-1.6	1.3
970700	Eduardo Castex (M Tamagnoni)	-5.3	-27	-7.3	+8.6			0.12	0.70	0.33	-2.5	-0.32	0.73	-2.1	0.5
970701	Lake next to Tamagnoni	-2.3	-16					-0.11	-0.56	-1.42	-3.6	-3.00	0.48	-4.0	0.6
970702	Eduardo Castex (Omar Piorno)	-4.8	-24					0.20	0.58	0.18	-1.2	-0.84	0.79	-1.2	0.8
970703	Establ Fuentes	-4.7	-27	-6.9				0.25	0.72	0.36	-1.5	-0.20	0.80	-1.5	0.8
970704	Establ Las Toscas	-4.7	-32					0.12	0.58	0.22	-2.3	-0.31	0.78	-2.2	0.8
970705	La Gloria							0.31	1.05	-0.06	-1.9	-0.80	0.79	-1.7	0.5
970706	Establ Enrigue Villalba	-3.9	-23	-12.8	+7.7			0.31	1.06	0.27	-0.9	-1.05	0.76	-0.8	1.2
970707	Establ Winschel Hermanos							0.40	1.14	-0.01	-1.8	-0.49	0.78	-1.8	0.5
970708	Establ El Cencerro (Barbero)	-5.1	-25					0.16	0.86	0.16	-2.4	-0.43	0.73	-2.0	0.3
970776	Arata No 2	-4.8	-24	-6.2	+7.9	0.1	60.0	-0.07	0.37	0.21	-2.4	-0.48	0.73	-2.2	0.3
970777	Establ Los Tauras							0.20	0.90	0.44	-2.2	-0.37	0.75	-2.0	0.2
970778	La Ocasión	-5.3	-30					0.10	0.79	-0.11	-1.5	-1.16	0.74	-1.3	2.0
970779	Establ Las Mercedes	-4.1	-25	-9.4				0.04	0.62	0.03	-1.5	-1.15	0.74	-1.3	1.2
970780	Establ La Pebeta (Viglione)	-4.7	-24	-5.3				0.30	0.80	0.27	-2.0	0.08	0.75	-1.9	0.2
970781	Caleufu No 2	-4.9	-28	-5.9	+7.7	0.6	70.6	0.01	0.39	0.20	-2.3	-1.18	0.72	-2.1	-0.3
970782	Caleufu (R Destouches)							0.09	0.46	0.18	-2.5	-1.54	0.76	-2.2	-0.1
970783	Caleufu (F Coronel E Hijos)	-4.5	-26	-10.2				0.11	0.46	0.50	-0.7	-3.79	0.79	-0.7	1.2

APPENDIX 1.7 cont'd...

Sample	Locality	$\delta^{18}O$ ‰	$\delta^{2}H$ ‰	$\delta^{13}C$ ‰	$\delta^{34}S$ ‰	^{3}H TU	^{14}C pmc	calcite	dolomite	barite	gypsum	fluorite	quartz	celestite	gibbsite
970784	Caleufu, El Destino	-4.5	-23					0.47	1.19	0.31	-0.9	-1.31	0.71	-0.8	0.7
970785	Caleufu (Groppo)							0.40	1.12	0.37	-1.6	-0.08	0.71	-1.2	0.4
970786	Caleufu, B Assone Lote 6			-4.6				0.42	0.94	0.43	-2.2	-0.01	0.71	-1.9	0.4
970787	Caleufu, molino 2km NECaleufu							0.07	0.31	0.19	-2.8	-0.27	0.72	-2.5	0.6
970788	Trenel No 2	-5.1	-27	-6.9	+7.8	1.8	58.6	0.04	0.61	0.16	-1.8	-0.47	0.74	-1.5	0.7
970789	Trenel (J Peinado)							0.27	0.74	0.45	-1.4	-0.31	0.73	-1.3	1.2
970790	H Massa							0.15	0.81	0.21	-1.8	-0.34	0.74	-1.3	0.7
970791	Simonetti Hermanos							0.46	0.98	0.40	-1.6	-0.57	0.76	-1.6	0.8
970792	Estancia Cnia, Trenel (Feninger)	-4.7	-23					-0.22	-0.14	-0.02	-2.7	-0.81	0.79	-2.4	0.1
970793	A Lovera	-4.6	-28	-8.8				0.30	0.60	0.20	-0.3	-1.15	0.76	-0.6	1.4
970794	F Fuchs							0.31	1.03	0.29	-1.2	-0.34	0.76	-1.0	0.9
970795	Ing Foster, Est Las Margaritas	-4.8	-36	-12.3		0.3	53.3	0.06	0.45	-0.06	-2.6	-1.53	0.71	-2.5	-0.5
970796	Establ La Costera (Barale)	-4.9	-27	-9.5				0.04	0.48	0.08	-2.4	-1.37	0.71	-2.2	0.5
970797	La Maruja No 2	-6.4	-35	-9.1	+7.1	5.8	38.4	0.02	0.49	0.25	-1.8	-1.07	0.72	-1.7	0.4
970798	La Marina (La Nelioa)							0.28	0.81	0.05	-1.8	-0.41	0.71	-1.7	0.2
970799	Establ Los Dos Pinos (Ferroro)	-4.6	-25					0.10	0.68	-0.09	-1.7	-0.57	0.74	-1.4	0.5
970800	Pichi Huinca No 3	-4.9	-27	-8.9	+6.8			0.26	0.93	0.08	-1.8	-0.73	0.70	-1.7	0.3
970801	Eduardo Castex No 9	-4.9	-27					0.13	0.60	0.26	-1.7	0.01	0.73	-1.6	0.6
970802	Rolando			-8.6				0.30	1.04	0.38	-2.8	-0.65	0.73	-2.1	0.3
970803	Establ La Loma (Gaiottino)							0.06	0.56	-0.13	-2.3	-1.81	0.75	-2.3	0.1
970804	Las Torcacitas (Heinz)							0.14	0.79	-0.06	-2.4	-1.16	0.74	-2.1	0.2
970805	Caleufu No 3	-4.8	-28					-0.03	0.30	-0.04	-2.6	-1.04	0.72	-2.3	-0.2
970806	Caleufu No 1			-4.9				0.01	0.30	0.19	-2.4	-1.55	0.73	-2.2	0.4
970807	Caleufu Establ El Caldén	-4.6	-29					0.17	0.59	0.21	-1.0	-2.36	0.78	-1.1	0.8
970808	Caleufu Establ El Ontoño	-5.2	-27	-5.8				0.16	1.04	0.12	-2.6	-0.58	0.71	-1.9	0.2
970809	Caleufu Establ La Pichincha							0.36	1.25	0.15	-1.8	-0.93	0.73	-1.2	0.5
970810	Galcerán							0.42	1.24	0.32	-1.0	-0.32	0.74	-0.5	1.7
970811	Caleufu (M Bauduco)							0.31	0.56	0.70	-1.8	0.19	0.68	-1.7	1.0
970812	Blanco	-4.9	-32					0.19	0.47	0.27	-2.0	0.14	0.78	-2.0	0.7
970813	Molino 7 km S of El Cruce			-4.0				0.74	1.72	0.17	-2.1	0.75	0.76	-1.9	1.1
970814	Estancia Los Olmos	-4.4	-28	-7.4				0.63	1.35	0.21	-1.8	0.36	0.78	-1.9	0.8
970815	José Gariglio							0.21	0.48	-0.17	-2.7	-0.25	0.77	-2.7	0.1
970816	Estancia Las Tres Hermanas							0.17	0.41	0.13	-2.7	-0.72	0.82	-2.7	0.2
970817	El Peral	-4.3	-23	-5.9				0.80	1.81	0.89	-1.9	0.62	0.73	-0.6	0.9

APPENDIX 1.7 cont'd...

Sample	Locality	$\delta^{18}O$ ‰	$\delta^{2}H$ ‰	$\delta^{13}C$ ‰	$\delta^{34}S$ ‰	^{3}H TU	^{14}C pmc	calcite	dolomite	barite	gypsum	fluorite	quartz	celestite	gibbsite
970818	Estancia La Leonor							0.04	0.43	0.13	-2.2	-0.10	0.74	-1.7	1.0
970819	Campo Arduino	-4.8	-24	-8.4				0.28	1.03	0.28	-2.6	-0.42	0.65	-2.1	0.2
970820	Establ Don Fidel	-5.3	-31	-6.9				0.20	0.95	0.47	-2.3	-0.46	0.71	-1.7	0.6
970821	Ing. Luiggi No 3 (Mun'palidad)							0.14	0.73	0.18	-2.2	-0.57	0.73	-1.7	0.6
970822	Establ La Querencía (Armitano)							0.31	0.68	0.29	-2.0	-0.34	0.76	-2.1	0.6
970823	Estancia La Dulce	-3.8	-25					0.31	0.69	0.21	-1.9	-0.87	0.69	-2.1	0.7
970824	Establ La Rebollada	-4.5	-27		+6.3			0.20	0.68	0.26	-1.1	-1.01	0.79	-1.1	1.4
970825	Estancia Jagüel Grande				+8.3			0.10	0.72	0.09	-1.1	-0.60	0.77	-0.8	1.3
970826	Establ El Amanecer (Ferrero)							0.23	0.51	-0.04	-2.4	-1.55	0.75	-2.4	0.5

Mineral saturation indices calculated using equilibrium constants from the PHREEQC database

APPENDIX 2.1 Description of core material from Talleres Norte and Tamagnoni cored boreholes, La Pampa

Sample	Top depth m	Bottom depth m	Colour	Lithology	Secondary minerals	Hydrogeology
Talleres Norte						
TN1	0.00	0.50	Blackish brown	Silty sand		Unsaturated
TN2	0.50	1.00	Blackish brown	Silty sand		Unsaturated
TN3	1.00	1.45	Blackish brown	Slightly clayey silty sand	Calcrete at 1.45m	Unsaturated
TN4	1.45	4.20	Brown	Silty sand		Unsaturated
TN5	4.33	4.45	Brown	Fine sand		Aquifer
TN6	4.45	4.90	Grey-brown	Interlayered calcrete, clayey silty sand bands		
TN7	4.90	5.40	Grey-brown	Variable: med-coarse sand, conglomeratic sand	Much calcrete, sometimes in bands	Aquifer
TN8	5.40	5.90	Grey-brown	Slightly clayey silty fine sand	Many sub-angular pieces of calcrete, <10 mm	Aquifer
TN9	5.90	6.40	Brown	Medium sand	Many angular to sub-angular pieces of calcrete, <15 mm	Aquifer
TN10	6.40	6.90	Brown	Fine sand	Very few pieces of calcrete disappearing with depth	Aquifer
TN11	6.90	7.33	Brown	Med-coarse sand becoming finer towards the base	Sub-angular pieces of calcrete, <20 mm	Aquifer
TN12	7.63	7.79	Grey-brown	Silty fine sand, layer of white sand at ca. 7.71 m		Aquifer
	7.79	7.89	Grey-white	Solid calcrete (tosca)		
TN13	7.90	8.35	Grey-brown sand	Alternating bands of calcrete and fine sand		
TN14	8.40	8.78	Dark grey-brown	Fine sand	Sub-angular calcrete pieces, dark brown nodules at base, <20 mm	Aquifer
TN15	8.90	9.38	Dark grey-brown	Fine sand		Aquifer
TN16	9.40	9.90	Dark grey-brown	Fine sand		Aquifer
TN17	9.90	10.40	Dark grey-brown	Fine sand	Few small rounded pieces of calcrete, <1 mm	Aquifer
TN18	10.40	10.89	Dark grey-brown	Fine sand	Very few crumbly calcretions, <2 mm	Aquifer
TN19	10.90	11.25	Dark grey-brown	Fine sand	Calcretes increasing in number and size with depth to < 8 mm	Aquifer
TN20	11.40	11.75	Dark grey-brown	Fine sand	Large sub-angular to angular pieces of calcrete, <60 mm	Aquifer
TN21	12.20	12.40	Dark grey-brown	Fine sand		Aquifer
TN22	13.20	13.30	Dark grey-brown	Coarse sand, coarser with depth	Increasing no of large angular/sub-angular calcretes with depth, <12 mm	Aquifer
TN23	13.69	13.90	Dark grey-brown	Coarse sand/gravel	Many angular calcretes, <15 mm, more compact at base	Aquifer
TN24	14.00	14.40	Brown	Gravel/coarse sand	Some large calcretes, ca. 20 mm	Aquifer
TN25	14.60	14.72	Dark grey-brown	Gravel/coarse sand	Some large calcretes, ca. 20 mm	Aquifer
TN26	15.06	15.36	Brown	Slightly clayey silty fine sand	Few sub-rounded calcretes, <10 mm	Aquifer

APPENDIX 2.1 cont'd...

Sample	Top depth m	Bottom depth m	Colour	Lithology	Secondary minerals	Hydrogeology
TN27	15.50	16.00	Brown	Clayey sandy silt	Many calcrete pieces in the bottom 17 cm, <10 mm	Aquifer
TN28	16.00	16.42	Brown, grey-brown	Slightly clayey silt-sand, variable fine to crse	Poorly sorted calcretes, <30 mm	Aquifer
TN29	16.50	16.71	Brown	Slightly clayey silty fine sand	Some calcrete pieces, <3 mm	Aquifer
TN30	16.50	16.84	Dark brown	Calcrete with slightly clayey silty fine sand		Aquifer
TN31	17.00	17.31	Dark brown	Slightly clayey silty medium sand	Many sub-angular calcrete pieces, <8 mm	Aquifer
TN32	17.31	17.50	Dark brown	Slightly sandy clayey silt	Some small calcrete pieces, <2 mm	Aquifer
TN33	17.50	17.83	Dark brown	Blocks/small fragments calcrete, slightly clayey silty med-crse sand, clayey sandy silt		Aquifer
TN34	18.00	18.38	Brown	Clayey sandy silt, wet silty sand at 18.32 m	Few calcretes, <4 mm	Aquifer
TN35	18.50	18.89	Dark brown	Slightly clayey silty fine sand	Calcrete pieces more larger with depth, <10 mm	Aquifer
TN36	19.00	19.33	Dark brown	Silty fine sand	Some calcrete pieces, smaller with depth, <10 mm	Aquifer
TN37	19.50	19.83	Dark brown	Clayey silty fine sand	Many angular pieces calcrete, <12 mm, plus few large sub-angular calcretes, 30 mm	Aquifer
TN38	20.00	20.50	Dark grey-brown	Slightly clayey silty fine sand	Some calcrete, <8 mm, becoming more silty and with fewer calcretes with depth	Aquifer
TN39	20.50	20.83	Dark grey-brown	Slightly clayey silty fine sand	Poorly sorted pieces of calcrete, 1 – 50 mm, increasing in number with depth	Aquifer
TN40	21.00	21.33	Brown	Clayey silty fine sand, gravel at base	Band with high calcrete content and medium sand	Aquifer
TN41	21.50	21.66	Dark grey-brown	Slightly clayey silty fine sand	Many small pieces of calcrete, <3 mm, + few larger angular calcretes ca. 10 mm	Aquifer
TN42	21.66	21.88	Dark grey-brown	Slightly clayey sandy silt	Few rounded pieces of calcrete, <3 mm	Aquifer
TN43	22.00	22.50	Brown	Clayey sandy silt	Some rounded calcretes, <2 mm, + one large calcrete ca. 80 mm	Aquifer
TN44	22.50	23.00	Brown	Slightly clayey silty sand to fine sandy silt	Some sub-rounded calcrete, <5 mm	Aquifer
TN45	23.00	23.50	Brown	Clayey silty sand	Some calcrete, <2 mm, + very large boulder at base ca. 100 mm	Aquitard
TN46	23.50	23.83	Brown	Clayey silt, slightly sandy	Some small calcrete, <2 mm, + few larger pieces, <40 mm	Aquitard
TN47	24.00	24.39	Brown	Clayey silty sand	Some rounded calcrete, <2 mm, + few larger angular fragments	Aquitard, wet
TN48	24.50	24.90	Dark brown	Clayey silty sand to coarse sandy silt	Some sub-rounded calcretes, <2 mm, + few larger calcretes, <30 mm	Aquitard
TN49	25.00	25.35	Dark brown	Slightly clayey silty sand	Some calcrete, <3 mm	Aquitard
TN49	25.35	25.50	Dark brown	Slightly clayey silty sand	Many larger angular calcrete fragments, <40 mm	Aquitard
TN50	25.50	25.83	Brown	Slightly clayey silty fine sand	Some calcrete, <15 mm	Aquitard
TN51	26.00	26.50	Brown	Slightly clayey silty fine sand, med in parts	Calcrete, <12 mm	Aquifer
Tamagnoni						
TAM1	0.00	0.65	Dark brown	Silt	None	Unsaturated
TAM2	0.65	1.32	Dark brown	Clayey silt	None	Unsaturated
TAM3	1.32	1.98	Brown	Clayey silt	None	Unsaturated, wetter than above
TAM4	1.98	2.64	Brown	Clayey silt	None	Unsaturated

APPENDIX 2.1 cont'd...

Sample	Top depth m	Bottom depth m	Colour	Lithology	Secondary minerals	Hydrogeology
TAM5	2.64	3.00	Brown	Clayey silt	Calcareous nodules	Unsaturated
TAM6	3.00	3.50	Brown	Clayey silt	Calcareous nodules	Unsaturated
TAM7	3.50	4.10	Brown	Silt	Calcareous nodules	
TAM8	4.10	4.45	Brown	Sandy silt	Calcareous nodules	
TAM9	4.45	5.00	Brown	Sandy silt, compact at base	None	Aquifer
TAM10	5.00	5.18	Brown	Very compact silt	Calcareous nodules	Aquitard
TAM11	5.18	5.50	Dark brown	Compact silt	None	Aquitard
TAM12	5.50	6.00	Brown	Slightly clayey silt	Rounded calcretions of silt, 2mm diameter, black mottling	
TAM13	6.30	6.78	Brown	Clayey silt	Sub-rounded calcretions of silt, ca. 4mm, black mottling	
TAM14	6.80	7.10	Brown	Slightly clayey silt	Many sub-rounded calcretions of silt, <4mm, black mottling	
TAM15	7.10	7.30	Brown	Slightly clayey silt	Silt calcretions, <4mm	Aquifer
TAM15	7.30	7.60	Brown	Clayey silt	30% angular to sub-angular pieces of calcrete, ca. 10 mm	Aquifer
TAM16	7.60	8.04	Brown	Silt becoming sand with depth	30% angular pieces of calcrete	Aquifer
TAM16	8.04	8.10	Brown	Layering of calcrete + clayey silt	None	Aquifer
TAM17	8.10	8.54	Brown	Silt with thick band of calcrete, ca. 100 mm	None	Aquifer
TAM18	8.60	9.10	Brown	Silt or fine sand	10% calcrete, angular becoming rounded with depth, hard layer	Aquifer
TAM19	9.10	9.55	Brown	Silty sand	No calcrete	Aquifer
TAM20	9.60	9.87	Brown	Silty clay	Few nodules of calcrete	Aquifer
TAM21	10.14	10.40	Brown	Silty clay	Few calcrete nodules	
TAM22	10.40	10.90	Brown	Fine sandy clay	Two large nodules, >40 mm, no finer calcrete pieces	
TAM23	10.90	11.20	Brown	Silt	Few small calcrete pieces, <3mm, some 50 mm, sub-rounded to sub-angular	
TAM24	11.28	11.50	Dark brown	Unconsolidated fine to medium sand	Many small black specks, angular calcrete pieces, <1mm, few larger not so black	Aquifer
TAM25	11.50	11.90	Brown	Silt	Calcrete, <3mm	
TAM25	11.90	12.00	Brown	Clayey silt	Calcrete clasts, ca. 70mm	
TAM26	12.00	12.50	Brown	Silt	Very few small pieces of calcrete, <1mm, black mottling evident	
TAM27	12.50	12.75	Brown	Clayey silt	Small calcrete pieces + large sub-rounded nodules, ca. 50 mm	Aquifer
	12.75	12.80	Dark brown	Calcrete	50% poorly sorted angular fragments of calcrete, <15mm	
TAM28	13.00	13.45	Dark brown	Medium sand	Many angular pieces of calcrete, <5mm	Aquifer
	13.50	13.90	Brown	Clayey sand	30% calcretes, ranging from 1-50 mm	
TAM29	13.90	14.00	Brown	Clayey silt	Few calcrete (clasts), ca. 15 mm	Aquifer
TAM30	14.25	14.35	Dark brown	Poorly sorted coarse sand	Some angular to sub-rounded fragments of calcrete	Aquifer
TAM31	14.50	15.00	Brown	Slightly clayey sandy silt	Small pieces calcrete <2 mm, some large clasts, many small black particles (amphibole?)	

APPENDIX 2.1 cont'd...

Sample	Top depth m	Bottom depth m	Colour	Lithology	Secondary minerals	Hydrogeology
TAM32	15.00	15.50	Brown	Clayey sandy silt becoming sandier with depth	Many small black particles, <2 mm, + rounded clasts	
TAM33	15.50	15.74	Dark brown	Silty medium sand	Many black particles, <3 mm	Aquifer
TAM34	15.74	16.00	Dark brown	Clayey sandy silt	Many black specks, <1 mm	
TAM35	16.00	16.43	Brown	Slightly clayey sandy silt	Some silt concretions	
TAM36	16.50	16.79	Dark brown	Fine to medium sand	None	Aquifer, wet
TAM37	16.87	17.50	Brown	Sandy silt	Many silt concretions (some with black surround), one large clast, ca. 80mm	Aquifer
TAM38	17.50	18.00	Brown	Slightly clayey silty fine sand	Many silt concretions	Aquifer
TAM39	18.00	18.11	Brown	Silty medium sand	Silt concretions, <2 mm	Aquifer
TAM40	18.11	18.30	Brown	Compact silt	Many black specks	
TAM41	18.30	18.80	Brown	Slightly clayey sandy silt	Black specks	
TAM42	18.80	19.40	Brown	Slightly clayey silty sand	Many calcrete pieces, 2-40 mm	Aquifer
TAM43	19.40	19.70	Brown	Silt	Many sub-rounded calcretes, + sub-rounded clasts, <4 mm	Very dry
TAM44	19.70	20.15	Dark brown	Sandy silt	Many angular fragments becoming sub-angular with increasing size, 1-50 mm, silt concretions/calcretes?	
TAM45	20.15	20.70	Dark brown	Silty fine sand	Many calcretes, <4 mm, + some silt concretions	
TAM46	?20.70	?21.60	Brown	Slightly clayey compact silt	Many calcretes and clast, <40 mm	
TAM47	21.60	22.03	Dark brown	Silty coarse sand	Many angular pieces of calcrete, <8 mm, + many clasts, <4 mm	Aquifer
TAM48	?22.10	?22.75	Dark brown	Silty coarse sand	Many calcrete pieces and clasts, <2 mm	Aquifer
TAM49	22.75	23.00	Dark brown	Clayey sandy silt	Many calcretes and clasts, <4 mm	
TAM50	23.00	23.50	Dark brown	Clayey silt	Many small black sub-round particles of calcrete, <3 mm and larger clasts, ca 30 mm	
TAM51	23.50	24.00	Dark brown	Slightly clayey sandy silt	Many small calcrete fragments, <3 mm	Aquifer
TAM52	24.00	24.20	Dark brown	Medium sandy silt	Many calcretes, <3 mm	Aquifer
TAM53	24.20	24.50	Dark brown	Slightly clayey sandy silt	Many calcretes, <4 mm, although less than above	
TAM54	24.50	24.95	Brown	Slightly clayey sandy silt	Some silt concretions and clasts, 20-40 mm	Very dry
TAM55	25.00	25.32	Brown	Slightly clayey sandy silt	Many black specks	
	25.32	25.38		No matrix	Sub-angular fragments of calcrete	
TAM55	25.38	25.50	Brown	Slightly clayey silt	Black specks + clasts, ca. 40 mm	
TAM56	25.50	26.00	?	Clayey silt	Many black specks, high clay content, plastic	Very dry
TAM57	26.00	26.50	Dark brown	Clayey silt	Many black specks, high clay content, plastic	Very dry
TAM58	26.50	27.00	Dark brown	Slightly silty sand	Black specks, as above but sandier and less clayey, + 2 elongate calcrete nodules	
TAM59	27.00	27.50	Dark brown	Clayey sandy silt, more sand with depth	Many black specks	Very dry
TAM60	27.50	28.00	Dark brown	Sandy clayey silt	Many black specks + some calcretes, rounded crumbly, <2 mm	Very dry
TAM61	28.00	28.45	Dark brown	Clayey sandy silt	Some sub-rounded calcrete nodules, <6 mm	

APPENDIX 2.1 cont'd...

Sample	Top depth m	Bottom depth m	Colour	Lithology	Secondary minerals	Hydrogeology
	28.15	28.24		Calcrete band		
TAM62	28.50	29.00	Dark brown	Clayey sandy silt	Many black specks, some calcretes, one large boulder	
TAM63	29.00	29.20	Dark brown	Clayey sandy silt	Many black specks	Aquifer
TAM63	29.20	29.50	Dark brown	Slightly clayey silty sand	Many sub-angular fragments of black calcrete, calcrete finger	Aquifer
TAM64	29.50	29.95	Dark brown	Slightly clayey silty sand	Many angular fragments black calcrete, black calcrete banding, large nodule	Aquifer
TAM65	30.00	30.30	Dark brown	Clayey sandy silt	Many sub-angular fragments of calcrete, <6 mm, becoming more sandy and less clayey with depth	?

APPENDIX 3.1 Chemical data for porewaters extracted from cored sediments at Talleres Norte (Eduardo Castex) and Tamagnoni (10 km south of Eduardo Castex) and from augered sediments.

Sample	Locality	Top depth m	Bottom depth m	pH*	SEC µS cm^{-1}	Moisture content % dry wt	Ca mg l^{-1}	Mg mg l^{-1}	Na mg l^{-1}	K mg l^{-1}	Cl mg l^{-1}	SO_4 mg l^{-1}	HCO_3* mg l^{-1}	NO_3-N mg l^{-1}	NH_4-N mg l^{-1}	Si mg l^{-1}	Al mg l^{-1}
Talleres Norte borehole																	
980401	TN4	1.45	4.20	8.27	1300	28.6	56.5	38.4	195	15.4	67.3	150	596	<0.2	0.014	17.8	0.04
980402	TN5	4.33	4.45	8.27	702	22.3	10.3	6.52	150	2.7	13.8	70.6	275	8.7	<0.01	22.7	1.15
980403	TN6	4.45	4.90	8.30	752	24.7	8.05	5.26	162	2.3	13.3	99.5	270	6.8	nd	20.4	0.35
980404	TN7	4.90	5.40	8.39	774	26.1	6.88	4.29	171	2.2	17.8	87.7	286	8.0	<0.01	20.5	0.59
980405	TN8	5.40	5.90	8.40	741	26.0	6.21	3.70	163	2.5	16.9	66.2	296	8.0	<0.01	22.1	0.89
980406	TN9	5.90	6.40	8.34	717	25.8	5.67	2.91	162	2.1	16.1	51.8	309	7.7	<0.01	21.3	0.56
980407	TN10	6.40	6.90	8.46	782	33.8	7.49	3.20	179	2.0	17.0	50.0	381	7.6	nd	19.7	0.22
980408	TN11	6.90	7.33	8.38	892	29.0	10.2	5.66	204	2.3	19.4	70.5	477	0.4	nd	18.2	0.17
980409	TN12	7.63	7.79	8.38	661	25.0	5.16	2.10	155	1.8	17.9	39.8	348	1.0	<0.01	20.4	0.19
980410	TN13	7.90	8.35	8.37	611	22.6	4.47	1.76	138	1.7	13.8	25.3	322	5.1	<0.01	20.7	0.10
980411	TN14	8.40	8.78	8.40	598	39.3	11.2	5.06	141	2.2	10.8	22.2	365	6.3	<0.01	21.8	0.08
980412	TN15	8.90	9.38	8.31	612	37.0	14.0	6.90	141	2.3	9.9	23.1	380	6.5	<0.01	22.4	0.07
980413	TN16	9.40	9.90	8.33	607	30.3	11.0	5.34	142	2.2	8.8	23.7	372	6.2	nd	21.3	0.06
980414	TN17	9.90	10.40	8.42	657	32.1	11.0	5.12	160	2.5	8.1	24.5	429	5.4	nd	21.0	0.07
980415	TN18	10.40	10.90	8.50	689	36.7	4.15	3.95	181	2.3	6.1	19.0	454	4.3	nd	37.2	3.45
980416	TN19	10.90	11.25	8.53	756	37.5	4.65	2.72	199	2.4	5.2	27.5	493	3.8	nd	26.1	1.05
980417	TN20	11.40	11.75	8.42	607	28.8	2.93	1.95	158	2.1	6.4	22.6	366	3.5	0.01	26.0	0.96
980418	TN21	12.20	12.40	8.54	685	30.8	3.31	2.47	177	2.4	8.1	28.3	416	3.6	<0.01	29.1	1.48
980419	TN22	13.20	13.30	8.66	929	30.1	4.17	2.84	247	2.9	11.1	48.2	596	3.2	nd	22.8	0.09
980420	TN23	13.69	13.90	8.53	825	27.8	2.94	2.22	205	2.7	13.4	36.0	468	2.2	<0.01	25.8	0.75
980421	TN24	14.00	14.40	8.48	823	31.1	2.85	2.21	233	2.5	13.9	34.8	532	1.1	<0.01	23.7	0.46
980422	TN25	14.60	14.72	8.52	816	27.4	3.88	2.67	222	2.7	13.0	49.2	559	0.9	<0.01	24.3	0.77
980423	TN26	15.06	15.36	8.64	1070	33.9	3.88	3.67	286	3.1	16.9	46.3	655	3.0	<0.01	25.2	1.03
980424	TN27	15.50	16.00	8.76	1180	32.0	3.97	3.47	320	3.2	28.4	67.1	701	1.0	nd	22.9	0.38
980425	TN28	16.00	16.42	8.60	1190	29.2	4.63	4.70	317	3.6	23.7	72.6	719	<0.2	<0.01	26.6	1.47
980426	TN29	16.50	16.71	8.55	1050	33.3	2.81	3.23	256	2.7	38.3	74.7	511	0.6	<0.01	27.6	1.78
980427	TN30	16.50	16.84	8.61	1030	28.7	2.56	2.75	247	2.6	40.6	66.8	504	<0.2	<0.01	25.5	1.39
980428	TN31	17.00	17.31	8.59	1020	31.0	2.54	2.63	261	2.6	45.0	69.3	495	<0.2	<0.01	25.8	1.04
980429	TN32	17.31	17.50	8.67	1100	26.0	2.91	2.70	270	2.4	50.3	89.1	487	<0.2	<0.01	22.8	0.30
980430	TN33	17.50	17.83	8.66	1160	28.8	2.83	2.77	275	2.5	52.5	75.6	521	<0.2	<0.01	21.8	0.27

APPENDIX 3.1 cont'd...

Sample	Locality	Top depth m	Bottom depth m	pH*	SEC µS cm^{-1}	Moisture content % dry wt	Ca mg l^{-1}	Mg mg l^{-1}	Na mg l^{-1}	K mg l^{-1}	Cl mg l^{-1}	SO_4 mg l^{-1}	HCO_3* mg l^{-1}	NO_3-N mg l^{-1}	NH_4-N mg l^{-1}	Si mg l^{-1}	Al mg l^{-1}
980431	TN34	18.00	18.38	8.44	1550	35.0	5.34	5.52	411	3.3	55.5	82.5	903	<0.2	<0.01	23.5	<0.12
980432	TN35	18.50	18.89	8.46	1640	33.6	5.59	6.19	438	4.0	61.7	84.2	955	<0.2	<0.01	22.6	0.47
980433	TN36	19.00	19.33	8.33	1440	37.2	4	4.08	378	3.7	66.4	80.5	769	<0.2	<0.01	22.6	0.12
980434	TN37	19.50	19.83	8.45	1530	33.4	4.39	4.67	390	4.0	71.4	97.2	799	<0.2	<0.01	23.2	0.29
980435	TN38	20.00	20.50	8.67	1500	35.3	4.11	4.33	385	3.7	74.8	99.5	756	<0.2	<0.01	22.7	0.17
980436	TN39	20.50	20.83	8.49	1430	24.2	3.23	3.68	336	3.5	79.3	122	645	<0.2	<0.01	21.9	0.25
980437	TN40	21.00	21.33	8.54	1470	33.1	3.19	3.54	332	3.4	79.4	108	651	<0.2	<0.01	20.5	0.08
980438	TN41	21.50	21.66	8.48	1370	25.8	4.49	4.27	342	3.7	57.7	105	684	<0.2	0.019	22.4	0.44
980439	TN42	21.66	21.88	8.56	1760	33.9	5.49	6.18	450	4.8	79.6	123	899	<0.2	0.01	25.1	0.15
980440	TN43	22.00	22.50	8.65	1740	37.0	5.19	5.49	426	4.8	84	143	807	<0.2	0.01	24.9	0.54
980441	TN44	22.50	23.00	8.58	1720	33.3	5.25	5.31	417	4.5	88	149	782	<0.2	<0.01	25.1	0.90
980442	TN45	23.00	23.50	8.66	1770	40.1	4.94	5.63	450	5.1	91	160	814	<0.2	<0.01	22.6	0.04
980443	TN46	23.50	23.83	8.70	1840	32.3	4.97	5.94	454	5.2	99	199	781	<0.2	<0.01	21.8	0.09
980444	TN47	24.00	24.39	8.45	2060	36.5	6.18	7.73	505	6.0	108	219	919	<0.2	<0.01	21.9	<0.04
980445	TN48	24.50	24.90	8.39	2110	31.5	6.34	7.64	505	6.2	120	258	838	<0.2	<0.01	23.0	0.35
980446	TN49	25.00	25.50	8.47	2070	31.0	5.88	6.96	465	5.9	133	287	713	<0.2	<0.01	21.6	0.08
980447	TN50	25.50	25.83	8.39	1890	34.5	4.41	5.25	392	4.8	143	291	493	<0.2	<0.01	20.3	0.08
980448	TN51	26.00	26.50	8.42	2020	36.5	4.69	6.44	458	6.0	161	370	483	<0.2	<0.01	22.0	0.08
Tamagnoni borehole																	
980449	TAM7	3.50	4.10	7.20	9710	31.0	849	330	1269	106	1440	2355	49	560	<0.01	28.0	<0.12
980450	TAM8	4.10	4.45	7.52	9440	32.0	606	249	1521	89.7	1380	1683	182	620	<0.01	26.2	<0.12
980451	TAM9	4.45	5.00	7.77	9240	28.6	678	267	1545	101	1320	2106	474	493	<0.01	27.6	<0.12
980452	TAM10	5.00	5.18	7.39	8780	27.3	511	181	1590	92.6	1240	1760	67	510	0.02	24.8	0.06
980453	TAM11	5.18	5.50	7.55	7470	27.5	104	43.2	1690	49.9	1110	643	125	510	<0.01	23.5	<0.04
980454	TAM12	5.50	6.00	8.00	6710	31.4	45.3	22.3	1520	41.9	960	501	255	434	<0.01	26.1	<0.04
980455	TAM13	6.30	6.78	8.10	4620	34.7	12.4	8.28	1070	24.8	628	339	306	270	<0.01	26.6	0.05
980456	TAM14	6.80	7.10	8.18	4010	30.0	7.54	5.45	928	19.2	509	324	309	213	<0.01	26.1	0.08
980457	TAM15	7.10	7.30	8.31	4020	29.3	5.76	5.40	939	17.7	456	333	410	200	<0.01	26.3	0.15
980458	TAM16	7.60	8.04	8.32	4020	27.0	6.36	5.97	963	15.6	429	360	369	208	nd	25.1	0.12
980459	TAM17	8.10	8.54	8.47	3920	29.8	5.13	5.34	927	14.7	408	354	454	185	nd	24.8	<0.12
980460	TAM18	8.60	9.10	8.27	3590	28.1	5.37	5.01	849	14.7	369	354	434	161	nd	26.3	0.33
980461	TAM19	9.10	9.55	8.57	3140	33.2	3.15	3.60	750	12.6	280	291	592	109	nd	27.5	0.27
980462	TAM20	9.60	9.87	8.50	2870	28.3	3.06	3.51	702	10.8	206	257	796	77	nd	25.9	0.15

APPENDIX 3.1 cont'd...

Sample	Locality	Top depth m	Bottom depth m	pH*	SEC μS cm^{-1}	Moisture content % dry wt	Ca mg l^{-1}	Mg mg l^{-1}	Na mg l^{-1}	K mg l^{-1}	Cl mg l^{-1}	SO$_4$ mg l^{-1}	HCO$_3$* mg l^{-1}	NO$_3$-N mg l^{-1}	NH$_4$-N mg l^{-1}	Si mg l^{-1}	Al mg l^{-1}
980463	TAM21	10.14	10.40	8.63	3110	32.4	4.24	4.32	729	12.9	200	247	1010	72	nd	25.0	0.16
980464	TAM22	10.40	10.90	8.61	2390	31.1	2.53	2.83	566	9.5	171	230	698	62	nd	24.2	0.21
980465	TAM23	10.90	11.20	8.61	2520	27.1	2.73	2.89	582	9.7	170	247	685	58	nd	25.0	0.16
980466	TAM24	11.28	11.50	8.29	3040	37.1	4.80	4.49	726	14.8	205	284	928	72	nd	25.3	0.12
980467	TAM25	11.50	12.00	8.69	2410	30.5	2.34	3.00	606	10.5	150	265	692	49	nd	28.7	0.24
980468	TAM26	12.00	12.50	8.62	2240	31.1	2.40	2.61	543	9.3	121	270	686	33	nd	26.6	0.30
980469	TAM27	12.50	12.75	8.66	2510	31.6	2.98	3.61	611	10.0	107	262	968	27	nd	24.1	0.15
980470	TAM28	13.00	13.45	8.77	2070	30.8	2.17	2.72	488	7.9	92	254	666	21	nd	25.7	0.99
980471	TAM29	13.90	14.00	8.61	1810	28.1	2.62	1.96	441	7.3	76	294	534	14.9	nd	23.2	0.20
980472	TAM30	14.25	14.35	8.61	2310	37.0	2.51	3.12	533	10.5	123	282	694	31.2	nd	27.3	0.82
980473	TAM31	14.50	15.00	8.66	1770	30.9	2.38	1.76	401	7.3	56	266	548	9.5	nd	26.5	0.37
980474	TAM32	15.00	15.50	8.56	1820	30.4	2.46	2.04	397	7.6	54	259	594	7.3	nd	25.3	0.39
980475	TAM33	15.50	15.74	8.66	2500	37.4	3.23	3.56	576	11.2	150	300	713	41	nd	25.3	0.27
980476	TAM34	15.74	16.00	8.68	1780	32.1	2.28	2.10	429	7.5	59	282	563	7.9	nd	28.1	0.36
980477	TAM35	16.00	16.43	8.66	1720	32.0	2.07	2.10	420	7.5	53	268	566	5.9	nd	28.9	0.54
980478	TAM36	16.50	16.79	8.62	2220	34.7	2.76	3.30	528	9.6	110	292	679	26	nd	25.9	0.30
980479	TAM37	16.87	17.50	8.59	1790	33.7	2.14	2.28	414	7.7	63	254	585	7.9	nd	26.1	0.45
980480	TAM38	17.50	18.00	8.60	1960	31.9	2.43	2.76	471	9.0	72	284	672	9.0	nd	28.7	0.36
980481	TAM39	18.00	18.11	8.61	1940	29.8	2.34	3.10	450	9.1	85	292	568	12	nd	29.5	1.42
980482	TAM40	18.11	18.30	8.66	1930	26.9	2.22	2.56	431	8.5	72	272	632	7.0	nd	25.7	0.16
980483	TAM41	18.30	18.80	8.59	1910	30.3	2.44	2.72	434	8.7	59	260	670	5.2	nd	26.7	0.47
980484	TAM42	18.80	19.40	8.72	1810	29.9	2.09	2.90	390	8.3	53	245	623	4.2	nd	29.8	1.68
980485	TAM43	19.40	19.70	8.78	1850	25.8	2.58	2.65	424	9.1	55	280	619	3.0	nd	29.4	0.54
980486	TAM44	19.70	20.15	8.69	1880	26.2	2.55	2.99	427	9.2	62	280	631	3.2	nd	31.9	1.18
980487	TAM45	20.15	20.70	8.62	1780	28.5	2.19	3.06	429	9.3	61	297	562	4.4	nd	36.3	2.19
980488	TAM46	20.70	21.60	8.56	2160	27.4	4.78	4.26	497	9.8	105	342	615	17	nd	25.5	0.62
980489	TAM47	21.60	22.03	8.46	2000	30.4	2.64	3.33	441	9.0	111	372	404	13	nd	32.1	1.59
980490	TAM48	22.10	22.75	8.63	2430	35.7	4.2	4.71	579	12.3	99	360	848	11	nd	26.3	<0.12
980491	TAM49	22.75	23.00	8.65	2090	36.8	3.09	3.15	483	9.9	96	375	569	9.7	nd	26.9	0.15
980492	TAM50	23.00	23.50	8.59	2430	31.1	4.38	5.22	578	11.4	82	336	1000	4.4	nd	24.4	0.11
980493	TAM51	23.50	24.00	8.72	2010	34.0	2.94	3.36	474	9.0	73	333	667	3.2	nd	26.8	0.27
980494	TAM52	24.00	24.20	8.62	2300	40.0	3.33	3.75	531	10.2	146	321	526	38	nd	26.1	0.18
980495	TAM53	24.20	24.50	8.66	1860	31.4	2.73	2.70	435	8.4	71	318	561	<0.5	nd	25.4	0.15
980496	TAM54	24.50	24.95	8.56	1950	28.2	3.48	2.70	441	7.8	77	369	539	1.6	nd	23.0	0.15

APPENDIX 3.1 cont'd...

Sample	Locality	Top depth m	Bottom depth m	pH*	SEC µS cm^{-1}	Moisture content % dry wt	Ca mg l^{-1}	Mg mg l^{-1}	Na mg l^{-1}	K mg l^{-1}	Cl mg l^{-1}	SO_4 mg l^{-1}	HCO_3* mg l^{-1}	NO_3-N mg l^{-1}	NH_4-N mg l^{-1}	Si mg l^{-1}	Al mg l^{-1}
980497	TAM55	25.00	25.50	8.59	1790	33.0	3.09	2.37	408	8.1	73	345	434	1.6	nd	25.8	0.30
980498a	TAM56	25.50	26.00	8.38		31.6					104		341	6.1			
980498b	TAM57	26.00	26.50			31.7											
980499	TAM58	26.50	27.00	8.63	1860	33.8	3.36	2.22	423	8.1	82	366	482	<0.5	nd	26.5	<0.12
980500	TAM59	27.00	27.50	8.42	1700	31.9	2.70	1.74	366	7.2	89	324	401	1.2	nd	27.6	0.15
980501	TAM60	27.50	28.00	8.51	1650	33.8	2.11	1.92	371	7.2	83	298	429	<0.5	nd	23.7	0.15
980502	TAM61	28.00	28.45	8.66	1920	33.3	2.85	2.58	426	7.5	86	345	546	<0.5	nd	23.0	0.12
980503	TAM62	28.50	29.00	8.67	1980	31.8	2.91	2.72	438	8.0	92	380	525	0.8	nd	21.5	0.07
980504	TAM63	29.00	29.50	8.59	1940	30.3	2.60	2.40	423	8.6	97	411	431	0.8	nd	24.2	0.06
980505	TAM64	29.50	29.95	8.46	1970	29.5	2.94	3.09	477	9.6	107	510	365	<0.5	nd	32.1	1.11
980506	TAM65	30.00	30.30	8.55	2060	33.3	2.94	2.79	453	10.0	106	463	426	1.2	nd	27.7	0.34
Augered sediments																	
970829	La Invernada	0.2	1.0	8.52	3200	nd	15.0	9.97	927	24.7	32.9	225	2330	0.54	nd	18.0	0.24
970830	La Invernada	1.0	2.0	8.50	3790	nd	13.1	22.8	1060	33.4	151	598	1969	0.46	nd	34.1	0.19
970831	Nicola	0.0	0.3	8.38	1158	nd	34.5	7.12	53.5	306	25.1	97.8	546	7.64	nd	16.6	0.10
970832	Santa Rita	0.2	1.0	8.45	1461	nd	17.7	11.5	376	35.9	32.6	319	457	12.7	nd	60.8	22.0

*Laboratory measurements; nd: not determined

APPENDIX 3.2 **Trace-element data for porewaters extracted from cored sediments at Talleres Norte (Eduardo Castex) and Tamagnoni (10 km south of Eduardo Castex) and from augered sediments**

Sample	Locality	P_T mg l^{-1}	B mg l^{-1}	V mg l^{-1}	Li µg l^{-1}	As_T µg l^{-1}	Fe µg l^{-1}	Mn µg l^{-1}	Sr µg l^{-1}	Ba µg l^{-1}	Zn µg l^{-1}	F mg l^{-1}	Br µg l^{-1}	I µg l^{-1}	Li* µg l^{-1}	Be* µg l^{-1}	Al* µg l^{-1}	Cr* µg l^{-1}
Talleres Norte borehole																		
980401	TN4	1.0	0.91	0.043	14	<20	15	79	699	347	146	5.61	468	87	16.9	0.080	16	0.72
980402	TN5	1.4	0.67	0.490	13	80	932	50	137	66	18	9.21	203	47	16.7	0.087	nd	4.56
980403	TN6	1.0	0.82	0.544	14	70	234	10	116	76	8	11.4	192	87	13.3	0.095	273	2.28
980404	TN7	0.7	0.75	0.486	13	120	623	11	100	64	18	16.8	195	50	15.0	0.085	nd	2.11
980405	TN8	0.7	0.69	0.526	14	120	907	15	89.2	58	19	16.5	193	48	14.9	0.096	nd	1.67
980406	TN9	0.6	0.61	0.534	12	120	612	10	81.4	55	18	15.1	182	42	13.4	0.054	nd	1.45
980407	TN10	0.4	0.52	0.376	15	70	330	10	102	56	12	6.39	188	31	14.1	0.067	177	1.19
980408	TN11	0.5	0.78	0.289	16	60	167	6	147	62	13	7.77	193	153	17.4	0.107	159	0.83
980409	TN12	0.5	0.4	0.302	13	50	204	6	74.4	30	<8	6.09	190	47	13.6	0.037	151	2.31
980410	TN13	0.5	0.37	0.208	13	40	98	2	66.5	28	9	3.69	168	31	13.0	0.038	85	1.92
980411	TN14	0.2	0.41	0.111	20	<20	53	5	163	72	20	2.88	148	30	27.9	0.035	57	1.39
980412	TN15	<0.2	0.44	0.149	19	20	52	3	212	101	23	3.06	149	27	25.6	0.057	42	1.53
980413	TN16	0.3	0.42	0.179	16	60	36	3	173	67	14	3.84	172	28	21.2	0.039	38	1.56
980414	TN17	0.3	0.38	0.196	17	70	61	3	180	72	16	4.56	142	30	23.4	0.039	56	1.82
980415	TN18	0.6	0.41	0.296	21	110	3990	89	86.3	86	29	7.77	104	36	25.1	0.099	nd	3.35
980416	TN19	0.4	0.38	0.406	19	100	1190	31	99.3	92	17	7.29	87	45	23.3	0.055	nd	2.42
980417	TN20	0.5	0.37	0.691	11	130	1110	37	66.6	72	12	9.57	164	47	13.7	0.044	nd	1.51
980418	TN21	0.5	0.42	0.662	11	130	1660	37	76.1	65	16	10.1	78	53	14.3	0.074	nd	2.01
980419	TN22	<0.2	0.44	0.433	10	130	67	2	105	57	<8	8.34	89	88	9.8	0.036	78	0.74
980420	TN23	<0.6	0.45	0.660	<3	210	768	9	72.3	24	<24	9.57	101	57	9.1	0.060	nd	15.6
980421	TN24	<0.2	0.49	0.742	4	180	500	6	71.7	22	<8	9.57	115	49	8.7	0.057	441	2.32
980422	TN25	<0.2	0.46	0.555	7	170	782	10	86.7	35	12	9.57	113	72	11.5	0.063	nd	1.31
980423	TN26	<0.2	0.59	1.03	9	280	1040	22	103	39	11	13.8	138	56	12.6	0.061	nd	3.29
980424	TN27	<0.2	0.88	1.21	10	320	321	9	105	101	19	16.9	177	65	11.8	0.076	333	4.36
980425	TN28	0.5	0.77	0.800	13	200	1380	40	128	79	27	13.1	161	301	17.9	0.081	nd	2.19
980426	TN29	<0.2	0.77	1.57	12	340	2270	41	79.3	46	14	21.8	203	57	12.4	0.10	nd	3.27
980427	TN30	<0.2	0.75	1.47	10	300	1250	24	71.4	42	12	22.2	215	58	11.7	0.101	nd	2.93
980428	TN31	<0.2	0.76	1.50	8	320	957	15	71.7	30	12	22.1	232	54	11.5	0.094	nd	2.57
980429	TN32	<0.6	0.72	1.68	<9	350	246	18	82.8	72	<24	24.1	249	61	8.5	0.056	459	3.99
980430	TN33	<0.2	0.84	1.60	9	410	187	8	85	45	<8	25.2	258	76	8.8	0.091	217	3.26
980431	TN34	<0.6	1.2	1.17	9	310	48	3	175	111	<24	17.4	258	69	14.4	0.098	67	3.20

APPENDIX 3.2 cont'd...

Sample	Locality	P_T mg l^{-1}	B mg l^{-1}	V mg l^{-1}	Li µg l^{-1}	As_T µg l^{-1}	Fe µg l^{-1}	Mn µg l^{-1}	Sr µg l^{-1}	Ba µg l^{-1}	Zn µg l^{-1}	F mg l^{-1}	Br µg l^{-1}	I µg l^{-1}	Li* µg l^{-1}	Be* µg l^{-1}	Al* µg l^{-1}	Cr* µg l^{-1}
980432	TN35	<0.2	1.2	0.981	12	290	397	11	178	60	<8	16.2	295	66	17.6	0.08	nd	3.98
980433	TN36	<0.2	1.13	1.45	9	350	104	8	125	75	<8	18.5	360	73	10.6	0.121	111	2.76
980434	TN37	<0.2	1.35	1.39	12	360	228	13	137	72	13	18.6	322	82	12.3	0.137	274	4.09
980435	TN38	<0.2	1.32	1.59	9	380	148	12	129	51	<8	21.7	319	77	10.2	0.152	220	3.67
980436	TN39	<0.2	1.16	1.44	12	460	209	14	108	45	<8	23	326	97	10.3	0.098	193	7.61
980437	TN40	<0.2	1.19	1.62	9	530	38	2	104	51	<8	25.7	309	103	10.8	0.127	51	3.77
980438	TN41	0.3	0.99	0.68	12	140	433	17	134	67	<8	17.2	259	207	13.7	0.10	388	1.04
980439	TN42	<0.6	1.74	1.44	12	420	147	6	191	108	27	20.8	310	107	16.2	0.176	146	5.26
980440	TN43	<0.6	1.95	1.54	12	470	279	12	167	153	24	23.5	332	127	10.6	0.199	435	4.74
980441	TN44	<0.6	2.13	1.49	12	460	360	12	162	108	39	23.8	348	142	11.4	0.212	754	5.24
980442	TN45	<0.2	2.67	1.41	8	460	37	1	166	139	25	22.8	329	148	10.6	0.198	75	4.77
980443	TN46	<0.2	2.6	1.13	8	450	53	2	173	125	32	18.7	370	150	12.3	0.198	110	7.28
980444	TN47	<0.2	3.1	1.00	10	420	37	<1	221	140	34	17.6	420	158	11.2	0.261	70	4.95
980445	TN48	0.3	3.38	1.00	10	350	174	9	220	111	37	17.6	440	197	10.7	0.326	383	4.77
980446	TN49	0.3	3.04	0.97	10	410	41	4	203	110	25	18.4	490	217	11.1	0.308	93	5.18
980447	TN50	0.3	2.5	1.03	9	450	44	3	153	45	<8	22.2	520	232	9.6	0.304	79	5.22
980448	TN51	0.3	2.99	1.05	7	440	42	2	190	71	<8	21.6	570	248	8.5	0.181	61	4.99
Tamagnoni borehole																		
980449	TAM7	<0.6	0.39	0.024	69	<20	<18	6	8670	123	180	1.14	8100	387	83.3	<0.065	29	1.13
980450	TAM8	0.9	0.45	0.027	69	<20	<18	6	7650	171	255	1.08	7700	331	77.2	<0.065	17	1.07
980451	TAM9	<0.6	0.6	0.027	84	<20	99	12	8250	234	381	1.86	7200	356	100	<0.065	53	1.51
980452	TAM10	0.3	0.38	0.023	64	<20	14	5	5500	145	174	1.53	6200	292	91.1	<0.095	24	8.21
980453	TAM11	0.2	0.46	0.037	37	<20	16	3	1840	139	81	1.44	38000	172	31.5	<0.072	54	3.88
980454	TAM12	0.3	0.66	0.069	34	<20	14	6	1010	116	125	1.83	33000	154	38.6	<0.05	34	1.93
980455	TAM13	0.4	0.84	0.359	19	50	26	2	427	170	33	2.49	3080	129	20.6	0.072	52	2.04
980456	TAM14	0.3	1.25	0.554	17	130	39	4	273	173	51	5.01	2770	129	20.0	0.072	72	3.98
980457	TAM15	<0.6	1.68	0.933	12	430	108	6	260	126	<24	7.53	2610	122	21.3	0.19	138	2.81
980458	TAM16	<0.6	1.83	1.12	12	570	96	6	282	207	27	9.75	2440	126	20.9	0.15	129	3.87
980459	TAM17	<0.6	1.86	2.03	15	570	33	6	245	138	42	10.2	2340	137	19.0	0.19	51	4.00
980460	TAM18	<0.6	1.89	1.64	15	500	249	6	227	99	<24	10.9	2150	143	17.3	0.12	319	3.71
980461	TAM19	<0.6	1.98	3.48	<3	550	150	6	156	108	<24	10.7	1560	137	12.8	0.23	208	3.48
980462	TAM20	<0.6	1.8	3.48	<3	440	72	<4	142	138	36	10.7	1160	126	15.4	0.21	77	3.46
980463	TAM21	0.3	1.8	3.06	13	470	74	4	170	187	23	9	1090	126	20.6	0.13	131	3.97
980464	TAM22	0.3	1.78	4.26	11	740	85	4	106	114	23	13	1060	131	10.6	0.19	126	3.03

APPENDIX 3.2 cont'd…

Sample	Locality	P_T mg l^{-1}	B mg l^{-1}	V mg l^{-1}	Li μg l^{-1}	As_T μg l^{-1}	Fe μg l^{-1}	Mn μg l^{-1}	Sr μg l^{-1}	Ba μg l^{-1}	Zn μg l^{-1}	F mg l^{-1}	Br μg l^{-1}	I μg l^{-1}	Li* μg l^{-1}	Be* μg l^{-1}	Al* μg l^{-1}	Cr* μg l^{-1}
980465	TAM23	0.2	2.02	4.82	10	820	45	3	109	200	36	14	970	142	15.2	0.22	64	4.68
980466	TAM24	0.5	2.35	1.68	15	250	66	4	182	154	38	9.3	1140	210	20.4	0.22	86	0.88
980467	TAM25	<0.6	3.21	7.02	<3	1280	99	6	114	135	<24	15.9	800	173	14.4	0.36	123	3.47
980468	TAM26	<0.6	3.21	6.78	12	1330	129	9	98.7	225	45	15.3	650	174	10.3	0.23	164	8.06
980469	TAM27	0.3	3.24	6.31	9	1390	48	2	129	156	49	14.4	580	181	14.1	0.32	99	3.92
980470	TAM28	0.4	3.22	8.48	10	1880	481	6	87.5	62	11	19.8	520	193	10.4	0.37	789	4.24
980471	TAM29	0.4	3.39	8.22	7	2010	36	2	74.9	266	39	16	400	211	11.0	0.34	98	6.32
980472	TAM30	0.5	3.53	6.03	13	1030	477	15	105	71	12	16.5	710	226	13.0	0.44	769	2.94
980473	TAM31	0.4	3.72	12.0	6	2290	108	5	65.3	249	50	20.4	310	218	8.0	0.29	237	5.89
980474	TAM32	0.4	3.42	8.06	9	2360	153	9	73.8	301	47	20	270	256	9.3	0.37	284	16.7
980475	TAM33	0.5	3.31	6.13	11	1130	129	7	129	127	17	16.6	840	262	16.0	0.43	202	2.06
980476	TAM34	<0.6	3.72	9.45	<3	2720	105	<4	72	150	51	22.2	300	279	9.5	0.34	202	4.97
980477	TAM35	<0.6	4.26	9.06	<3	3210	258	12	69.9	147	48	22.4	270	337	10.4	0.43	386	4.70
980478	TAM36	<0.6	4.02	6.93	12	2160	90	6	114	99	<24	19	570	306	10.9	0.35	138	3.42
980479	TAM37	0.4	4.28	7.91	8	3300	188	7	72.9	90	13	22.2	300	247	10.0	0.41	383	4.73
980480	TAM38	<0.6	4.86	7.77	<3	3200	132	6	93.3	123	33	21	360	310	11.6	0.36	245	7.17
980481	TAM39	0.5	4.3	6.54	10	2850	806	47	88.9	94	18	18.8	520	304	13.6	0.39	1238	6.51
980482	TAM40	0.4	4.15	7.40	8	3050	25	<1	82.7	101	<8	22.7	330	257	12.8	0.44	77	4.88
980483	TAM41	0.5	4.39	7.30	10	3460	211	8	84.5	150	27	21.7	290	531	11.8	0.57	391	6.14
980484	TAM42	0.5	4.06	7.01	12	3630	947	63	77.2	87	24	25.1	260	313	12.5	0.48	1481	4.50
980485	TAM43	0.5	4.41	7.03	10	3480	301	11	83.4	168	25	25.2	260	281	12.5	0.56	448	7.38
980486	TAM44	0.7	4.47	6.25	12	3230	681	30	89.3	87	26	25	290	334	13.1	0.43	950	5.95
980487	TAM45	<0.6	5.31	7.14	<3	4260	1359	63	82.8	69	27	20.7	270	298	15.5	0.51	nd	4.74
980488	TAM46	0.9	3.49	3.79	15	2280	354	21	147	216	50	19.4	480	284	16.4	0.32	540	33.6
980489	TAM47	<0.6	4.38	4.71	9	3900	957	42	97.5	72	27	19.4	450	298	16.4	0.47	nd	5.08
980490	TAM48	<0.6	4.98	4.02	12	2610	33	6	155	180	51	15.4	450	296	19.0	0.47	47	3.75
980491	TAM49	<0.6	4.47	4.92	12	3990	39	<4	109	153	39	19.4	460	276	16.8	0.62	58	3.95
980492	TAM50	0.5	4.69	3.37	16	2660	35	3	165	135	37	14	330	253	21.0	0.39	84	4.95
980493	TAM51	<0.6	4.35	4.35	12	3960	129	6	113	93	<24	18.5	270	295	13.3	0.33	218	5.47
980494	TAM52	<0.6	3.78	3.81	<3	2530	93	6	129	87	<24	18.7	750	306	18.9	0.40	140	3.44
980495	TAM53	<0.6	4.17	3.90	<3	5100	72	6	93.9	96	<24	19.9	240	274	15.5	0.52	128	6.32
980496	TAM54	<0.6	3.72	3.45	9	4920	60	6	101	213	36	19.4	260	276	15.9	0.44	108	6.74
980497	TAM55	<0.6	4.47	3.93	12	5070	117	6	86.7	237	51	16.6	240	250	11.6	0.44	224	6.54
980498a	TAM56																	
980498b	TAM57																	

APPENDIX 3.2 cont'd...

Sample	Locality	P_T mg l^{-1}	B mg l^{-1}	V mg l^{-1}	Li µg l^{-1}	As_T µg l^{-1}	Fe µg l^{-1}	Mn µg l^{-1}	Sr µg l^{-1}	Ba µg l^{-1}	Zn µg l^{-1}	F mg l^{-1}	Br µg l^{-1}	I µg l^{-1}	Li* µg l^{-1}	Be* µg l^{-1}	Al* µg l^{-1}	Cr* µg l^{-1}
980499	TAM58	<0.6	4.71	2.38	<3	7490	39	3	88.8	201	57	16.4	270	295	13.9	0.41	108	4.03
980500	TAM59	<0.6	4.92	2.17	<3	6500	69	3	68.4	186	63	17.5	290	305	13.7	0.55	127	4.32
980501	TAM60	0.5	3.94	1.99	9	6480	75	4	65.9	110	33	17.5	250	274	13.7	0.35	166	3.41
980502	TAM61	<0.6	3.45	1.76	9	5230	60	6	93.6	156	42	18.4	270	280	14.9	0.29	93	4.97
980503	TAM62	0.4	3.18	1.61	10	4670	32	3	94.9	148	29	16.4	300	260	14.6	0.27	106	4.53
980504	TAM63	0.5	3.90	2.02	10	5100	21	1	87.4	90	10	17.3	420	334	15.0	0.29	78	5.76
980505	TAM64	<0.6	4.68	2.50	12	4710	702	24	103	84	30	16.6	330	353	16.1	0.46	974	5.72
980506	TAM65	0.5	4.10	1.99	12	4000	234	9	98.1	111	28	16.2	330	364	13.5	0.43	311	7.25
Augered sediments																		
970829	La Invernada	1.2	6.90	0.168	50	36.6	156	38	418	342	173	1.8	nd	nd	72	0.23	341	3.39
970830	La Invernada	0.6	5.86	0.379	67	133	138	29	1000	341	148	7.6	nd	nd	84	0.099	216	4.02
970831	Nicola	7.2	0.66	0.050	40	34.7	101	43	341	599	261	0.7	nd	nd	50	<0.15	150	1.51
970832	Santa Rita	9.2	3.09	0.189	27	1890	13840	288	203	337	362	10.1	nd	nd	28	1.08	26374	19.6

*Analysed by ICP-MS (metals analysed by ICP-AES where not otherwise specified, halogen elements by ion chromatography); nd: not determined

APPENDIX 3.3 Trace-element data for porewaters extracted from cored sediments at Talleres Norte (Eduardo Castex) and Tamagnoni (10 km south of Eduardo Castex) and from augered sediments (analysed by ICP-MS)

Sample	Locality	Mn μg l^{-1}	Co μg l^{-1}	Ni μg l^{-1}	Cu μg l^{-1}	Zn μg l^{-1}	Ga μg l^{-1}	Ge μg l^{-1}	As μg l^{-1}	Rb μg l^{-1}	Sr μg l^{-1}	Y μg l^{-1}	Mo μg l^{-1}	Cd μg l^{-1}	Sb μg l^{-1}	Cs μg l^{-1}	Se μg l^{-1}	Pb μg l^{-1}	U μg l^{-1}
Talleres Norte borehole																			
980401	TN4	63.4	0.91	4.38	2.11	110	<0.024	0.017	10	5.79	686	0.125	29.3	0.11	0.30	<0.011	<0.33	0.45	14.6
980402	TN5	40.3	1.13	2.10	2.95	15.1	0.427	0.117	108	1.72	122	3.48	5.5	<0.11	0.18	0.060	<0.71	2.06	9.0
980403	TN6	7.6	0.29	1.48	2.75	5.6	0.114	0.068	83	1.13	102	0.792	7.6	<0.11	0.20	0.023	<0.63	0.35	10.8
980404	TN7	9.2	0.52	1.31	1.08	12.9	0.235	0.083	126	1.06	89	0.493	4.2	<0.11	0.30	<0.016	<0.29	0.85	10.0
980405	TN8	12.2	0.64	1.93	1.88	16.6	0.276	0.066	140	1.45	81	1.13	3.6	<0.11	0.28	0.034	<0.42	1.18	9.0
980406	TN9	7.7	0.42	1.26	1.10	14.9	0.237	0.086	130	0.99	69	1.10	2.8	<0.11	0.26	0.018	<1.67	0.76	7.3
980407	TN10	8.6	0.41	2.33	1.77	10.7	0.151	0.077	91	0.80	97	0.608	3.2	<0.11	0.18	<0.016	<1.00	1.04	10.0
980408	TN11	5.1	0.34	2.44	1.74	10.8	0.078	0.108	77	1.04	144	0.291	12.7	<0.11	0.25	<0.016	<1.00	0.58	19.5
980409	TN12	4.7	0.80	1.29	1.30	3.7	0.092	0.089	58	0.79	69	1.01	8.3	<0.11	0.29	<0.016	0.76	0.52	11.0
980410	TN13	2.3	0.19	3.49	1.49	5.8	0.041	0.022	41	0.70	62	0.108	4.6	<0.11	0.17	<0.016	<0.63	0.32	11.0
980411	TN14	4.0	0.19	1.57	0.70	15.1	<0.024	0.064	26	0.76	151	0.085	2.1	<0.05	0.10	<0.011	0.33	0.22	12.2
980412	TN15	2.2	0.18	0.84	0.84	17.3	<0.024	0.032	34	0.85	202	0.088	1.9	<0.05	0.11	<0.011	<0.36	0.11	10.6
980413	TN16	1.8	0.20	1.41	0.97	9.2	<0.024	0.029	51	0.75	163	0.069	2.1	<0.05	0.31	<0.011	<1.00	1.40	8.8
980414	TN17	2.5	0.20	1.72	0.92	11.7	<0.024	0.034	61	0.83	167	0.077	5.4	<0.05	0.71	<0.011	<0.83	0.22	10.2
980415	TN18	65.4	3.58	2.46	3.59	22.1	1.008	0.143	83	2.46	72	4.45	1.4	<0.11	0.31	0.14	<1.25	2.14	8.9
980416	TN19	26.7	1.67	1.85	1.73	14.4	0.291	0.060	99	1.43	93	1.02	1.4	<0.11	0.32	0.039	<0.56	1.15	9.5
980417	TN20	29.8	2.08	1.35	1.16	9.0	0.300	0.063	109	1.19	59	1.12	1.6	<0.11	0.29	0.034	<1.00	1.05	4.6
980418	TN21	28.6	1.66	1.02	1.52	11.3	0.443	0.095	110	1.59	68	1.25	2.3	<0.11	0.37	0.075	0.32	1.13	6.9
980419	TN22	1.6	0.10	0.76	0.55	4.5	0.047	0.052	121	1.09	99	0.149	5.5	<0.11	0.17	<0.016	<0.38	0.15	16.1
980420	TN23	8.8	0.28	1.21	0.70	7.3	0.212	0.067	149	1.06	57	0.852	6.5	<0.11	0.15	0.039	<0.50	0.80	8.4
980421	TN24	5.9	0.90	0.58	0.79	4.0	0.154	0.027	162	1.24	67	0.196	4.9	<0.11	0.15	0.022	<1.25	0.39	11.7
980422	TN25	8.8	0.40	1.01	1.06	9.5	0.271	0.070	141	1.37	79	0.598	9.7	<0.11	0.50	0.029	1.06	0.50	10.7
980423	TN26	18.1	0.73	1.12	1.54	7.6	0.326	0.098	232	1.50	97	0.451	5.7	<0.11	0.22	<0.016	0.65	0.58	29.9
980424	TN27	8.2	0.32	0.89	1.51	15.3	0.120	0.081	282	1.25	101	0.366	9.8	<0.11	0.18	0.016	1.31	0.43	37.5
980425	TN28	33.4	1.07	1.69	2.58	20.2	0.402	0.061	166	1.71	120	0.751	26.7	<0.11	0.46	0.049	0.85	1.22	33.7
980426	TN29	31.7	1.14	0.96	1.44	9.9	0.530	0.118	310	1.86	73	1.91	9.4	<0.11	0.21	0.06	1.11	2.51	19.1
980427	TN30	20.9	0.51	5.74	2.36	16.8	0.573	0.148	306	1.58	69	0.864	9.5	<0.43	<0.34	<0.065	1.17	1.46	19.6
980428	TN31	12.5	0.47	1.58	1.24	10.0	0.313	0.077	312	1.38	68	0.66	10.0	<0.11	0.18	0.058	<1.25	0.92	19.4
980429	TN32	17.1	0.24	1.00	2.98	10.2	0.123	0.097	393	1.02	78	0.110	11.9	<0.32	<0.26	<0.049	1.61	0.84	22.3
980430	TN33	6.2	0.13	0.67	2.73	3.1	0.051	0.043	400	0.98	77	0.101	11.9	<0.11	0.23	<0.016	1.57	0.41	32.0
980431	TN34	3.6	0.07	1.54	4.86	21.6	<0.072	0.037	298	1.18	162	0.043	9.9	<0.16	<0.17	<0.032	1.36	0.37	46.7
980432	TN35	11.5	0.35	3.34	4.02	12.2	0.176	0.108	284	1.93	170	0.627	10.1	<0.43	<0.34	<0.065	1.26	1.02	45.3

APPENDIX 3.3 cont'd...

Sample	Locality	Mn µg l^{-1}	Co µg l^{-1}	Ni µg l^{-1}	Cu µg l^{-1}	Zn µg l^{-1}	Ga µg l^{-1}	Ge µg l^{-1}	As µg l^{-1}	Rb µg l^{-1}	Sr µg l^{-1}	Y µg l^{-1}	Mo µg l^{-1}	Cd µg l^{-1}	Sb µg l^{-1}	Cs µg l^{-1}	Se µg l^{-1}	Pb µg l^{-1}	U µg l^{-1}
980433	TN36	7.5	0.13	0.53	0.92	4.6	0.052	0.060	340	1.37	123	0.167	12.2	<0.11	0.15	<0.016	1.37	0.47	44.8
980434	TN37	11.7	0.19	0.92	1.25	16.2	0.210	0.079	352	1.44	132	0.250	15.0	<0.43	<0.34	<0.065	2.03	1.18	49.3
980435	TN38	12.0	0.43	11.83	10.96	43.3	0.096	0.133	408	3.68	126	0.158	15.9	<0.43	<0.34	<0.065	1.37	7.00	50.2
980436	TN39	11.9	0.15	0.36	0.53	3.4	0.061	0.062	411	1.38	107	0.065	32.4	<0.11	0.20	<0.016	1.50	0.52	50.1
980437	TN40	1.6	0.08	0.82	1.28	<1.7	<0.024	0.028	462	1.19	109	0.049	25.5	<0.05	0.17	<0.011	2.63	0.06	54.7
980438	TN41	13.7	0.27	0.71	1.25	3.4	0.121	0.072	130	1.42	123	0.177	29.8	<0.11	0.75	<0.016	0.91	0.65	35.2
980439	TN42	6.4	0.12	1.26	0.90	28.7	<0.072	0.074	410	1.84	182	0.075	24.8	<0.16	0.29	<0.032	2.38	0.51	75.8
980440	TN43	12.4	0.10	0.93	<0.89	26.1	0.162	0.127	461	2.12	158	0.207	27.7	<0.32	<0.26	<0.049	2.95	0.42	79.3
980441	TN44	9.7	0.16	1.27	1.40	34.0	0.170	0.050	454	2.36	146	0.235	31.0	<0.32	<0.26	0.209	2.56	0.36	86.1
980442	TN45	1.7	0.07	0.52	2.38	29.2	<0.097	0.054	447	1.66	165	0.064	32.0	<0.21	<0.23	0.052	2.01	0.29	87.1
980443	TN46	2.3	0.12	0.90	1.44	34.6	<0.097	0.048	411	1.63	173	0.070	48.3	<0.21	<0.23	<0.043	2.34	0.18	79.8
980444	TN47	1.4	0.05	1.55	1.11	35.0	<0.097	0.143	372	1.95	234	0.088	55.1	<0.21	0.25	<0.043	3.67	0.11	94.5
980445	TN48	7.7	0.16	0.56	<1.19	37.2	0.107	0.109	358	2.44	222	0.138	100	<0.43	<0.34	<0.065	3.91	0.39	94.4
980446	TN49	3.6	0.11	0.44	0.94	25.4	<0.097	0.088	383	1.94	212	0.12	195	<0.21	0.26	<0.043	3.50	0.34	77.3
980447	TN50	2.7	0.08	0.63	1.29	9.7	<0.097	0.096	458	1.60	167	0.050	310	0.22	0.28	<0.043	4.29	<0.11	37.5
980448	TN51	1.5	0.06	0.86	1.06	9.4	<0.097	<0.048	427	2.00	183	<0.018	435	0.31	0.30	<0.043	4.89	0.14	33.3
Tamagnoni borehole																			
980449	TAM7	4.0	3.14	30.27	16.63	177.1	<0.217	<0.11	21	32.4	10018	0.22	3.3	<0.47	0.59	<0.096	1.73	2.21	0.8
980450	TAM8	3.6	2.37	22.18	11.88	242.1	<0.217	<0.11	18	25.9	8320	0.18	<2.2	<0.47	<0.52	0.113	1.96	2.64	8.5
980451	TAM9	12.4	2.24	23.71	13.96	342.8	<0.217	0.116	17	28.4	9068	0.34	<2.2	<0.47	<0.52	0.109	1.55	1.95	36.2
980452	TAM10	5.1	2.46	21.33	15.83	223.0	<0.321	<0.159	19	32.7	8690	0.17	6.1	<0.69	0.83	<0.142	1.37	2.19	1.5
980453	TAM11	2.3	0.72	4.40	9.08	78.4	<0.242	0.150	13	11.8	1644	0.063	4.8	<0.52	<0.57	<0.107	1.15	1.23	0.9
980454	TAM12	4.4	0.75	19.74	2.64	116.3	<0.169	0.090	12	14.5	1172	0.055	13.5	<0.36	<0.40	<0.075	1.08	1.30	1.3
980455	TAM13	1.6	0.41	1.12	1.92	36.3	<0.121	<0.06	54	8.18	446	<0.02	62.9	<0.26	<0.29	<0.053	<1.25	0.28	1.9
980456	TAM14	3.5	0.35	1.15	2.60	51.1	<0.097	0.132	151	6.19	295	0.079	88.9	<0.21	0.32	<0.043	1.52	0.64	1.8
980457	TAM15	3.0	0.39	1.33	5.96	16.3	<0.072	0.079	368	5.17	240	0.12	67.2	<0.16	0.36	<0.032	1.00	0.51	3.0
980458	TAM16	3.0	0.45	1.01	3.47	23.8	<0.072	<0.036	515	4.67	266	0.066	77.4	<0.16	0.20	<0.032	1.40	0.33	3.8
980459	TAM17	2.0	0.34	1.10	2.02	27.3	<0.072	0.069	565	4.66	241	0.055	91.5	<0.16	0.37	<0.032	1.49	0.23	5.1
980460	TAM18	6.6	0.44	1.28	2.35	19.1	0.148	0.043	484	5.18	217	0.16	95.8	<0.32	<0.26	<0.049	1.25	0.92	4.6
980461	TAM19	5.8	0.29	5.52	3.11	16.3	0.079	0.167	536	4.29	148	0.13	97.2	<0.32	0.55	<0.049	1.44	0.73	7.9
980462	TAM20	2.1	0.17	1.39	2.82	23.5	<0.072	<0.036	428	3.18	129	0.081	96.5	<0.16	0.31	<0.032	1.66	0.35	12.1
980463	TAM21	3.8	0.28	0.88	1.70	55.3	<0.072	<0.036	455	4.37	198	0.20	109	<0.16	0.45	<0.032	1.46	0.22	20.4
980464	TAM22	2.7	0.14	0.97	2.03	20.2	0.058	0.066	628	3.11	106	0.066	108	<0.21	0.32	<0.032	1.46	0.27	10.6
980465	TAM23	1.7	0.15	0.54	1.22	30.7	<0.053	0.055	776	2.65	109	0.075	135	<0.11	0.22	<0.024	1.28	0.23	13.2

APPENDIX 3.3 cont'd...

Sample	Locality	Mn µg l^{-1}	Co µg l^{-1}	Ni µg l^{-1}	Cu µg l^{-1}	Zn µg l^{-1}	Ga µg l^{-1}	Ge µg l^{-1}	As µg l^{-1}	Rb µg l^{-1}	Sr µg l^{-1}	Y µg l^{-1}	Mo µg l^{-1}	Cd µg l^{-1}	Sb µg l^{-1}	Cs µg l^{-1}	Se µg l^{-1}	Pb µg l^{-1}	U µg l^{-1}
980466	TAM24	3.4	0.15	0.72	1.24	32.9	<0.072	<0.036	236	4.22	183	0.11	123	<0.16	0.85	<0.032	1.39	0.21	24.3
980467	TAM25	2.8	0.17	0.78	1.23	16.8	<0.072	0.131	1122	3.14	99	0.092	141	<0.16	0.27	<0.032	1.67	0.33	15.5
980468	TAM26	6.5	0.18	0.84	1.56	39.1	<0.071	0.184	1356	3.25	90	0.225	163	<0.32	<0.26	<0.049	1.71	0.34	15.1
980469	TAM27	2.0	0.37	0.67	0.74	43.5	<0.097	<0.048	1281	2.77	127	0.11	154	<0.21	0.26	<0.043	2.46	0.37	41.2
980470	TAM28	6.1	0.12	1.22	1.35	24.0	0.162	0.102	1808	2.59	85	0.16	154	<0.43	0.34	<0.065	3.45	0.25	19.7
980471	TAM29	2.3	0.13	0.52	0.69	154.6	<0.097	0.112	1870	1.85	72	0.11	226	<0.21	0.37	<0.043	2.64	0.45	10.7
980472	TAM30	15.0	0.28	1.10	1.83	22.7	0.224	0.163	960	4.36	109	0.29	177	<0.43	2.29	0.075	1.59	0.82	22.7
980473	TAM31	5.5	0.06	0.64	<1.19	52.4	<0.095	0.11	2138	2.36	64	0.15	201	<0.43	3.57	<0.065	1.88	0.58	12.4
980474	TAM32	8.6	0.16	0.62	1.24	51.1	0.113	0.204	2204	2.67	76	0.17	228	<0.43	0.54	<0.065	2.05	0.61	19.6
980475	TAM33	6.0	0.25	1.05	1.57	21.9	<0.097	0.073	1069	3.16	127	0.14	157	<0.21	3.96	<0.043	2.00	0.43	24.5
980476	TAM34	3.8	0.10	1.36	1.40	44.2	<0.071	0.13	2851	2.72	67	0.053	213	<0.32	<0.26	<0.049	2.07	0.25	20.0
980477	TAM35	11.2	0.17	1.09	1.23	43.4	0.143	0.089	3229	2.44	65	0.18	240	<0.32	0.48	<0.049	1.71	0.35	24.5
980478	TAM36	3.2	0.13	0.66	1.21	13.6	<0.071	0.125	2220	3.43	108	0.066	197	<0.32	0.94	<0.049	1.61	0.33	32.9
980479	TAM37	6.9	0.08	2.12	1.87	30.2	<0.095	0.169	3486	2.75	71	0.11	226	0.53	<0.34	<0.065	2.32	0.43	26.1
980480	TAM38	5.5	0.17	0.58	0.94	29.4	<0.071	0.127	3085	3.19	86	0.16	248	<0.32	0.44	<0.049	1.74	0.59	42.6
980481	TAM39	43.0	0.61	1.08	2.82	27.0	0.407	0.203	2948	3.70	86	0.44	253	<0.43	<0.34	<0.065	3.87	1.00	46.6
980482	TAM40	1.2	0.13	0.33	0.90	9.0	<0.097	0.167	2855	2.89	84	0.024	275	<0.21	<0.23	<0.043	3.10	<0.11	52.3
980483	TAM41	8.2	0.11	0.56	<1.19	34.2	0.135	0.069	3524	3.15	87	0.086	273	<0.43	0.35	<0.065	2.98	0.24	62.1
980484	TAM42	57.6	0.73	0.94	1.59	31.8	0.406	0.164	3497	3.90	74	0.63	255	<0.43	<0.34	<0.065	2.91	1.31	47.7
980485	TAM43	10.4	0.18	0.92	1.36	36.1	0.126	0.142	3929	3.59	87	0.12	346	<0.43	<0.34	<0.065	3.40	0.62	58.3
980486	TAM44	25.1	0.30	0.71	1.40	26.3	0.264	<0.048	3091	3.77	80	0.28	289	<0.43	0.42	0.074	3.41	0.88	65.0
980487	TAM45	55.7	0.76	1.01	1.55	28.7	0.604	0.164	3987	4.80	75	0.45	285	<0.32	0.27	0.104	2.56	1.38	29.6
980488	TAM46	20.0	0.33	0.85	1.93	48.5	0.118	0.057	2575	3.85	144	0.26	428	<0.43	<0.34	<0.065	2.73	0.89	56.1
980489	TAM47	38.4	0.61	1.35	1.88	27.7	0.324	0.212	3476	4.02	89	0.56	355	<0.32	0.46	0.099	3.03	1.24	19.0
980490	TAM48	2.6	0.16	0.66	1.05	44.1	<0.072	0.099	2455	3.94	144	0.074	279	0.24	0.27	<0.032	2.90	0.13	99.0
980491	TAM49	2.0	0.10	0.28	0.70	30.5	<0.072	0.14	3354	3.40	102	0.031	360	0.35	0.32	<0.032	2.94	0.21	41.5
980492	TAM50	2.9	0.15	0.84	1.20	36.2	<0.097	0.136	2434	3.38	165	0.066	272	<0.21	0.26	<0.043	nd	0.28	118.5
980493	TAM51	2.2	0.07	1.18	1.22	16.8	0.131	0.191	3956	2.88	108	0.058	301	<0.32	0.37	<0.049	nd	0.40	47.4
980494	TAM52	2.2	0.17	4.05	0.77	13.9	<0.072	0.09	2486	3.29	121	0.050	237	0.31	0.52	<0.032	nd	0.12	27.2
980495	TAM53	2.2	0.06	0.72	0.86	16.3	<0.072	0.179	4563	2.56	89	0.056	368	0.17	0.45	<0.032	nd	0.37	31.8
980496	TAM54	3.5	0.12	1.34	1.16	35.0	<0.072	0.134	4570	2.50	94	0.18	369	<0.16	0.20	<0.032	nd	0.73	28.1
980497	TAM55	4.8	0.09	1.15	1.29	47.1	<0.071	0.183	5384	2.57	81	0.14	286	0.41	0.28	<0.049	3.08	0.73	20.9
980498a	TAM56																nd		
980498b	TAM57																		
980499	TAM58	4.3	0.09	0.80	1.01	48.3	<0.072	0.158	5549	2.77	83	0.12	380	0.30	0.30	<0.032	3.89	0.79	14.3

APPENDIX 3.3 cont'd...

Sample	Locality	Mn µg l^{-1}	Co µg l^{-1}	Ni µg l^{-1}	Cu µg l^{-1}	Zn µg l^{-1}	Ga µg l^{-1}	Ge µg l^{-1}	As µg l^{-1}	Rb µg l^{-1}	Sr µg l^{-1}	Y µg l^{-1}	Mo µg l^{-1}	Cd µg l^{-1}	Sb µg l^{-1}	Cs µg l^{-1}	Se µg l^{-1}	Pb µg l^{-1}	U µg l^{-1}
980500	TAM59	3.3	0.10	0.56	1.30	52.8	<0.072	0.227	5392	2.63	62	0.084	339	<0.16	0.55	<0.032	3.46	1.23	9.0
980501	TAM60	4.0	0.14	2.19	1.73	35.3	<0.097	0.254	5734	2.09	66	0.074	305	0.27	0.26	<0.043	6.97	0.58	13.2
980502	TAM61	3.5	0.08	0.90	1.45	33.2	<0.072	0.136	4481	2.11	87	0.095	355	0.24	0.28	<0.032	3.13	0.33	25.2
980503	TAM62	3.1	0.39	3.51	1.04	37.5	<0.097	0.214	4389	2.21	98	0.14	417	<0.21	0.37	<0.043	4.49	0.38	27.3
980504	TAM63	1.6	0.65	7.04	1.41	40.0	<0.097	<0.048	4668	3.06	94	0.036	549	0.58	0.35	<0.043	nd	0.38	13.7
980505	TAM64	20.6	0.31	1.17	1.72	28.5	0.218	0.262	4071	3.83	92	0.33	569	0.59	0.29	<0.049	3.38	1.03	11.3
980506	TAM65	7.7	0.09	0.70	1.46	33.4	<0.095	0.195	3814	3.52	97	0.27	498	0.73	<0.34	<0.065	3.08	0.79	14.0
Augered sediments																			
970829	La Invernada	42	1.66	18.0	13	164	<0.41	<0.5	50	11.6	nd	1.58	576	1.7	<2.1	<0.44	nd	3.14	79.3
970830	La Invernada	30	1.43	19.7	8.8	141	<0.55	<0.6	149	13.0	nd	0.70	400	1.4	<2.7	<0.58	nd	<1.78	72.0
970831	Nicola	40	2.33	15.2	21	229	<1.37	<1.5	37	58.7	nd	1.36	50	<0.4	<6.9	<1.46	nd	<4.46	1.1
970832	Santa Rita	234	6.29	34.2	74	329	9.8	<1.5	1826	43.6	nd	15.11	278	0.9	<6.9	2.56	nd	12.40	19.7

nd: not determined

APPENDIX 3.4

Trace-element data for porewaters extracted from cored sediments at Talleres Norte (Eduardo Castex) and Tamagnoni (10 km south of Eduardo Castex) and from augered sediments (analysed by ICP-MS)

Sample	Locality	La μg l^{-1}	Ce μg l^{-1}	Pr μg l^{-1}	Nd μg l^{-1}	Eu μg l^{-1}	Sm μg l^{-1}	Gd μg l^{-1}	Tb μg l^{-1}	Dy μg l^{-1}	Ho μg l^{-1}	Er μg l^{-1}	Tm μg l^{-1}	Yb μg l^{-1}	Lu μg l^{-1}	Tl μg l^{-1}	Bi μg l^{-1}	Th
Talleres Norte borehole																		
980401	TN4	0.05	0.065	0.019	0.063	<0.013	<0.009	0.016	0.005	0.016	<0.003	0.01	<0.004	0.009	<0.003	0.05	<0.05	<0.05
980402	TN5	3.73	18.6	1.23	5.06	0.178	1.13	1.03	0.146	0.838	0.138	0.439	0.054	0.332	0.051	0.016	<0.03	1.58
980403	TN6	0.806	1.58	0.223	0.991	0.055	0.243	0.217	0.039	0.131	0.024	0.088	<0.007	0.061	0.013	<0.007	<0.03	0.28
980404	TN7	0.491	4.34	0.143	0.646	0.021	0.143	0.173	0.013	0.112	0.02	0.073	<0.007	0.043	0.012	<0.007	<0.03	0.39
980405	TN8	0.894	5.95	0.386	1.381	0.075	0.398	0.443	0.044	0.188	0.044	0.122	<0.007	0.109	0.01	0.012	<0.03	0.75
980406	TN9	1.12	7.08	0.453	1.835	0.071	0.430	0.492	0.041	0.254	0.059	0.14	<0.007	0.086	0.019	<0.007	<0.03	0.77
980407	TN10	0.627	7.85	0.223	0.946	0.037	0.178	0.287	0.034	0.185	0.027	0.062	<0.007	0.043	0.006	<0.007	<0.03	0.40
980408	TN11	0.296	2.44	0.076	0.359	0.009	0.114	0.101	0.006	0.062	0.016	0.021	<0.007	0.035	0.004	<0.007	<0.03	0.19
980409	TN12	0.514	1.99	0.189	0.93	0.041	0.163	0.23	0.023	0.168	0.041	0.09	<0.007	0.058	0.01	<0.007	<0.03	0.30
980410	TN13	0.084	1.30	0.031	0.142	0.01	0.040	0.035	<0.004	0.023	<0.005	0.014	<0.007	<0.013	<0.003	<0.007	<0.03	0.10
980411	TN14	0.039	0.287	0.016	0.064	<0.013	<0.009	<0.016	<0.004	0.019	0.003	0.008	<0.004	0.005	<0.003	0.009	<0.05	<0.05
980412	TN15	0.033	0.322	0.013	0.05	<0.013	<0.009	0.017	<0.004	<0.008	<0.003	0.011	<0.004	<0.005	<0.003	0.011	<0.05	<0.05
980413	TN16	0.013	0.19	<0.006	0.025	<0.013	<0.009	<0.016	<0.004	0.01	0.005	<0.008	<0.004	<0.005	<0.003	0.011	<0.05	0.11
980414	TN17	0.019	0.151	0.011	0.015	<0.013	0.015	<0.016	<0.004	<0.008	0.003	<0.008	<0.004	0.012	<0.003	0.007	<0.05	0.06
980415	TN18	4.95	7.83	1.74	7.59	0.276	1.55	1.41	0.216	1.11	0.173	0.592	0.059	0.295	0.047	0.013	<0.03	3.02
980416	TN19	1.19	3.10	0.455	1.70	0.061	0.421	0.454	0.051	0.247	0.054	0.103	0.011	0.096	0.016	<0.007	<0.03	1.09
980417	TN20	1.26	4.35	0.484	1.85	0.06	0.398	0.356	0.051	0.331	0.061	0.169	0.02	0.104	0.012	<0.007	<0.03	1.06
980418	TN21	1.57	6.29	0.608	2.45	0.099	0.571	0.564	0.067	0.358	0.092	0.174	0.019	0.146	0.019	<0.007	<0.03	1.70
980419	TN22	0.138	0.322	0.044	0.171	0.012	0.026	<0.028	<0.004	0.013	0.008	0.02	<0.007	<0.013	0.004	<0.007	<0.03	0.08
980420	TN23	0.932	2.01	0.296	1.46	0.071	0.226	0.41	0.027	0.228	0.042	0.125	0.009	0.082	0.01	<0.007	<0.03	0.25
980421	TN24	0.202	0.639	0.041	0.274	<0.008	0.069	<0.028	0.01	0.047	<0.005	0.046	<0.007	0.036	0.004	<0.007	<0.03	0.17
980422	TN25	0.569	1.42	0.151	0.975	0.031	0.185	0.223	0.02	0.125	0.027	0.054	<0.007	0.038	0.011	<0.007	<0.03	0.42
980423	TN26	0.476	0.699	0.159	0.621	0.029	0.123	0.17	0.012	0.106	0.019	0.067	0.008	0.049	0.006	<0.007	<0.03	0.43
980424	TN27	0.303	0.552	0.115	0.378	0.021	0.061	0.064	0.009	0.056	0.017	0.081	<0.007	0.04	0.007	<0.007	<0.03	0.25
980425	TN28	0.842	1.12	0.252	1.16	0.059	0.239	0.202	0.023	0.223	0.039	0.093	0.008	0.091	0.013	0.013	<0.03	0.61
980426	TN29	2.38	3.20	0.885	3.91	0.196	0.69	0.739	0.107	0.523	0.105	0.259	0.022	0.182	0.023	0.014	0.04	1.93
980427	TN30	0.858	1.90	0.282	1.46	0.062	0.275	0.401	0.018	0.235	0.048	0.138	<0.027	0.117	<0.012	<0.027	<0.11	1.10
980428	TN31	0.731	1.12	0.24	0.721	0.034	0.214	0.287	0.024	0.153	0.025	0.058	<0.007	0.069	0.007	0.01	<0.03	0.71
980429	TN32	0.102	0.229	<0.032	0.149	<0.023	<0.025	<0.084	<0.013	<0.032	<0.014	<0.013	<0.02	<0.039	<0.009	<0.021	<0.08	<0.10
980430	TN33	0.087	0.21	0.021	0.143	<0.008	<0.008	0.039	<0.004	0.03	0.006	0.012	<0.007	<0.013	<0.003	0.015	<0.03	0.21
980431	TN34	<0.022	0.051	<0.018	0.059	<0.038	<0.027	<0.047	<0.013	<0.025	<0.009	<0.023	<0.013	0.03	<0.01	0.018	<0.16	<0.16
980432	TN35	0.734	1.23	0.163	1.20	0.073	0.326	0.151	<0.017	0.191	0.024	0.08	<0.027	0.144	<0.012	<0.027	<0.11	0.60

APPENDIX 3.4 cont'd...

Sample	Locality	La μg l^{-1}	Ce μg l^{-1}	Pr μg l^{-1}	Nd μg l^{-1}	Eu μg l^{-1}	Sm μg l^{-1}	Gd μg l^{-1}	Tb μg l^{-1}	Dy μg l^{-1}	Ho μg l^{-1}	Er μg l^{-1}	Tm μg l^{-1}	Yb μg l^{-1}	Lu μg l^{-1}	Tl μg l^{-1}	Bi μg l^{-1}	Th
980433	TN36	0.095	0.182	<0.011	0.139	0.029	0.022	0.05	<0.004	0.017	0.007	0.012	<0.007	<0.013	<0.003	<0.007	<0.03	0.07
980434	TN37	0.34	0.538	<0.042	0.368	<0.031	0.099	<0.112	<0.017	0.06	<0.018	0.042	<0.027	<0.052	<0.012	<0.027	<0.11	0.21
980435	TN38	0.159	0.326	<0.042	0.247	<0.031	0.071	<0.112	<0.017	0.062	<0.018	<0.017	<0.027	<0.052	<0.012	<0.027	<0.11	<0.14
980436	TN39	0.058	0.126	0.012	0.048	<0.008	<0.008	<0.028	<0.004	<0.011	0.006	0.005	<0.007	<0.013	<0.003	<0.007	<0.03	0.09
980437	TN40	0.016	0.05	0.007	0.028	<0.013	<0.009	<0.016	<0.004	<0.008	0.005	<0.008	<0.004	0.008	<0.003	0.009	<0.05	0.08
980438	TN41	0.162	0.433	0.052	0.171	0.031	<0.008	<0.028	<0.004	0.043	0.008	0.016	<0.007	0.013	<0.003	0.009	<0.03	0.17
980439	TN42	0.073	0.132	0.037	0.19	<0.038	<0.027	0.055	<0.013	0.038	<0.009	<0.023	<0.013	<0.015	<0.01	0.023	<0.16	<0.16
980440	TN43	0.183	0.332	<0.032	0.238	<0.023	0.090	<0.084	<0.013	0.032	0.019	0.017	<0.02	0.042	<0.009	0.023	<0.08	0.10
980441	TN44	0.245	0.547	<0.032	0.234	<0.023	0.080	<0.084	<0.013	0.038	0.016	0.019	<0.02	<0.039	<0.009	<0.021	<0.08	0.18
980442	TN45	<0.03	0.077	0.034	<0.037	<0.051	0.067	<0.062	<0.017	<0.033	<0.011	<0.031	<0.018	<0.02	<0.013	0.032	<0.21	0.35
980443	TN46	<0.03	0.076	<0.024	0.045	<0.051	<0.036	<0.062	<0.017	<0.033	<0.011	<0.031	<0.018	<0.02	<0.013	<0.021	<0.21	<0.22
980444	TN47	0.032	0.03	<0.024	0.041	<0.051	<0.036	<0.062	<0.017	<0.033	<0.011	<0.031	<0.018	<0.02	<0.013	0.045	<0.21	<0.22
980445	TN48	0.121	0.313	<0.042	0.25	0.037	0.091	<0.112	<0.017	<0.043	0.02	0.022	<0.027	<0.052	<0.012	<0.027	<0.11	0.17
980446	TN49	0.034	0.126	0.028	0.08	<0.051	<0.036	<0.062	<0.017	<0.033	<0.011	<0.031	<0.018	<0.02	<0.013	<0.021	<0.21	<0.22
980447	TN50	<0.03	0.051	<0.024	<0.037	<0.051	<0.036	<0.062	<0.017	<0.033	<0.011	<0.031	<0.018	<0.02	<0.013	<0.021	<0.21	<0.22
980448	TN51	<0.03	0.042	<0.024	0.077	<0.051	<0.036	<0.062	<0.017	<0.033	<0.011	<0.031	<0.018	0.02	<0.013	0.059	<0.21	<0.22
Tamagnoni borehole																		
980449	TAM7	0.103	<0.057	<0.054	0.335	<0.114	<0.082	<0.14	<0.038	<0.075	<0.026	<0.07	<0.04	<0.044	<0.03	0.167	<0.47	<0.49
980450	TAM8	<0.067	0.095	<0.054	0.12	<0.114	0.084	<0.14	<0.038	<0.075	<0.026	<0.07	<0.04	<0.044	<0.03	0.12	<0.47	<0.49
980451	TAM9	<0.067	<0.057	0.055	0.336	<0.114	0.095	<0.14	<0.038	<0.075	0.034	<0.07	<0.04	0.082	<0.03	0.135	<0.47	<0.49
980452	TAM10	<0.099	0.203	<0.079	0.279	<0.169	<0.121	<0.207	<0.056	<0.111	0.048	<0.104	<0.058	<0.066	<0.044	0.19	<0.70	<0.72
980453	TAM11	<0.075	0.125	<0.06	<0.092	<0.127	<0.091	<0.155	<0.042	<0.084	<0.028	<0.078	<0.044	<0.049	<0.033	0.093	<0.53	<0.54
980454	TAM12	<0.052	<0.044	<0.042	0.18	<0.089	<0.064	0.125	<0.03	<0.059	<0.02	<0.055	<0.031	<0.035	<0.023	0.093	<0.37	<0.38
980455	TAM13	<0.037	0.076	<0.03	0.075	<0.064	<0.046	<0.078	<0.021	<0.042	<0.014	<0.039	<0.022	<0.025	<0.017	0.047	<0.26	<0.27
980456	TAM14	0.038	0.157	0.04	0.104	<0.051	<0.036	<0.062	<0.017	<0.033	<0.011	<0.031	<0.018	<0.02	<0.013	0.039	<0.21	<0.22
980457	TAM15	0.122	0.305	0.075	0.233	<0.038	0.047	0.107	0.019	<0.025	<0.009	<0.023	<0.013	0.023	<0.01	0.033	<0.16	<0.16
980458	TAM16	0.094	0.175	0.019	0.088	<0.038	<0.027	<0.047	<0.013	<0.025	<0.009	<0.023	<0.013	0.015	<0.01	0.043	<0.16	<0.16
980459	TAM17	0.048	0.115	0.032	0.044	<0.038	<0.027	<0.047	<0.013	<0.025	<0.009	<0.023	<0.013	0.021	<0.01	0.043	<0.16	0.18
980460	TAM18	0.198	0.391	<0.032	0.34	<0.023	<0.025	<0.084	<0.013	0.081	0.014	<0.013	<0.02	<0.039	<0.009	<0.021	<0.08	0.13
980461	TAM19	0.167	0.376	0.035	0.228	<0.023	0.083	<0.084	<0.013	<0.032	<0.014	<0.013	<0.02	<0.039	<0.009	<0.021	<0.08	<0.10
980462	TAM20	0.038	0.16	0.028	<0.027	<0.038	<0.027	<0.047	<0.013	<0.025	0.01	<0.023	<0.013	<0.015	<0.01	0.017	<0.16	<0.16
980463	TAM21	0.121	0.363	0.05	0.127	<0.038	<0.027	<0.047	<0.013	0.032	<0.009	<0.023	<0.013	<0.015	<0.01	0.029	<0.16	<0.16
980464	TAM22	0.034	0.208	<0.021	0.095	<0.016	<0.017	<0.056	<0.008	<0.021	<0.009	0.01	<0.013	<0.026	<0.006	<0.014	<0.05	0.08
980465	TAM23	<0.016	0.067	0.02	0.064	<0.028	<0.02	<0.034	0.009	<0.018	<0.006	<0.017	<0.01	<0.011	<0.007	0.018	<0.12	<0.12

APPENDIX 3.4 cont'd…

Sample	Locality	La μg l^{-1}	Ce μg l^{-1}	Pr μg l^{-1}	Nd μg l^{-1}	Eu μg l^{-1}	Sm μg l^{-1}	Gd μg l^{-1}	Tb μg l^{-1}	Dy μg l^{-1}	Ho μg l^{-1}	Er μg l^{-1}	Tm μg l^{-1}	Yb μg l^{-1}	Lu μg l^{-1}	Tl μg l^{-1}	Bi μg l^{-1}	Th
980466	TAM24	0.088	0.178	0.023	0.146	<0.038	<0.027	<0.047	<0.013	<0.025	0.011	<0.023	<0.013	<0.015	<0.01	<0.015	<0.16	<0.16
980467	TAM25	0.044	0.124	<0.018	0.066	<0.038	<0.027	<0.047	<0.013	<0.025	<0.009	0.033	<0.013	<0.015	<0.01	0.018	<0.16	<0.16
980468	TAM26	0.139	0.361	<0.032	0.185	<0.023	<0.025	<0.084	<0.013	0.041	<0.014	0.019	<0.02	<0.039	<0.009	<0.021	<0.08	0.12
980469	TAM27	0.174	0.121	<0.024	<0.037	<0.051	0.043	<0.062	<0.017	<0.033	<0.011	<0.031	<0.018	<0.02	<0.013	0.024	<0.21	0.81
980470	TAM28	0.202	0.533	<0.042	0.246	<0.031	0.057	<0.112	<0.017	<0.043	<0.018	0.023	<0.027	<0.052	<0.012	<0.027	<0.11	0.37
980471	TAM29	0.041	0.12	<0.024	<0.037	<0.051	0.046	<0.062	<0.017	<0.033	<0.011	<0.031	<0.018	<0.02	<0.013	0.03	<0.21	<0.22
980472	TAM30	0.31	0.636	<0.042	0.354	<0.031	<0.033	<0.112	<0.017	0.046	0.026	0.041	<0.027	<0.052	<0.012	<0.027	<0.11	0.32
980473	TAM31	0.142	0.366	<0.042	<0.079	<0.031	0.072	<0.112	<0.017	<0.043	<0.018	0.062	<0.027	<0.052	<0.012	<0.027	<0.11	0.28
980474	TAM32	0.164	0.339	<0.042	<0.079	<0.031	<0.033	<0.112	<0.017	<0.043	<0.018	0.043	<0.027	<0.052	<0.012	<0.027	<0.11	<0.14
980475	TAM33	0.221	0.418	0.048	0.262	<0.051	<0.036	0.116	<0.017	0.043	0.014	<0.031	<0.018	<0.02	<0.013	0.033	<0.21	<0.22
980476	TAM34	0.113	0.15	<0.032	0.086	0.024	<0.025	<0.084	<0.013	<0.032	<0.014	<0.013	<0.02	<0.039	<0.009	<0.021	<0.08	0.37
980477	TAM35	0.165	0.48	<0.032	0.08	<0.023	0.031	<0.084	<0.013	0.035	<0.014	0.017	<0.02	<0.039	<0.009	<0.021	<0.08	0.30
980478	TAM36	0.112	0.165	<0.032	0.102	<0.023	<0.025	<0.084	<0.013	0.033	<0.014	<0.013	<0.02	<0.039	<0.009	<0.021	<0.08	0.37
980479	TAM37	0.114	0.272	<0.042	0.275	<0.031	<0.033	<0.112	<0.017	<0.043	<0.018	<0.017	<0.027	<0.052	<0.012	<0.027	<0.11	0.15
980480	TAM38	1.47	0.244	<0.032	0.07	<0.023	<0.025	<0.084	<0.013	<0.032	<0.014	0.038	<0.02	<0.039	<0.009	0.031	<0.08	0.24
980481	TAM39	0.54	1.10	<0.042	0.55	<0.031	0.118	<0.112	<0.017	0.11	0.025	0.053	<0.027	<0.052	<0.012	<0.027	<0.11	0.39
980482	TAM40	0.035	0.09	<0.024	<0.037	<0.051	<0.036	<0.062	<0.017	<0.033	<0.011	<0.031	<0.018	<0.02	<0.013	<0.021	<0.21	<0.22
980483	TAM41	0.14	0.274	<0.042	0.206	0.044	0.050	<0.112	<0.017	<0.043	<0.018	0.03	<0.027	<0.052	<0.012	<0.027	<0.11	<0.14
980484	TAM42	0.82	1.31	0.179	0.816	0.051	0.204	0.2	<0.017	0.163	0.022	0.083	<0.027	0.056	0.02	<0.027	<0.11	0.63
980485	TAM43	0.326	0.32	<0.042	0.166	<0.031	<0.033	<0.112	<0.017	<0.043	<0.018	<0.017	<0.027	<0.052	<0.012	<0.027	<0.11	0.14
980486	TAM44	0.396	0.771	0.06	0.556	<0.031	0.096	<0.112	<0.017	0.087	<0.018	<0.017	<0.027	<0.052	0.016	<0.027	<0.11	0.34
980487	TAM45	0.741	1.19	0.2	0.76	0.044	0.158	0.176	<0.013	0.084	0.014	0.034	<0.02	0.053	0.011	<0.021	<0.08	0.78
980488	TAM46	0.194	0.433	<0.042	0.414	<0.031	0.045	<0.112	<0.017	0.064	<0.018	<0.017	<0.027	<0.052	<0.012	<0.027	<0.11	0.36
980489	TAM47	0.707	2.16	0.181	0.677	<0.023	0.169	0.116	0.021	0.103	0.023	0.105	<0.02	0.066	0.011	<0.021	<0.08	1.17
980490	TAM48	0.195	0.032	<0.018	0.104	<0.038	<0.027	<0.047	<0.013	<0.025	<0.009	<0.023	<0.013	<0.015	<0.01	0.017	<0.16	<0.16
980491	TAM49	0.038	0.049	0.027	0.029	<0.038	<0.027	<0.047	<0.013	<0.025	<0.009	<0.023	<0.013	0.016	<0.01	0.017	<0.16	<0.16
980492	TAM50	0.097	0.132	<0.024	<0.037	<0.051	<0.036	<0.062	<0.017	<0.033	<0.011	<0.031	<0.018	<0.02	<0.013	<0.021	<0.21	0.29
980493	TAM51	0.367	0.155	<0.032	0.113	<0.023	0.051	<0.084	<0.013	<0.032	<0.014	<0.013	<0.02	<0.039	<0.009	<0.021	<0.08	0.14
980494	TAM52	0.104	0.131	<0.018	0.108	<0.038	<0.027	<0.047	<0.013	0.031	<0.009	<0.023	<0.013	<0.015	<0.01	<0.015	<0.16	<0.16
980495	TAM53	0.054	0.142	<0.018	<0.027	<0.038	<0.027	<0.047	<0.013	<0.025	<0.009	<0.023	<0.013	<0.015	<0.01	0.017	<0.16	<0.16
980496	TAM54	0.142	0.070	0.026	0.03	<0.038	0.037	<0.047	<0.013	<0.025	0.01	0.036	<0.013	0.021	<0.01	0.02	<0.16	<0.16
980497	TAM55	0.317	0.127	<0.032	0.066	0.043	<0.025	<0.084	<0.013	0.055	<0.014	0.02	<0.02	<0.039	<0.009	0.021	<0.08	0.32
980498a	TAM56																	
980498b	TAM57																	
980499	TAM58	0.428	0.113	0.023	0.063	<0.038	<0.027	0.057	<0.013	<0.025	<0.009	<0.023	0.013	<0.015	<0.01	0.016	<0.16	<0.16

APPENDIX 3.4 cont'd...

Sample	Locality	La μg l^{-1}	Ce μg l^{-1}	Pr μg l^{-1}	Nd μg l^{-1}	Eu μg l^{-1}	Sm μg l^{-1}	Gd μg l^{-1}	Tb μg l^{-1}	Dy μg l^{-1}	Ho μg l^{-1}	Er μg l^{-1}	Tm μg l^{-1}	Yb μg l^{-1}	Lu μg l^{-1}	Tl μg l^{-1}	Bi μg l^{-1}	Th
980500	TAM59	0.121	0.192	0.027	0.087	<0.038	<0.027	<0.047	<0.013	<0.025	<0.009	<0.023	<0.013	<0.015	<0.01	0.029	<0.16	0.38
980501	TAM60	0.308	0.152	<0.024	<0.037	<0.051	<0.036	<0.062	<0.017	<0.033	0.013	<0.031	<0.018	0.036	<0.013	0.026	<0.21	<0.22
980502	TAM61	0.094	0.108	0.024	0.038	<0.038	<0.027	<0.047	<0.013	<0.025	<0.009	<0.023	<0.013	<0.015	<0.01	<0.015	<0.16	<0.16
980503	TAM62	0.099	0.109	<0.024	0.093	<0.051	<0.036	<0.062	<0.017	<0.033	<0.011	<0.031	<0.018	<0.02	<0.013	0.03	<0.21	<0.22
980504	TAM63	0.15	0.055	<0.024	0.078	<0.051	<0.036	<0.062	<0.017	<0.033	<0.011	<0.031	<0.018	<0.02	<0.013	0.035	<0.21	<0.22
980505	TAM64	0.715	0.614	0.084	0.337	<0.023	0.049	0.125	<0.013	<0.032	0.017	0.05	<0.02	0.051	<0.009	<0.021	<0.08	0.27
980506	TAM65	1.14	0.249	<0.042	0.17	<0.031	<0.033	<0.112	<0.017	<0.043	0.02	0.042	<0.027	<0.052	<0.012	0.031	<0.11	0.19
Augered sediments																		
970829	La Invernada	1.4	1.6	0.30	1.4	<0.17	0.22	0.37	<0.16	0.35	<0.14	<0.17	<0.17	0.20	<0.15	<0.447	<0.72	0.23
970830	La Invernada	0.60	1.2	<0.19	0.6	<0.23	<0.26	<0.24	<0.22	<0.21	<0.19	<0.23	<0.23	<0.20	<0.20	<0.596	<0.96	0.16
970831	Nicola	1.5	2.0	<0.47	1.7	<0.58	<0.66	<0.60	<0.54	<0.51	<0.47	<0.57	<0.57	<0.51	<0.51	<1.49	<2.40	0.33
970832	Santa Rita	13.9	33.2	3.88	16.6	0.66	3.70	5.0	<0.54	3.17	0.57	1.52	<0.57	1.61	<0.51	<1.49	<2.40	4.07

APPENDIX 4.1 Major-oxide concentrations (analysed by XRF) and organic carbon (by TOC analyser) in sediments from La Pampa

Sample	Lithology	Depth m	Location	SiO_2 %	TiO_2 %	Al_2O_3 %	Fe_2O_{3T} %	Mn_3O_4 %	MgO %	CaO %	Na_2O %	K_2O %	P_2O_5 %	LOI %	TOC %	Total %
DDA archive samples																
E. Castex, No 9 Cooperative	Brown silt	6-9	35°54.48'S 64°18.28'W	48.25	0.60	12.20	4.08	0.10	1.83	16.06	2.48	1.60	0.15	12.81	0.05	100.29
E. Castex, No 9 Cooperative	Brown silt	15-18	35°54.48'S 64°18.28'W	53.57	0.74	14.38	5.02	0.12	2.29	10.01	2.20	2.00	0.15	9.64	0.06	100.27
E. Castex, No 9 Cooperative	Brown silt	27-30	35°54.48'S 64°18.28'W	53.15	0.76	14.41	5.18	0.13	2.16	10.05	2.10	1.96	0.17	9.94	0.05	100.14
E. Castex, No 9 Cooperative	Brown silt	42-45	35°54.48'S 64°18.28'W	55.33	0.80	15.15	5.45	0.13	2.43	7.85	2.17	2.09	0.17	8.55	0.05	100.33
E. Castex, Campo de Soria	Brown silt	30-33	36°0.32'S 64°22.29'W	57.16	0.80	15.45	5.38	0.12	2.23	6.43	2.20	2.08	0.18	7.06	0.05	99.22
Ing. Luiggi No 7	Brown silt	6-12	35°23.84'S 64°27.74'W	60.73	0.82	16.23	5.60	0.07	2.10	4.24	2.71	2.30	0.21	4.59	0.05	99.88
Ing. Luiggi No 7	Brown silt	24-30	35°23.84'S 64°27.74'W	39.25	0.51	10.18	3.35	0.11	2.80	21.97	2.16	1.32	0.20	18.27	0.05	100.28
Ing. Luiggi No 7	Brown silt	36-42	35°23.84'S 64°27.74'W	65.59	0.53	12.52	3.42	0.06	1.19	6.41	3.00	1.99	0.12	4.75	0.06	99.72
La Maruja No 3	Brown silt	42-48	35°40.33'S 64°56.97'W	54.56	0.72	14.55	5.02	0.11	2.26	9.24	2.18	2.12	0.19	8.86	0.04	99.95
La Maruja No 3	Brown silt	72-78	35°40.33'S 64°56.97'W	55.76	0.73	14.82	5.20	0.10	2.37	8.10	2.08	2.19	0.24	8.38	0.07	100.08
La Maruja No 3	Brown silt	96-102	35°40.33'S 64°56.97'W	54.83	0.70	14.74	5.12	0.13	1.88	9.69	2.45	1.97	0.22	8.08	0.08	99.93
Quarry and road cutting sampes																
LPS2, E of E. Castex	Rhyolitic ash	Near surface	35°54.244'S 64°9.025'W	69.41	0.39	14.72	2.20	0.07	0.48	1.58	4.71	3.94	0.11	1.91	0.14	99.65
LPS3, N of Ing. Luiggi No 8	Rhyolitic ash	Near surface	35°23.822'S 64°27.759'W	67.42	0.54	15.15	3.35	0.07	0.95	2.75	3.79	2.79	0.13	2.48	0.05	99.55
LPS4, Conhelo	Rhyolitic ash	Near surface	35°55.217'S 64°36.349'W	69.36	0.37	14.76	2.10	0.07	0.50	1.57	4.79	4.00	0.13	1.89	0.12	99.67
?Tertiary sed, Toay cutting	Brown silt	1-2	36°43.082'S 64°29.584'W	61.64	0.85	16.72	5.76	0.10	2.12	3.52	2.85	1.92	0.15	4.26	0.02	100.03
?Quaternary sediment, Toay "	Fine brown sand	<1	36°43.082'S 64°29.584'W	64.99	0.77	15.38	4.89	0.08	1.38	3.38	3.31	2.16	0.08	2.83	0.34	99.39
4 km N of Conhelo, above ash	Dark brown silt	Near surface	35°51.8'S 64°36.1'W	66.15	0.58	15.02	3.73	0.08	1.12	2.79	3.39	2.75	0.15	4.05	0.83	99.94
4 km N of Conhelo	Rhyolitic ash (2cm*)	Near surface	35°51.8'S 64°36.1'W	69.24	0.37	14.66	2.10	0.07	0.49	1.51	4.72	4.04	0.13	2.37	0.12	99.83
4 km N of Conhelo below ash	Dark brown clay-silt	Near surface	35°51.8'S 64°36.1'W	64.34	0.67	15.12	4.64	0.10	1.33	2.89	2.77	2.39	0.15	5.07	0.94	99.59
14 km E of E. Castex	Brown sandy silt	Near surface	35°54.20'S 64°6.9'W	67.56	0.56	15.01	3.51	0.07	0.88	2.43	3.52	2.75	0.10	3.22	0.52	99.73
14 km E of E. Castex	Impure ash (1cm*)	Near surface	35°54.20'S 64°6.9'W	68.17	0.46	14.78	2.78	0.07	0.66	1.91	4.13	3.40	0.11	3.01	0.42	99.61
14 km E E. Castex, below ash	Grey-brown silt	Near surface	35°54.20'S 64°6.9'W	68.12	0.59	14.61	3.75	0.07	0.90	2.44	3.22	2.54	0.08	3.23	0.58	99.67
LPS9, Caleufu	Silt	0.5-0.7	35°35.472'S 64°34.903'W	68.12	0.54	14.79	3.44	0.06	1.09	3.16	3.54	2.49	0.10	2.15	0.23	99.62
LPS10, Caleufu	Silt	1.3-1.5	35°35.472'S 64°34.903'W	67.13	0.60	14.80	3.89	0.07	1.21	3.14	3.21	2.43	0.11	3.08	0.46	99.81
LPS11, Caleufu	Silt	2-2.2	35°35.472'S 64°34.903'W	65.46	0.63	14.93	4.11	0.08	1.35	3.29	3.13	2.43	0.14	3.75	0.51	99.44
LPS12, La Maruja	Silt	1	35°43.265'S 64°55.953'W	65.67	0.66	15.78	4.35	0.08	1.47	3.78	3.46	2.25	0.12	2.30	0.15	100.08
LPS13, Ing. Luiggi	Silt	0.5	35°24.598'S 64°27.939'W	66.64	0.61	15.40	3.98	0.08	1.36	3.30	3.31	2.39	0.13	2.76	0.25	100.10
Augered samples																
Santa Rita	Grey-brown silt	0.2-0.8	35°59.830'S 64°22.142'W	63.59	0.71	15.75	5.16	0.11	1.56	2.50	2.74	2.59	0.16	4.77	0.45	99.77
Santa Rita	Brown sandy silt	0.8-1.4	35°59.830'S 64°22.142'W	60.51	0.82	16.31	5.76	0.09	2.25	3.04	2.38	2.51	0.17	5.72	0.20	99.70
La Invernada	Brown sandy silt	0.2-1	35°57.93'S 64°11.23'W	62.38	0.63	14.67	4.47	0.09	1.53	4.89	2.96	2.46	0.13	5.47	0.20	99.82
La Invernada	Brown sand	1-2	35°57.93'S 64°11.23'W	55.26	0.69	14.03	4.76	0.10	1.96	8.68	2.37	2.14	0.14	9.42	0.07	99.68
Nicola	Brown silt	0-0.3	35°56.53'S 64°35.72'W	59.90	0.66	14.65	4.54	0.09	1.55	5.88	2.67	2.78	0.22	6.44	0.48	99.50

APPENDIX 4.1 cont'd...

Sample	Lithology	Depth m	Location	SiO_2 %	TiO_2 %	Al_2O_3 %	Fe_2O_{3T} %	Mn_3O_4 %	MgO %	CaO %	Na_2O %	K_2O %	P_2O_5 %	LOI %	TOC %	Total %
Piorno	Brown silt	1-1.4	35°56.70'S 64°10.80'W	64.05	0.71	15.90	4.99	0.11	1.46	2.47	2.75	2.51	0.15	4.96	0.46	100.18
Talleres Norte, E. Castex	Dark brown silt	0-0.25	35°54.33'S 64°18.07'W	65.44	0.69	15.36	4.27	0.08	1.33	2.98	3.13	2.46	0.12	3.92	0.56	99.90
Cored boreholes																
Talleres Norte																
TN6	Clay-sand, calcrete	4.45-4.90	35°54.3'S 64°18.07'W	44.01	0.57	11.60	3.89	0.09	1.90	18.10	2.06	1.54	0.16	15.27		99.31
TN8	Silty fine sand	5.40-5.90	35°54.3'S 64°18.07'W	60.08	0.75	15.58	5.09	0.07	2.01	5.66	2.92	2.11	0.12	5.22	0.05	99.73
TN18	Fine sand	10.40-10.89	35°54.3'S 64°18.07'W	63.29	0.74	16.37	4.72	0.07	1.76	4.46	3.69	1.94	0.13	1.83		99.14
TN30	Silty fine sand	16.50-16.84	35°54.3'S 64°18.07'W	62.19	0.83	16.26	5.57	0.07	2.04	3.31	2.96	2.23	0.21	3.58		99.40
TN40	Silty fine sand	21.00-21.33	35°54.3'S 64°18.07'W	57.94	0.78	15.52	5.51	0.11	2.29	6.04	2.54	2.13	0.16	6.37		99.54
TN46	Clayey silt	23.50-23.83	35°54.3'S 64°18.07'W	60.42	0.82	16.20	5.74	0.13	2.47	3.64	2.42	2.25	0.17	5.40	0.04	99.80
TN50	Silty fine sand	25.50-25.83	35°54.3'S 64°18.07'W	60.67	0.84	16.29	5.83	0.12	2.46	2.81	2.39	2.22	0.15	5.52	0.05	99.42
Tamagnoni																
TAM8	Sandy silt	4.10-4.45	35°59.55'S 64°15.57'W	60.54	0.79	16.03	5.52	0.12	1.96	4.05	2.41	2.35	0.17	5.11	0.07	99.19
TAM14	Clayey silt	6.80-7.10	35°59.55'S 64°15.57'W	61.74	0.82	16.62	5.86	0.15	2.09	2.51	2.61	2.48	0.16	4.47		99.65
TAM24	Fine to med sand	11.28-11.50	35°59.55'S 64°15.57'W	61.13	0.84	16.33	5.87	0.10	2.08	3.10	2.58	2.41	0.17	4.60	0.07	99.35
TAM34	Clayey-sandy silt	15.74-16.00	35°59.55'S 64°15.57'W	62.02	0.81	16.71	5.81	0.13	2.25	2.17	2.48	2.36	0.15	4.21		99.23
TAM40	Compact silt	18.11-18.30	35°59.55'S 64°15.57'W	40.86	0.52	10.90	3.70	0.09	1.54	20.73	1.68	1.54	0.14	18.28	0.04	100.09
TAM44	Sandy silt	19.70-20.15	35°59.55'S 64°15.57'W	51.01	0.63	13.45	4.46	0.11	1.70	12.52	2.11	1.91	0.15	11.49		99.65
TAM56	Clayey silt	25.38-25.50	35°59.55'S 64°15.57'W	61.33	0.80	16.63	5.97	0.14	2.51	1.92	2.32	2.46	0.17	4.87	0.04	99.26
TAM58	Silty sand	26.50-27.00	35°59.55'S 64°15.57'W	61.36	0.79	16.55	5.84	0.13	2.47	2.28	2.36	2.41	0.14	4.80		99.26
TAM64	Clayey silty sand	29.50-29.95	35°59.55'S 64°15.57'W	62.31	0.79	16.57	5.75	0.15	2.21	2.12	2.43	2.36	0.18	4.30		99.33

Values are given in weight %; total Fe given as Fe_2O_{3T}; LOI: loss on ignition; *: refers to thickness of ash band

APPENDIX 4.2 Trace-element data for sediment samples from La Pampa (analysed by XRF)

Sample	F mgkg^{-1}	V mgkg^{-1}	Cr mgkg^{-1}	Co mgkg^{-1}	Ba mgkg^{-1}	Sb mgkg^{-1}	Cs mgkg^{-1}	Ni mgkg^{-1}	Cu mgkg^{-1}	Zn mgkg^{-1}	As mgkg^{-1}	Se mgkg^{-1}	Rb mgkg^{-1}	Sr mgkg^{-1}	Mo mgkg^{-1}	Th mgkg^{-1}	U mgkg^{-1}	Cd mgkg^{-1}
DDA archive samples																		
E. Castex, No 9 Cooperative	496	nd	18	11	385	<1	<2	8	18	43	5	<1	51	411	3	nd	1	nd
E. Castex, No 9 Cooperative	970	nd	21	14	484	<1	<2	11	26	56	5	<1	65	353	4	nd	3	nd
E. Castex, No 9 Cooperative	776	nd	23	14	404	<1	2	12	28	58	5	<1	64	366	5	nd	2	nd
E. Castex, No 9 Cooperative	844	nd	23	16	989	<1	<2	13	31	61	6	<1	67	405	4	nd	2	nd
E. Castex, Campo de Soria	890	nd	24	18	420	<1	<2	12	30	61	7	<1	69	363	4	nd	2	nd
Ing. Luiggi No 7	749	nd	24	14	1430	<1	<2	13	27	65	9	<1	73	438	4	nd	1	nd
Ing. Luiggi No 7	589	nd	14	10	276	<1	<2	7	17	36	8	<1	38	752	4	nd	2	nd
Ing. Luiggi No 7	475	nd	16	9	587	<1	<2	6	11	39	6	<1	62	307	3	nd	2	nd
La Maruja No 3	710	nd	25	15	485	<1	<2	13	29	57	7	<1	66	351	4	nd	2	nd
La Maruja No 3	776	nd	26	15	378	<1	2	13	29	62	9	<1	69	332	4	nd	2	nd
La Maruja No 3	725	nd	21	17	399	<1	<2	11	27	54	12	<1	60	343	5	nd	3	nd
Quarry and road cutting samples																		
LPS2, E of E. Castex	151	nd	<2	6	654	<1	<2	<1	6	42	10	<1	115	151	5	nd	4	nd
LPS3, N of Ing. Luiggi No 8	309	nd	13	9	632	<1	<2	6	13	50	7	<1	86	278	4	nd	2	nd
LPS4, Conhelo	224	nd	<2	5	663	<1	<2	1	7	43	12	<1	118	146	6	nd	4	nd
?Tertiary sed, Toay cutting	829	116	32	17	438	<1	<2	13	27	56	6	<1	64	376	<1	5	3	<1
?Quaternary sed, Toay cutting	<500	87	24	12	530	<1	<2	11	17	48	3	<1	72	335	<1	8	3	1
4 km N of Conhelo, above ash	<500	65	18	10	562	<1	<2	8	17	52	7	<1	89	278	2	8	3	1
4 km N of Conhelo	<500	22	<2	5	656	<1	<2	2	7	43	10	<1	117	142	2	12	4	<1
4 km N of Conhelo below ash	<500	82	23	14	539	<1	<2	12	23	66	8	<1	86	270	<1	8	3	1
14 km E of E. Castex	<500	58	18	9	570	<1	<2	8	14	50	5	1	92	269	1	8	3	<1
14 km E of E. Castex	<500	39	8	7	628	<1	<2	5	10	47	8	<1	104	195	2	9	4	1
14 km E E. Castex, below ash	<500	66	20	10	534	<1	<2	8	14	46	5	<1	87	278	<1	6	2	<1
LPS9, Caleufu	<500	58	19	7	593	<1	<2	6	12	42	4	<1	81	328	<1	5	4	2
LPS10, Caleufu	<500	68	21	10	588	<1	<2	8	16	51	6	<1	79	313	1	6	1	1
LPS11, Caleufu	<500	73	19	11	603	<1	<2	10	18	52	7	<1	82	313	1	7	2	2
LPS12, La Maruja	<500	77	25	11	599	<1	<2	11	17	49	6	<1	74	381	<1	6	2	<1
LPS13, Ing. Luiggi	<500	70	19	10	625	<1	<2	9	17	48	6	<1	77	335	<1	6	2	2
Augered samples																		
Santa Rita	633	84	26	15	512	<1	<2	14	29	67	18	<1	87	271	<1	8	3	<1
Santa Rita	984	108	30	14	498	<1	<2	15	33	105	16	<1	80	324	<1	7	2	<1
La Invernada	514	74	20	13	526	<1	<2	12	21	55	6	<1	84	370	<1	7	4	1
La Invernada	698	85	21	15	375	<1	<2	14	27	55	7	<1	70	439	1	7	3	<1

APPENDIX 4.2 cont'd...

Sample	F mgkg^{-1}	V mgkg^{-1}	Cr mgkg^{-1}	Co mgkg^{-1}	Ba mgkg^{-1}	Sb mgkg^{-1}	Cs mgkg^{-1}	Ni mgkg^{-1}	Cu mgkg^{-1}	Zn mgkg^{-1}	As mgkg^{-1}	Se mgkg^{-1}	Rb mgkg^{-1}	Sr mgkg^{-1}	Mo mgkg^{-1}	Th mgkg^{-1}	U mgkg^{-1}	Cd mgkg^{-1}
Nicola	<500	75	21	12	467	<1	<2	12	26	59	6	<1	80	304	1	7	3	<1
Piorno	<500	92	25	16	521	<1	<2	14	28	62	6	<1	85	283	<1	7	2	1
Talleres Norte, E. Castex	<500	72	20	11	567	<1	<2	11	19	53	8	<1	85	287	<1	7	3	<1
Cored boreholes																		
Talleres Norte																		
TN6	<500	70	18	9	421	<1	3	10	20	51	7	<1	56	439	<1	6	2	<1
TN8	<500	111	28	11	578	<1	7	12	23	67	9	<1	75	412	1	9	2	<1
TN18	<500	100	26	8	564	<1	<3	10	17	54	7	<1	62	517	1	7	4	<1
TN30	<500	111	25	11	477	<1	3	13	28	74	7	<1	78	417	<1	8	3	<1
TN40	<500	117	27	13	475	<1	4	15	29	78	7	<1	73	410	<1	8	2	1
TN46	<500	145	32	18	559	<1	5	16	33	78	11	<1	79	395	<1	9	3	<1
TN50	<500	148	33	18	472	<1	4	16	35	78	11	<1	81	397	<1	9	3	<1
Tamagnoni																		
TAM8	<500	114	30	13	511	<1	4	16	32	76	6	<1	80	381	<1	8	2	<1
TAM14	<500	126	28	14	528	<1	6	18	34	80	7	<1	87	335	<1	10	3	<1
TAM24	<500	142	33	14	516	1	5	15	34	76	8	<1	85	345	<1	9	3	<1
TAM34	<500	174	31	16	514	<1	5	18	35	74	10	<1	84	345	<1	9	3	<1
TAM40	<500	96	23	10	334	<1	3	13	25	49	9	<1	56	324	<1	7	2	1
TAM44	<500	108	24	12	410	<1	6	13	26	60	9	<1	67	333	<1	7	1	<1
TAM56	<500	157	33	17	634	<1	7	19	36	77	18	<1	93	319	<1	8	5	<1
TAM58	<500	146	30	16	631	<1	4	17	35	79	17	<1	90	325	<1	8	5	<1
TAM64	<500	140	30	19	620	<1	7	17	36	79	13	<1	87	340	<1	8	3	<1

APPENDIX 5.1 Chemical data for acid-oxalate extract solutions of sediments from La Pampa

Sample	Locality	Lithology	Top depth m	Bottom depth m	Mg mg kg^{-1}	Na mg kg^{-1}	K mg kg^{-1}	As$_T$ mg kg^{-1}	Fe mg kg^{-1}	Mn mg kg^{-1}	B mg kg^{-1}	Li mg kg^{-1}	S mg kg^{-1}	P mg kg^{-1}	Si mg kg^{-1}	Al mg kg^{-1}	Sr mg kg^{-1}
Quarry and road cutting samples																	
981467	Cantera de Lorda*	Silt	<1		190	14	215	0.35	494	70	1.08	0.40	4.3	91	163	361	0.83
981468	Tertiary, Toay cutting	Brown silt	1.0	2.0	1235	1269	270	0.68	327	269	2.56	1.05	7.9	228	591	1471	3.05
981469	Quaternary, Toay cutting	Fine brown sand	<1		217	18	305	0.61	679	114	1.72	0.48	15.3	71	305	730	0.71
981470	LPS3, N of Ing. Luiggi No 8	Rhyolitic ash	0.5		328	22	618	0.68	597	127	1.56	0.50	18.4	155	359	1016	1.07
981471	LPS12, La Maruja	Silt	1.0		227	20	229	0.57	518	106	0.99	0.31	11.8	129	304	767	0.74
981472	LPS12, La Maruja (duplicate)	Silt	1.0		217	20	223	0.60	536	108	1.02	0.36	11.9	127	290	761	0.78
981473	LPS9, Caleufu road cutting	Silt	0.5	0.7	124	10	336	0.46	513	58	1.18	0.41	8.5	96	230	586	0.62
981474	LPS10, Caleufu road cutting	Silt	1.3	1.5	218	12	671	0.79	998	157	1.73	0.42	16.2	158	419	984	0.77
981475	LPS11, Caleufu road cutting	Silt	2.0	2.2	283	12	583	0.86	793	148	1.81	0.46	26.0	192	460	1255	0.78
981476	14 km E of E. Castex	Brown sandy silt	Near surface		135	16	706	0.65	656	87	1.12	0.25	13.4	101	170	423	0.68
981477	14 km E of E. Castex	Impure ash (1cm)	Near surface		190	24	1189	1.03	1159	170	1.62	0.30	15.9	101	272	629	0.89
981478	14 km E E. Castex, below ash	Grey-brown silt	Near surface		217	10	1035	0.82	994	137	1.34	0.23	14.1	130	257	597	0.80
981479	4 km N of Conhelo, above ash	Dark brown silt	Near surface		234	12	1039	0.72	960	162	1.65	0.40	27.1	234	328	787	0.67
981480	4 km N of Conhelo	Rhyolitic ash (2cm)	Near surface		376	26	881	1.32	1815	307	2.66	0.34	26.0	257	595	1174	0.75
981481	4 km N of Conhelo below ash	Dk. brown clay-silt	Near surface		46	22	285	0.30	311	26	1.08	0.32	8.3	75	99	243	0.41
981490	UK Sherwood Sandstone	Red sandstone			2800	12	62	0.44	578	41	2.05	0.49	10.6	122	80	285	0.06
981491	UK Sherwood Sandstone	Red sandstone	443		3836	134	72	2.20	448	29	1.85	0.45	11.9	70	83	291	0.05
Augered samples																	
981466	Santa Rita	Brown sandy silt	0.8	1.4	1487	1074	1774	6.79	467	234	8.57	2.38	12.1	305	876	1179	1.90
981482	Piorno	Brown silt	0.15	1.0	1733	1158	1066	1.16	556	405	5.73	1.65	231.0	294	647	1047	1.51
981483	Piorno	Brown silt	1.0	1.4	1131	804	1305	1.27	844	359	5.31	0.79	209.8	251	490	1053	3.99
981486	La Invernada	Brown sandy silt	0.2	1.0	780	1534	850	0.74	443	263	7.38	1.14	27.9	194	461	1035	1.05
981484	La Invernada	Brown sand	1.0	2.0	1436	2140	1215	1.06	199	321	7.32	1.46	38.5	218	443	830	1.30
981485	La Invernada (duplicate)	Brown sand	1.0	2.0	1486	2098	1212	1.09	213	343	7.49	1.54	38.9	224	457	870	1.25
981487	Talleres Norte, E. Castex	Dark brown silt	0.0	0.25	323	26	513	0.97	1122	185	1.85	0.49	34.2	196	507	1501	0.90
981488	Talleres Norte (dupl.)	Dark brown silt	0.0	0.25	318	26	510	0.94	1014	175	1.76	0.44	34.2	194	497	1434	0.87
981489	E. Castex No 9 Cooperative	Dark brown silt	0.0	0.3	264	62	783	1.02	1098	156	2.56	0.39	89.8	229	398	877	0.74
Cored boreholes																	
Talleres Norte																	
982134	TN2	Silty sand	0.50	1.00	465	64	883	0.99	3573	290	1.98	0.36	36.6	238	804	1544	1.34
982135	TN4	Silty sand	1.45	4.20	854	246	557	0.94	944	72	1.52	0.59	34.2	109	576	1128	0.16
982136	TN6	Silty sand	4.45	4.90	1201	711	511	0.65	263	34	1.75	0.98	21.1	272	679	1188	0.18

APPENDIX 5.1 cont'd...

Sample	Locality	Lithology	Top depth m	Bottom depth m	Mg mg kg^{-1}	Na mg kg^{-1}	K mg kg^{-1}	As$_T$ mg kg^{-1}	Fe mg kg^{-1}	Mn mg kg^{-1}	B mg kg^{-1}	Li mg kg^{-1}	S mg kg^{-1}	P mg kg^{-1}	Si mg kg^{-1}	Al mg kg^{-1}	Sr mg kg^{-1}
982137	TN8	Silty fine sand	5.40	5.90	1035	855	522	0.98	1837	20	2.30	1.12	9.2	145	641	1450	0.57
982138	TN10	Fine sand	6.40	6.90	688	707	390	1.04	3594	31	2.31	0.86	6.2	100	512	1314	2.31
982139	TN12	Silty fine sand	7.63	7.79	1332	829	381	0.60	962	44	1.37	1.41	14.9	165	671	1240	0.21
982140	TN14	Fine sand	8.40	8.78	700	450	361	1.72	3636	39	2.02	0.68	5.4	178	511	1048	1.68
982141	TN16	Fine sand	9.40	9.90	620	424	343	0.98	3663	34	1.91	0.58	5.6	99	387	976	1.93
982142	TN18	Fine sand	10.40	10.90	483	726	347	1.13	4082	29	1.99	0.57	5.7	74	352	845	2.31
982143	TN20	Fine sand	11.40	11.75	538	656	376	1.20	4699	33	2.17	0.54	6.6	80	353	862	3.12
982144	TN22	Coarse sand	13.20	13.30	987	1122	553	1.37	5872	64	2.97	0.92	13.4	240	631	1178	0.37
982145	TN24	Coarse sand	14.00	14.40	1305	1645	877	0.86	599	52	2.29	1.45	10.0	467	1071	1695	1.11
982146	TN26	Silty fine sand	15.06	15.36	1341	1823	837	0.84	646	52	2.59	1.50	7.5	321	1087	1822	2.67
982147	TN28	Clayey silt	16.00	16.42	1227	1558	702	0.72	449	59	2.29	1.18	12.8	402	841	1386	0.29
982148	TN30	Silty fine sand	16.50	16.84	1309	1878	843	0.54	1224	26	3.18	1.76	9.3	462	1233	1829	3.30
982149	TN32	Clayey silt	17.31	17.50	1424	1904	782	0.55	451	102	2.66	1.49	18.8	379	429	1527	0.35
982150	TN34	Silty sand	18.00	18.38	1360	1976	765	0.87	453	149	3.27	1.45	17.1	244	968	1611	0.52
982151	TN36	Silty fine sand	19.00	19.33	1194	1626	649	0.78	457	108	3.43	1.48	12.2	229	956	1605	1.12
982152	TN38	Silty fine sand	20.00	20.50	1239	1866	704	0.77	413	122	3.14	1.43	12.5	219	954	1402	1.20
982153	TN40	Silty fine sand	21.00	21.33	1772	2023	833	1.09	481	228	4.61	1.82	15.4	345	1053	1719	0.63
982154	TN42	Sandy silt	21.66	21.88	1543	2151	871	0.83	508	112	4.11	1.86	9.1	188	1128	1732	4.61
982155	TN44	Silty sand	22.50	23.00	1959	2054	897	1.07	408	294	6.10	1.94	14.1	280	835	1722	0.92
982156	TN46	Clayey silt	23.50	23.83	2525	2160	950	1.43	442	516	7.50	2.47	18.2	347	1293	1547	1.39
982157	TN48	Silty sand	24.50	24.90	2335	2226	973	1.40	416	368	8.31	2.55	23.9	328	1324	1579	0.95
982158	TN50	Silty fine sand	25.50	25.83	2466	2267	1021	1.38	556	459	8.80	2.94	16.5	365	1108	1780	4.37
982159	TN51	Silty fine-med sand	26.00	26.50	2270	2338	1066	1.30	610	410	9.91	2.99	15.2	310	1493	2376	5.48
Tamagnoni																	
982102	TAM2	Clayey silt	0.65	1.32	713	42	2442	1.10	2207	482	1.55	0.54	18.0	353	1000	2184	2.29
982103	TAM4	Clayey silt	1.98	2.64	1223	697	1576	0.59	243	259	2.10	0.93	120.6	282	677	1032	0.11
982104	TAM6	Clayey silt	3.00	3.50	1385	1022	1879	0.58	412	239	2.10	1.77	272.7	264	855	1627	3.61
982105	TAM8	Sandy silt	4.10	4.45	1286	1409	1634	0.63	440	467	2.42	1.67	136.1	375	880	1602	1.90
982106	TAM10	Compact silt	5.00	5.18	1126	2570	1537	0.69	460	535	2.83	1.64	49.1	423	929	1505	0.93
982107	TAM12	Clayey silt	5.50	6.00	1110	3310	1650	0.68	534	740	3.24	2.08	41.9	420	976	1925	5.14
982108	TAM14	Clayey silt	6.80	7.10	1205	4322	1687	0.81	462	711	4.71	2.18	15.6	331	957	1735	4.88
982109	TAM16	Clayey silt	7.60	8.04	1235	4152	1610	1.15	577	421	5.51	2.34	15.9	410	1070	1750	5.68
982110	TAM18	Silt and fine sand	8.60	9.10	1223	3929	1531	0.97	796	446	5.54	2.19	15.4	273	957	1610	4.52
982111	TAM20	Silty clay	9.60	9.87	1312	4045	1436	1.02	450	415	5.23	2.41	15.7	489	1129	1584	1.81
982112	TAM22	Fine sandy clay	10.40	10.90	1339	3949	1422	1.01	441	495	5.60	2.44	12.6	418	1071	1539	3.40

APPENDIX 5.1 cont'd...

Sample	Locality	Lithology	Top depth m	Bottom depth m	Mg mg kg^{-1}	Na mg kg^{-1}	K mg kg^{-1}	As_T mg kg^{-1}	Fe mg kg^{-1}	Mn mg kg^{-1}	B mg kg^{-1}	Li mg kg^{-1}	S mg kg^{-1}	P mg kg^{-1}	Si mg kg^{-1}	Al mg kg^{-1}	Sr mg kg^{-1}
982113 TAM24		Fine-med sand	11.28	11.50	1333	3863	1589	0.78	817	392	6.22	2.31	19.2	381	1091	1966	3.91
982114 TAM26		Silt	12.00	12.50	1880	4435	1494	1.63	670	481	8.37	4.35	14.9	393	1469	1469	5.37
982115 TAM28		Medium sand	13.00	13.45	1601	4197	1500	1.11	332	179	8.60	2.98	10.1	284	1066	1845	6.45
982116 TAM30		Coarse sand	14.25	14.35	1598	3932	1483	1.32	483	662	8.33	2.97	15.5	370	1110	1612	1.96
982117 TAM32		Sandy silt	15.00	15.50	1909	4121	1457	2.40	719	627	9.19	4.06	15.9	394	1428	1585	6.33
982118 TAM34		Sandy silt	15.74	16.00	1830	3996	1445	2.24	587	824	9.16	3.77	13.7	389	1313	1477	6.45
982119 TAM36		Fine-med sand	16.50	16.79	1813	3927	1440	2.25	626	576	10.07	3.56	10.9	243	1154	1548	6.52
982120 TAM38		Silty fine sand	17.50	18.00	1779	3848	1454	2.63	556	760	10.02	3.40	12.3	357	1224	1831	5.85
982121 TAM40		Compact silt	18.11	18.30	1413	2900	1223	2.55	252	358	7.46	1.88	15.0	507	773	1076	0.40
982122 TAM42		Silty sand	18.80	19.40	1547	3330	1373	2.49	427	569	9.02	2.49	11.6	391	1098	1671	1.97
982123 TAM44		Sandy silt	19.70	20.15	1301	2644	1166	2.38	199	431	6.45	1.54	13.2	310	795	1144	0.20
982124 TAM46		Compact silt	20.70	21.60	1561	3238	1365	2.75	425	434	8.31	2.55	17.8	412	1194	1396	0.98
982125 TAM48		Coarse sand	22.10	22.75	2031	3762	1461	1.85	630	626	11.55	4.42	27.6	1111	1928	1666	4.31
982126 TAM50		Clayey silt	23.00	23.50	1761	3540	1426	3.64	463	660	10.29	3.21	22.2	822	1460	1496	2.34
982127 TAM52		Sandy silt	24.00	24.20	1490	3204	1295	3.21	408	525	9.10	2.85	17.2	583	1156	1505	3.04
982128 TAM54		Sandy silt	24.50	24.95	2004	3704	1327	7.72	742	682	10.47	3.46	18.2	300	1274	1294	1.25
982129 TAM56		Clayey silt	25.50	26.00	2372	4323	1552	9.55	832	613	11.48	3.79	19.8	447	1926	1126	6.36
982130 TAM58		Silty sand	26.50	27.00	2157	4155	1509	9.63	1015	676	10.61	3.55	15.7	375	1543	1458	4.59
982131 TAM60		Clayey silt	27.50	28.00	2064	3921	1432	9.04	667	608	10.56	3.69	23.7	354	1433	1293	6.45
982132 TAM62		Sandy silt	28.50	29.00	1807	3522	1323	7.40	679	679	9.29	3.14	17.2	391	1286	1409	1.87
982133 TAM64		Silty sand	29.50	29.95	1909	3778	1447	6.88	701	1031	10.19	3.31	19.6	540	1492	1594	5.85

*36°40.926'S 64°24.532'W

APPENDIX 5.2 Trace-element chemical data for acid-oxalate extract solutions of sediments from La Pampa

Sample	Locality	Lithology	Top depth m	Bottom depth m	Be mgkg^{-1}	Ba mgkg^{-1}	Sc mgkg^{-1}	Y mgkg^{-1}	Co mgkg^{-1}	Cu mgkg^{-1}	Zn mgkg^{-1}	Ni mgkg^{-1}	V mgkg^{-1}	Cd mgkg^{-1}	Mo mgkg^{-1}	Cr mgkg^{-1}	Pb mgkg^{-1}	La mgkg^{-1}	Zr mgkg^{-1}	F mgkg^{-1}
Quarry and road cutting samples																				
981467	Cantera de Lorda*	Silt	<1		0.08	33	0.39	1.03	1.5	1.4	1.73	2.5	3	0.42	0.86	0.6	3.9	1.3	6.1	nd
981468	Tertiary, Toay cutting	Silt	1.0	2.0	0.13	36	0.39	1.21	4.9	1.7	0.82	6.7	15	0.33	1.08	0.5	4.3	0.9	11.8	nd
981469	Quaternary, Toay cutting	Fine sand	<1		0.13	24	0.56	1.20	2.4	2.5	1.41	3.7	6	0.47	1.02	0.7	4.1	1.2	12.0	nd
981470	LPS3, N Ing. Luiggi No 8	Rhyolitic ash	0.5		0.15	32	0.46	1.76	2.2	3.2	1.51	4.2	5	0.53	1.14	0.7	5.0	1.4	12.6	nd
981471	LPS12, La Maruja	Silt	1.0		0.11	25	0.34	0.90	1.8	3.0	1.51	3.5	4	0.37	0.65	0.6	3.4	0.9	9.6	nd
981472	LPS12, La Maruja (dupl.)	Silt	1.0		0.11	25	0.34	0.90	2.2	11.2	1.83	26.5	4	0.44	1.09	36.2	4.1	1.0	9.0	nd
981473	LPS9, Caleufu	Silt	0.5	0.7	0.08	16	0.25	0.57	1.2	1.7	2.15	2.4	3	0.43	1.03	0.8	4.6	1.1	7.2	nd
981474	LPS10, Caleufu	Silt	1.3	1.5	0.16	29	0.58	1.26	2.3	3.5	3.03	5.1	6	0.55	1.09	1.0	5.2	1.2	13.9	nd
981475	LPS11, Caleufu	Silt	2.0	2.2	0.16	30	0.48	1.27	2.4	3.8	2.07	4.8	6	0.52	1.45	0.9	5.6	1.2	15.0	nd
981476	14 km E of E. Castex	Sandy silt	Near surface		0.10	16	0.52	1.39	1.4	2.2	3.95	2.8	4	0.31	0.87	0.5	3.1	1.1	9.5	nd
981477	14 km E of E. Castex	Impure ash	Near surface		0.18	21	0.95	1.90	2.4	2.5	2.74	4.7	6	0.50	1.27	0.9	4.3	1.4	15.6	nd
981478	14 km E Castex, below ash	Silt	Near surface		0.16	21	0.77	1.78	2.0	2.4	6.34	3.7	5	0.44	1.03	0.7	4.0	1.3	14.8	nd
981479	4 km N Conhelo, above ash	Silt	Near surface		0.16	24	0.53	1.52	3.0	13.1	4.29	45.4	6	0.48	1.29	62.7	4.3	1.1	14.4	nd
981480	4 km N of Conhelo	Rhyolitic ash	Near surface		0.28	37	1.18	2.41	4.2	6.8	4.46	8.6	11	0.68	1.03	1.0	5.0	1.2	23.6	nd
981481	4 km N Conhelo below ash	Clay-silt	Near surface		0.04	9	0.15	0.44	0.9	1.7	1.01	1.5	2	0.34	0.73	0.5	2.8	0.8	3.5	nd
981490	UK Sherwood Sandstone	Sandstone			0.25	2	0.34	0.25	1.6	78	15.8	4.1	1	0.52	1.12	5.0	4.4	1.0	2.8	nd
981491	UK Sherwood Sandstone	Sandstone	443		0.23	9	0.33	0.20	1.0	14.8	5.68	2.5	1	0.41	0.93	0.8	3.0	0.8	3.7	nd
Augered samples																				
981466	Santa Rita	Sandy silt	0.8	1.4	0.18	32	0.62	2.43	4.1	4.0	3.35	7.8	19	0.48	1.38	0.9	4.9	1.5	22.3	nd
981482	Piorno	Silt	0.15	1.0	0.21	51	0.69	1.55	6.3	4.2	2.09	12.0	23	0.49	1.37	0.9	5.0	1.1	19.0	nd
981483	Piorno	Silt	1.0	1.4	0.25	42	1.18	3.39	5.4	5.7	2.69	12.3	16	0.53	1.37	1.0	6.5	1.9	21.8	nd
981486	La Invernada	Sandy silt	0.2	1.0	0.15	19	0.55	0.42	4.4	4.0	1.37	8.9	8	0.56	1.64	0.9	5.2	1.1	15.0	nd
981484	La Invernada	Sand	1.0	2.0	0.13	18	0.34	0.31	6.1	2.5	0.83	9.7	14	0.41	1.58	0.8	4.4	0.9	9.9	nd
981485	La Invernada (duplicate)	Sand	1.0	2.0	0.13	17	0.37	0.34	6.4	2.7	0.93	10.2	15	0.48	1.66	0.9	4.8	1.0	10.3	nd
981487	Talleres Norte, E. Castex	Silt	0.0	0.25	0.21	37	0.67	2.13	2.8	4.8	2.27	5.6	7	0.61	1.25	0.9	6.4	1.5	18.7	nd
981488	Talleres Norte (dupl.)	Silt	0.0	0.25	0.21	36	0.66	2.08	2.8	4.8	2.16	5.4	7	0.55	1.25	0.8	5.9	1.4	18.9	nd
981489	E. Castex No 9 Coop'tive	Silt	0.0	0.3	0.17	27	0.66	1.43	2.3	6.5	20.46	4.7	7	0.54	1.13	0.9	6.1	1.0	15.9	nd
Cored boreholes																				
Talleres Norte																				
982134	TN2	Silty sand	0.50	1.00	nd	53	nd	2.80	3.5	5.2	4.77	6.6	15	0.8	1.37	1.2	3.8	1.0	nd	16
982135	TN4	Silty sand	1.45	4.20	nd	12	nd	0.06	1.9	2.1	1.80	2.4	9	0.2	0.79	0.6	<1.2	<0.2	nd	64
982136	TN6	Silty sand	4.45	4.90	nd	17	nd	0.06	1.2	0.9	1.02	1.1	5	<0.2	0.62	<0.4	<1.2	<0.2	nd	57

APPENDIX 5.2 cont'd...

Sample	Locality	Lithology	Top depth	Bottom depth	Be	Ba	Sc	Y	Co	Cu	Zn	Ni	V	Cd	Mo	Cr	Pb	La	Zr	F
			m	m	mgkg^{-1}	mgkg^{-1}	mgkg^{-1}	mgkg^{-1}	mgkg^{-1}	mgkg^{-1}	mgkg^{-1}	mgkg^{-1}	mgkg^{-1}	mgkg^{-1}	mgkg^{-1}	mgkg^{-1}	mgkg^{-1}	mgkg^{-1}	mgkg^{-1}	mgkg^{-1}
982137 TN8		Silty fine sand	5.40	5.90	nd	29	nd	0.18	1.3	1.3	2.50	1.0	15	0.4	0.73	1.0	1.6	<0.2	nd	21
982138 TN10		Fine sand	6.40	6.90	nd	31	nd	1.26	1.5	1.3	3.51	1.5	26	0.8	0.83	1.6	1.8	0.2	nd	14
982139 TN12		Silty fine sand	7.63	7.79	nd	9	nd	0.16	1.8	1.1	1.91	1.7	10	0.2	0.68	0.8	1.6	<0.2	nd	49
982140 TN14		Fine sand	8.40	8.78	nd	31	nd	0.26	2.0	1.5	4.30	1.9	26	0.8	0.70	2.0	2.2	<0.2	nd	51
982141 TN16		Fine sand	9.40	9.90	nd	32	nd	0.16	1.7	1.5	3.76	1.8	21	0.8	0.58	2.2	1.8	<0.2	nd	30
982142 TN18		Fine sand	10.40	10.90	nd	32	nd	0.16	1.5	1.5	4.13	1.7	23	0.8	0.81	2.6	2.0	<0.2	nd	8
982143 TN2		Fine sand	11.40	11.75	nd	40	nd	0.16	1.9	1.7	4.27	2.0	25	1.0	0.66	3.0	2.2	<0.2	nd	15
982144 TN22		Coarse sand	13.20	13.30	nd	26	nd	0.12	3.3	1.9	7.31	3.0	33	1.2	0.87	4.2	2.0	<0.2	nd	23
982145 TN24		Coarse sand	14.00	14.40	nd	27	nd	0.31	2.4	1.2	1.71	2.0	14	<0.2	0.46	<0.4	1.6	<0.2	nd	57
982146 TN26		Silty fine sand	15.06	15.36	nd	35	nd	0.56	2.1	1.4	1.56	1.8	18	0.2	0.76	<0.4	2.2	0.2	nd	45
982147 TN28		Clayey silt	16.00	16.42	nd	22	nd	0.24	2.3	1.2	1.17	1.8	16	<0.2	0.69	<0.4	<1.2	<0.2	nd	25
982148 TN30		Silty fine sand	16.50	16.84	nd	29	nd	1.12	1.8	1.6	2.23	1.1	20	0.4	0.88	0.8	2.0	0.4	nd	50
982149 TN32		Clayey silt	17.31	17.50	nd	29	nd	0.10	2.5	1.5	1.21	2.6	18	<0.2	0.90	<0.4	<1.2	<0.2	nd	32
982150 TN34		Silty sand	18.00	18.38	nd	32	nd	0.20	3.0	1.5	1.34	3.3	20	0.2	0.83	<0.4	2.0	0.2	nd	35
982151 TN36		Silty fine sand	19.00	19.33	nd	29	nd	0.38	3.5	1.5	1.32	3.8	18	0.6	2.00	0.8	4.0	0.9	nd	23
982152 TN38		Silty fine sand	20.00	20.50	nd	34	nd	0.26	3.0	1.5	1.22	3.1	18	0.2	0.88	<0.4	2.2	<0.2	nd	27
982153 TN40		Silty fine sand	21.00	21.33	nd	27	nd	0.34	5.3	2.1	1.89	5.7	23	0.6	1.52	0.8	4.6	1.0	nd	nd
982154 TN42		Sandy silt	21.66	21.88	nd	39	nd	1.06	2.9	1.6	1.24	2.9	24	0.4	1.24	0.6	3.6	0.8	nd	25
982155 TN44		Silty sand	22.50	23.00	nd	29	nd	0.42	5.9	2.4	1.74	7.2	26	0.6	1.49	1.0	5.4	1.2	nd	30
982156 TN46		Clayey silt	23.50	23.83	nd	59	nd	0.64	9.0	3.3	2.30	12.4	34	0.8	1.78	1.2	6.2	1.3	nd	42
982157 TN48		Silty sand	24.50	24.90	nd	35	nd	0.46	7.2	3.2	2.31	9.4	33	0.8	1.74	1.2	6.2	1.3	nd	33
982158 TN50		Silty fine sand	25.50	25.83	nd	40	nd	1.63	8.4	3.3	2.52	11.0	34	0.8	1.95	1.4	7.6	1.9	nd	52
982159 TN51		Silty f-m sand	26.00	26.50	nd	40	nd	2.04	7.2	3.1	2.49	8.9	35	1.0	2.15	1.4	9.2	2.2	nd	28
Tamagnoni																				
982102 TAM2		Clayey silt	0.65	1.32	nd	53	nd	3.22	5.4	8.2	3.11	10.1	13	0.8	1.33	0.8	4.0	1.2	nd	2
982103 TAM4		Clayey silt	1.98	2.64	nd	15	nd	0.06	5.3	2.2	0.99	5.7	12	<0.2	0.54	<0.4	<1.2	<0.2	nd	19
982104 TAM6		Clayey silt	3.00	3.50	nd	60	nd	1.14	5.0	1.9	1.16	5.6	20	<0.2	0.73	<0.4	2.0	0.3	nd	30
982105 TAM8		Sandy silt	4.10	4.45	nd	54	nd	0.76	4.6	2.5	1.24	8.9	19	0.2	0.96	<0.4	1.8	<0.2	nd	31
982106 TAM10		Compact silt	5.00	5.18	nd	50	nd	0.26	6.8	3.5	1.33	11.3	18	<0.2	0.74	<0.4	1.6	<0.2	nd	35
982107 TAM12		Clayey silt	5.50	6.00	nd	67	nd	1.54	6.2	3.5	1.41	13.9	19	<0.2	0.79	0.8	2.2	0.2	nd	37
982108 TAM14		Clayey silt	6.80	7.10	nd	83	nd	2.00	6.6	3.4	1.51	15.1	27	<0.2	0.93	<0.4	3.4	0.4	nd	28
982109 TAM16		Clayey silt	7.60	8.04	nd	80	nd	1.72	5.1	2.8	1.48	8.3	34	<0.2	0.95	<0.4	2.6	0.3	nd	32
982110 TAM18		Silt, fine sand	8.60	9.10	nd	81	nd	1.42	5.8	2.8	1.88	8.9	35	0.2	0.72	<0.4	3.4	0.3	nd	31
982111 TAM20		Silty clay	9.60	9.87	nd	58	nd	0.50	5.1	2.9	1.44	8.8	34	<0.2	0.84	<0.4	2.0	<0.2	nd	38
982112 TAM22		Sandy clay	10.40	10.90	nd	77	nd	1.08	8.6	3.1	1.51	11.1	37	<0.2	0.92	<0.4	2.6	<0.2	nd	49

APPENDIX 5.2 cont'd...

Sample	Locality	Lithology	Top depth m	Bottom depth m	Be mgkg^{-1}	Ba mgkg^{-1}	Sc mgkg^{-1}	Y mgkg^{-1}	Co mgkg^{-1}	Cu mgkg^{-1}	Zn mgkg^{-1}	Ni mgkg^{-1}	V mgkg^{-1}	Cd mgkg^{-1}	Mo mgkg^{-1}	Cr mgkg^{-1}	Pb mgkg^{-1}	La mgkg^{-1}	Zr mgkg^{-1}	F mgkg^{-1}
982113	TAM24	Fine-med sand	11.28	11.50	nd	70	nd	0.96	4.7	2.8	2.66	7.7	35	0.2	1.01	0.4	2.8	<0.2	nd	39
982114	TAM26	Silt	12.00	12.50	nd	95	nd	2.58	7.7	3.6	1.54	10.1	72	0.2	1.19	<0.4	3.2	0.8	nd	32
982115	TAM28	Medium sand	13.00	13.45	nd	69	nd	1.88	4.3	2.1	1.01	4.0	51	<0.2	0.79	<0.4	3.0	0.6	nd	80
982116	TAM30	Coarse sand	14.25	14.35	nd	98	nd	0.74	5.7	3.7	1.54	11.7	56	<0.2	1.05	0.6	2.8	<0.2	nd	36
982117	TAM32	Sandy silt	15.00	15.50	nd	106	nd	2.89	7.5	3.5	1.69	13.1	81	0.2	1.12	<0.4	3.2	0.9	nd	45
982118	TAM34	Sandy silt	15.74	16.00	nd	148	nd	2.98	8.5	4.0	1.73	17.5	76	0.2	0.98	0.4	5.0	0.9	nd	61
982119	TAM36	Fine-med sand	16.50	16.79	nd	87	nd	2.14	6.8	3.4	1.38	12.1	68	<0.2	0.77	<0.4	3.2	0.6	nd	40
982120	TAM38	Silty fine sand	17.50	18.00	nd	105	nd	2.10	8.5	3.4	1.60	14.5	60	<0.2	0.86	<0.4	3.2	0.6	nd	41
982121	TAM40	Compact silt	18.11	18.30	nd	26	nd	0.14	7.1	2.6	1.30	9.3	41	0.1	0.77	<0.3	1.2	<0.2	nd	34
982122	TAM42	Silty sand	18.80	19.40	nd	65	nd	0.50	7.5	3.0	1.33	11.0	46	<0.2	0.74	<0.4	2.2	<0.2	nd	44
982123	TAM44	Sandy silt	19.70	20.15	nd	24	nd	0.08	6.2	2.3	1.06	8.1	34	<0.2	0.69	<0.4	<1.2	<0.2	nd	24
982124	TAM46	Compact silt	20.70	21.60	nd	55	nd	0.30	6.4	3.1	1.31	9.9	44	<0.2	0.80	<0.4	1.8	<0.2	nd	43
982125	TAM48	Coarse sand	22.10	22.75	nd	122	nd	1.75	7.9	4.6	1.77	12.3	64	0.2	1.41	0.4	3.8	0.3	nd	134
982126	TAM50	Clayey silt	23.00	23.50	nd	119	nd	0.90	7.0	3.8	1.53	13.0	54	0.2	1.10	0.6	3.2	<0.2	nd	99
982127	TAM52	Sandy silt	24.00	24.20	nd	114	nd	1.20	6.0	3.0	1.15	9.6	50	<0.2	1.60	0.8	2.2	<0.2	nd	70
982128	TAM54	Sandy silt	24.50	24.95	nd	84	nd	0.52	8.5	3.6	1.50	11.9	67	<0.2	0.97	<0.4	2.0	<0.2	nd	22
982129	TAM56	Clayey silt	25.50	26.00	nd	150	nd	3.28	9.6	4.5	1.81	14.3	68	0.4	0.96	0.6	3.2	1.0	nd	63
982130	TAM58	Silty sand	26.50	27.00	nd	139	nd	2.38	7.9	3.5	1.18	11.1	54	<0.2	1.03	<0.4	2.2	0.4	nd	34
982131	TAM60	Clayey silt	27.50	28.00	nd	118	nd	2.68	10.2	3.4	1.35	13.3	46	0.2	1.11	0.4	3.6	0.8	nd	39
982132	TAM62	Sandy silt	28.50	29.00	nd	92	nd	0.74	8.3	3.1	1.41	11.5	41	0.2	0.93	0.4	2.6	0.2	nd	45
982133	TAM64	Silty sand	29.50	29.95	nd	160	nd	3.28	12.0	4.0	1.36	16.8	53	<0.2	0.91	0.8	3.8	1.0	nd	59

*36°40.926'S 64°24.532'W

APPENDIX 6.1 Chemical data for hydroxylamine-hydrochloride extract solutions of sediments from La Pampa

Sample	Locality	Top depth m	Bottom depth m	As_T mgkg^{-1}	Ca mgkg^{-1}	Mg mgkg^{-1}	Na mgkg^{-1}	K mgkg^{-1}	Mn mgkg^{-1}	Fe mgkg^{-1}	Si mgkg^{-1}	Al mgkg^{-1}	Sr mgkg^{-1}	Ba mgkg^{-1}	B mgkg^{-1}	S mgkg^{-1}	P mgkg^{-1}	Co mgkg^{-1}	Ni mgkg^{-1}	V mgkg^{-1}	Zn mgkg^{-1}	Y mgkg^{-1}	La mgkg^{-1}
990499	TN2	0.50	1.00	0.02	2220	361	65	386	130	86.9	230	140	12.2	52	13.9	14.9	8	1.6	<0.9	1.2	1.13	0.23	0.25
990500	TN4	1.45	4.20	0.47	28052	875	400	371	118	21.0	180	6.9	50.4	35	14.9	63.7	8	1.0	1.0	3.2	0.28	0.12	<0.09
990501	TN6	4.45	4.90	0.47	41098	1317	1117	411	117	31.8	204	2.4	62.9	48	20.5	48.3	33	<1	<1.0	2.4	<0.24	0.25	0.16
990502	TN8	5.40	5.90	0.22	24590	993	1175	326	92	6.8	174	4.5	46.2	45	11.3	23.9	17	1.1	<0.8	20.9	<0.19	0.68	0.41
990504	TN10	6.40	6.90	0.11	1998	540	931	353	11	17.7	231	371	26.6	65	17.0	11.4	90	<1	<1.0	3.6	0.72	0.64	0.68
990505	TN12	7.63	7.79	0.26	41095	1234	1252	380	133	27.7	154	5.3	74.9	33	17.5	36.6	12	<1	<1.0	2.7	<0.25	2.13	0.78
990506	TN14	8.40	8.78	0.20	1847	480	527	293	24	27.2	181	273	27.0	34	12.2	<9	230	<1	<0.9	2.2	0.39	1.04	0.81
990507/8	TN16	9.40	9.90	0.14	1523	431	500	304	20	16.3	226	390	24.7	37	14.8	<10	134	82.1	0.0	2.0	0.10	0.83	0.66
990509	TN18	10.40	10.90	0.12	1290	342	895	318	14	12.1	206	382	22.7	33	8.2	10.0	120	<1	0.9	1.9	1.55	0.71	0.57
990510	TN20	11.40	11.75	0.08	1036	376	810	318	13	12.2	224	259	24.2	44	10.2	<10	119	<1	<1.0	2.5	0.57	0.50	0.46
990511	TN22	13.20	13.30	0.30	23289	933	1639	400	94	30.0	168	11	53.3	36	11.5	22.1	67	<1	<0.9	2.8	<0.24	0.78	0.49
990512	TN24	14.00	14.40	0.31	16814	1177	2335	431	78	32.3	240	15	61.6	39	15.8	19.0	88	1.0	<1.0	4.7	<0.25	0.35	0.29
990513	TN26	15.06	15.36	0.47	3356	1008	2435	392	47	25.9	464	177	50.3	42	12.5	<9	258	<1	<0.9	6.6	0.33	1.14	0.86
990514	TN28	16.00	16.42	0.21	21995	1088	2251	415	92	34.4	190	5.0	57.4	40	13.6	15.9	26	1.2	<1.0	5.2	<0.24	0.46	0.37
990515	TN30	16.50	16.84	0.67	2851	974	2514	409	15	5.8	394	219	44.9	37	15.4	9.5	402	<1	<0.9	6.3	0.27	1.74	1.28
990516	TN32	17.31	17.50	0.28	25649	1223	2768	420	149	1.5	285	6.5	1.3	59	21.5	24.7	11	<1	<1.0	7.2	1.15	0.15	0.17
990518	TN34	18.00	18.38	0.32	9404	1010	2638	447	134	32.4	165	21	51.7	46	18.6	20.8	23	<1	<1.0	6.9	<0.26	0.49	0.36
990519/20	TN36	19.00	19.33	0.36	6115	925	2402	462	99	2.3	963	67	44.1	38	17.0	13.7	78	1.6	<0.0	6.2	0.05	0.81	0.62
990521	TN38	20.00	20.50	0.36	4983	894	2409	401	101	39.0	113	39	41.1	35	15.9	13.0	80	1.5	<0.9	5.9	<0.23	0.61	0.42
990522	TN40	21.00	21.33	0.43	18182	1494	3275	422	230	1.1	224	8.7	65.6	58	13.6	18.1	22	2.1	<1.0	9.3	<0.24	0.39	0.33
990523	TN42	21.66	21.88	0.50	2102	1174	2894	440	94	8.5	311	229	46.1	40	14.5	<10	236	2.4	<1.0	8.9	<0.25	0.92	0.75
990524	TN44	22.50	23.00	0.52	11776	1684	3226	426	215	1.2	316	24	58.1	48	15.1	14.1	51	1.9	1.3	9.5	0.38	0.50	0.51
990525	TN46	23.50	23.83	0.62	9957	2064	3024	772	129	41.5	439	93	74.5	95		11.8	71	3.9	1.3	16.9	1.79	0.64	0.25
990526	TN48	24.50	24.90	0.51	11625	1873	3716	419	321	2.2	509	21	59.1	65	49.5	52.9	43	2.6	<1.0	12.7	<0.24	0.39	0.41
990527	TN50	25.50	25.83	0.72	2761	2058	3606	527	355	16.1	193	94	59.0	54	22.8	15.0	178	4.2	1.1	14.4	<0.24	1.03	0.72
990528	TN51	26.00	26.50	0.78	2427	1801	3659	862	261	10.2	406	191	57.5	46	20.1	13.0	266	4.2	<0.9	15.0	0.36	1.33	0.89
990460	TAM2	0.65	1.32	0.18	2583	589	83	2091	373	57.2	649	588	24.0	88	11.7	<10	264	4.1	2.1	2.8	1.32	2.65	2.45
990461	TAM4	1.98	2.64	0.25	48709	1224	1100	1743	365	12.3	254	3.5	58.4	49	16.4	106	41	2.7	1.6	5.0	<0.25	0.81	0.84
990462	TAM6	3.00	3.50	0.27	4113	1191	1332	1705	272	39.7	1087	667	38.8	67	17.9	309	371	<0.9	1.5	7.0	0.48	2.98	2.42
990463	TAM8	4.10	4.45	0.44	13555	1210	1882	1603	489	23.3	686	677	58.1	91	22.0	146	510	3.9	1.8	9.3	0.60	4.71	3.65
990464	TAM10	5.00	5.18	0.44	14246	934	3466	932	536	13.6	394	184	50.4	75	16.8	40.1	354	5.2	2.0	8.2	<0.23	2.78	2.03
990465	TAM12	5.50	6.00	0.45	3303	896	4287	1572	624	60.2	542	645	49.4	69	20.4	38.5	562	5.4	3.1	11.2	1.22	4.07	2.90
990467	TAM14	6.80	7.10	0.49	2709	861	5390	1529	456	40.6	470	581	48.2	73	17.2	12.5	426	4.4	2.1	13.6	0.36	3.35	2.32

APPENDIX 6.1 cont'd...

Sample	Local-ity	Top depth m	Bottom depth m	As_T $mgkg^{-1}$	Ca $mgkg^{-1}$	Mg $mgkg^{-1}$	Na $mgkg^{-1}$	K $mgkg^{-1}$	Mn $mgkg^{-1}$	Fe $mgkg^{-1}$	Si $mgkg^{-1}$	Al $mgkg^{-1}$	Sr $mgkg^{-1}$	Ba $mgkg^{-1}$	B $mgkg^{-1}$	S $mgkg^{-1}$	P $mgkg^{-1}$	Co $mgkg^{-1}$	Ni $mgkg^{-1}$	V $mgkg^{-1}$	Zn $mgkg^{-1}$	Y $mgkg^{-1}$	La $mgkg^{-1}$
990468	TAM16	7.60	8.04	1.02	2564	962	5390	1494	395	20.3	494	491	52.5	92	20.6	19.8	743	4.4	1.6	19.5	0.58	3.58	2.48
990469	TAM18	8.60	9.10	0.55	2771	949	5017	1417	376	36.8	804	478	45.7	86	20.4	12.3	353	4.8	1.8	19.2	0.87	2.12	1.62
990470/1	TAM20	9.60	9.87	0.65	17577	1030	5351	1394	414	21.3	401	259	56.1	87	22.7	18.3	433	3.6	2.3	21.2	0.07	3.04	2.43
990472	TAM22	10.40	10.90	0.84	4627	1083	5016	1412	557	62.0	430	564	54.0	114	27.8	14.1	593	5.9	2.9	28.1	0.86	4.13	3.15
990473	TAM24	11.28	11.50	0.57	4010	1062	5050	1515	329	29.5	467	562	51.9	86	20.0	17.1	483	3.7	1.4	19.2	1.33	3.31	2.74
990475	TAM26	12.00	12.50	1.19	2122	1339	5716	1423	405	24.3	578	334	51.4	101	21.2	12.1	498	6.5	1.6	51.0	0.51	2.15	1.73
990476	TAM28	13.00	13.45	0.69	1650	1271	5500	1444	240	14.6	545	502	52.0	84	21.4	9.3	352	4.1	<0.9	33.8	0.35	1.95	1.56
990477	TAM30	14.25	14.35	0.75	15676	1243	5367	1405	410	81.0	433	89	55.7	103	23.1	17.6	222	3.4	1.0	31.1	<0.2	2.01	1.67
990478	TAM32	15.00	15.50	1.77	1754	1376	5258	1395	476	52.9	631	350	51.5	110	36.0	17.3	478	6.1	2.4	58.1	0.56	2.32	1.91
990479	TAM34	15.74	16.00	1.76	1786	1378	5237	1407	454	23.4	390	362	52.3	105	23.2	11.2	510	5.9	2.4	52.7	0.55	2.39	1.93
990480	TAM36	16.50	16.79	1.50	1603	1355	5135	1366	576	38.8	519	293	50.2	115	37.6	14.7	317	6.7	2.7	50.1	0.56	1.61	1.24
990481	TAM38	17.50	18.00	2.02	1934	1290	4790	1335	508	18.8	533	391	49.3	100	22.0	11.1	449	6.3	2.8	40.8	0.53	2.03	1.58
990482/3	TAM40	18.11	18.30	1.00	45978	1229	4207	1285	393	23.2	250	6.3	57.0	77	21.0	16.3	27	3.1	2.2	26.0	<0.2	0.24	0.38
990484	TAM42	18.80	19.40	1.77	7248	1150	4274	1242	386	10.1	414	300	45.2	78	18.3	9.5	400	4.8	2.0	28.0	0.52	2.28	1.75
990485	TAM44	19.70	20.15	1.16	42669	1125	3798	1219	370	96.8	226	21	51.3	74	14.8	14.2	47	2.7	1.9	21.5	<0.2	0.45	0.54
990486	TAM46	20.70	21.60	2.16	17332	1215	4292	1329	445	25.2	377	258	53.2	96	28.4	22.5	392	5.4	2.3	27.7	0.45	2.68	2.17
990488	TAM48	22.10	22.75	3.34	2093	1177	4818	1219	460	21.4	266	162	47.7	115	33.0	23.0	756	4.4	0.9	39.7	0.27	1.20	0.82
990489/90	TAM50	23.00	23.50	1.86	6731	1128	4599	1190	451	7.7	272	27	44.0	118	20.3	14.1	184	3.1	1.1	30.0	<0.2	0.25	0.24
990491	TAM52	24.00	24.20	1.43	8872	1150	4685	1218	471	3.2	385	12	44.5	132	23.1	12.8	116	3.2	0.9	28.9	<0.2	0.17	0.22
990492	TAM54	24.50	24.95	2.38	12111	1379	5045	1287	596	10.7	273	3.3	50.8	149	26.4	17.7	37	4.6	1.6	44.4	<0.2	0.23	0.31
990493	TAM56	25.50	26.00	4.72	1619	1299	5497	1307	430	15.4	488	82	43.6	117	33.2	18.4	379	5.3	1.4	40.4	0.32	0.86	0.71
990494	TAM58	26.50	27.00	3.97	3102	1266	5571	1343	369	4.2	440	41	38.8	111	35.2	18.4	200	4.3	1.1	30.9	0.25	0.63	0.57
990495/6	TAM60	27.50	28.00	4.18	1535	1248	5014	1258	458	<7.6	147	120	45.2	102	26.2	21.7	380	6.7	1.7	26.6	0.11	0.87	0.74
990497	TAM62	28.50	29.00	2.93	15448	1552	4609	1204	514	42.0	520	68	65.8	143		17.6	124	4.7	1.8	28.8	0.86	0.40	0.15
990498	TAM64	29.50	29.95	3.05	125	1182	4949	1263	441	9.9	295	148	43.4	102	23.6	16.1	486	5.8	1.2	27.2	0.55	1.33	1.02